

Jishuang Chen

Experimental Plant Virology

With 126 figures

 ZHEJIANG UNIVERSITY PRESS
浙江大学出版社

 Springer

**ADVANCED TOPICS
IN SCIENCE AND TECHNOLOGY IN CHINA**

ADVANCED TOPICS IN SCIENCE AND TECHNOLOGY IN CHINA

Zhejiang University is one of the leading universities in China. In Advanced Topics in Science and Technology in China, Zhejiang University Press and Springer jointly publish monographs by Chinese scholars and professors, as well as invited authors and editors from abroad who are outstanding experts and scholars in their fields. This series will be of interest to researchers, lecturers, and graduate students alike.

Advanced Topics in Science and Technology in China aims to present the latest and most cutting-edge theories, techniques, and methodologies in various research areas in China. It covers all disciplines in the fields of natural science and technology, including but not limited to, computer science, materials science, life sciences, engineering, environmental sciences, mathematics, and physics.

Author

Dr. Jishuang Chen
Institute of Bioengineering
Zhejiang Sci-Tech University
Hangzhou 310029, China
E-mail: chenjs@zstu.edu.cn

ISSN 1995-6819 e-ISSN 1995-6827
Advanced Topics in Science and Technology in China

ISBN 978-7-308-07369-1
Zhejiang University Press, Hangzhou

ISBN 978-3-642-14118-8 e-ISBN 978-3-642-14119-5
Springer Heidelberg Dordrecht London New York

Library of Congress Control Number: 2010929389

© Zhejiang University Press, Hangzhou and Springer-Verlag Berlin Heidelberg 2010

This work is subject to copyright. All rights are reserved, whether the whole or part of the material is concerned, specifically the rights of translation, reprinting, reuse of illustrations, recitation, broadcasting, reproduction on microfilm or in any other way, and storage in data banks. Duplication of this publication or parts thereof is permitted only under the provisions of the German Copyright Law of September 9, 1965, in its current version, and permission for use must always be obtained from Springer-Verlag. Violations are liable to prosecution under the German Copyright Law. The use of general descriptive names, registered names, trademarks, etc. in this publication does not imply, even in the absence of a specific statement, that such names are exempt from the relevant protective laws and regulations and therefore free for general use.

Cover design: Frido Steinen-Broo, EStudio Calamar, Spain

Printed on acid-free paper

Springer is a part of Springer Science+Business Media (www.springer.com)

Preface

Plant Virology, the study of plant viruses and their diseases, is an important branch of science comprised of challenges and opportunities in China and developing countries, where agriculture is of key importance to date. The discovery of principles and the development of new techniques are helpful in feeding the population more safely and in providing more healthy systems of food production, along with many other aspects of social life such as ornamentals and natural medicine.

It is easy to show people fish, no matter how they are obtained, but it is more difficult to tell others how to fish, no matter how simple it becomes after years of practice. Based on the progress of biological studies over the last decades, molecular biology techniques have established a good foundation for realizing the investigation of viral genomes, which is the “stem” for plant virus exploration. Using *Cucumber mosaic virus* (CMV) with its satellite RNA and several other plant viruses with single stranded RNA genome as examples, some newly-obtained principles and the progress of the research are shown in this book, which is composed of six chapters. Chapters 1 to 5 mainly involve topics of genomic characterization, detection and quantitative techniques, especially the infection clone systems of CMV. Host responses to virus infection through plant microRNAs have also been demonstrated as groundwork. In Chapter 6, several plant cryptic viruses with double stranded virus genomes have been described for the first time, treating an understanding of plant viruses as a kind of bio-resource.

I hope this book will provide some practical clues and insight for people who work in this field and in related areas.

I warmly thank all the contributors who have worked with me in the same laboratory, during the year 2000 to 2009, including Ph.D candidates, Junli Feng, Zhiyou Du, Qiansheng Liao, Liqiang Li, Shaoning Chen and Qiulei Lang, with Master Students Liang Cheng, Yanfei chen, Rong Zeng, Jianguang Zhang, Zuodong Qin, Liping Zhu, Qinghua Tian, Hong Guo, Shijie Yan and Susu Shentu.

Dr. Jishuang
Hangzhou, China
December, 2009

Contents

1 Gene Cloning of <i>Cucumber Mosaic Virus</i> and Some Related Viral Agents.....	1
1.1 Introduction.....	1
1.2 A Tomato Strain of <i>Cucumber Mosaic Virus</i> , a Natural Reassortant Between Subgroups IA and II.....	5
1.3 The <i>Araceae</i> Strain of <i>Cucumber Mosaic Virus</i> Infecting <i>Pinellia ternate</i> Suggested to be a Novel Class Unit Under Subgroup I.....	10
1.3.1 Phylogenetic and Sequence Divergence Analysis of 3a and CP ORFs.....	15
1.3.2 Phylogenetic and Sequence Divergence Analysis of 5' UTR and 3' UTR, 2a and 2b ORFs of RNA3.....	15
1.4 The Potyvirus Infecting <i>Pinellia ternata</i> is a Recombinant Contributed by <i>Soybean Mosaic Virus</i> and <i>Lettuce Mosaic Virus</i>	17
1.4.1 DAS-ELISA Analysis of Field Samples for Detecting the Potyvirus.....	18
1.4.2 Sequencing and Nucleotide Sequence Analysis of the Potyvirus Infecting <i>Pinellia</i>	20
1.4.3 Amino Acid Sequence Analysis for CP of the Potyvirus Infecting <i>Pinellia</i>	22
1.4.4 Nucleotide Sequence Analysis for CP N-terminal of the Potyvirus Infecting <i>Pinellia</i>	24
1.4.5 Amino Acid Sequences for N-terminal and for the Conserved Region of the Potyvirus Infecting <i>Pinellia</i>	25
1.4.6 Nucleotide Sequences for 3' UTR of the Potyvirus Infecting <i>Pinellia</i>	27
1.4.7 The General Character and Possible Origin of the Potyvirus Infecting <i>Pinellia</i>	27
1.5 The 5' Terminal and a Single Nucleotide Determine the Accumulation of <i>Cucumber Mosaic Virus</i> Satellite RNA.....	31
1.5.1 GUUU- in 5' Terminal is Necessary to Initiate Replication of <i>2msatRNA</i>	32

1.5.2	Typical Structure at the 5' Terminal is Necessary for Long-distance Movement or High Accumulation of <i>2msat</i> RNA.....	34
1.5.3	Low Accumulation of 2mF5sat Mutants is Related to Single Nucleotide Mutation.....	36
1.5.4	Secondary Structure of 2mF5sat Impaired its Replication Capacity.....	38
1.6	Methodology.....	40
1.6.1	Purification of CMV Virions from Plant Tissue.....	40
1.6.2	RT-PCR and cDNA Cloning for Full-length Genomic RNAs of <i>Cucumber Mosaic Virus</i>	41
1.6.3	RT-PCR and Gene Cloning for 3'-end of Viral Genome of <i>Soybean Mosaic Virus</i>	42
1.6.4	Sequence Analysis and Phylogenetic Analysis.....	43
1.6.5	Pseudo-recombination of Satellite RNA of <i>Cucumber Mosaic Virus</i> and the Helper Virus.....	43
	References.....	44
2	Molecular Detection of <i>Cucumber Mosaic Virus</i> and Other RNA Viruses Based on New Techniques.....	47
2.1	Introduction.....	47
2.2	Multiplex RT-PCR System for Simultaneous Detection of Five Potato Viruses.....	51
2.2.1	Comparison of 18S rRNA and <i>nad2</i> mRNA as Internal Controls.....	52
2.2.2	The Optimized System for Simultaneous Detection of Potato Viruses with Multiplex RT-PCR.....	54
2.2.3	Sensitivities of Multiplex RT-PCR and DAS-ELISA in Detecting Potato Viruses.....	55
2.3	Detection of <i>Cucumber Mosaic Virus</i> Subgroups and Tobamoviruses Infecting Tomato.....	57
2.3.1	Multiplex RT-PCR for Simultaneous Detection of Strains of CMV and ToMV in Tomato.....	58
2.3.2	Field Detection of Tomato Viruses by Multiplex RT-PCR.....	62
2.3.3	Identification of CMV Subgroups by Restriction Enzymes.....	62
2.4	A Novel Glass Slide Hybridization for Detecting Plant RNA Viruses and Viroids.....	65
2.4.1	Preparation of Highly Sensitive Fluorescent-labeled Probes...	66
2.4.2	Effect of Spotting Solutions on Spot Quality.....	67
2.4.3	Effect of Glass Surface Chemistries on Efficiencies of RNA	

	Binding.....	68
2.4.4	Detection Limits of Glass Slide Hybridization and Nylon Membrane Hybridization.....	69
2.4.5	Specificity of Glass Slide Hybridization.....	71
2.4.6	Detection of PVY and PSTVd from Field Potato Samples.....	72
2.5	Quantitative Determination of CMV Genome RNAs in Virions by Real-time RT-PCR.....	74
2.5.1	Optimization of Real-time RT-PCR and the Specificity.....	76
2.5.2	Quantification of CMV Genomic RNAs by RT-PCR and Comparison of the Quantification with Lab-on-a-Chip and Northern Blot Hybridization Assays.....	76
2.6	Accurate and Efficient Data Processing for Quantitative Real-time PCR.....	81
2.6.1	Quantification of CMV RNAs in Virions with Standard Curves.....	82
2.6.2	Quantification of CMV RNAs in Virions by SCF.....	83
2.6.3	Quantification of CMV RNAs in Virions by LinReg PCR and DART Programs.....	85
2.6.4	Determination of the Suppression Effect of Satellite RNA on CMV Accumulation in Plant Tissues Using N_0 Values.....	87
2.7	Methodology.....	88
2.7.1	Primers Design and Specificity Tests in RT-PCR.....	88
2.7.2	Comparison of 18S rRNA and <i>nad2</i> mRNA as Internal Controls.....	89
2.7.3	Optimization of Multiplex RT-PCR.....	90
2.7.4	Comparison of Sensitivities for Multiplex RT-PCR and DAS-ELISA.....	91
2.7.5	Glass Slide Hybridization.....	91
	References.....	94
3	Infectious Clones and Chimerical Recombination of <i>Cucumber Mosaic Virus</i> and its Satellite RNAs.....	97
3.1	Introduction.....	97
3.2	<i>Cucumber Mosaic Virus</i> -mediated Regulation of Disease Development Against <i>Tomato Mosaic Virus</i> in the Tomato.....	98
3.2.1	ToMV-N5 Initiated Necrosis on Tomato Can be Protected by Previous Inoculation with Wild-type CMV.....	100
3.2.2	ToMV-N5 Initiated Necrosis on Tomato Cannot be Protected by Previous Inoculation with CMV Δ 2b.....	102

3.2.3	ToMV-N5-initiated Necrosis on Tomato Cannot be Protected by Previous Inoculation with Potato Virus X.....	103
3.2.4	CMV-initiated Protection against ToMV-N5 is Related to the Replication and Accumulation of Challenging Virus.....	104
3.3	Pseudo-recombination between Subgroups of <i>Cucumber Mosaic Virus</i> Demonstrates Different Pathotype and Satellite RNA Support Characters.....	105
3.3.1	Wildtype and Pseudo-recombinants and with or without satRNA Induce Different Symptoms on <i>N. glutinosa</i>	105
3.3.2	Wildtype and Pseudo-recombinants with or without satRNA Induce Different Symptoms on <i>N. benthamiana</i>	107
3.3.3	Wildtype and Pseudo-recombinants with or without satRNA Induce Different Symptoms on Tomato Varieties.....	108
3.3.4	The Pathogenicity of Wildtype and Pseudorecombinants with or without satRNA-Tsh are Related to Viral Accumulation.....	110
3.4	Synergy via <i>Cucumber Mosaic Virus</i> and <i>Zucchini Yellow Mosaic Virus</i> on Cucurbitaceae Hosts.....	111
3.4.1	Assessment of Symptom and Synergic Interaction by <i>Cucumber Mosaic Virus</i> and <i>Zucchini Yellow Mosaic Virus</i> ...	112
3.4.2	Accumulation Kinetics for CMV ORFs in Single or Complex Infection.....	113
3.4.3	Accumulation Kinetics of ZYMV CP ORF in Single or Complex Infection.....	116
3.5	Methodology.....	117
3.5.1	The Interaction Study on CMV and ToMV Interaction.....	118
3.5.2	Pseudo-recombination of CMV Subgroups.....	119
3.5.3	Synergy between CMV and ZYMV on <i>Cucurbitaceae</i>	121
	References.....	122
4	Gene Function of <i>Cucumber Mosaic Virus</i> and its Satellite RNA Regarding Viral-host Interactions.....	125
4.1	Introduction.....	125
4.2	The 2b Protein of <i>Cucumber Mosaic Virus</i> is a Determinant of Pathogenicity and Controls Symptom Expression.....	127
4.2.1	Infectivity and Stability of Fny-CMV Derived Mutants.....	128
4.2.2	Replacement of the 2b ORF Affected Capsidation of Viral RNA 2.....	130
4.2.3	Intraspecies Hybrid Viruses by Changing 2b Gene Induce Different Virulence.....	132

4.2.4	Divertive Virulence is Mediated by the 2b Protein Rather than by the C-terminal Overlapping Parts of the 2a Protein.....	132
4.2.5	Virulence is Associated with the Accumulation of Viral Progeny RNAs Affected by 2b Protein.....	134
4.3	Function of CMV 2b Protein and the C-terminus of 2a Protein in Determining Viral RNA Accumulation and Symptom Development...	137
4.3.1	The Systemic Necrosis-inducing Domain is Related to a 125-nucleotide Region of RNA 2.....	138
4.3.2	Effect of 2b Protein Amino Acid 55 on Viral Accumulation and Symptom Development.....	140
4.3.3	Sequence Analyses of the 2b Proteins and the C-top of the 2a Proteins.....	141
4.3.4	Effect of the C-terminus of 2a Protein on Symptom Expression and Virus Accumulation.....	143
4.4	Satellite RNA-mediated Reduction in Accumulation of CMV Genomic RNAs in Tobacco Related to 2b Gene of the <i>Helper Virus</i>	146
4.4.1	Symptom Expression on <i>N. Tabacum</i> Inoculated with CMV-Fsat.....	146
4.4.2	Effect of satRs on the Accumulation of CMV-Fny Genomic RNAs.....	148
4.4.3	Symptom Expression on the Host Plants Inoculated with CMV-Fny Δ 2b.....	148
4.4.4	Accumulation of CMV-Fny Δ 2b Genomic RNAs and the Effect of satRNAs.....	149
4.4.5	Accumulation of CMV-Fny Genomic RNAs in the Inoculated Leaves and the Effect of satRNAs.....	151
4.4.6	The Effect of satRNAs on Long-distance Movement of CMV-Fny Genomic RNAs.....	152
4.5	Methodology.....	153
4.5.1	Plants, Viruses and Plasmid Constructs.....	153
4.5.2	Plant Inoculation and Viral Progeny RNA Analysis.....	158
4.5.3	Quantifying the Accumulation of Viral RNAs in Leaf Tissue...	159
	References.....	159
5	Plant MicroRNAs and Their Response to Infection of Plant Viruses...	163
5.1	Introduction.....	163
5.2	Methodology.....	165
5.2.1	Computational Prediction of miRNAs and Their Target Genes	

	for Plant Species with Known Genome Sequences.....	165
5.2.2	Use Plant miRNA Microwares to Identify Conservative miRNAs from New Host Plants.....	167
5.2.3	Use Plant miRNA Microarrays to Identify Conservative miRNAs Response to Virus Infection.....	169
5.2.4	Quantitative Determination of miRNAs by Stem-loop Real-time RT-PCR.....	170
5.2.5	Design of Plant miRNA-array and Data Analysis.....	173
5.2.6	Confirmation of miRNAs by Northern Blotting and Target mRNA by 3'-RACE.....	174
5.3	Tomato miRNAs Predicted from Known Genomic Sequences and Discovered by miRNA Microarray.....	174
5.3.1	Potential Tomato miRNAs Predicted Computationally According to Known Genomic Sequences.....	175
5.3.2	Potential Targets of Newly Predicted miRNAs and Their Function.....	178
5.3.3	Confirmation of Tomato miRNAs Expression and Survey by Microarray.....	180
5.4	Mechanisms Involved in Plant miRNA Expression with Regard to Infection of ssRNA Viruses.....	185
5.4.1	Phenotype in Tomato Under Infection with CMV/satRNA Combinations and ToMV.....	186
5.4.2	Response of Tomato miRNA Expression to Virus Infection...	187
5.4.3	MiRNA Expression Profiles between CMV-Fny and CMV-FnyΔ2b Infections.....	193
5.4.4	MiRNAs Expression Profiles Altered with Addition of satRNAs.....	194
5.4.5	A Comparison of miRNAs Expression Profiles between CMV and ToMV Infections.....	195
5.5	Tomato miRNA Response to Virus Infection Quantified by Real-time RT-PCR.....	197
5.5.1	Identification of Tomato ARF8- and AGO1-like Genes.....	199
5.5.2	Analytical Validation of Real-time RT-PCR for Amplification of miRNAs.....	200
5.5.3	Quantification of Tomato miRNAs Expression by Stem-loop Real-time RT-PCR.....	202
5.5.4	Quantification of miRNAs Targets in Tomato under <i>Cucumovirus</i> Infection.....	204
	References.....	206

6	Genomic Characterization of New Viruses with Double Stranded RNA Genomes.....	211
6.1	Introduction.....	211
6.2	Novel dsRNA Viruses Infecting <i>Raphanus sativus</i>	212
6.2.1	Yellow Edge Symptoms and dsRNA Patterns in the Radish...	213
6.2.2	Genome Characterization of <i>Raphanus sativus</i> Cryptic Virus 1.....	217
6.2.3	Genome Characterization of <i>Raphanus sativus</i> Cryptic Virus 2.....	222
6.2.4	Correlation of <i>Raphanus sativus</i> Cryptic Virus 2 with <i>Raphanus sativus</i> Cryptic Virus 1.....	224
6.2.5	Genome Characterization of Suggested <i>Raphanus sativus</i> Cryptic Virus 3.....	226
6.2.6	The Possible Existence of More dsRNA Viruses in Radish.....	229
6.3	Double Stranded Viruses in <i>Vicia faba</i>	229
6.3.1	Two dsRNA Viruses Infecting <i>V. faba</i>	230
6.3.2	A Partitiviruss Infecting <i>Aspergillus</i> sp. Associated with Leaf Tissue of <i>Vicia faba</i>	237
6.4	A Novel dsRNA Virus Infecting <i>Primula malacoides</i> Franch.....	243
6.5	Derivation and Evolutionary Relationship of dsRNA Viruses Infecting plants.....	249
6.6	Conclusion.....	257
6.7	Methodology.....	258
6.7.1	Plant Material and dsRNA Extraction.....	258
6.7.2	Purification of Virus Particles.....	260
6.7.3	Amplification of Unknown dsRNA Sequence by Modified Single-primer Amplification Technique (SPAT).....	260
6.7.4	Sequence Analysis.....	261
6.7.5	Dot-Blot Hybridization.....	262
	References.....	262
	Index.....	267

Gene Cloning of *Cucumber Mosaic Virus* and Some Related Viral Agents

1.1 Introduction

Cucumber mosaic virus (CMV) is a typical member of the genus *Cucumovirus*. It has infected more than 1,000 species of monocots and dicots, including many economically important crops (Palukaitis and García-Arenal, 2003; Palukaitis et al., 1992). In China, CMV is commonly detected as the principal virus infecting field crops in the families *Solanaceae* (including tobacco, tomato, potato, pepper, etc.), *Brassicaceae* (including brassicas, radish, turnip, etc.) and *Fabaceae* (including soybean, cowpea, etc.). As shown in Fig. 1.1, CMV strain containing a satellite RNA co-infected with *Tomato mosaic virus* (ToMV), brought fruit necrosis and killed off the whole plant when the temperature was high. CMV infection in early spring used to bring a major lost of radishes and other cruciferous crops.



Fig. 1.1. Symptoms caused by infection of *Cucumber mosaic virus* in the field (a) Field tomato plant complexly infected by *Cucumber mosaic virus* with a satellite RNA and a strain of *Tomato mosaic virus*; (b) Field radish plant infected by CMV

CMV can easily transmit mechanically to a wide range of plants. This characteristic makes it easier to do more research for virus-host interactions, and also for virus-virus interactions. Typical symptoms induced by CMV are supplied in Fig. 1.2. The rapid replication and high accumulation in leaf tissues of systemic hosts provide another advantage for genomic and quantitative studies. As shown in Fig. 1.3, CMV particles reach a high accumulation condition within four days of inoculation in cells of the inoculated leaf. And the potyvirus infection also shows distinguished characteristics.

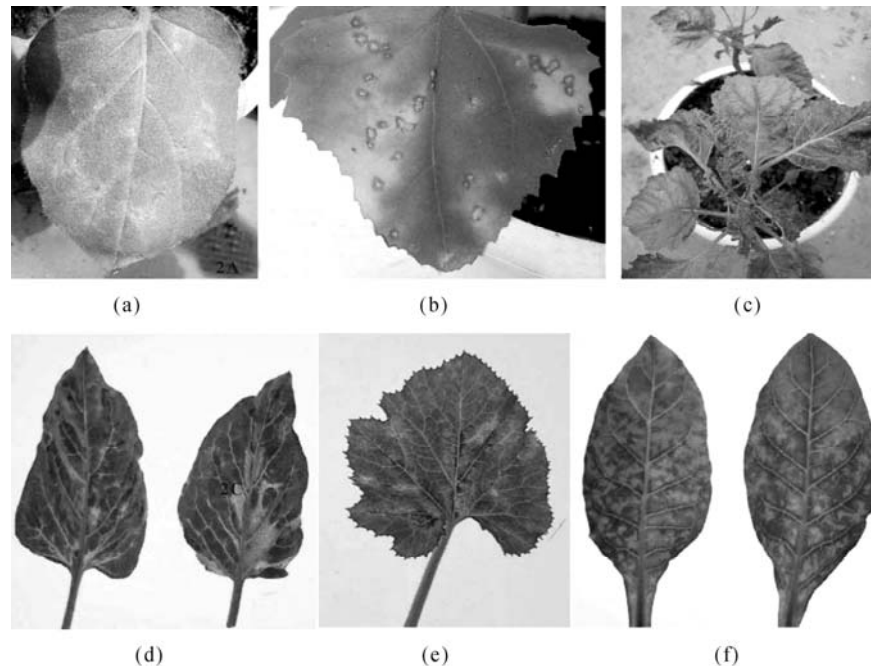


Fig. 1.2. Typical symptoms caused by inoculation of *Cucumber mosaic virus*
 (a) *Nicotiana glutinosa*, presenting irregular yellowing spots on the inoculated leaves; (b) *Chenopodium amaranticolor*, presenting local lesions on the inoculated leaves; (c) *Nicandra physalodes*, presenting systemic mosaic and distortion the lower leaves inoculated dropped; (d) *N. glutinosa*, presenting systemic mosaic; (e) *Lagenaria siceraria*, presenting systemic mosaic; (f) *N. tabacum* (cv. HuangMiaoYu), presenting systemic mosaic

Major differences are also characterized for CMV and the co-infection potyvirus, for CMV is more a hot time virus occurring in seasons with higher temperature, whilst potyvirus such as TuMV is more likely to occur in cool seasons (Table 1.1).

In the same ecological position and transmitted via similar methods (both by aphids and by mechanical transmission), CMV and potyvirus are found to have infected the same crops and express typical mosaic symptoms. It could be considered that the two kinds of viruses can be evaluated together or with similar mechanisms. The morphological characteristics are presented in Fig. 1.4.

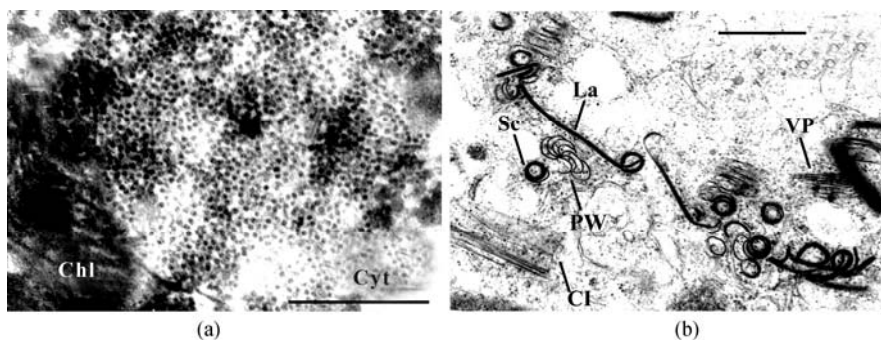


Fig. 1.3. Cytoplasmic alteration of the host tissues by infection of *Cucurbit mosaic virus* and *Turnip mosaic virus* (TuMV)

(a) Cytoplasm structure of *N. glutinosa* (inoculated leaf 4 days post inoculation) infected by *Cucurbit mosaic virus*, presenting numerous spherical virus particles in the cytoplasm and the remaining chloroplast layers (Chl: chloroplast layer; Cyt: cytoplasm), bar = 750 nm; (b) Cell structure of *Brassica campestris* ssp. *chinensis* infected with TuMV, presenting different structures of cylindrical inclusion body and aggregated filamentous virus particles (PW: pinwheel structure; CI: cylindrical structure; Sc: scroll-like structure; La: laminated aggregates; VP: virus particle), bar = 600 nm

Table 1.1 Seasonal occurrence in frequencies of principal viruses infecting cruciferous crops

Seasons	CMV	TuMV	CMV +TuMV	CMV (%)	TuMV (%)	CMV/TuMV	Total isolate obtained
Spring (March–May)	12	22	5	44.0	69.2	0.63	39
Summer (June–August)	5	5	0	50.0	50.0	1.00	10
Autumn (September–November)	24	9	5	72.5	35.0	2.10	40
Winter (December–February)	42	51	7	43.3	51.3	0.85	113

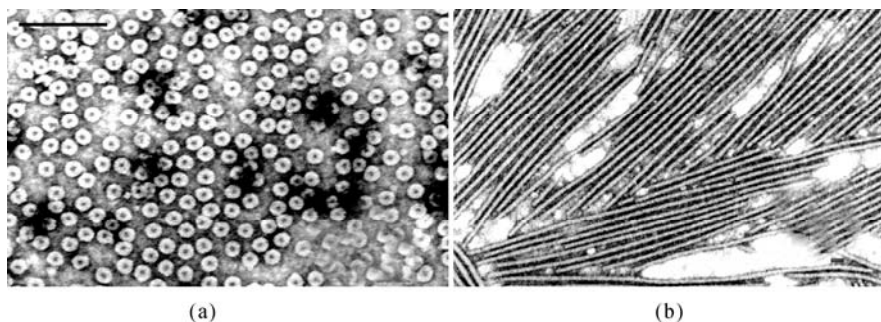


Fig. 1.4. Morphological characteristics of *Cucurbit mosaic virus* and potyvirus infecting crucifers

(a) Virus particles of *Cucurbit mosaic virus*, bar = 150 nm; (b) Virus particles of *Turnip mosaic virus*, bar = 350 nm

The survey was done during 1997 and 2001, in Zhejiang Province, eastern China.

In comparison with conventional techniques, viral genome sequence analysis is the most direct and one of the most valid methods to date. As a tripartite RNA virus, CMV contains three capped single-stranded positive-sense genomic RNAs named RNA1, RNA2 and RNA3. RNA1 and RNA2 encode 1a protein and 2a protein respectively, which are involved in virus replication (Hayes and Buck, 1990). RNA3 encodes 3a protein (MP) and coat protein (CP). 3a protein is responsible for virus movement (Ding et al., 1995; Li et al., 2001). CP is translated via a subgenomic RNA4 and involved in virus movement and aphid-mediated transmission (Kaplan et al., 1998; Perry et al., 1994). In addition, 2b protein encoded by subgenomic RNA4A via RNA2 functions in long-distance movement and as a post-transcriptional gene silencing suppressor (Brigneti et al., 1998; Ding et al., 1994; 1995).

A major advantage in using CMV as model ssRNA virus is that it has high copies of double stranded RNAs of the full-length genome. The dsRNA segments are easily extracted and analyzed, and can be regarded as replication forms, as shown in Fig. 1.5.

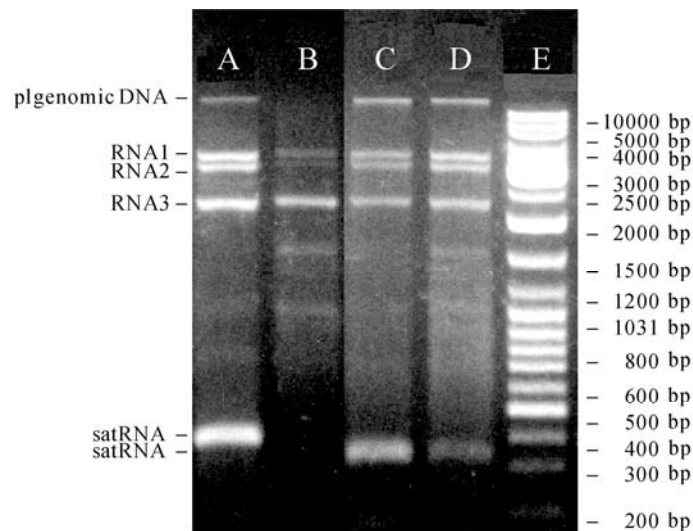


Fig. 1.5. Patterns of dsRNA analysis of several *Cucumber mosaic virus* isolates
The dsRNA pattern shows relative copy numbers of carried satellite RNA and the genome RNAs

When determining the symptom development by host, coat protein is involved in quite a few functions. It is highly expressed via subgenomic RNA4. To outline the fine functional domain and related sequence of CMV RNA3 subgenomic promoter region (SgPr) as a region for regulation between 3a protein and CP sequence, the sequences for SgPr are determined and compared to the reported sequences for CMV RNA3 with different origins. Among the CMV isolates compared, SgPrs are found to consist of 284–323 nt, varying among the isolates.

The SgPr sequence for subgroup I is obviously different from that of subgroup II because of a sequence similarity of <70% between them. This indicates that the SgPr region may have additional biological significance and that the SgPr may have no direct relationship with the presence or absence of a satRNA in CMV (Fig. 1.6).

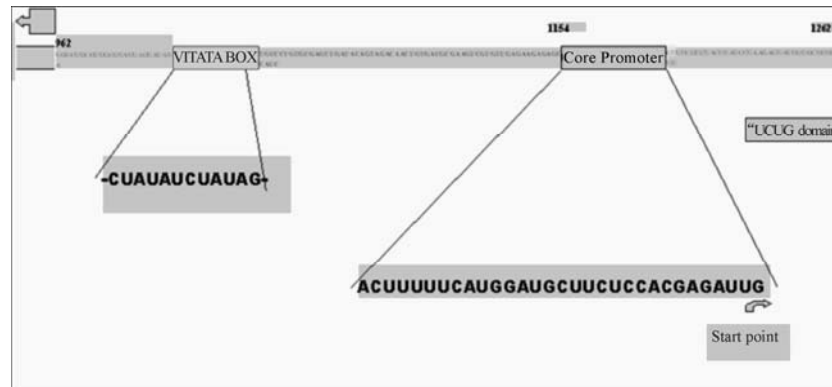


Fig. 1.6. Fine structure and functional motifs of RNA3 subgenomic core promoter region of *Cucumber mosaic virus*

Introduced in this chapter, the evolution mechanism between CMV and the co-infecting potyvirus and the evolution mechanism between CMV and its satellite RNAs (satRNAs) could be different from each other. CMV, as a multipartite ssRNA virus, pseudo-recombination is considered frequently, while potyvirus infecting new host plants seems to utilize a combination among and within gene motifs. For example, the new CMV strain infecting the tomato is discovered as a natural reassortment between the strain of the same virus, but to fit the infection to *Pinellia ternata* from the *Araceae* family, a potyvirus jointly coming from *Soybean mosaic virus* (SMV) and *Watermelon mosaic virus* (WMV). At the same time, an unusual strain of CMV infects *P. ternata* after a period of fitness to vegetative propagation of the host plant displays site mutation and deletion (insertion) mechanisms, with some independent evolution at their UTR terminus (Figs. 1.3 and 1.4). It is believed that the host and geographical environment had an impact on evolutionary types of this virus.

As for satRNA of CMV, the secondary structures are essential for replication and stability. Changes at a single base could influence survival or interaction.

1.2 A Tomato Strain of *Cucumber Mosaic Virus*, a Natural Reassortant Between Subgroups IA and II

According to serological relationships and nucleic acid identities, CMV isolates have been classified into two main subgroups, namely subgroup I and subgroup II (Palukaitis et al., 1992). The analysis of a larger numbers of CP genes and 5'

non-translated regions of CMV isolates' RNA3 has led to a further division of subgroup I into subgroups IA and IB (Roossinck et al., 1999). The nucleotide sequence identity between CMV subgroups I and II strains ranges from 69% to 77%, while it is above 90% within a subgroup (Palukaitis et al., 1992). CMV strains of subgroups IA and II have been reported from most parts of the world, while subgroup IB strains are considered to be mainly restricted to Asia (Roossinck, 2002). Considering the tripartite nature of the CMV genome, reassortment is one of the mechanisms for genetic variation and new strain generation of multipartite RNA viruses (Chao, 1997). Reassortment of multipartite RNA viruses has been displayed for many animal viruses and plant viruses, such as the influenza virus (McCullers et al., 1999) and tobnavirus (Robinson et al., 1987). Among cucumoviruses, an interspecific reassortant, composed of CMV RNA3 and *Peanut stunt virus* (PSV) RNAs 1 and 2, and an intraspecific reassortant of PSV, have been discovered (Hu and Ghabrial, 1998; White et al., 1995). Studies of natural CMV populations have showed that mixed infection by different CMV strains is frequent and genetic exchange by reassortment occurred (Bonnet et al., 2005; Fraile et al., 1997).

However, natural reassortants between CMV subgroups and strains should survive against selection and could not become established as dominating populations before a favorite condition appears. Furthermore, reassortment does not occur randomly. The fraction of reassortants between CMV subgroups IA and IB is found to be larger than that of reassortants between subgroups I and II. Before, only one naturally occurring reassortant between CMV subgroups I and II strains was found by Bonnet et al. (2005).

A CMV strain, represented as an isolate, namely CMV-Tsh has been detected for its wide distribution in a tomato field in Shanghai, emerging in spring 2005. This isolate is found to be a natural reassortant between subgroups I and II based on sequence analysis.

Based on biological inoculation, virus isolation, serological identification and, especially, double stranded RNA analysis, the existence of CMV with a satRNA is found to co-exist with ToMV to cause severe systemic mosaic and necrosis synergy. After gene cloning with full-length cDNA amplified with primer pairs against all the subgroups I and II strains, the genomic sequences of this CMV are obtained. The full length RNA1 is obtained by cloning two RT-PCR products respectively. The primers used for amplification CMV genomic RNAs are listed in Table 1.2. The full length sequences of CMV-Tsh RNA1, RNA2 and RNA3 have been submitted to GenBank under the accession number EF202595, EF202596 and EF202597, respectively. CMV-Tsh RNA1 is found to consist of 3,394 nucleotides (nt), encoding 1a protein of 994 amino acids from 96 to 3,077 nt. RNA2 is consisted of 3,047 nt, containing two partially overlapped ORFs 2a and 2b. The 2a ORF encoding 2a protein of 858 amino acids extends from 86 to 2659 nt, and the 2b ORF is positioned at the sequence from 2,418 to 2,750 nt, encoding 2b protein of 111 amino acids. RNA3 contains 2,206 nt, encoding 3a protein of 280 amino acids and CP of 219 amino acids, corresponding to the sequences from 97 to 936 nt, and 1,229 to 1,885 nt respectively.

Table 1.2 Primers for RT-PCR amplification of CMV genomic RNAs

Primer ^a	Positions ^b	Nucleotide sequence ^c	Enzyme site
RNA1-F	5' end of RNA1	5'-AATCGGATCCTAATACGACTCACTATA GGTTTATTACAAGAGCGTA-3'	<i>Bam</i> HI
RNA1-R	3' end of gRNAs	5'-AATTGTCGACTGGTCTCCTT-3'	<i>Sal</i> I
RNA2-F	5' end of RNA2	5'-AATCGGATCCTAATACGACTCACTATA GGTTATTYWCAAGAGCGTA-3'	<i>Bam</i> HI
RNA3-F	5' end of RNA3	5'-AATCGGATCCTAATACGACTCACTATA GGTAATCTTACCACT-3'	<i>Bam</i> HI
RNA23-R	3' end of gRNAs	5'-AATTCTGCAGTGGTCTCCTT-3'	<i>Pst</i> I
RNA1-1750-R	1607–1623 nt	5'-AATTGTCGACGATGATATCACGTCCCA-3'	<i>Sal</i> I
RNA1-1600-F	1607–1623 nt	5'-AATCGGATCCTGGGACGTGATATCATC-3'	<i>Bam</i> HI

^a: “F” represent forward primer, “R” represent reverse primers. All primers are useful against all CMV subgroups; ^b: combining area (for against CMV-Fny), “gRNAs” represent all genomic RNA; ^c: Underlined are sites for restriction enzymes, blocked are T7 promoter sequences, Y= C or T, W= A or T

The sequence comparison results between CMV-Tsh and other strains from subgroups I and II are shown in Table 1.3. RNA1 and 1a ORF of CMV-Tsh show 97.5% nucleotide sequence identity with those of the strain Q and less than 78% with those of the two strains CMV-Fny and CMV-Sd, which are obtained from Shandong, China. These results revealed that CMV-Tsh RNA1 is derived from a CMV subgroup II strain. Comparisons of the nucleotide sequences of CMV-Tsh 2a, 2b and RNA2 to those of CMV-Fny, CMV-Sd and Q strain revealed that CMV-Tsh is more closely related to the CMV-Fny (with over 96% sequence identity) than to CMV-Sd (less than 91% identity) and Q strain (less than 73% identity). So, it is most likely that CMV-Tsh RNA2 is derived from a CMV subgroup IA strain. The nucleotide sequences of CMV-Tsh RNA3, 3a and CP ORF show over 98% sequence identity with those of the strain Q and less than 80% sequence identity with those of the CMV-Fny and CMV-Sd. These results indicated that CMV-Tsh RNA3 is derived from a CMV subgroup II strain. The same classification of CMV-Tsh RNAs 1, 2 and 3 are observed by comparing the deduced amino acid sequences of five ORFs.

The results of phylogenetic analysis for five ORFs between CMV-Tsh and another 15 CMV strains are shown in Fig. 1.7. For 1a, 3a and CP genes, CMV-Tsh forms an independent clade with subgroup II strains with supporting values of 100%, while 2a and 2b ORFs of CMV-Tsh form a clade with subgroup IA strains, supported by >98% bootstrap values. These results are similar to those obtained from the sequence comparisons.

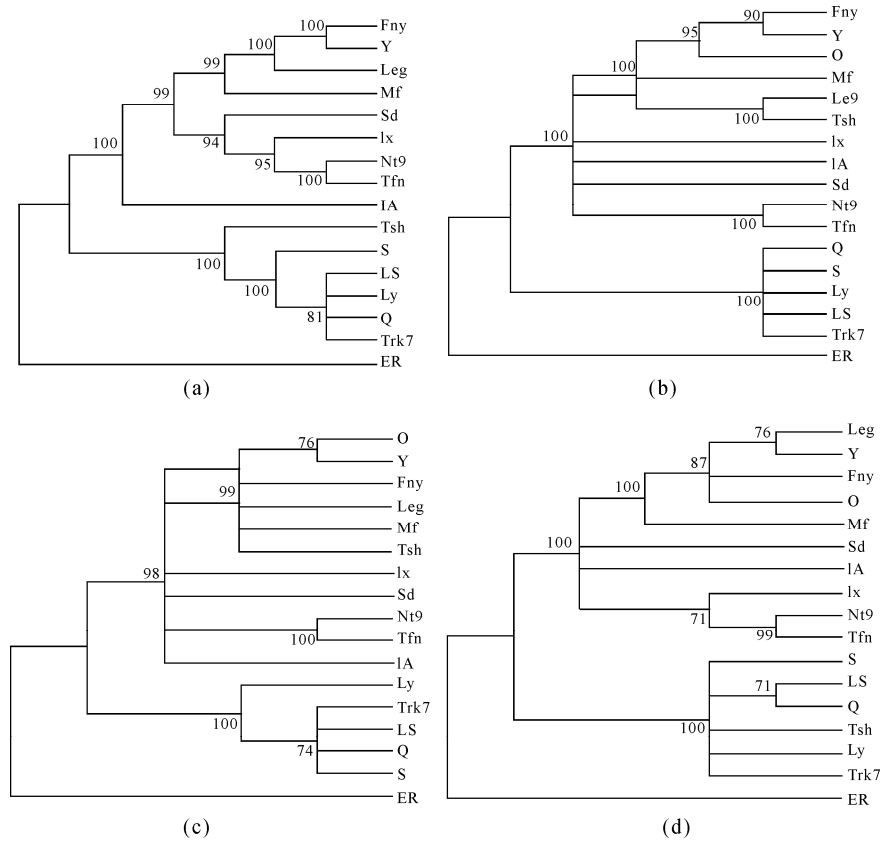
Using a restriction enzyme analysis, firstly described by Rizos et al. (see Chapter 2), RT-PCR products obtained from 15 field tomato samples collected across 2006–2008 in Shanghai has shown the same results of occurrence for

reassortant between CMV subgroups IA and II strains. It is thus judged that this new strain of CMV has become stable in certain tomato varieties in this area.

Table 1.3 Sequence comparisons of CMV-Tsh genomic RNAs and deduced amino acids sequences with those of subgroups I and II strains

RNAs	Identity of nucleotide sequence between CMV-Tsh and other CMV strains (%)			Identity of deduced amino acid sequences between CMV-Tsh and other CMV strains (%)		
	CMV-Fny ^a	CMV-Sd	Q strain	CMV-Fny	CMV-Sd	Q strain
1a	77.9	77.8	97.5	85.5	85.4	97.6
2a	96.1	91.2	72.4	97.1	92.9	72.7
2b	96.1	86.9	64.0	96.4	81.1	48.6
3a	78.9	78.9	98.5	83.9	83.6	98.7
CP	76.9	77.8	99.2	82.6	82.6	100
RNA1	76.9	76.6	97.5			
RNA2	96.0	90.4	71.2			
RNA3	74.0	74.3	98.3			

^a CMV-Fny, CMV-Sd and Q strains are used as representative for subgroups IA, IB and II respectively. The GenBank accession numbers are given in Fig. 1.7



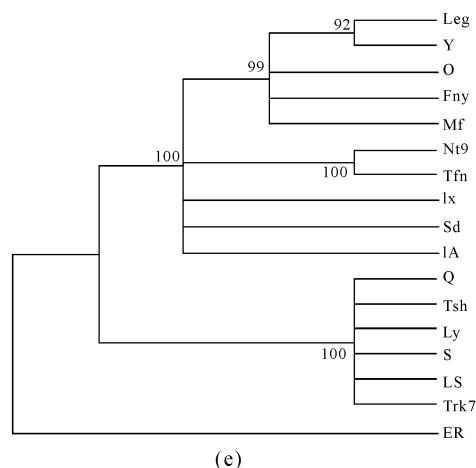


Fig. 1.7. Bootstrap majority rule consensus trees of the five ORFs of selected CMV strains ORFs are listed as (a) 1a; (b) 2a; (c) 2b; (d) 3a; (e) CP. Bootstrap percentage values are placed at major nodes. Fny, Leg, Mf, Y and O are subgroup IA strains; Nt9, Tfn, Ix, Sd and IA are subgroup IB strains; Q, Ly, S, LS and Trk7 are subgroup II strains. PSV ER strain is used as an outgroup. The GenBank accession numbers of nucleotide sequences used here are as follows: CMV-Fny (D00356, D00355, D10538); Leg (D16403, D16406, D16405); Mf (AJ276479, AJ276480, AJ276481); Y (D12537, D12538, D12499); O (*, D10209, D00385); Nt9 (D28778, D28779, D28780); Tfn (Y16924, Y16925, Y16926); Ix (U20220, U20218, U20219); Sd (AF071551, D86330, AB008777); IA (AB042292, AB042293, AB042294); Q (X02733, X00985, M21464); Ly (AF198101, AF198102, AF198103); S (Y10884, Y10885, U37227 and AF063610); LS (AF416899, AF416900, AF4127976); Trk7 (AJ007933, AJ007934, L15336); ER (U15728, U15729, U15730)

Reassortment has been proposed as an important mechanism in the evolution of the RNA virus with divided genomes. Reassortment would offset the fitness losses induced by deleterious mutations of nucleotides and recombination of viral genes (Henderson et al., 1995). CMV has been successful in adapting to different hosts and environments, leading to an extremely large host range and a worldwide distribution. Bonnet et al. (2005) analyzed the role of recombination and reassortment in the evolution of CMV with 159 filed Spanish CMV isolates collected from 1989 to 2002. According to their results, only 5% of isolates were reassortants between CMV subgroups. Amongst them, only one reassortant between CMV subgroups I and II was detected. This suggested that the occurrence of natural reassortants between strains of CMV subgroups IA and IB is more frequent than those between subgroups I and II. This phenomenon can be interpreted by the following reasons. First, CMV subgroup I strains have a higher incidence (Lin et al., 2003) and more rapid viral accumulation (Wang et al., 2002) compared with subgroup II strains. Thus, CMV subgroup I strains have competitive advantages in mixed infection. Second, the thermal optima of CMV subgroup I strains are much higher than those of subgroup II strains (Fraile et al., 1997). The resultant possibility of mixed infections between subgroups IA and IB is much higher than that between subgroups I and II. In

addition, the high nucleotide sequence divergence between CMV subgroups I and II strains is one of the important influencing factors that induce a low possibility of forming viable natural reassortants between subgroups I and II.

Although some studies have revealed that the reassortment between CMV subgroups is a rare event, it does not mean that reassortment is not important in CMV evolution. The phylogenetic analysis of 15 CMV strains have shown that reassortment had led to the high genetic diversity and evolutionary success of CMV (Roossinck, 2002). CMV-Tsh is found to be a natural reassortant between CMV subgroups IA and II strains. The sequence analysis and restriction enzyme analysis of CMV-Tsh genomic RNAs demonstrate that RNAs 1 and 3 of CMV-Tsh are derived from one or two subgroup II strain(s), while RNA2 is derived from a subgroup I strain. Furthermore, the restriction pattern of the CMV-Tsh-infected tomato plant is the same as the other five tomato plants sampled from the same planting area. It is suggested that the infection of CMV-Tsh occurred frequently in this planting area. It could be hypothesized that CMV-Tsh might be derived from a mixed infection by CMV subgroups IA and II strains, and it is likely that the subgroup II RNA2 has been washed out by the subgroup IA RNA2 because of its low efficiency in inhibiting host responses during the mixed infection of parental viruses of CMV-Tsh. In addition, a ToMV isolate and a CMV satRNA are found to co-exist with CMV-Tsh in the diseased tomato plants from Shanghai, China. Some studies have found that other plant viruses and CMV satRNAs may change the accumulation levels of different genomic RNAs of CMV in the co-infected plants (Palukaitis et al., 1992; Poolpol, 1986). Wang et al. found that Fny-CMV (subgroup IA strain) and LS-CMV (subgroup II strain) showed obviously different changes in accumulation profiles of viral RNAs, while each virus co-infected with *Zucchini yellow mosaic virus* (ZYMV) in zucchini squash and similar results are to be introduced in Chapter 3 in this book. It is also possible that ToMV and CMV satRNA co-infected with CMV-Tsh give different selection pressures on the genomic RNAs of parental strains of CMV-Tsh and bring on the occurrence of CMV-Tsh.

As a widely distributed plant virus with tripartite ssRNA genome, CMV is chosen as a good model virus for studying its mutation, detection, qualification and interaction with host plants.

1.3 The *Araceae* Strain of *Cucumber Mosaic Virus* Infecting *Pinellia ternate* Suggested to be a Novel Class Unit Under Subgroup I

As a kind of traditional Chinese medicinal plant, *Pinellia ternata* has been used for thousands of years. It has been cultivated since the end of the 1970s, and it is propagated mostly in a vegetative manner. This cultivated plant is found to be commonly infected by viral diseases which have been found recently with a new

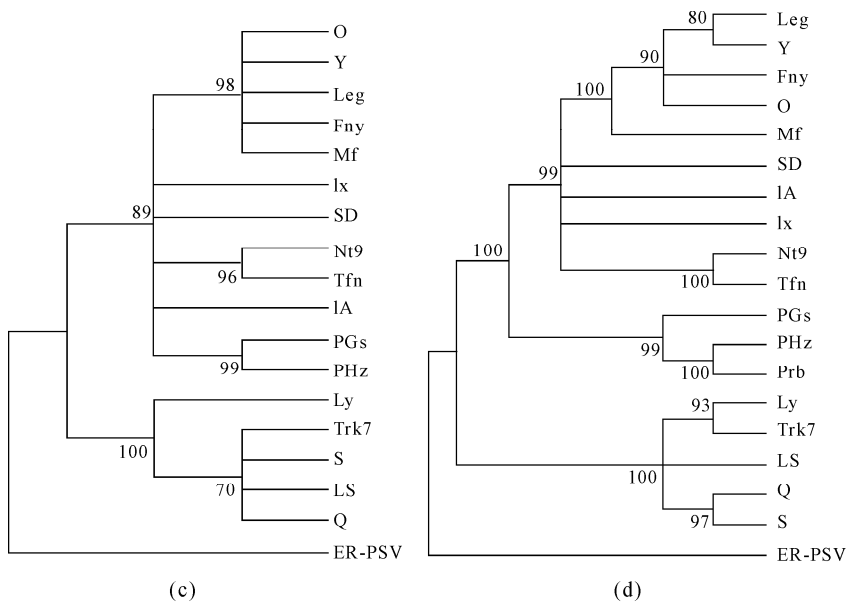
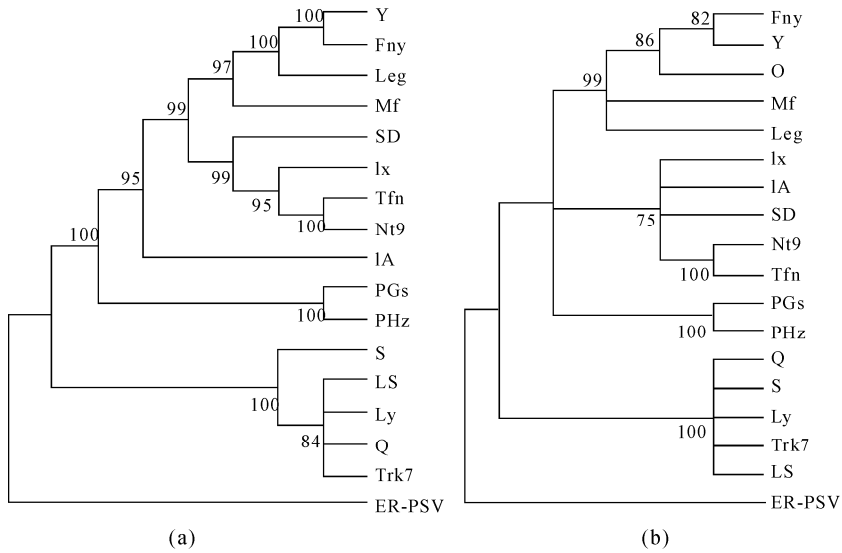
strain of *Cucumber mosaic virus* and a potyvirus. At the same time, the above viruses are seldom found in wild plants. Depending on dsRNA analysis and RT-PCR amplification, combined with full-length cDNA cloning by modified single-primer amplification technique (SPAT, see description in Chapter 6), full genomes of the newly discovered CMV strain are determined. Based on the serological and biological characteristics, the new strain of CMV limited to *Araceae* but not transported mechanically to *Solaniose* species is considered as subgroup IC strain. Two isolates, namely CMV-PHz isolated from *P. ternata* grown in Hangzhou, eastern China, and CMV-PGs isolated from *P. ternata* grown in Gansu Province, northwest China, are sequenced for genomic phylogenetic and sequence divergence analysis with known CMV strains. The two isolates were obtained during 2005-2008. Partial sequence of other isolates, CMV-PNb isolated from cultivated *P. ternata* grown in Ningbo, eastern China, in 2003 has also been obtained and compared. The accession numbers of full length sequences for CMV-PHz RNA1, RNA2 and RNA3 are EU723568, EU723570 and EU723569, respectively. The accession numbers of the full length sequences of CMV-PGs RNA1, RNA2 and RNA3 are DQ399548, DQ399549 and DQ399550, respectively. The sizes of genomic RNAs and positions for each ORF of consensus CMV I, consensus CMV II, CMV-PGs, PHz and CMV-PNb are shown in Table 1.4.

Table 1.4 Size of genomic RNAs and position of each ORF in the CMV (CMV I, CMV II, CMV-PGs, CMV-PHz and CMV-PNb)

	CMV I	CMV II	CMV-PGs	CMV-PHz	CMV-PNb
RNA1	3357—3365	3389—3391	3336	3346	
1a ORF	95—98 to 3076—3079	96—98 to 3073—3078	86—3067	95—3076	
RNA2	3036—3060	3038—3053	3037	3037	
2a ORF	78—79 to 2652—2673	93 to 2612—2615	76—2652	76—2652	
2b ORF	2414—2432 to 2746—2836	2409—2413 to 2712—2715	2411—2743	2411—2743	
RNA3	2213—2220	2197—2209	2179	2180	2179
3a ORF	120—123 to 959—973	96—97 to 935—936	98—937	96—935	96—935
CP ORF	1255—1263 to 1911—1918	1220—1232 to 1876—1888	1232—1888	1237—1893	1237—1893

Phylogenetic and sequence divergence analysis of 1a ORF: The products of 1a ORF have been found to be related for determining the host range of CMV strains. Phylogenetic analysis shows that CMV-PHz and CMV-PGs could be clustered into a single clade with 100% supporting values apart from other strains of subgroup I, with the rest forming their own clusters (Fig. 1.8(a)). The 1a gene of CMV-PHz and CMV-PGs shows 12.0%–13.2% and 11.2%–12.8% nucleotide divergence with subgroup IA strains, respectively. They have 13.2% to 14.1% and 13.3%–14.1% nucleotide divergence with subgroup IB strains respectively. In

addition, they are 26.2%–27.0% and 26.8%–27.5% divergent when they are compared pairwise with subgroup II strains (Table 1.5). The pairwise comparison results between subgroups of Ia divergence with remarkable difference are a/b/c models for both CMV-PHz and CMV-PGs according to subgroup II/IB/IA (Table 1.6).



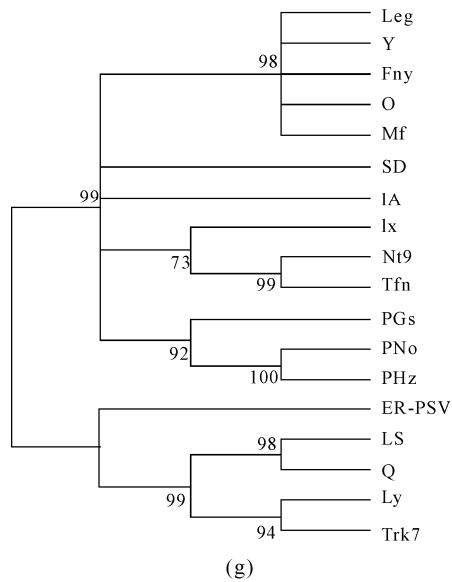
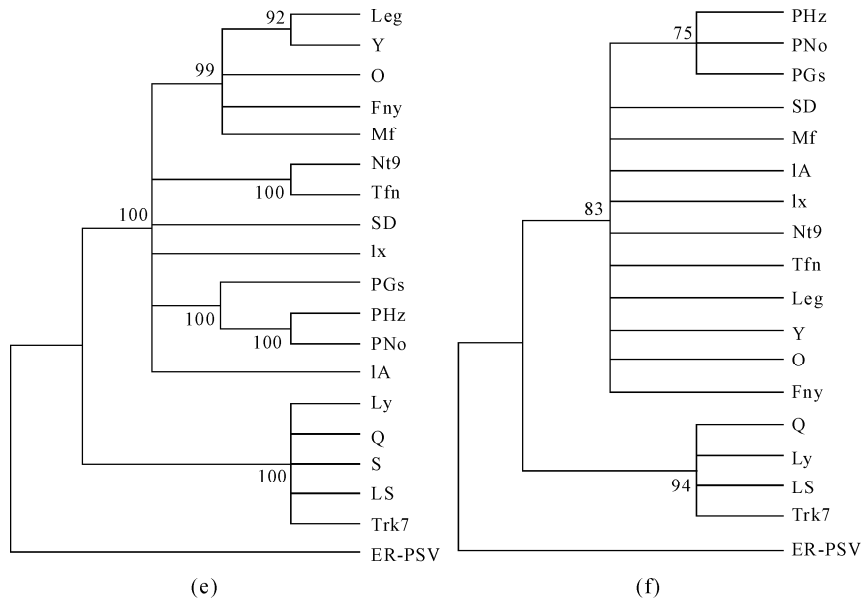


Fig. 1.8. Phylogenetic trees of nucleotide sequences of the five ORFs of isolates CMV-PGs and CMV-PHz and other CMV isolates as references (a) 1a; (b) 2a; (c) 2b; (d) 3a; (e) CP; (f): 5' UTR of RNA3; (g) 3' UTR of RNA3. The dendrograms were conducted by NJ with 1,000 bootstrap replications. Bootstrap scores exceeding 70% are placed at major nodes. ER-PSV was used as an outgroup. The GenBank accession numbers of referenced strains are listed in Table 1.4

Table 1.5 The sequence divergence between different CMV isolates and subgroups. The ORFs or 5' UTR or 3' UTR of RNA3 are compared using Kimura's 2-parameter model, with minimum and maximum percentage numbers of different cases as shown

RNA	PHz/ PGs	PHz/ PNb	PNb/ PGs	PHz/ IA	PHz/ IB	PHz/ II	PGs/ IA	PGs/ IB	PGs/ II
1a	5.7			12.0— 13.2	13.2— 14.1	26.2— 27.0	11.2— 12.8	13.3— 14.1	26.8— 27.5
2a	3.4			11.1— 11.7	12.7— 14.5	34.5— 35.0	11.2— 12.0	12.5— 14.1	33.5— 33.9
2b	5.1			21.8— 26.0	20.2— 24.1	55.3— 58.0	21.4— 28.5	19.2— 23	55.5— 58.2
3a	3.6	0.4	3.7	10.3— 11.6	9.5— 11.2	21.7— 22	10.6— 11.8	10.1— 11.3	22.6— 22.9
CP	3.9	0.3	4.2	8.1— 9.6	8.5— 10.8	29.1— 30.7	9.0— 9.8	7.8— 10.1	28.6— 30.2
5' UTR	1.4	0	1.4	4.2— 13.3	5.6— 7.1	49.8— 53.0	2.8— 11.7	4.2— 5.6	53.0— 56.5
3' UTR	9.8	0.4	9.3	14.8— 16.4	15.4— 20.2	36.5— 38.8	10.6— 12.1	12.1— 17	34.3— 36.4

Table 1.6 Comparison of the pairwise comparison results between different CMV isolates and subgroups. The ORFs or 5' UTR or 3' UTR of RNA3 with remarkable difference are compared

PHz	1a	2a	2b	3a	CP	5' UTR	3' UTR	PGs	1a	2a	2b	3a	CP	5' UTR	3' UTR
II	a	a	a	a	a	a	a	II	a	a	a	a	A	a	a
IB	b	b	b	b	b	b	b	IB	b	b	b	b	B	b	b
IA	c	c	b	b	b	b	c	IA	c	c	b	b	B	c	c

The phylogenetic and sequence divergence analysis of 2a and 2b ORFs: As partially involved in virus replication, 2a phylogeny analysis shows that CMV-PHz and CMV-PGs are grouped in a separate branch while IA and IB form their own clade within subgroup I, radically. Subgroup II forms a single group (Fig. 1.8(b)). The 2a gene of CMV-PHz and CMV-PGs has nucleotide divergence of 11.1% to 11.7% and 11.2% to 12.0% with subgroup IA, 12.7% to 14.5% and 12.5% to 14.1% with subgroup IB, 34.5% to 35.0% and 33.5% to 33.9% with subgroup II, respectively (Table 1.5). When CMV-PHz or CMV-PGs are pairwise compared with other subgroup strains, remarkable differences in the pairwise comparison between different subgroups are both a/b/c patterns, subgroup II, subgroup IB and subgroup IA, respectively. It is also shown in Table 1.6. As a newly discovered gene of CMV for determining symptom development, the 2b phylogeny analysis shows a radial pattern. They are clustered into a single clade within subgroup IB with high values (Fig. 1.8(c)). The 2b ORF shows the highest divergence with other subgroups. The nucleotide divergence for CMV-PHz and CMV-PGs sequences taken in pairs ranged from 21.8% to 26.0% and 21.4% to 28.5% with subgroup IA, 20.0% to 24.1% and 19.2% to 23.0% with subgroup IB, 55.3% to 58% and 55.5% to 58.2% with subgroup II, respectively. Remarkable difference models in both of them are a/b/b corresponding to subgroup II/IB/IA.

1.3.1 Phylogenetic and Sequence Divergence Analysis of 3a and CP ORFs

Phylogenetic analysis of 3a shows that more branches and compact trees within the groups, CMV-PHz, CMV-PGs and CMV-PNb (DQ512476) are clustered into a separate branch away from subgroup IA and IB (Fig. 1.8(d)). The 3a sequence divergence between CMV-PHz or CMV-PGs and other subgroups is found to range from 10.3% to 11.6% and 10.6% to 11.8% with subgroup IA, 9.5% to 11.2% and 10.1% to 11.3% with subgroup IB, 21.7% to 22% and 22.6% to 22.9% with subgroup II, respectively. Corresponding remarkable differences are both a/b/b patterns for subgroup II/IB/IA. As the most important determinant of the host range and symptom expression, the CP phylogeny analysis is quite similar to that of 3a, but absolutely different in the degree of the branch, and the three strains form a single clade within subgroup IB with high bootstrap scores (Fig. 1.8(e)). CP of CMV-PHz and CMV-PGs displays the degree of divergence from other subgroups: 8.1% to 9.6% and 9.0% to 9.8% with subgroup IA, 8.5% to 10.8% and 7.8% to 10.1% with subgroup IB, 29.1% to 30.7% and 28.6% to 30.2% with subgroup II, separately. The according remarkable difference patterns are both a/b/b models for subgroup II/IB/IA, as shown in Table 1.6.

1.3.2 Phylogenetic and Sequence Divergence Analysis of 5' UTR and 3' UTR, 2a and 2b ORFs of RNA3

In the tree of 5' UTR it is hard to distinguish subgroup IA from IB; they are congregated in a whole clade, and the three *Pinellia* isolates are a branch within the group (Fig. 1.8(f)). The pairwise nucleotide-sequence divergence of 5'UTR of CMV-PHz and CMV-PGs RNA3 ranged from 4.2% to 13.3% and 2.8% to 11.7% with subgroup IA, 5.6% to 7.1% and 4.2% to 5.65% with subgroup IB, 49.8% to 54.0% and 53.0% to 56.5% with subgroup II, respectively (Table 1.5). The remarkable difference of CMV-PHz is different from CMV-PGs; a/b/b is for CMV-PHz; a/b/c is for CMV-PGs (Table 1.6). From the structure of their RNA3, it is found that the positions of RNA3 ORFs of *Pinellia* isolates are different from other documented subgroup I strains with about 25 base regions deleted. The "shorter" 5' UTR structure is more similar to the position of subgroup II (Fig. 1.9). Thus, we consider the results for the alignment and regard the three *Pinellia* isolates as some intermediate between CMV subgroup I and subgroup II, since consensus sequences of IA, IB, II and RIB can be considered to be the closest ancestral 5' UTR (Roossinck et al., 1999). The alignment can be divided into 7 motifs (A, B, C, D1, D2, E and F) as in (Roossinck et al., 1999). In their reports, boxes A and F are conserved in all strains, and are also found from CMV-PHz, CMV-PNb and CMV-PGs. Boxes B, C and E are found to vary in different subgroups, the motifs analysis supported the same conclusion, with CMV-PHz, CMV-PNb and CMV-PGs containing boxes B and C, but imperfect E. Only box D1 was found in CMV-PHz, CMV-PNb and CMV-PGs. However, box D is a fore-and-aft repeat in subgroups I, D1 and D2, respectively. Besides, CMV-PGs

are two nucleotides more than CMV-PNb and CMV-PGs. Phylogenetic analysis of 3'UTR shows that subgroup IA is clustered as a clade with 99% bootstrap values, with others clustered together. CMV-PHz, CMV-PGs and CMV-PNb are found to form a single branch with high bootstraps (Fig. 1.8(g)). The sequence divergence of 3' UTR of CMV-PHz and CMV-PGs RNA3 are 14.8% to 16.4% and 10.6% to 12.1% with subgroup IA, 15.4% to 20.2% and 12.1% to 17.0% with subgroup IB, 36.5% to 38.8% and 34.3% to 36.4% with subgroup II, separately. The remarkable difference patterns in both CMV-PHz and CMV-PGs are a/b/c according to subgroup II/IB/IA.

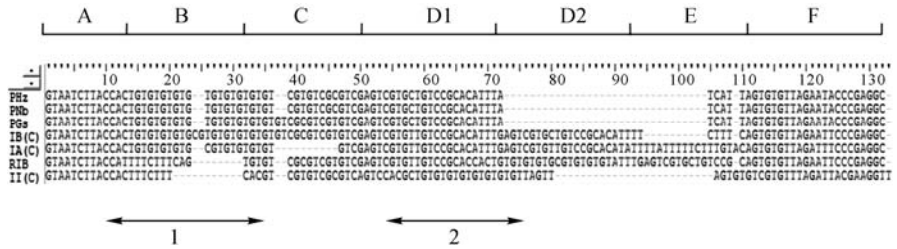


Fig. 1.9. Alignment of 5' UTR of CMV-PHz and CMV-PGs and CMV-PNb, consensus IA (C IA), IB (C IB), II (C II) and RIB strains. The whole 5' UTRs are divided into 7 boxes (A, B, C, D1, D2, E and F). 1 and 2 are considered as two fragments which RIB deleted and rearranged to form other strains

The phylogenetic results only showed that they are clustered into subgroup I. It is difficult to distinguish them from subgroup IA and subgroup IB. It has been concluded that subgroup IA strains may radiate from subgroup IB strains (Roossinck, 2002; Roossinck et al., 1999). The *Araceae* strain of CMV is found to be clustered into a single branch with high bootstrap support, and the phylogenetic analysis revealed that their 1a, 2a and 3a are not raised from previous subgroup IB strains, but are closer to the subgroup II ancestor. It seemed that they have evolved in a different way to form their own branches. 2b, CP and UTRs are clustered together with others; However, they are found to have formed a branch of their own with high divergence within subgroup I. It looks as if 1a, 2a and 3a have less select stress than 2b, CP and UTRs. It might be due to the fact that they are constrained by virus-host interactions or the environment, especially the vertical propagation of the *Araceae* plant, such as *Pinellia* spp. The new strain of CMV should have been developed with fitness to a new host plant, and more new isolates from the *Araceae* family are expected to provide a clearer reason of its origination.

It should be mentioned that quite a lot of CMV isolates, either from subgroups IA, IB or subgroup II have been used to inoculate *P. ternata*, but none of them have been found to successfully infect this plant, and the new strain of CMV has been found to infect none of the *Solanaceae* species by mechanical inoculation.

In conclusion, the CMV strain infecting *Pinellia* spp. and other possible species from the *Araceae* family have been suggested as being from subgroup ID, since other strains have been suggested as being from CMV subgroup IC.

1.4 The Potyvirus Infecting *Pinellia ternata* is a Recombinant Contributed by *Soybean Mosaic Virus* and *Lettuce Mosaic Virus*

Dasheen mosaic virus (DsMV) and other potyviruses are found to commonly occur in *Araceae* plants, which are used as ornamental, medicinal and food crops worldwide. China is one of the centers for the origination of *Araceae* plants. The spread of DsMV has been repeatedly reported in this area. A typical mosaic disease has been found to occur frequently in cultivated *P. ternata*, but unlike the *Araceae* strain of CMV, the potyvirus could be readily transmitted to new seedlings. Serological tests show that this virus has a positive reaction serologically with antibodies of *Soybean mosaic virus* (SMV) but also with potato virus Y and DsMV. Sequence analysis of this potyvirus has revealed that its major portion contains the sequence of SMV and its minor part of it is complementary to *Watermelon mosaic virus* (WMV).

During the years 2003–2006, 29 *Pinellia ternata* specimens were collected from representative areas in China, including the major producing provinces of Zhejiang, Henan, Shanxi, Hunan, Shandong and Hubei. Seven isolates are related to the SMV, which could be pathogenic *P. ternata* as well as some soybean [*Glycine max* (L.) Merr.]. Cultivars are detected by using RT-PCR amplification performed with degenerate primer of potyvirus and serological experiment. This also revealed that the common potyvirus infecting *P. ternata* is, indeed, SMV rather than DsMV as previously reported. Further molecular phylogenetic analysis and comparison of all the CP genes of these SMV isolates from *P. ternata* and some SMV isolates from *G. max*, along with other potyvirus members, such as DsMV and WMV, reconstructed the evolutionary routine on both nucleotide and amino acid levels. Similarity and homology of nucleotide sequences for SMV CP genes show high apparent host correlativity and partially unapparent geographic correlation, while alignment and comparison of amino acid sequences show that the host correlativity is more notable than the geographic correlation. The highly variational region (N-terminal) within CP genes of SMV isolates from *P. ternata* is, on the one hand, due to recombination of SMV from *G. max* and WMV and, on the other hand, obviously the results of evolutionary selection pressure. The amino acid sequence of the conserved region within CP determines the main function, which shows high similarity or little diversity between species. This study has primarily displayed the evolutionary strategies, especially rapid variation and recombination, through which SMV, as a (+) ssRNA virus, adapted itself naturally to quite different hosts.

The pinellia strain of SMV is thus named to describe the population of such a novel viral strain for its adaptation to hosts from a new plant family.

1.4.1 DAS-ELISA Analysis of Field Samples for Detecting the Potyvirus

Plants of *P. ternata* are found to be susceptible to SMV either by natural infection or by artificial inoculation. The results from a disease survey are shown in Table 1.7 and Table 1.8. Fourteen out of twenty-nine *P. ternata* samples with mosaic and distortion symptoms observed from field plants collected from Zhejiang, Henan, Shanxi, Hunan, Shandong and Hubei provinces were found to be both SMV, PVY and DsMV positive using DAS-ELISA with specific antibodies. From this routine serological detection, the infected rate is found to be 48.2% from those symptomized samples with mosaic and distortion, and the serological cross-reaction between SMV and DsMV has also been observed.

Table 1.7 Isolates of related potyviruses used for phylogenetic analysis

Virus*	Strain/ Isolate	Site	Specific host	Genbank accession	Annotation
DsMV	M13	Zhejiang, China	<i>Zantedeschia aethiopica</i>	NC_003537	Chen J. et al., 30/03/2006 Complete Genome
DsMV	SY1	Jiangsu, China	<i>Pinellia ternata</i>	AJ628756	Shi Y.H. et al., 15/04/2005 Partial Genome (Nib, CP)
DsMV	TW	Utsunomiya, Japan	<i>Colocasia esculenta</i>	AJ298036	Chen J. et al., 30/03/2006 Partial Genome (NIb, CP)
DsMV	DK	Utsunomiya, Japan	<i>Colocasia esculenta</i>	AJ298035	Chen J. et al., 02/10/2001 Partial Genome (Nib, CP)
DsMV	ND	Zhejiang, China	<i>Zantedeschia aethiopica</i>	AJ298034	Chen J. et al., 02/10/2001 Partial Genome (NIb, CP)
DsMV	Caladium	Florida, USA	<i>Caladium hortulanum</i>	AF048981	Li R.H. et al., 12/03/1998 Partial Genome (NIa, NIB, CP)
SMV	G2	Illinois, USA	<i>Glycine max</i> (L.) Merr.	S42280	Jayaram C. et al., 05/08/1999 Complete Genome
SMV	G3	Illinois, USA	<i>Glycine max</i> (L.) Merr.	AH008452	Latorre I.J. et al., 30/11/1999 Partial Genome (HC-Pro, P1, CP)
SMV	G5	Illinois, USA	<i>Glycine max</i> (L.) Merr.	AH008453	Latorre I.J. et al., 30/11/1999 Partial Genome (HC-Pro, P1, CP)
SMV	G6	Illinois, USA	<i>Glycine max</i> (L.) Merr.	AH008454	Latorre I.J. et al., 30/11/1999 Partial Genome (HC-Pro, P1, CP)
SMV	G7	Illinois, USA	<i>Glycine max</i> (L.) Merr.	AF241739	Latorre I.J. et al., 30/11/1999 Partial Genome (HC-Pro, P1, CP)
SMV	G7a	Illinois, USA	<i>Glycine max</i> (L.) Merr.	AH008455	Latorre I.J. et al., 30/11/1999 Partial Genome (HC-Pro, P1, CP)
SMV	G7F	Illinois, USA	<i>Glycine max</i> (L.) Merr.	AH008456	Latorre I.J. et al., 30/11/1999 Partial Genome (HC-Pro, P1, CP)
SMV	ChGs1	Gansu, China	<i>Glycine max</i> (L.) Merr.	AH008404	Latorre I.J. et al., 18/11/1999 Partial Genome (HC-Pro, P1, CP)

(To be continued)

(Table 1.7)

Virus*	Strain/ Isolate	Site	Specific host	Genbank accession	Annotation
SMV	ChGs2	Gansu, China	<i>Glycine max</i> (L.) Merr.	AH008402	Latorre I.J. et al., 18/11/1999 Partial Genome (HC-Pro, P1, CP)
SMV	ChGs3	Gansu, China	<i>Glycine max</i> (L.) Merr.	AH008447	Latorre I.J. et al., 30/11/1999 Partial Genome (HC-Pro, P1, CP)
SMV	ChH1	Hebei, China	<i>Glycine max</i> (L.) Merr.	AH008448	Latorre I.J. et al., 30/11/1999 Partial Genome (HC-Pro, P1, CP)
SMV	ChH2	Hebei, China	<i>Glycine max</i> (L.) Merr.	AH008403	Latorre I.J. et al., 18/11/1999 Partial Genome (HC-Pro, P1, CP)
SMV	ChJ	Jiangsu, China	<i>Glycine max</i> (L.) Merr.	AH008449	Latorre I.J. et al., 30/11/1999 Partial Genome (HC-Pro, CP)
SMV	ChS1	Shanxi, China	<i>Glycine max</i> (L.) Merr.	AH008450	Latorre I.J. et al., 30/11/1999 Partial Genome (HC-Pro, P1, CP)
SMV	IL1	Illinois, USA	<i>Glycine max</i> (L.) Merr.	AH008458	Latorre I.J. et al., 30/11/1999 Partial Genome (HC-Pro, P1, CP)
SMV	413/IL2	Illinois, USA	<i>Glycine max</i> (L.) Merr.	AH012606	Domier L.L. et al., 12/03/2003 Partial Genome (HC-Pro, CP)
SMV	452/IL3	Illinois, USA	<i>Glycine max</i> (L.) Merr.	AH012607	Domier L.L. et al. 12/ 03/ 2003 Partial Genome (HC-Pro, CP)
SMV	1071/IL4	Illinois, USA	<i>Glycine max</i> (L.) Merr.	AH012604	Domier L.L. et al., 12/03/2003 Partial Genome (HC-Pro, CP)
SMV	1083/IL5	Illinois, USA	<i>Glycine max</i> (L.) Merr.	AH012605	Domier L.L. et al., 12/03/2003 Partial Genome (HC-Pro, CP)
SMV	VA1	Virginia, USA	<i>Glycine max</i> (L.) Merr.	AH008457	Latorre I.J. et al., 30/11/1999 Partial Genome (HC-Pro, P1, CP)
SMV	VA2	Virginia, USA	<i>Glycine max</i> (L.) Merr.	AH008459	Latorre I.J. et al., 30/11/1999 Partial Genome (HC-Pro, P1, CP)
SMV	A2/To	Tottori, Japan	<i>Glycine max</i> (L.) Merr.	AB181492	Saruta M. et al., 06/01/2005 Partial Genome (CP)
SMV	D/Ok	Okayama, Japan	<i>Glycine max</i> (L.) Merr.	AB181493	Saruta M. et al., 06/01/2005 Partial Genome (CP)
SMV	CN3	Daejeon, R.O. Korea	<i>Glycine max</i> (L.) Merr.	AJ609298	Choi B.K. et al., 30/11/2003 Partial Genome (CP)
SMV	BZ	Beizhang, China	Henan, <i>Pinellia ternata</i>	DQ360817	ShenTu S. et al., 07/02/2006 Partial Genome (NIb, CP)
SMV	HN2	Henan, China	<i>Pinellia ternata</i>	DQ360818	ShenTu S. et al., 07/02/2006 Partial Genome (NIb, CP)
SMV	JZX	Lizhou, China	Henan, <i>Pinellia ternata</i>	DQ360819	ShenTu S. et al., 07/02/2006 Partial Genome (NIb, CP)
SMV	LB	Liangbei, China	Henan, <i>Pinellia ternata</i>	DQ360820	ShenTu S. et al., 07/02/2006 Partial Genome (NIb, CP)
SMV	SX	Shanxi, China	<i>Pinellia ternata</i>	DQ360821	ShenTu S. et al., 07/02/2006 Partial Genome (NIb, CP)
SMV	XY	Xiangyang, China	Hubei, <i>Pinellia ternata</i>	DQ360822	ShenTu S. et al., 07/02/2006 Partial Genome (NIb, CP)

(To be continued)

(Table 1.7)

Virus*	Strain/ Isolate	Site	Specific host	Genbank accession	Annotation
SMV	YW	Yangwang, China	Shanxi, <i>Pinellia ternata</i>	DQ360823	ShenTu S. et al., 07/02/2006 Partial Genome (NIb, CP)
SMV	YZ	Yuzhou, China	Henan, <i>Pinellia ternata</i>	AJ628755	Shi Y.H. et al., 15/04/2005 Partial Genome (NIb, CP)
SMV	WH1	Wuhan, China	Hubei, <i>Pinellia ternata</i>	AJ628753	Shi Y.H. et al., 15/04/2005 Partial Genome (NIb, CP)
SMV	WH2	Wuhan, China	Hubei, <i>Pinellia ternata</i>	AJ628754	Shi Y.H. et al., 15/04/2005 Partial Genome (NIb, CP)
SMV	P/SY1	Sheyang, China	Jiangsu, <i>Pinellia ternata</i>	AJ628752	Shi Y.H. et al., 15/04/2005 Partial Genome (NIb, CP)
WMV	Pak	Frontier, Pakistan	<i>Trichsanthes anguina</i>	AB127934	Ali A. et al., 03/12/2004 Partial Genome (NIb, CP)
WMV	Habenari a	Japan	<i>Habenaria radiata</i>	AB001994	Gara I.W. et al., 13/02/1999 Partial Genome (CP)
WMV	Israel	Israel	<i>Cucurbit</i>	AF322376	Wang Y. et al., 28/12/2000 Partial Genome (CP)
WMV	WMV-Fr	France	<i>Zucchini squash</i>	NC_006262	Desbiez C. et al., 02/06/2006 Complete Genome

*DsMV: *Dasheen mosaic virus*; SMV: *Soybean mosaic virus*; WMV: *Watermelon mosaic virus*

Table 1.8 Disease observation on cultivated *P. ternata* from different areas in China

Source	Total numbers	Symptoms ^a					Pathologic index
		N	miM	M or CoM	seM or Cr	Stu or D	
Ningbo (Zhejiang)	35	3	12	15	5	0	54.29
Hangzhou (Zhejiang)	65	24	10	15	16	5	41.54
Hebei	23	1	6	7	9	1	55.43
Beijing	14	3	6	3	2	0	42.86
Anhui	18	0	16	2	0	1	33.33
Sichuan	47	39	8	0	0	0	17.02

^a N: no symptom; miM: mild mosaic; M: mosaic; CoM: common mosaic; Cr: crinkle; seM: severe mosaic; Stu: stunt; D: distortion

1.4.2 Sequencing and Nucleotide Sequence Analysis of the Potyvirus Infecting *Pinellia*

The nucleotide sequences of partial *NIb* gene, complete *CP* gene and 3' UTR within SMV genome are determined with products of RT-PCR using potyvirus specific primers. The *CP* genes of all seven isolates from *P. ternata* are found to be quite similar to those of SMV, with identical length of 846 nt, which could determine 282 amino acids and the size of 3' UTR is 251–252 nt (excluding Poly (A) tail). Sequence information for these seven SMV isolates has been submitted to GenBank with accession numbers from DQ360817 to DQ360823. The identity of SMV *CP* nucleotide sequences from 35 isolates tested is found to be 75.4%–99.5% (\bar{a} = 86.9%) and the procedure of the sequence alignment contains

952 informative characters consisting of 421 successive, 96 non-parsimony informative and 435 parsimony informative characters. The identity of SMV CP nucleotide sequences amongst 24 soybean isolates is 89.6%–99.5% ($\bar{a} = 93.8\%$) and the identity of SMV CP nucleotide sequences amongst eleven *P. ternata* isolates is 91.3%–99.2% ($\bar{a} = 93.4\%$). The tree files consisting of the un-weighted pair group method with neighbor-joining (NJ) tree are tested using K-H tests with the minimum tree length (Fig. 1.10).

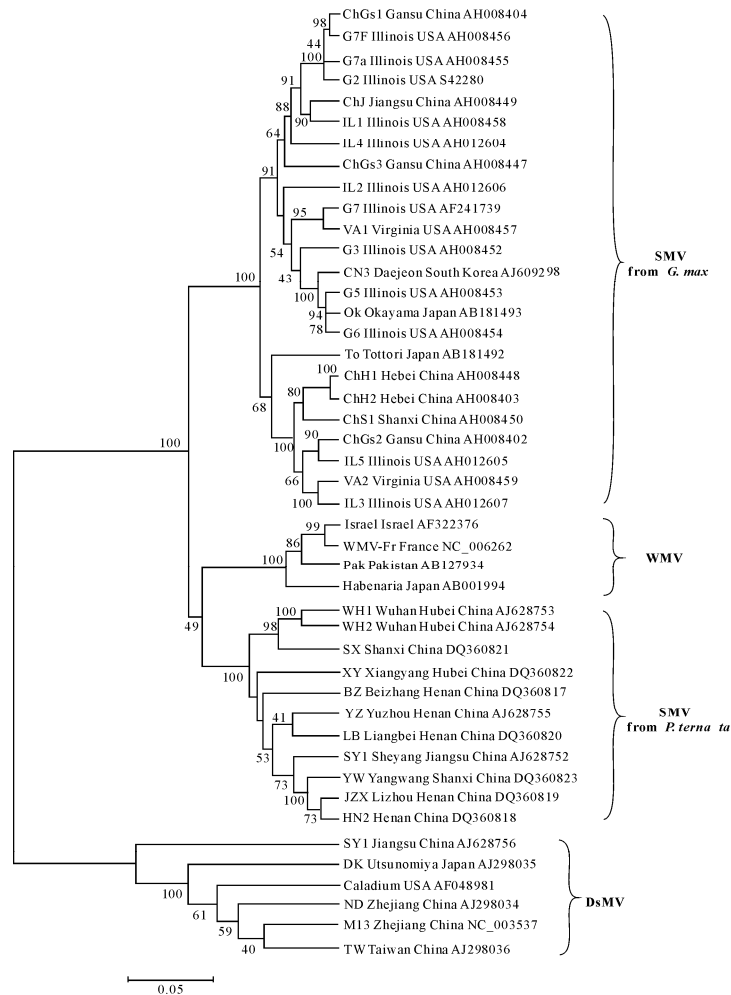


Fig. 1.10. Neighbor-joining (NJ) tree resulting from nucleotide sequences of potyviruses CP gene isolates and strains of different origins are compared. The numbers at each major node indicate the bootstrapping values (shown only when >40%) out of 100 replicates occurring. RefSeq accession number and abbreviation for the organism, respectively, are shown at each relevant branch. The scale bar shows the number of character substitutions per base to indicate the total nucleotide diversity among taxa

WMV isolates and SMV isolates from *P. ternata* are found to form an unreliable clade clustering 49 out of 100 times. The relationship between any two and the other among these three clades cannot be definitely distinguished. Phylogenetic analysis suggests discrete distribution and separation of *G. max* isolates from China, USA, R.O. Korea and Japan. Although the high sequence identity of five SMV *P. ternata* isolates JZX, LB, BZ, HN2, YZ was 92%–98.7% ($\bar{a} = 93.7\%$), there is no grouping direction according to the result of phylogenetic tree analysis, but the *P. ternata* isolates HN2 and JZX from Henan and YW from Shanxi present reliable subclades because of the close geographic location.

1.4.3 Amino Acid Sequence Analysis for CP of the Potyvirus Infecting *Pinellia*

The sequence identity of the potyvirus CP amino acids from 35 isolates is found to be higher than that of the nucleotides (>80%, $\bar{a} = 90.96\%$), and the procedure of the sequence alignment contains 319 informative characters consisting of 177 successive, 34 non-parsimony informative and 108 parsimony informative characters. The significance of SMV-host correlation is indicated by the phylogenetic tree and three reliable evolution clades are formed by WMV isolates and SMV isolates infecting soybean and *P. ternata* respectively with bootstrap value of 100. These three evolution clades are clustered into one reliable major clade with 100% bootstrapping support. The genetic diversity (horizontal scale indicated) and subclades is less than the nucleotides tree under SMV from soybean clade, which indicates that SMV-habitat correlation on the same host is less notable than SMV-host correlation. There is high correlation between amino acid sequences of SMV CP and its host, and on the same host there is habitat correlation between amino acid sequences of SMV CP and its habitat source. The sequence identity of SMV CP amino acids amongst 24 soybean isolates is 95.5%–100% ($\bar{a} = 98.4\%$) and the sequence identity of SMV CP amino acids amongst eleven *P. ternata* isolates is 94.3%–100% ($\bar{a} = 96.25\%$). It is obvious that the sequence identity of SMV CP amino acids from *P. ternata* isolates is lower than that from *G. max* according to the comparison of the scale. The sequence identity of the between isolates infecting *G. max* and *P. ternata* is 79.8%–83.0% ($\bar{a} = 83.1\%$). The tree files consisting of the maximum parsimony (MP) tree are tested using K-H tests with the minimal tree length (Fig. 1.11).

Through phylogenetic tree analysis, three reliable evolution clades are formed by WMV isolates and SMV isolates from *G. max* and *P. ternata*. WMV isolates and SMV isolates from *P. ternata* form an unreliable clade clustering 42 out of 100 times. The relationship between any two and the other one among these three clades could not be definitely distinguished either. This result accords with the nucleotide tree. The evolution clade of *G. max* isolates is constrictive and most of their subclades are unreliable (<50% bootstrapping support). The differences of

character substitution rates (horizontal distance) in the amino acid tree are greater than in their nucleotide tree, especially for the clade of the SMV isolates from *G. max*. Furthermore, the number of reliable subclades within the clade of the SMV isolates from *G. max* in the amino acid phylogenetic tree has also been noticeably reduced. The natural selection pressure in the genome and its functional evolution studies are reflected by the differences at the nucleotide level. Due to the principle of codon degeneracy, these are reduced at the amino acid residue level (Gojobori et al., 1990).

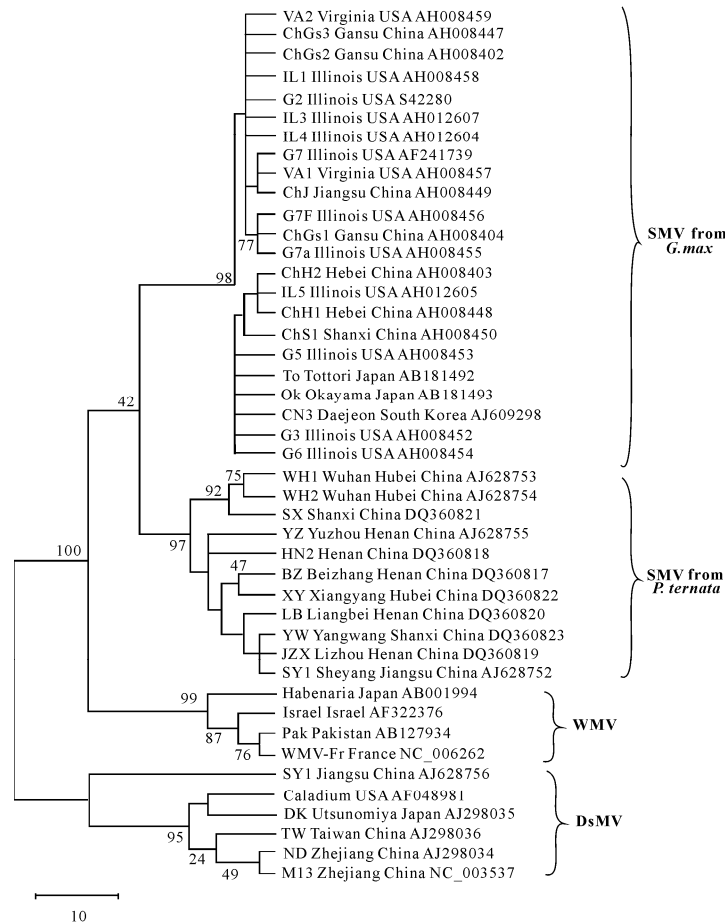


Fig. 1.11. Maximum parsimony (MP) trees resulting from CP aa sequences encoded of related potyviruses of different origin. The numbers at each fork node indicate the bootstrapping values (shown only when >40%). RefSeq accession number and abbreviation for the organism, respectively, are shown at each relevant branch. The scale bar indicates the number of character substitutions

The sequence identities of SMV CP amino acids from six soybean isolates obtained from China are 97.4%–99.6% ($\bar{a} = 98.7\%$), and the identities from fifteen

US and two Japanese soybean isolates are 97.4%–100% ($\bar{a} = 98.8\%$) and 96.6% respectively. In the sequence comparison of the V2 isolate from Virginia compared with other US isolates, the sequence identities for the isolates of G2, G3, G5, G6, G7a and G7F from Illinois are lower (91.9%–94.0%) than those for two other Illinois isolates IL2 and IL3 (99.7%–98.7%). The sequence identity amongst the five SMV isolates BZ, HN2, JZX, YZ and LB from Henan, China, is 92.0%–98.7% ($\bar{a} = 93.7\%$), while the sequence identity of the LB isolate from Henan with the YW isolate from Shanxi is 99.6%, which is obviously higher than the other four isolates from Henan. The *P. ternata* isolates from China are found to form two subclades, of which the WH1 and WH2 isolates from Hubei and the isolate from Shanxi presented a reliable subclade. This result is coincident with the result of the phylogenetic tree analysis for CP nucleotides.

1.4.4 Nucleotide Sequence Analysis for CP N-terminal of the Potyvirus Infecting *Pinellia*

Based on the results of the amino acid sequence alignment with the 35 SMV isolates, the structure of the CP amino acid sequence can be divided into three domains, namely, CP core domain, C-terminal conserved domain and N-terminal highly variable domain with approximately 41–60 amino acids, respectively. The most variations always occurred in the highly variable domain within interspecies or interstrains, while a few nucleotide variations always occurred in the CP core domain, only with the presence of molecular clock variations such as transition, transversion or site missing. Therefore, further nucleotide level analysis for molecular variations of the N-terminal highly variable domain is undertaken in order to find out the variation mechanism of the SMV CP gene as well as the relationship between the variation and the host. Of the 35 SMV isolates whose sequence identity of the CP N-terminal nucleotides is found to be 38.5%–100% ($\bar{a} = 70.5\%$), 24 are from *G. max* with the sequence identity 82.9%–100% ($\bar{a} = 92.6\%$) and 11 are from *P. ternata* with the sequence identity 86.8%–94.3% ($\bar{a} = 91.1\%$). In this region, however, the nucleotide sequence homology between isolates from *G. max* and from *P. ternata* is only 38.5%–45.4% ($\bar{a} = 43.1\%$) and great diversity exists in the length of their nucleotides. According to the alignment result by both CLUSTAL W and BLASTN, the CP N-terminal highly variable region of SMV isolates from *P. ternata* is very close to that of WMV for homology as well as the length of nucleotide sequences. In detail, the potyvirus, mostly SMV, infecting *Pinellia* has some 47 nt coming from WMV in this area. Moreover, there are variations with equal transition or transversion found in the highly variable region of SMV and WMV by nucleotide sequence alignment (Fig. 1.12). This suggested they became relatively stable genotypes in the natural selection process of host adaptability evolution, and the potyvirus infecting *Pinellia* is considered as an SMV strain with a fragment of the genome obtained from WMV to fit the new host.

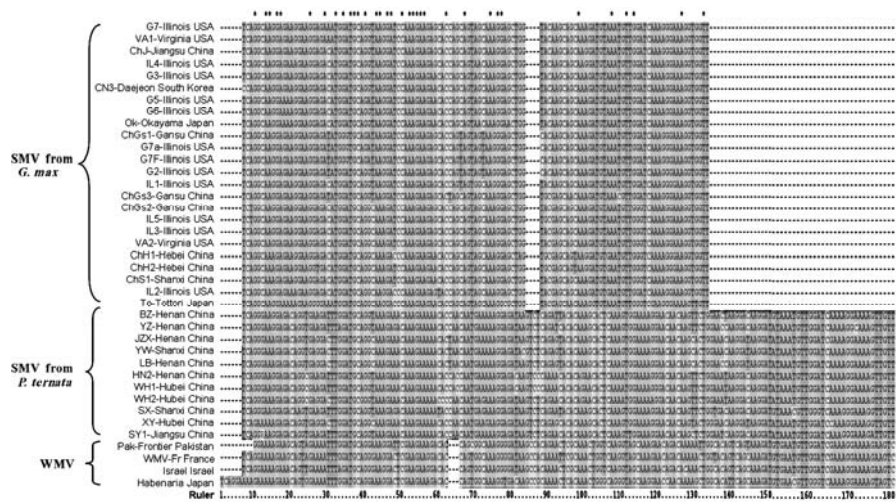


Fig. 1.12. Alignment of nucleotide sequences in the CP N-terminal region

1.4.5 Amino Acid Sequences for N-terminal and for the Conserved Region of the Potyvirus Infecting *Pinellia*

Of the 35 SMV isolates whose sequence identity of the CP N-terminal amino acids is 30%–100% ($\bar{a} = 63.5\%$), 24 are from *G. max* with the sequence identity 81.2%–100% ($\bar{a} = 92.5\%$) and 11 are from *P. ternata* with the sequence identity 82.0%–100% ($\bar{a} = 90.2\%$). In contrast, the CP N-terminal amino acid sequence identity of the isolates between *G. max* and *P. ternata* is 30.0%–42.9% ($\bar{a} = 37.5\%$). As a result of the great diversity within the highly variable region at amino acid level between both of the *G. max* and *P. ternata* isolates, they are divided into two reliable clades which are obviously distinct from each other in the phylogenetic tree. Little variation is found in the CP amino acid conserved region including C-terminal and core region of CP. The identity of 35 SMV isolates is 89.3%–100% ($\bar{a} = 95.4\%$), and there are 47 pairs of combinations with an identity of 100%. The sequence identity of the SMV CP amino acid conserved region from *G. max* isolates is 96.2%–100% ($\bar{a} = 99.1\%$) and that from *P. ternata* isolates is 95.7%–100% ($\bar{a} = 97.4\%$). The sequence identity of the isolates between *G. max* and *P. ternata* is 89.3%–96.3% ($\bar{a} = 92\%$). The homology between WMV and SMV *P. ternata* isolates is 88.8%–90.6% and it is 90.9% between WMV and SMV *G. max* isolates. Therefore, these results indicate that there is little variation in the CP amino acid conserved region of WMV and SMV. The procedure of the amino acid sequence alignment for the CP conserved region contains 224 informative characters consisting of 146 successive, 24 non-parsimony informative and 54 parsimony informative characters. There is obvious distinction between WMV and SMV in the phylogenetic tree at amino acid level and SMV from *G. max* and *P.*

ternata isolates could form two reliable evolution clades in the phylogenetic tree with bootstrapping supports of 93% and 97% respectively (Fig. 1.13). This indicates that SMV CP has, at the amino acid level, obvious distinctions from different hosts. The tree topology of the nucleotide sequence phylogenetic tree is similar to its amino acid sequence phylogenetic tree, but there are more reliable subclades under the clade of SMV isolates from *G. max*, which are indicated by high bootstrap values and horizontal distance. It is difficult to definitely distinguish the CP amino acid conserved region of WMV and SMV from the two host plants for the clustering forms by SMV isolates from *G. max* and *P. ternata* fail to obtain the required high bootstrapping support.

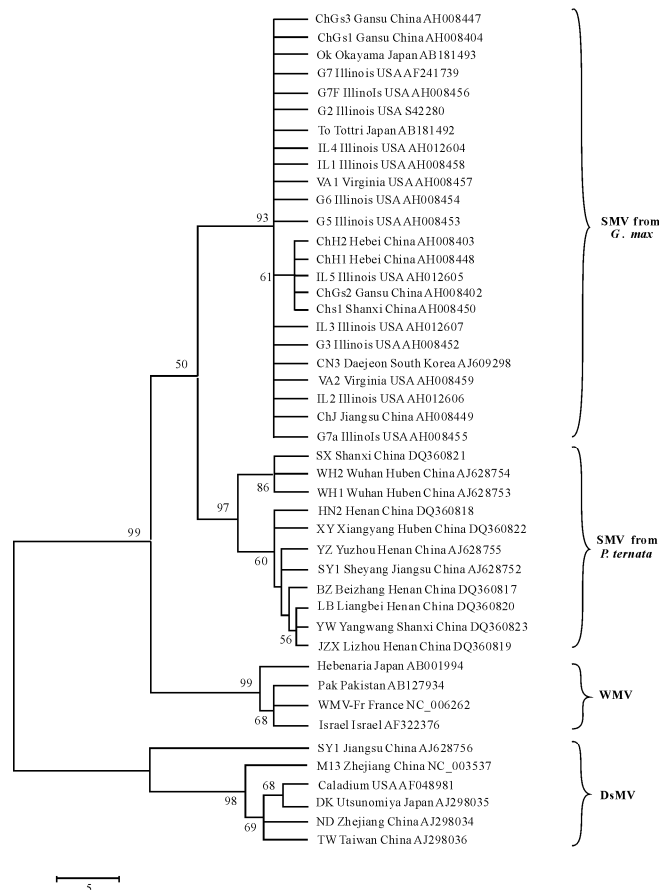


Fig. 1.13. Maximum parsimony (MP) trees resulting from CP core region aa sequences of related potyviruses of different origin

The numbers at each fork node indicate the bootstrapping values (shown only when >50%). RefSeq accession number and abbreviation for the organism respectively are indicated at each relevant branch. The scale bar indicates the number of character substitutions

Through habitat correlation analysis, of the 19 SMV isolates from USA soybeans whose CP conserved region amino acid sequence identity is 97.9%–100% ($\bar{a} = 99.4\%$), 7 have high identities of up to 100%. This indicates that this region is highly conserved. The sequence identity of these 7 sequences with ChJ isolate from Jiangsu, China and Ok isolate from Japan is also 100%. Of the 7 SMV *P. ternata* isolates in China (DQ360817–DQ360823) whose sequence identity of the CP conserved region amino acids is 98.3%–100% ($\bar{a} = 99.4\%$), three are from Hebei, Shanxi and Gansu with an identity of 100 % and two are from Gansu with an identity of 98.1%. In the SMV *P. ternata* isolates, the identities of the WH1 and WH2 isolates from Hubei is 100%, but there is not high identity corresponding with other SMV isolates from the same site. Although the identity of five SMV *P. ternata* isolates from Henan is 97%, only JZX and LB isolates are in the same group and others are discretely distributed and separated in the phylogenetic tree. Thus, the habitat correlation of SMV is not strong and this result is consistent with previous trees for the complete sequences of CP nucleotides and amino acids in the phylogenetic tree.

1.4.6 Nucleotide Sequences for 3' UTR of the Potyvirus Infecting *Pinellia*

The nucleic acid lengths of 3' UTR of the analyzed potyviruses are found to differ from each other, ranging from 251 to 256 nt, 251–252 nt of which are found from *P. ternata* isolates and 253–256 nt are found from *G. max* isolates. Each evolution clade of the isolates between *P. ternata* and *G. max* could be formed in the phylogenetic tree. There is no clear evidence of a grouping rule for the variation of 3' UTR. The identities of thirteen SMV *P. ternata* isolates and only two SMV *G. max* isolates are above 80%, with an average of 89.1%, which is higher than the average identity of nucleotide sequences and amino acid sequences of SMV CP, but lower than the amino acid sequence identity of the C-terminal and core region of SMV CP. The nucleotide sequence identity of SMV 3' UTR from 11 *P. ternata* isolates is 88.4%–100% ($\bar{a} = 94.2\%$). The homology and variation rule of SMV 3' UTR are not definitely related to the nucleotide sequences of SMV CP, so there is need for further study on its evolution mechanism. Just like the other potyviruses, the 3' UTR provides less information of host fitness.

1.4.7 The General Character and Possible Origin of the Potyvirus Infecting *Pinellia*

It is shown that both the habitat correlation and host correlation exist in the evolution of SMV CP nucleotides and amino acids, with the latter being more pronounced than the former. In the molecular phylogenetic analysis, both the

SMV CP nucleotides and amino acids from *P. ternata* and soybean isolates can form stable evolution clades, demonstrating the great influence the host exerted on the viral evolution. Accordingly, the host appears to be the dominant factor affecting the viral evolution. The hereditary diversity of SMV *G. max* isolates at amino acid level is more striking than that at nucleotide level. On account of the different combination results of the three clades of WMV isolates and SMV isolates from *G. max* and *P. ternata* with different methods, and the bootstrap values being also too low to give a strong support at the major node, the relationships cannot be well distinguished from each other. Nevertheless, it can be concluded that SMV isolates from *P. ternata* do not belong to DsMV from the individual clade with 100% bootstrapping support in phylogenetic analysis. WMV and SMV isolates from *G. max* and *P. ternata* respectively, clustered into three individual clades, may be three factors in a great undefined clade of SMV which derived from a monophyletic group. As a cultivar, *G. max* has undergone a long process of domestic cultivation with a quite simplex genotype derived from the wild progenitor (Xu et al., 2002; Zhu et al., 1994). This perhaps restricts the direction and velocity for SMV evolution at the functional level. Moreover, the molecular phylogenetic trees of SMV *P. ternata* isolates are similar among themselves at nucleotide and amino acid level. This may partially be due to the complicated genome type and chromosome nucleus type and the fact that all the germ-lines are wild, including the *P. ternata* cultivars, without uniform artificial breed (Zhu et al., 1994). In addition, the interaction of the polyproteins of SMV, aphid vector and *P. ternata* host also play a role in this evolution. As a typical viral pathogen, the infectious ability of SMV depends largely upon the level of primary inoculums, the virulence in the seeds and the activity of non-persistent aphid transmission. The diversity of SMV transmission methods determines its unusual rules of geobiological distribution. For example, in the phylogenetic trees of SMV CP nucleotides and amino acid, the SMV isolates of ChGS1 (Nelson), G7a and G7F (Cho and Goodman, 1982), as well as those from different sites could always form stable evolution clades. This homology indicates that the genotype may well be one of the SMV ancestors and is more likely to be caused by the introduction of soybean varieties. Under the reliable clade of SMV isolates from *G. max* in the amino acid tree, the number of reliable subclades within the major clades and the character substitution rates (horizontal distance) are reduced compared with the nucleotide tree. As a result of the selection pressure derived from the host, the evolution velocity in these subclades is reduced at a functional level. This suggests that soybean is a monophyletic group as one group of species of domestic plants.

CLUSTAL X 1.83 alignment of nucleotide sequences shows some evidence that the N-terminals of CP genes of SMV from *P. ternata* are highly similar to those of WMV. The small difference between these two viruses is random transition and transversion, which is calculated by molecular clock estimation (trees construction process) and Partition-Homogeneity analysis of PAUP software. For the conserved core region of SMV CP from all isolates the average homology value is 95.4%. The average identity of SMV isolates from *P. ternata* and *G. max* is more than 92%, which accords with the criteria for species discrimination

within genus potyvirus presented by Shukla and Ward, who proposed that the homology of CP core region amino acid sequences from the same virus should be above 92% (Shukla and Ward, 1988). The homology of SMV CP N-terminal amino acid sequences from *G. max* and *P. ternata* isolates is as low as 30%–42.9% ($\bar{a} = 37.5\%$) usually accompanied with variation, yet in the conserved core and C-terminal regions, the diversity at the amino acid level is minimal. potyvirus CP is divided into different functional regions of the N-terminal amino acid region (about 41 amino acids exposed to the surface of the virions), core region (related to the virion packaging and transportation) and C-terminal amino acid region (about 20 amino acids exposure to the surface of the virions) based on the spatial structure of amino acid residues as previously reported (Shukla et al., 1988). These two regions of CP should therefore be compared separately for the classification of SMV in a more reliable manner. From the predicted secondary structure analysis of the CP, it is found that the beta-sheet of SMV isolate from *G. max* distinctly reduced compared with the other four isolates (Fig. 1.14). The CP protein secondary structures are very similar to each other amongst SMV *P. ternata* isolate, WMV *Zucchini squash* isolate, DsMV *P. ternata* isolate and *Caladium hortulanum* isolate. This could probably interpret the phenomenon of serological cross-reaction between SMV and DsMV.

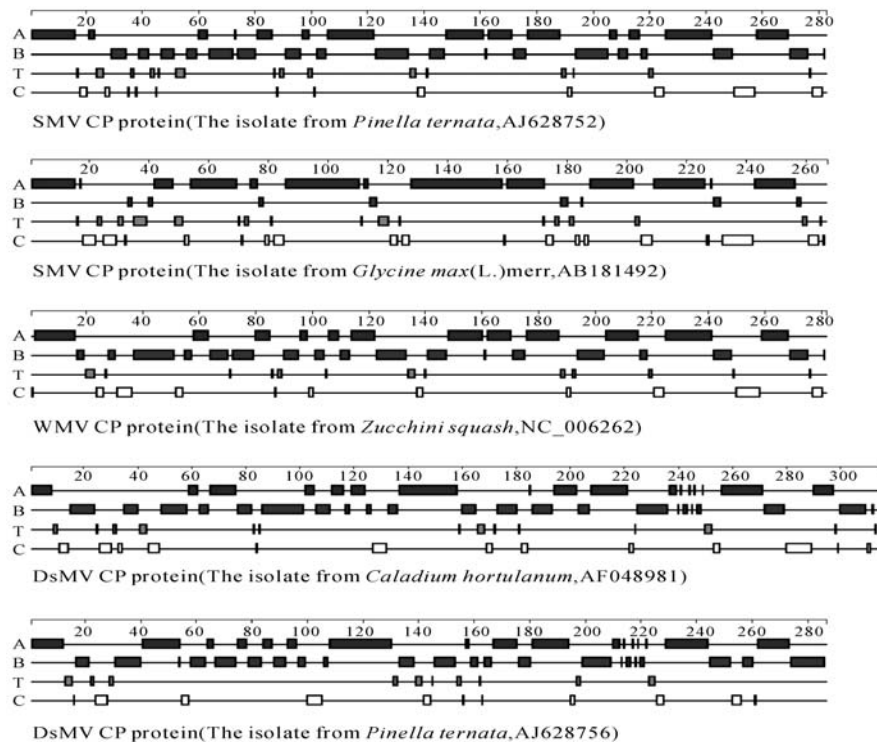


Fig. 1.14. The predicted secondary structure of the CP protein of different potyviruses
A: alpha helix; B: beta sheet; T: turn; C: coil

The notion of Muller's ratchet predicts the gradual build-up of slightly deleterious alleles in an asexual population. *P. ternata* is a typical population of asexual reproduction via corm buds. Otherwise, the random loss of those individuals in a SMV population has the fewest deleterious alleles. Muller's ratchet provides for an advantage of sex reproduction when the rate of deleterious mutations is high and population size is small. Accordingly, sexual reproduction can be helpful to escape from accumulated deleterious mutations (Chao, 1997; Shukla and Ward, 1988). The majority of evolutionary changes at the molecular level are caused not by Darwinian natural selection but by random fixation of neutral or nearly neutral mutations which are governed by genetic drift. In light of the neutral theory, the synonymous substitutions always predominate over non-synonymous substitutions and the ratios of nonsynonymous to synonymous mutations (Ka/Ks) are relatively greater between species than within species, which can be best explained by the deleterious-compensatory model. For SMV evolution, more compensatory mutations are important for SMV survival during genetic drift or recombination. A certain SMV mutant may obtain relatively more predominance than others. Its offspring will become dominant and may further adapt to the new host species (Wang et al., 2006). High viral mutation rates are not necessary for its adapting to the host. Nevertheless, a recombination event has played a significant role in the evolution of RNA viruses. As a single-stranded positive-sense RNA virus, SMV adapts itself to the new host rapidly through the genomic evolution mechanism of genetic drift and recombination. This progress of ancient recombination involves crossovers at homologous sites (Worobey et al., 1999; Zhong et al., 2005). Furthermore, as a kind of adaptive ruderal host, *P. ternata* in a mixed-growing environment with legumes provides the virus with the chance to interinfect different hosts, in addition to aphid transmission vectors. This phenomenon has also been observed in other potyvirus species such as ZYMV and TuMV (Ohshima et al., 2002), so we can conclude that potyvirus can generally adapt itself to the new host rapidly through the evolution mechanism of genome RNA variation.

There are at least two possibilities for becoming the present *Pinellia* strain of SMV. Firstly, the ancestor virus could be a pathogen infecting Araceae species such as pinellia, when pinellia was cultivated with soybeans; the virus was transmitted to the neighboring plants and changed by deleting about 47nt to fit new hosts. Secondly, the parent virus could be a normal soybean virus. When pinellia was cultivated with soybean crops, the virus moved onto the new medicinal host. In case of complex infection with WMV, some recombination happened and after the selection by replication or accumulation in favorite conditions, it brought the existence of a relatively stable virus in pinellia and transmitted vertically to offspring and horizontally to other individuals. A field survey has shown that a certain portion of pinellia plants are infected, for over 30% depend on the origin of seedlings, and wild plants are less infected. Thus, combining with aphid transmission characters of this potyvirus, the second route is more possible.

1.5 The 5' Terminal and a Single Nucleotide Determine the Accumulation of *Cucumber Mosaic Virus* Satellite RNA

satRNAs of CMV are small (330–405 nt), linear, non-coding RNA molecules that rely on their helper virus for replication, encapsulation and transmission (Palukaitis and García-Arenal, 2003; Roossinck et al., Sleat et al., 1992; Simon, Roossinck et al., 2004). To date, over 100 CMV satRNAs variants have been documented associating with over 65 CMV isolates. Despite their small size and usual absence of any potential gene products, CMV-satRNAs have dramatic effects on the symptoms induced by their helper virus, ranging from amelioration to severe exacerbation (Simon et al., 2004; Roossinck et al., 1992; Palukaitis and García-Arenal, 2003; García-Arenal and Palukaitis, 1999). It has been proposed that the resulting symptoms in plants depend on direct interaction between satRNAs, and virus or the species of the host plant. In most cases, the presence of satRNAs attenuates the symptoms induced by CMV, and reduces the titer of the helper virus (Gal-On et al., 1995).

CMV-satRNAs have highly ordered secondary structures with base pairings that range from 49% to 52% and form many loop-stems, which are probably responsible for the high stability and survivability (Simon et al., 2004; Collmer and Howell, 1992). In solanaceous hosts, several chimerical and mutational analyses have identified the regions among satRNA molecules involved in the induction of chlorosis and/or necrosis. The structures proposed for several non-necrogenic CMV-satRNAs have been found to be identical and the nucleotide differences at the primary structure level are suspected of causing a variation in pathogenesis. The mutation causing functional changes could affect the global RNA structure rather than having a local effect, and additional data support the theory that the function of CMV-satRNA is due to a structural motif specific for each variant. The phenotype changed from chlorosis-inducing to non-pathogenic when 149 U of WL2-satRNA was converted into C residue (Fraile et al., 1997).

One CMV strain could harbor several satRNAs in host plants but many satRNAs are not supported efficiently by strains of CMV in cucurbit hosts (Gal-on et al., 1995). Among several CMV strains tested, the inability to replicate the WL1-satRNA to a detectable level in zucchini squash was unique to the CMV-Sny. CMV-Fny has been found to be incapable of being the helper virus for WL1-satRNA and at least in one case the genetic determinant is Cys at residue 978 in the 1a protein, proximal to the helicase domain VI (Roossinck et al., 1997). Ix-satRNA of CMV could be maintained by strain A of *Tomato aspermy virus* (TAV) in tobacco protoplasts and in the inoculated leaves, but A-TAV was not found to support the encapsulation or long-distance movement of Ix-satRNA. The nucleotide determinants for the unusually low accumulation of Ix-sat in the tissues of *Nicotiana tabacum* are mapped to three domains (Fraile et al., 1997; McGarvey et al., 1995; Bernal et al., 1994).

Terminal of GUUUU exists in most satRNAs; an unusual CMV satRNA, namely 2msatRNA (GeneBank accession number: EU022373) lacking two U nucleotides in 5' terminal, has been found to exist stably. The nucleotide U added

or deleted in the 5' terminal of 2msatRNA does not significantly affect its replication efficiency in *N. tabaccum*, but it is found that 2mF5sat has an especially low accumulation in systemic leaves, and for which the 5' terminal is the same as that of commonly reported CMV-satRNA. Only C₂₈₈ is a different nucleotide compared with T1sat, so we analyzed the 2mF5sat accumulation level on different days post inoculation (dpi) and confirmed that the C nucleotide of 2mF5sat at 288 position is a determinant for low accumulation phenotype in *N. tabaccum*.

1.5.1 GUUU- in 5' Terminal is Necessary to Initiate Replication of 2msatRNA

With primers listed in Table 1.9, several artificial mutants have been obtained by PCR initiated protocol and transcribed satRNAs of positive sense. To analyze the effect of 5' terminal structure on the replication and accumulation, especially the initiation of satRNA replication, we used a mixed RNA transcript together with pF109,

Table 1.9 Mutations of satRNA and primers used for constructing them

Name of satRNA to be obtained	Primer name	Up stream primer sequences
2msat (wild type)	2m primer F	5'-GTTGTTTGATGGAGAATTGC-3'
2mF1sat	2mF1(2m-T)	5'-GTGTTTGATGGAGAATTGC-3'
2mF2sat	2mF2(2m-TT)	5'-GGTTTGATGGAGAATTGC-3'
2mF3sat	2mF3(2m-TTG)	5'-GTTTGATGGAGAATTGC-3'
2mF6sat	2mF4(2m-GTTG)	5'-TTTGATGGAGAATTGCGC-3'
2mF7sat	2mF5(2m-GTTGT)	5'-TTGATGGAGAATTGCG-3'
2mF4sat	2mF6(2m+T)	5'-GTTTGTTTGATGGAGAATTG-3'
2mF5sat	2mF6(2m+TT)	5'-GTTTTGTTTGATGGAGAATTG-3'
Primers for 288 site mutation	2m primerR	5'-GGGTCTGTAGAGGAATGTG-3'
	2mF5AF	5'-GAGGCTAAGGCATATGCTATGCTG-3'
	2mF5AR	5'-CAGCATAGCATATGCCTTAGCCTC-3'
	2mF5GF	5'-GAGGCTAAGGCGTATGCTATGCTG-3'
	2mF5GR	5'-CAGCATAGCATAACGCCTTAGCCTC-3'
	SatF	5'-AATTCAGCAGTAATACGACTCACTATAAGGTTT
	SatR	TGTTTGTG-3'
		5'-AATTGGGCCCGGGTCCTGCAGAGGAATG-3'
CP gene	CP F	5'-GTGGGTGACGGTCCGTAA-3'
	CP R	5'-AGATGTGGGAATGCGTTGG-3'
CP ORF	Cp-F1661	5'-CGTTGCCGCTATCTCTGCTAT-3'
	Cp-R1731	5'-GGATGCTGCATACTGACAAACC-3'
18s rRNA	18s rRNAF1564	5'-TTCCTAGTAAGCGCGAGTCATCAGC-3'
	18s rRNAR1630	5'-GCGACGGGCGGTGTGT-3'
Full satRNA	satF81	5'-CTACGGCGGTTGAGAGATG-3'
	satR226	5'-ATTTCACGTAACGGCA-3'

The sequence in square is complementary to T7 promoter; CTGAG: *Pst* I; GGGCCC: *Sma*

pF209 and pF309 to build up CMV-Fny, and the RNA transcripts above with 2msatRNA or its mutants to build up a series of pseudo-recombinants between CMV-Fny and satRNA, and then inoculated them onto the seedlings of tobacco host (*N. tabaccum*). At 3 dpi, 2msatRNA and all mutants were detected for their replication in the inoculated leaves with CMV-Fny as helper virus, except for 2mF6 and 2mF7, of which the first complete GUUU- at the 5' terminal was omitted, resulting in "5'-UUU... -3'" and "5'-UU... -3'". It is shown that the lack of the first GUUG-at the 5' terminal of satRNA could not support the replication of 2msatRNA, and only the mutants containing 5' GUUU- may initiate its replication (Table 1.10). In systemic leaves, 2mF1 and 2mF2 could not be detected, but all 2mF3–2mF5 were found accumulated at a certain level. The results for real time RT-PCR used to analyze the relative accumulation of 2msatRNA and its mutants in both inoculated and systemic leaves are shown in Figs. 1.15 and 1.16. Setting the wild type T1 satRNA as positive control, normalized to 1.0, the relative accumulation amounts of 2msatRNA, 2mF1–2mF5 are 0.39±0.07, 0.42±0.06, 0.76±0.10, 0.63±0.02, 0.79±0.02 and 0.63±0.01, respectively. This suggests that, based on the replication, deletion or addition of one or two U nucleotides at the 5' terminal of 2msatRNA does not significantly affect the replication, but obviously influence the systemic distribution or accumulation to a certain extent (Table 1.11).

Table 1.10 Mutants obtained from 2msatRNA and their existence in host tissues

	5' terminal structure	3 dpi I	S	7 dpi S	14 dpi S	21 dpi S
2msat	5'-GUUGUUUG...- 3'	+	+	+	-	-
2mF1	5'-GUGUUUG...- 3'	+	+	-	-	-
2mF2	5'-GGUUUG...- 3'	+	+	-	-	-
2mF3	5'-GUUUG...- 3'	+	+	+	+	-
2mF4	5'-GUUUGUUUG...- 3'	+	+	+	+	+
2mF5	5'-GUUUUGUUUG...- 3'	+	+	+	+	-
2mF6	5'-UUUG...- 3'	-	-	NT	NT	NT
2mF7	5'-UUG...- 3'	-	-	NT	NT	NT

+: detected; -: un-detected ; NT: not tested

Table 1.11 Relative accumulation of 2mF5/T1sat in tobacco tissues at different dpi

Inoculated leaves	2 dpi	3 dpi	5 dpi	7 dpi	14 dpi
T1sat	2.55±0.21	5.76±0.40	6.50±0.53	8.03±0.77	6.44±1.26
2mF5sat	1.47±0.20	3.26±0.26	5.07±0.38	7.26±0.93	8.02±1.03
Systemic leaves		3 dpi	5 dpi	7 dpi	14 dpi
T1sat		0.08±0.01	1.35±0.10	4.64±0.37	5.23±0.60
2mF5sat		0	0.02±0.01	0.16±0.02	0.24±0.02
T1sat I/S		0.01	0.21	0.58	0.81
2mF5sat I/S		6.13E-05	0	0.02	0.03

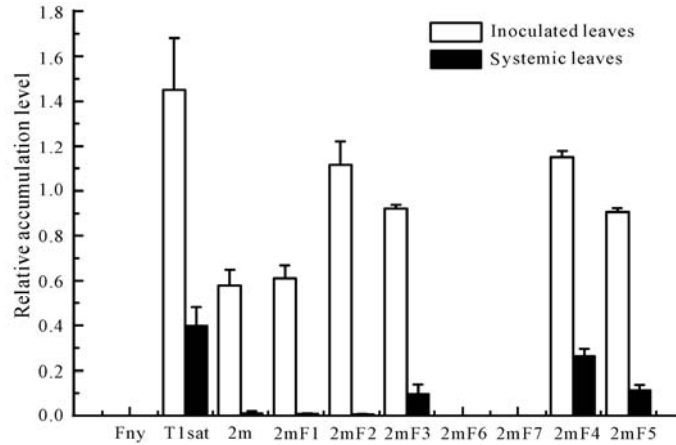


Fig. 1.15. Relative accumulation of 2msat and its mutants in tobacco at 3 dpi. Total RNA was extracted from the tissues of six individual plants inoculated with CMV-Fny with or without T1sat. The relative accumulation of satRNA was analyzed by real-time RT-PCR amplified with specific pairs and was repeated three times, with 18s rRNA used as endogenous control and relative quantization with data was performed according to the comparative C_T method ($2^{-\Delta C_T}$), for example relative accumulation of 2msat = $2^{-(\text{aver } 2\text{msat } C_T - \text{aver } 18\text{s } C_T)}$.



Fig. 1.16. Detection of CMV and satRNA in systemic leaves of tobacco at different dpi. Specific primer pairs against CMV-Fny partial CP gene and 2msatRNA were used. 1: pF309; 2: Mock; 3: CMV-Fny; 4: CMV-Fny plus 2m; 5: CMV-Fny plus 2mF1; 6: CMV-Fny plus 2mF2; 7: CMV-Fny plus 2mF3; 8: CMV-Fny plus 2mF4; 9: CMV-Fny plus 2mF5; 10: p2msat

1.5.2 Typical Structure at the 5' Terminal is Necessary for Long-distance Movement or High Accumulation of 2msatRNA

When the existence of 2msatRNA and its mutants in tobacco leaf tissues are analyzed by RT-PCR, it is found that at 7 dpi, 2mF1 and 2mF2 do not exist in the leaf tissues above the inoculated leaves when co-inoculated with CMV-Fny, whilst 2mF3–2mF5 together with 2msatRNA are found to be replicated. At 14 dpi, 2msatRNA could not be detected by RT-PCR, but 2mF3–2mF5, those with nucleotides added back, are detected for relatively higher accumulation. At 21 dpi, however, only 2mF4 is found to consistently exist but 2mF5 is not easily detected in the systemic leaves at this time point. Though the level of 2msatRNA and its

mutants are almost equal in the inoculated leaves at the early stage, the effect of deleting or adding at the 5' terminal on replication in systemic leaves has a marked effect. Adding one to two nucleotides at the 5' terminal raised the level of replication and accumulation of 2msatRNA in systemic tissues (Fig. 1.17). Further quantitative analysis of satRNAs conducted by real-time RT-PCR, showed that 2msatRNA, 2mF3 and 2mF5 are supported by CMV-Fny for replication and distribution in systemic leaf tissue in *N. tabaccum* at 7 dpi, but their accumulation levels are much lower compared to 2mF4. At 14 and 21 dpi, the accumulation of 2mF4 satRNA is noticeably above those of 2mF3 or 2mF5, suggesting that the 5' terminal of satRNA might be responsible for long-distance movement or replication efficiency of 2msatRNA in tobacco. The "5'-GUUUGUUUG...-3'" are considered as the most suitable terminae for replication and accumulation of those mutants.

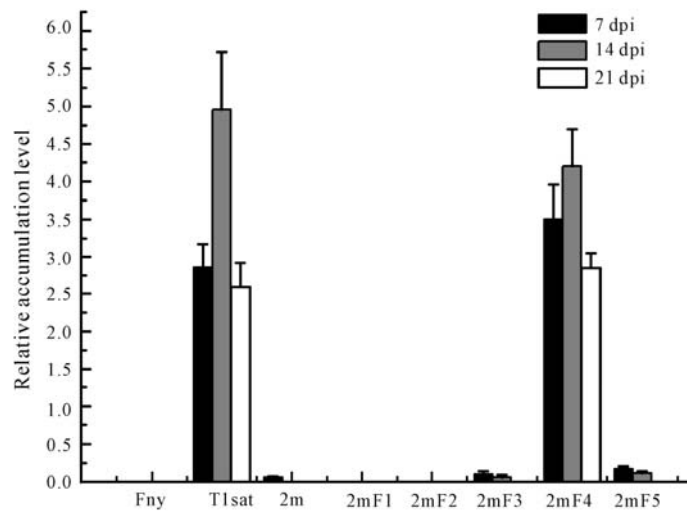


Fig. 1.17. Relative accumulation of 2msat and its mutants in systemic tobacco leaves at different dpi

Wildtype T1sat is used as the positive control of satRNAs, and the relative accumulation of satRNA is analyzed by real-time RT-PCR amplified with specific pairs. The same amount of leaves 2–3 above the inoculated leaves are detected for 7 dpi. Leaves 4–6 above the inoculated leaves are detected for 14 dpi. All the systemic leaves are detected for 21 dpi

Previous studies have demonstrated that a number of cis-acting elements were important for viral RNA's replication and infectivity, modified symptoms, and enhanced their fitness on host plants (Kim et al., 1996; Ravelonandro et al., 1983; Huisman et al., 1989). When series of mutants with different 5' terminals were constructed, of the 7 mutants, 2mF6sat and 2mF7sat with their 5' terminals lacked the integrated GUUU, and could not be found to replicate in *N. tabaccum*. It is suggested that the 5' UTR should contain a certain extent sequence, less than the limitative nucleotide for CMV-satRNA accumulation in host plants. U base deletion or addition in 5' terminal of 2msatRNA does not significantly affect the replication of 2msat in the inoculated tissues when CMV-Fny supports the

replication of 2msatRNA. In addition, 5' terminal might be responsible for long-distance movement of 2msatRNA in accumulation of satRNA in *N. tabaccum* because the accumulation level deduced as time goes by affected its long-distance movement, and finally contributed to its low accumulation. Earlier studies have indicated that one or few nucleotide variations can greatly change the viral or satellite RNA phenotype (Kobiler et al., 1999) and, after alteration of sequences, satellite RNA also effects accumulation (Sleat et al., 1992). The necessary 5' terminal structure seems to be more flexible for replication. To answer a comprehensive question, the 3' terminal structure should be comparably studied.

1.5.3 Low Accumulation of 2mF5sat Mutants is Related to Single Nucleotide Mutation

Fig. 1.17 shows that the relative accumulation of 2mF4sat is always highest in systemic leaf tissue among all 2msat mutants at different detecting time points. Its level of accumulation is close to those of wild-type T1sat, and the accumulation level of 2mF5sat in *N. tabaccum* is much less, although there is only one nucleotide, namely at 288 site, that differs between them. To detect the accumulation of 2mF5sat in mass *N. tabaccum*, compared with 2mF4sat and T1sat, direct gel electrophoresis is adopted to analyze RNAs in plant tissue. Over 80% of individual seedlings inoculated by CMV-Fny plus 2mF5sat could not support detectable accumulation of satRNA by gel electrophoresis of the total RNAs in systemic leaves (Fig. 1.18).

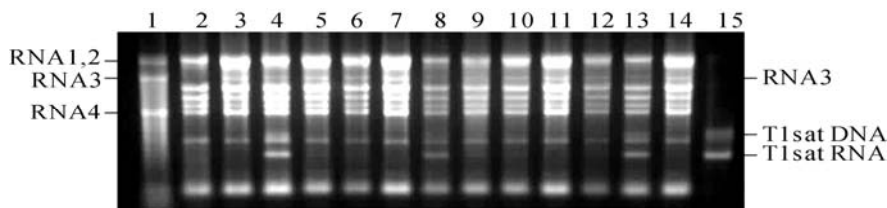


Fig. 1.18. Agarose gel electrophoresis of total RNAs extracted from systemic leaves of *N. tabaccum* at 14 dpi

1: CMV-Fny viral RNA; 2: Mock; 3: CMV-Fny; 4: CMV-Fny plus T1sat; 5–14: Tissues infected by CMV-Fny plus 2mF5; 15: T1sat RNA transcripts

Thus, a common phenotype of low accumulation of 2mF5sat in *N. tabaccum* results when CMV-Fny serves as helper virus. Symptoms in the seedlings of *N. tabaccum* inoculated with CMV-Fny and CMV-Fny plus 2mF5sat develop similar symptoms as sever mosaic, systemically deformed and stunted, whereas seedlings inoculated with CMV-Fny plus T1sat expressed only slight mosaic symptoms with no deformation, and dsRNA extraction results confirmed this. Northern blotting analysis has designated that 2mF5sat could only accumulate to a low level in systemic leaves though it is highly accumulated in the inoculated leaves, to levels

similar to T1sat, which is highly accumulated in both leaves. For a better understanding of the long distance movement of 2mF5sat compared with the wild-type T1sat, their relative accumulation is examined at 2, 3, 5, 7 and 14 dpi. As shown in Fig. 1.19, accumulation levels are comparatively similar for both satRNAs in the inoculated leaves at different inoculating time points. In systemic leaves, however, T1sat presents a gradual increase during the inoculation times, while 2mF5sat shows considerably low accumulation at all times. The ratios of the amount in systemic leaf tissue to that in the inoculated leaf tissue are about 300 multiples for T1sat against 2mF5sat (Table 1.11). The high accumulation of 2mF5sat in the inoculated leaves suggests that the low accumulation level of 2mF5sat in *N. tabaccum* is not significantly related to the replication efficiency of this mutant satRNA.

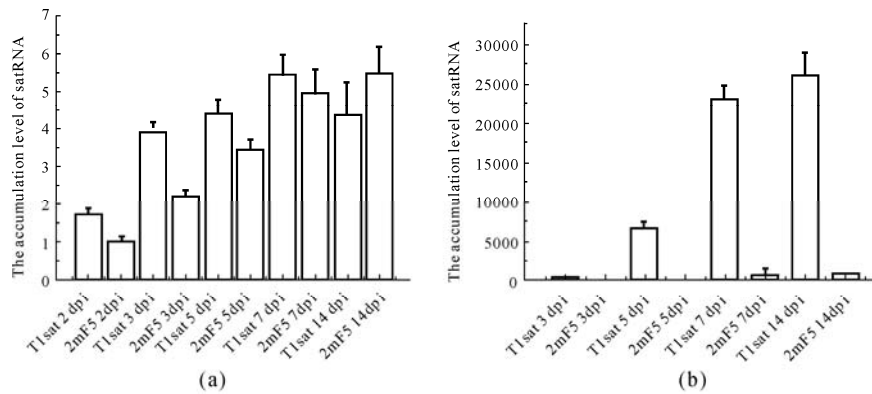


Fig. 1.19. The accumulation level of T1sat and 2mF5 in tobacco leaf tissue at different dpi. The relative accumulations of satRNAs are analyzed by real-time RT-PCR amplified with specific pairs described above. (a) Inoculated leaves; (b) Systemic leaves

Between T1sat and 2mF5sat, there is only one nucleotide different at 288 site ($U_{288}/T1sat: C_{288}/2mF5sat$), but the accumulation of 2mF5sat is much less than that of T1satRNA. This suggests that C_{288} nucleotide is probably the dominant factor for this phenotype expressed in *N. tabaccum*. To confirm whether nucleotide A or G at 288 site would have the same effect on the accumulation of 2mF5sat in *N. tabaccum*, C_{288} of 2mF5sat is mutated to A or G and their RNA transcripts are co-inoculated with CMV-Fny, respectively. At 14 dpi, the level of 2mF5sat C_{288} (2mF5sat), 2mF5sat A_{288} and 2mF5sat G_{288} is analyzed by Northern hybridization, compared with T1sat. Except for 2mF5sat, the other satRNA mutants can accumulate to relatively high levels (Fig. 1.20).

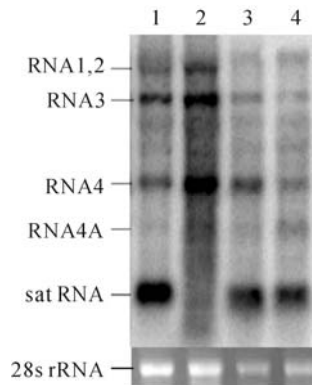


Fig. 1.20. Northern blot analysis of satRNA accumulation in tobacco leaf tissue at 14 dpi
1: CMV-Fny plus T1sat (T288); 2: CMV-Fny plus 2mF5 (C288); 3: CMV-Fny plus 2mF5 (A288);
4: CMV-Fny plus 2mF5 (G288)

Thus, C₂₈₈ of 2mF5sat determines the low accumulation of 2mF5sat in *N. tabaccum*.

1.5.4 Secondary Structure of 2mF5sat Impaired its Replication Capacity

The structural differences are made clear with the result predicted by RNA structure of the four satRNA mutants. T1sat, 2mF5sat (A₂₈₈) and 2mF5sat (G₂₈₈) have almost the same secondary structure. They are composed of three structural domains. Domain I (1–160 nt) has four short stem-loop, stringed series as a long stem, and three short stems converge at another stem-loop, called domain II (160–200 nt). Domain III (190–200 nt) resembles a sector with stems, with one of them having five small loops below it. The second structure of 2mF5sat is totally metamorphic with the first domain (1–30 nt) making the first stem with three small loops and domain II (40–280 nt) form a perfectly matched long stem, especially with two short stems at the apex, making a figure like the letter Y. The key point is that at domain III (300–330 nt), a notable, large sector-loop could be seen by computer analyses, including nt 307–309 (Fig. 1.21). The differences in secondary structure of the four satRNA affected by notable accumulation in *N. tabaccum* are interesting and await further investigation.

Conserved secondary structures are of functional significance in viral replication, transcription, recombination and pathogenesis by their highly conserved sequence or through the interaction of the secondary structure with viral or cellular proteins (Roossinck et al., 1992; Hofacker et al., 2004; Garcia et al., 2001). It can be postulated that the differences alter the secondary structure and may influence replicate recognition or systemic movement in plants (Chikara et al., 1989). Among the four 2mF5sat mutants in the 288 nucleotide, only the 2mF5sat

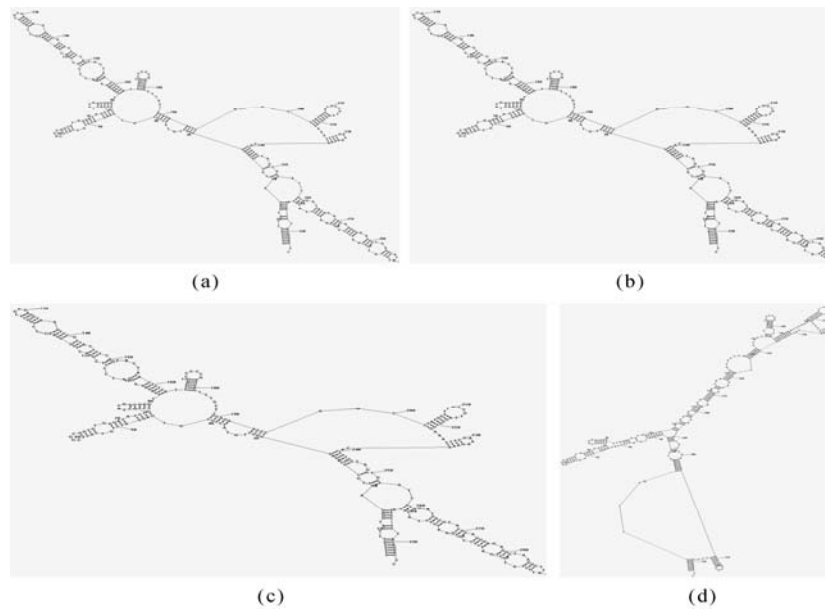


Fig. 1.21. Comparison of the second structure between 2mF5sat mutants (a) 2mF5 (A₂₈₈); (b) 2mF5 (G₂₈₈); (c) T1sat (U₂₈₈); (d) 2mF5 (C₂₈₈)

(C₂₈₈) could not be detected in systemic leaves. Specifically, satRNA with the 288 nucleotide (U/A/G) has a similar second structure and the structure of 2mF5satRNA is totally metamorphic. It has been shown that the changed C to U at position 20 incompletely restores the ability of the satRNA 6 to accumulate systemically, resulting in much lower systemic accumulation of satRNA (Garcia et al., 2001). This indicates that the phenotype determined by a U at position 20 shows a partial impairment of the long-distance systemic movement. It has been shown that encapsulation, or at least interaction with the coat protein, is required for long-distance systemic movement of the genomic RNAs of CMV (Suzuki et al., 1991). In the above case, 2mF5sat exists in inoculated leaves, but in systemic leaves, the level of satRNA has obviously declined. Different accumulation levels of 2mF5sat mutants could be dependent on a change of molecular conformation of satRNA in *N. tabaccum*. The analysis results of virus particles and viral RNA shows that the presence of satRNA reduced CMV-Fny virion titer and low accumulation of 2mF5sat in host plants had no relationship with its encapsulation efficiency. To a greater extent, there are some other ways to modulate the accumulation of 2mF5sat. It is reasonable to consider that T1sat might restrict the replication ability of the helper virus, and then cause the high accumulation level of satRNA in systemic leaves, as the encapsulation result has shown. On the other hand, satellite 2mF5sat could not strongly reduce such replication ability, and the replication efficiency of satRNA is slower than the helper virus, thus resulting in a low accumulation phenomenon in *N. tabaccum*. Similar reports have suggested that some amino acid changes at positions 876 and 891, responsible for satRNA

replication, do not occur in systemic leaves of lily, thereby suggesting that they may be essential for satRNA's systemic replication in lily (Yamaguchi et al., 2005). Another possible reason to explain the low replication and accumulation is viral long-distance movement. The accumulation level of 2mF5sat is obviously lower in systemic leaves than in inoculated leaves. Long-distance movement is a complex process requiring the interaction of virus and host components (Yamaguchi et al., 2005; Hull et al., 2002). Some studies indicate CP is more essential for virus long-distance movement and others supported MP better (Saito et al., 1990; Schmitz et al., 1998), but it seems the structure difference is mostly a deterrent to a high level of accumulation and movement.

It can be concluded that the mutation of a single nucleotide in CMV satellite RNA, causing structure alteration, is responsible for its long-distance movement efficiency and low accumulation in plant tissue.

1.6 Methodology

In this section, we introduce purification of CMV Virions from plant tissue, RT-PCR and cDNA cloning for Full-length genomic RNAs of *Cucumber mosaic virus*, RT-PCR and gene cloning for 3'-end of viral genome of *soybean mosaic virus*, sequence analysis and phylogenetic analysis, and pseudo-recombination of satellite RNA of *Cucumber mosaic virus* and the helper virus.

1.6.1 Purification of CMV Virions from Plant Tissue

The present protocol suggested here is firstly described by Francki et al. (1979). With some major modifications, it is described as follows.

Tobacco (*Nicotiana tabacum*) is recommended as host plant for virus inoculation for the purification. Seedlings of *N. glutinosa* are recommended as the host plants to keep the CMV strain either from subgroup I and subgroup II, to avoid contamination by Tobamoviruses which commonly occur in the greenhouse. CMV isolates are recommended to be activated for 4–10 d before transfer to tobacco seedlings as propagating host. The inoculated seedlings are kept at 22–25 °C under greenhouse conditions for 10–12 d before harvesting for virion extraction. The newly harvested leaf tissues, with vein removed, are recommended to be kept at –80 °C for 2 to 48 h before use. Keeping them a longer time at low temperature can reduce the ratio of virions purified and pre-freezing in liquid nitrogen would yield more indescribable components from cells. And then the following steps are recommended.

Step 1: 200 g fresh tobacco leaf tissue infected with CMV for 10–12 d with pre-freezing at –80 °C is to be used.

Step 2: Homogenize the tissue in 200 ml 0.5 mol/L (pH 7.4) potassium phosphate buffer (containing 0.1% 2-mercaptoethanol, 2% Triton X-100 and 0.01

mmol/EDTA).

Step 3: Add 10% cold chloroform/Pentanol (v/v=1:1) and mix well with short time homogenizing.

Step 4: Centrifuge the mixture at 8,000×g for 20 min, under 4 °C. Collect 90% of the aqueous phase.

Step 5: Add 6% PEG-8000, 0.1 mol/L NaCl to the aqueous phase and mix well. Keep at 4 °C for 6 h.

Step 6: Collect the pellet after centrifuging under the same conditions as above, and repeatedly suspend the pellet with 0.2 mol/L sodium phosphate buffer (pH 7.2, containing 1% Triton X-100, 0.01 mol/L EDTA).

Step 7: Centrifuge the suspension at 12,000×g for 25 min at 4 °C, during and after re-suspension. The suspension is used as a partially purified virus preparation.

Step 8: Layer 5 ml of partial purification preparation onto a glycerol grade of 5% to 40% and centrifuged at 78,000×g for 120 min, under 4 °C.

Step 9: Collect the pellets and suspend repeatedly with 0.2 mol/L sodium phosphate buffer (pH 7.2, with neither Triton X-100 nor EDTA) to a final value of 3–4 ml as the purified virus. During and after re-suspension, centrifuge the re-suspension at 12,000×g for 25 min, under 4 °C. The re-suspension should be done on ice and with a well vortex.

Step 10: Divide the purified virus into 300 µl value of 0.2 mol/L sodium phosphate buffer (pH 7.2, with neither Triton X-100 nor EDTA) and keep at 80 °C for further use.

The purified virions are ready to be used for quantitative analysis, RT-PCR and gene cloning, protein analysis and kept for infection, but further purification could be performed if more measurement is required.

1.6.2 RT-PCR and cDNA Cloning for Full-length Genomic RNAs of Cucumber Mosaic Virus

For unknown fragments, dsRNAs are suggested to be used as gene clone templates, while the simplified single-primer amplification technique (SPAT) is strongly suggested, see Chapter 6. With known genes or genomic fragments, primer design is based on the comparison of nucleotide sequences of over 15 known isolates of the same virus registered in GenBank, or all the possible documented descriptions of the same segment of viral genome. It needs to be considered for “known” viral genes for, in some cases, the reported sequences are not certain to be correct. For example, the primers used for amplification of genomic RNAs of CMV-Tsh are listed in Table 1.2. The downstream primer RNA23-R with a *Pst* I site is used to generate the first-strand cDNAs of CMV-Tsh RNAs 2 and 3. Primer RNA1-R with a *Sal* I site is used for generating the first-strand cDNA of RNA1, since there is a *Pst* I site in the cDNA of CMV-Tsh RNA1. The primer pair RNA1-F and RNA1-1842-R is used to amplify an approximately 1,840 bp cDNA fragment corresponding to the 5' end of RNA1,

and primer pair RNA1-1604-F and RNA1-R is used to amplify an approximately 1,750 bp cDNA fragment corresponding to the 3' end of RNA1. The primer pairs RNA2-F/RNA23-R and RNA3-F/RNA23-R are used to amplify the full-length cDNAs of RNA2 and RNA3 respectively.

First-strand cDNAs of genomic RNAs can be synthesized by *Avian myeloblastosis virus* (AMV) reverse transcriptase (Takara, Dalian) according to manufacturer's instructions with total RNAs extracted from systemic tissues or from virions. Second-strand cDNAs are generally synthesized by PCR using PrimeSTAR HS DNA polymerase (Takara, Dalian) according to manufacturer's instructions. PCR conditions are set according to the annealing temperatures of different primer pairs and the lengths of PCR products. RT-PCR products are fractionated by 1% agarose gel electrophoresis, and then target fragments are recovered using DNA Gel Extraction Kit (Axygen, USA) or any similar reagents. The purified fragments obtained by the above primers are to be digested with *Bam*H I-*Sal* I or *Bam*H I-*Pst* I, and then ligated into linearized plasmid pUC118 using T₄DNA ligase (Takara, Dalian). A T-vector can be used in many cases to obtain amplified fragments. Cells of the *E. coli* strain DH5 α are transformed with the ligation products. Recombinant colonies are screened by blue/white colony and identified by PCR or restriction enzymes.

1.6.3 RT-PCR and Gene Cloning for 3'-end of Viral Genome of Soybean Mosaic Virus

Total RNAs are extracted with TRIzol reagent from pulverized leaf tissues according to the manufacturer's protocol (Invitrogen, USA). Viral RNA preparation and virion purification are performed using routine methods described in the literature (Chen et al., 2001; Tan et al., 2004). First strand cDNA is synthesized with AMV reverse transcriptase as above and oligo dT-M13M4 (5'-GTTTTCCC AGTCACGAC (T)₁₆-3') according to the manufacturer's instructions. Complementary to the 3'-terminal Poly (A) tail of the viral genome, the initial primer oligo dT-M13M4 is used to ensure the successful amplification of complete 3'-terminal untranslated regions (UTR). As a template, reverse transcription (RT) products are amplified using *LA-Taq*[®] DNA polymerase system (TaKaRa, Japan) with the degenerate primer Sprimer (Chen and Adams, 2001; Chen et al., 2006) (5'-GGXAAYAAAYAGYGGXCAZCC-3', X=A, G, C or T; Y=T or C; Z=A or G) and primer M4 (5'-GTTTTCCCAGTCACGAC-3'). After optimizing the annealing temperature and time through Touch Down PCR (T-Gradient PCR, Germany), the optimal process for PCR amplifying is conducted as follows: predenaturing at 94 °C for 4 min, and then 94 °C for 30 s, 52 °C for 20 s, 68 °C for 2 min within 35 cycles, and final extension at 72 °C for 10 min. Successful amplification of the expected fragments is to be confirmed through electrophoresis with 1% (w/v) agarose gels. The target PCR products are excised into gel slices and purified by the QIAquick[™] Gel Extraction Kit (QIAGEN, Germany) and then directly ligated into the pGEM[®] T-Easy vector (Promega, USA) according to the manufacturers'

protocols. They are subsequently transformed into *E. coli* TG1 electroporation-competent cells culturing overnight. Individual positive colonies containing recombinant plasmid DNA are picked and grown in Luria-Bertani broth and the plasmids are isolated by a modified alkaline lyses method. Plasmids are certified by PCR and *EcoR* I restriction endonuclease (TaKaRa, Japan) analysis and selected clones are sequenced using the dideoxynucleotide chain termination method.

1.6.4 Sequence Analysis and Phylogenetic Analysis

It is suggested that clones containing the expected fragments be sequenced by a model 3730 ABI Prism DNA analyzer (Invitrogen, USA) or any other instruments. Two to four clones of each fragment should be sequenced and the consensus sequences are used for sequence analysis and phylogenetic analysis. The assemblage and comparison of sequences are done by using DNASTar version 6.1.3 (Madison, Wis., USA). Nucleotide sequence alignments are carried out by using CLUSTAL X (Thompson et al., 1997), with strains of other viruses from the same family as outgroups. In the case of CMV, some typical strains should be included as reference, including such as Fny, Leg, Mf, Y and O which are CMV subgroup IA strains; Nt9, Tfn, Ix, SD and IA which are CMV subgroup IB strains; Q, Ly, S, LS and Trk7 which are subgroup II strains. *Peanut stunt virus* (PSV) is suggested as the outgroup.

1.6.5 Pseudo-recombination of Satellite RNA of Cucumber Mosaic Virus and the Helper Virus

Infectious cDNA clones of CMV-Fny (pF109, pF209 and pF309) are firstly constructed and provided by Palukaitis (Scottish Crop Research Institute). Transcription reactions of CMV satRNA infections are essentially followed as a protocol described by Beckler (1992), with a cap added at the 5' terminal of each full-length genomic RNA. Full-length cDNAs with T7 promoter sequence, 5'-TAATACGACTCACTATA-3', at the 5' terminal of the positive strand are used as infectious clones. Transcripts of 2msatRNA and its mutant cDNA clones are obtained with Riboprobe® system-T7 (Promega, USA) according to manufacturer's instructions, without cap structure added at the 5' terminal. Full RNAs are transcribed from cDNA clones of pF109, pF209, and pF309 and 2msatRNA together with its mutants using T7 RNA polymerase. Prior to RNA transcription, plasmids of pF109, pF209 and pF309 should be linearized with *Pst* I, and clones of 2msatRNA and its mutants cDNAs are digested with *Sma* I. DNAs are removed from reaction mixtures with RQ1 RNase-free DNase (Promega, USA) and extracted with phenol-chloroform, and then precipitated with ethanol. RNA transcripts are suspended in nuclease-free ddH₂O to a concentration of 10–25

µg/ml. All the RNA transcripts are quantified by gel electrophoresis before inoculation. 2msatRNA has been cloned from systemic leaves of *N. tabaccum* infected by CMV-Fny plus an artificial 421 nt CMV-satRNA. Its full-length nucleotide is found to be 335 nt and the sequence of 5' terminal is "5'-GUUGUUU...-3'". After sequencing, 2msatRNA is found lacking the first two U nucleotides in 5' terminal compared to most CMV-satRNAs documented. PCR has been adopted to delete or add U in "5'-GUUGUUU...-3'" sequence of 2msatRNA to construct its mutants, using full-length cDNA clone of 2msat RNA (p2msat) as template, with primers listed in Table 1.9.

288 C of 2mF5sat is mutated to A or G by overlapping PCR, and fragments I and II are amplified with two PCR primer pairs SatF/2mF5AF and 2mF5AF/SatR, respectively. A mixture of two amplified fragments is used as template for a further amplification with primer pairs SatF/SatR. Using All the PCR products of mutants as template, 2msatRNA mutants containing T7 promoter at 5' terminal are obtained with primer pairs SatF/SatR. These resultant PCR fragments of 2msatRNA mutants are digested with *Pst* I and *Sma* I and then cloned into pUC118 vector. The exactness of site-directed mutagenesis in 2msatRNA is confirmed by sequencing. 20 µl RNA transcripts of CMV-Fny, containing about 0.05–0.01 µg RNA transcripts each, with or without T1sat/2msatRNA and its mutant RNA transcripts is used to inoculate. CMV-Fny with or without satRNAs is mechanically inoculated onto two seedlings of *N. glutinosa* or *N. tobaccum*, respectively. Systemic infection is to be confirmed by RT-PCR and double stranded RNA analysis according to previous reports (Liao et al., 2007). At 3 to 5 dpi, the inoculated leaf tissues are sampled for transmitting to new seedlings to enlarge the inoculation when necessary. Systemic diseased leaf samples are to be harvested according to the requirements or to be stored at -80 °C before further analysis.

Quantitative analysis of satRNA accumulation is followed by a realtime RT-PCR protocol which is to be described in Chapter 2 with additional primer pairs optimized for satellite RNAs of CMV, in addition to the primer pairs designed for genomic ORFs against CMV-Fny. Conventional northern blotting analysis is utilized for determining the expressing of CMV genomic RNAs and the satRNAs. Virus particles are purified according to recommended protocols introduced above, with viral RNAs and proteins analyzed according to conventional methods.

References

- Bernal OO, Maclaughlin DE, Lukefahr, et al. (1994) Copper NMR and Thermodynamics of $UCu_{5-x}Pd_x$: Evidence for Kondo Disorder. *Physical Review Letters* 75(10): 2023-2026.
- Bonnet J, Fraile A, Sacristán S, et al. (2005) Role of recombination in the evolution of natural populations of *Cucumber mosaic virus*, a tripartite RNA plant virus. *Virology* 332(1): 359-368.
- Brigneti G, Voinnet O, Li WX, et al. (1998) Viral pathogenicity determinants are suppressors of transgene silencing in *Nicotiana benthamiana*. *EMBO J* 17(22):

- 6739-6746.
- Chao L (1997) Evolution of sex and the molecular clock in RNA viruses. *Gene* 205(1-2): 301-308.
- Cho EK and Goodman RM (1982) Evaluation of resistance in soybeans to *Soybean mosaic virus* strains. *Crop Sci* 22(6): 1133-1136.
- Collmer CW and Howell SH (1992) Role of satellite RNA in the expression of symptoms caused by plant viruses. *Annu Rev Phytopathol* 30: 419-442.
- Ding B, Li Q, Nguyen L, et al. (1995) *Cucumber mosaic virus* 3a protein potentiates cell-to-cell trafficking of CMV RNA in tobacco plants. *Virology* 207(2): 345-353.
- Ding SW, Anderson BJ, Haase HR, et al. (1994) New overlapping gene encoded by the *Cucumber mosaic virus* genome. *Virology* 198(2): 593-601.
- Ding SW, Li WX and Symons RH (1995) A novel naturally occurring hybrid gene encoded by a plant RNA virus facilitates long distance virus movement. *EMBO J* 14(23): 5762-5772.
- Fraile A, Alonso-Prados JL, Aranda MA, et al. (1997) Genetic exchange by recombination or reassortment is infrequent in natural populations of a tripartite RNA plant virus. *J Virol* 71(2): 934-940.
- Gal-On A, Kaplan I and Palukaitis P (1995) Differential effects of satellite RNA on the accumulation of *Cucumber mosaic virus* RNAs and their encoded proteins in tobacco vs zucchini squash with two strains of CMV helper virus. *Virology* 208(1): 58-66.
- García-Arenal F and Palukaitis P (1999) Structure and functional relationships of satellite RNAs of *Cucumber mosaic virus*. In: *Satellites and Defective Viral RNAs* (Vogt PK and Jackson AO, Eds.), Springer-Verlag, Berlin, pp. 37-63.
- Gojobori T, Moriyama EN and Kimura M (1990) Molecular clock of viral evolution, and the neutral theory. *Proc Natl Acad Sci USA* 87(24): 10015-10018.
- Hayes RJ and Buck KW (1990) Complete replication of a eukaryotic virus RNA in vitro by a purified RNA-dependent RNA polymerase. *Cell* 63(2): 363-368.
- Henderson WW, Monroe MC, St. Jeor SC, et al. (1995) Naturally occurring *Sin nombre virus* genetic reassortants. *Virology* 214(2): 602-610.
- Hu CC and Ghabrial SA (1998) Molecular evidence that strain BV-15 of peanut stunt cucumovirus is a reassortant between subgroup I and II strains. *Phytopathology* 88(2): 92-97.
- Kaplan IB, Zhang L and Palukaitis P (1998) Characterization of *Cucumber mosaic virus*. *Virology* 246(2): 221-231.
- Li Q, Ryu KH and Palukaitis P (2001) *Cucumber mosaic virus*-plant interactions: identification of 3a protein sequences affecting infectivity, cell-to-cell movement, and long-distance movement. *Mol Plant Microbe Interact* 14(3): 378-385.
- Lin HX, Rubio L, Smythe A, et al. (2003) Genetic diversity and biological variation among California isolates of *Cucumber mosaic virus*. *J Gen Virol* 84(1): 249-258.
- McCullers JA, Wang GC, He S, et al. (1999) Reassortment and insertion-deletion are strategies for the evolution of influenza B viruses in nature. *J Virol* 73(9): 7343-7348.
- McGarvey PB, hammond J, dienett MM, et al. (1995) Expression of the rabies virus glycoprotein in transgenic tomatoes. *Biotechnology*, 13(13): 1484-1487.
- Morse SS (Ed.) (1994) *The Evolutionary Biology of Viruses*. Raven Press, New York, pp. 233-250.
- Ohshima K, Yamaguchi Y, Hirota R, et al. (2002) Molecular evolution of *Turnip*

- mosaic virus*: evidence of host adaptation, genetic recombination and geographical spread. *J Gen Virol* 83(Pt 6): 1511-1521.
- Palukaitis P and Garcia-Arenal F (2003) Cucumoviruses. *Adv Virus Res* 62: 241-323.
- Palukaitis P, Roossinck MJ, Dietzgen RG, et al. (1992) *Cucumber mosaic virus*. In: *Advances in Virus Research*, Academic Press, Vol. 41, pp. 281-348.
- Perry KL, Zhang L, Shintaku MH, et al. (1994) Mapping determinants in *Cucumber mosaic virus* for transmission by *Aphis gossypii*. *Virology* 205(2): 591-595.
- Poolpol PIT (1986) Enhancement of *Cucumber mosaic virus* multiplication by *Zucchini yellow mosaic virus* in doubly infected cucumber plants. *Ann Phytopathol Soc Jpn* 52: 22-30.
- Robinson DJ, Hamilton WDO, Harrison BD, et al. (1987) Two anomalous tobnavirus isolates: Evidence for RNA recombination in nature. *J Gen Virol* 68(10): 2551-2561.
- Roossinck MJ (2002) Evolutionary history of *Cucumber mosaic virus* deduced by phylogenetic analyses. *J Virol* 76(7): 3382-3387.
- Roossinck MJ, Sleat D and Palukaitis P (1992) Satellite RNAs of plant viruses: structures and biological effects. *Microbiol Rev* 56(2): 265-279.
- Roossinck MJ, Zhang L and Hellwald KH (1999) Rearrangements in the 5' nontranslated region and phylogenetic analyses of *Cucumber mosaic virus* RNA 3 indicate radial evolution of three subgroups. *J Virol* 73(8): 6752-6758.
- Shukla DD, Strike PM, Tracy SL, et al. (1988) The N and C termini of the coat proteins of potyviruses are surface-located and the N terminus contains the major virus-specific epitopes. *J Gen Virol* 69(7): 1497-1508.
- Shukla DD and Ward CW (1988) Amino acid sequence homology of coat proteins as a basis for identification and classification of the potyvirus group. *J Gen Virol* 69(11): 2703-2710.
- Simon AE, Roossinck MJ and Havelda Z (2004) Plant virus satellite and defective interfering RNAs: new paradigms for a new century. *Annu Rev Phytopathol* 42: 415-437.
- Wang H, Huang LF and Cooper JI (2006) Analyses on mutation patterns, detection of population bottlenecks, and suggestion of deleterious-compensatory evolution among members of the genus potyvirus. *Arch Virol* 151(8): 1625-1633.
- Wang Y, Gaba V, Yang J, et al. (2002) Characterization of synergy between *Cucumber mosaic virus* and potyviruses in cucurbit hosts. *Phytopathology* 92(1): 51-58.
- White PS, Morales F and Roossinck MJ (1995) Interspecific reassortment of genomic segments in the evolution of cucumoviruses. *Virology* 207(1): 334-337.
- Worobey M and Edward C (1999) Evolutionary aspects of recombination in RNA viruses. *J Gen Virol* 80 (Pt 10): 2535-2543.
- Xu H, Abe J, Gai Y, et al. (2002) Diversity of chloroplast DNA SSRs in wild and cultivated soybeans: evidence for multiple origins of cultivated soybean. *Theor Appl Genet* 105(5): 645-653.
- Zhong Y, Guo A, Li C, et al. (2005) Identification of a naturally occurring recombinant isolate of *Sugarcane mosaic virus* causing maize dwarf mosaic disease. *Virus Genes* 30(1): 75-83.
- Zhu T, Schupp JM, Oliphant A, et al. (1994) Hypomethylated sequences: characterization of the duplicate soybean genome. *Mol Gen Genet* 244(6): 638-645.

Molecular Detection of *Cucumber Mosaic Virus* and Other RNA Viruses Based on New Techniques

2.1 Introduction

Plant diseases caused by viruses and related pathogenic agents bring about substantial losses in agricultural and horticultural crops. And the study of plant viruses has contributed quite a lot to the agricultural progress and basic understanding of plant development as a molecular standard. For example, based on a virus's diagnosis, the omission of plant viruses from potato and many vegetative propagated crops has brought large progress for crop production. A majority of plant viruses, well studied to date, of economical importance are RNA viruses or viroids of RNA characters. The proper diagnostic method for causative viruses and viroids is the first requirement for the control of such diseases. To this day, the main techniques applied to the diagnosis of plant viruses include biological assays, electron microscopy, serological tests, viral double-stranded RNA analysis, nucleic acid hybridization, PCR (RT-PCR), and other molecular means. When large numbers of samples have to be handled, DAS-ELISA is most widely used for detection. Since viroids produce no specific protein, the serological test, applied so widely to viruses, cannot be used for their diagnosis. For this reason, nucleic acid hybridization on the membrane (Barker et al., 1985; McInnes, et al., 1989; Nakahara et al., 1998; Owens and Diener, 1981) and RT-PCR (Ito et al., 2002; Nie and Singh, 2001), with some modifications, was developed for the detection of viroids. Since the development of the microarray and its application in large scale scanning and detection, many objects have been changed. The leading objectives in the detection of plant viruses in practice are facets of the testing of a large amount of samples against a mono-target and the testing of a mono-sample against multiplex targets. In a laboratory, sensitivity and reliability are mostly considered even though the convenience and efficiency are less calculated.

On the other hand, more and more ssDNA viruses and dsRNA viruses are found through the plant kingdom, and their important role in plant-virus interaction and new emerging diseases is drawing more and more attention.

In this chapter, current diagnosis techniques are recommended, with novel qualitative and quantitative detection techniques being introduced now for laboratory use, using CMV as a model ssRNA virus.

Conventional methodology for plant virus diagnosis: Inoculation and transmission of plant viruses are of preliminary importance to a laboratory that works on this group of pathogens. Confirming the infectious clone and investigating host-virus interaction often invites us to introduce infectious viruses into the whole plant. Using plant tissue culture techniques, virus-infected plant materials can be propagated in mass and this provides us with the possibility to obtain more identical materials for experiments.

Observation of the virus particles and even the pathogenic alterations, including the inclusion structure, are of advantage for direct evidence. Combined with virions extraction and molecular laboring, electron-microscopy based observation is still one of the most effective methods used in a plant virus research laboratory.

Serological diagnosis and the immunoreactions based on antibody labeling are the most commercialized techniques used in clinical and agricultural use for virus detections. Kits of ELISA are now available on the market in millions, directly or indirectly. And the production of antibodies shows great promise after a basic study of viruses. Using sequence information obtained by gene cloning, antibodies can be more easily produced for experimental use, and thus can be used more easily to the research. In the present situation application is more important than improvement.

Nucleic acid hybridization used in plant virus detection: Most of the commercialized approaches to the application of nucleic acid hybridization for the diagnosis of plant viral diseases now involve the use of filter hybridization using radioactive probes, which use complementary cDNAs previously obtained or synthesized (Hsu et al., 2000). Nylon membrane is the most popular matrix for immobilizing nucleic acids (Dyson, 1991). When compared with nylon membrane, the glass slide used for immobilization of nucleic acids in DNA microarray systems has unique merits, including covalent immobilization of macro-molecules, durability to high temperature and high ionic strength, minimum hybridization volume and, especially, parallel hybridization capacities (Cheung et al., 1999). Presently, membrane hybridization with radioactive ³²P-phosphorous labels is still used widely in laboratories, although some of the non-radioactive report systems have been developed for the detection of plant viruses or viroids (Hull and Al-Hakim, 1988). Microarray as a relatively newly-developed molecular means possesses apparent advantages, including computerized data analysis, high throughput and parallelism with controlled conditions. In the past few years, DNA microarray has been mostly applied to the field of the diagnosis of human and animal pathogens (Chizhikov et al., 2002; Li et al., 2001; Wang et al., 2002; Wilson et al., 2002). This technique has been successfully used for detecting plant viruses just recently (Boonham et al., 2003; Bystricka et al., 2005; Deyong et al., 2005; Lee et al., 2003). Some microarrays combined the high sensitivity of PCR amplification and the high specificity of nucleic acid hybridization, by amplifying the target RNAs with RT-PCR before

chip hybridization. The targets are enlarged many times during detection. The hybridization signals could be again also enlarged by chemical dyes.

In light of the above, a newly developed system has been introduced by utilizing a DNA microarray system to improve the conventional dot blot hybridization, by directly spotting extracted RNAs onto surfaces of activated glass slides and then performing dot blot hybridization with CY5-labeled (or CY3-labeled) probes, for detecting plant RNA viruses and viroids. This modified method, namely glass slide hybridization, was developed from conventional RNA dot-blot hybridization, by replacing 32 P labels with CY5 labels (or CY3 labels) and by replacing membranes with positive-charged glass slides. An optimum efficiency of RNA binding onto surfaces of activated glass slides has been achieved using aminosilane-coated glass slides as a solid matrix, and the optimized glass slide hybridization could detect as little as 1.71 pg of TMV RNA. The sensitivity of the modified method is four times that of dot-blot hybridization on a nylon membrane with a 32 P-labeled probe, and it is demonstrated that this method is of high specificity. RNA glass slide hybridization provides a new option with obvious advantages for mass detection of 1–2 targets with high sensitivity. See details in Section 2.4.

RT-PCR and multiplex RT-PCR: As one of the most commonly used molecular approaches in bio-laboratories, PCR has high sensitivity, which is enough for most molecular detections, but PCR has many disadvantages, including contamination and being pseudo-positive. Thus, controls should be well arranged when PCR is delayed for an independent judgment. As mentioned above, the combination of PCR with other approaches can significantly improve the feasibility. Most plant viruses needing to be detected in practical diagnosis are of the ssRNA genome, thus a RT-PCR should be conducted and during the synthesis of the first strand cDNA, the specificity is increased by closing the targets. A majority of economically important crops are infected by several plant viruses or viroids. That means the detection often concerns many targets from a single sample. Multiplex RT-PCR accommodates several primer pairs in one reaction, saving time and other expense, especially when large numbers of samples need to be tested. Since the first multiplex PCR system was developed for the detection of mutations in the *dystrophin* gene (Chamberlain et al., 1988), this technique has been applied to the detection of plant viruses for years (Bertolini et al., 2001; Hauser et al., 2000; Nie and Singh, 2000; Nie et al., 2001; Nie and Singh 2002; Thompson et al., 2003). For example, two multiplex RT-PCR formats have been described for the diagnosis of multiple viruses infecting the potato (*Solanum tuberosum*). In the first format, oligo (dT) was used as a common primer for the synthesis of first-strand cDNA from viral RNA (Nie and Singh, 2000). It is said that this format effectively detected multiple potato viruses in tubers, but interference from plant mRNA made it unsuitable for the detection of the same viruses in leaves. In the second format, random primers were used for first-strand cDNA or a cDNA pool (Nie and Singh, 2001). This format detected several viruses from aphids, leaves and tubers. Both formats were developed through detecting viral RNA extracted from purified viral particles. To rule out false negative results due to factors such as the presence of PCR inhibitors, some

reports used a plant NADH dehydrogenase mRNA as an internal control for the success of RNA extraction and RT-PCR reaction (Bariana et al., 1994; Menzel et al., 2002; Thompson et al., 2003). Although the choice of using an internal control depends generally on the researcher's preference, it can facilitate troubleshooting of problems encountered during detection assays.

Real-time RT-PCR for quantitative detection of virus genes: Are the genes of a RNA virus expressed at the same time at the same level? Except for the subviral agents, such as satRNAs and the viroids, most RNA viruses have more than one gene but, to date, determination of the genomic RNA both in their virion and host tissue is still a big challenge. For example, to our present knowledge, it is hard to say, how a mono-genomic virus, such as a potyvirus, transcribes and expresses its genome, and how and when are its gene products controlled. It is unconscionable and uneconomical to produce all the proteins at the same time and of the same amount. It can also never be clearly evaluated if a tripartite virus, such as CMV, has the same amount of a gene fragment expressed or not. A reliable and convenient molecular measurement is required for understanding such key sects. The amounts of viral genomic RNAs which represent the expression levels of a viral gene, were previously quantified by electrophoresis, Northern blot hybridization and RT-PCR (Gal-On et al., 1995). However, the above methods vary in their usefulness for accurate quantification, being either time-consuming, laborious, insensitive, or having large variations in results. None of the above methods can be used for a full resolution of the quantitative measurement of viral RNAs singly. Present progress in gene sequencing and quantitative approaches provide the possibility for such an understanding of the realities. A highly sensitive laboratory method, PCR (RT-PCR for ssRNA viruses) provides much confidence for direct observation of the electrophoresis mass, but it cannot be considered as an accurate measurement. Real-time RT-PCR is a new method developed in recent years. By adding the fluorescent signal to the PCR reaction mixture, the whole PCR process is monitored through the increase in fluorescence, and the absolute amount of the target is calculated from a calibration curve. Due to its high sensitivity and reproducibility, real-time RT-PCR has been considered as the most reliable method currently and is used broadly in foreign gene (e.g. transgenic or pathogen) detection and quantification, and gene expression studies (Mackay et al., 2002; Valasek and Repa, 2005). Its applications in plant virology researches are increasing, and many economically important plant viruses have been detected by this method (Boonham et al., 2003; Zhu et al., 2003; Balaji et al., 2003; Delanoy et al., 2003). But most of these researches concern viral detection, taking advantages of its broad quantification range (≥ 7 magnitudes) and low titration limitation.

CMV is a type of species of the *Cucumovirus* genus, within the family *Bromoviridae*. It has a genome structure consisting of three single-stranded messenger sense RNAs (RNAs 1, 2 and 3) and two subgenomic RNA 4A and RNA 4 (Roossinck, 2001). Some strains of CMV harbor satRNAs, as small linear molecules ranging from 332 to around 400 nucleotides long. These satRNAs do not show any apparent homology to the viral genomic RNAs, but depend on CMV for their replication, encapsidation and transmission. Although there are no

apparent functional open reading fragments in satRNAs, they can usually modify symptoms induced by CMV. The success of this parasitism, and the extent to which symptoms have been modified, depend on the particular strains of CMV and satRNA, and the species of host plant as well. In many hosts, satRNA can attenuate the symptoms, but the molecular mechanism still remains unknown. Since the functions of CMV replication, movement and pathogenicity have been mapped to each of the five known genes, quantitative analysis of the effect of satRNA on their accumulation kinetics will contribute to a better understanding of the interaction of satRNA and its helper virus. Hereby, ways and means for quantitative determination of the helper virus and the satellite RNA will provide a better approach to understanding the effect of satRNA on the genes function of the helper virus.

The development of a real-time RT-PCR (SYBR Green I) assay, which allows an accurate quantification of CMV genomic RNAs, is to be introduced, with its use for the first termination of the genomic RNA ratio in virion and *in planta* for a tripartite, and for the satRNA affect on the accumulation of its helper viruses. Using the newly developed techniques, the copies of genomic RNA1, RNA2 and RNA3 and the subgenomic RNA4 in CMV particles are quantified by this method, and the ratios are determined as being about RNA1:RNA2:RNA3:RNA4 for 1:1.2:3.6:5.8, and the *in planta* accumulation levels of different ORFs among CMV genome can be determined. See details in Section 2.5.

The amounts of CMV genomic RNAs are usually quantified by Northern blot hybridization (Gal-On et al., 1995). Northern blot hybridization is considered to be the most specific in comparison with other conventional methods, but it is laborious and the results have larger variations, which could not meet the needs of most research, especially the RNA quantification assay, such as lab-on-a-chip measurement, RT-PCR and ultra-centrifugation combined measurements.

2.2 Multiplex RT-PCR System for Simultaneous Detection of Five Potato Viruses

More than 25 viruses have been reported to infect the potato (*Solanum tuberosum*). *Potato virus Y* (PVY), *Potato virus X* (PVX), *Potato virus A* (PVA), *Potato virus S* (PVS), and *Potato leaf roll virus* (PLRV) are known to cause serious diseases, and significantly reduce the yield and quality of potato crops. These viruses cause remarkable economic losses in potato production in China and North America. Accurate and timely diagnosis of the viruses is the first requirement for their control. Techniques used for the diagnosis of potato viruses include biological assay, electron microscopy, serology, virus-specific double-stranded RNA analysis, nucleic acid hybridization and PCR-based methods. Due to their rapidity and simplicity, molecular techniques (e.g., RT-PCR, real-time PCR, nucleic acid hybridization) and serological techniques (e.g., double-antibody sandwich enzyme-linked immunosorbent assay [DASELISA]) are popular in diagnostic

laboratories. However, most of the above techniques are designed for specific detection of a single virus. Recently, the potential of microarray technology for plant viral diagnosis has been investigated using a range of potato viruses as a model system. The microarray technique can detect multiple targets in a single assay, but high cost and the requirement for specific instruments limit its usefulness as a routine diagnostic tool for plant viruses.

The sequences and primers used for simultaneous detection of potato viruses are given in Table 2.1.

Table 2.1 List of primers used to prepare fluorescently labeled DNA probes

Virus	Abbreviation	Accession No.	Sequence (5'–3')	Position	Product (bp)
CMV	CMV-L	AF533968	TGTGGGTGACAGTCCGTAAAG	566–584	277
	CMV-R		AGATGTGGGAATGCGTTGGT	841–822	
TMV	TMV-L	AY360447	TCACKACTCCATCKCAGTTYGTGTT	538–562	223
	TMV-R		GGTCTARTACCGCATTGTACCTGT	760–736	
PVA	PVA-L	AY360381	TTTCTATGAGATCACTGCAACCACT	1–25	116
	PVA-R		TGACATTTCCGTCCAGTCCAA	116–96	
PVY	PVY-L	AY423428	ATACTCGRGCAACTCAATCACA	1–22	166
	PVY-R		CCATCCATCATAACCCAAACTC	166–145	
ZYMV	ZYMV-L	AY074809	CCAACGCTGCGACAAATAATG	493–513	287
	ZYMV-R		TGCCGTTCAAGTGTCTTCGC	779–761	
PSTVd	PSTV-L	AY360446	GGGAAACCTGGAGCGAACTG	96–115	116
	PSTV-R		CGAGGAAGGACACCCGAAGA	192–211	

2.2.1 Comparison of 18S rRNA and *nad2* mRNA as Internal Controls

Sensitivity of *Solalasooum* 18S rRNA internal control has been compared with that of *nad2* mRNA internal control by detecting 18S rRNA and *nad2* mRNA, respectively, with RT-PCR in serial dilutions of potato RNA extract. The 18S rRNA was detected in up to a 109 dilution, 105 times greater than *nad2* mRNA (Fig. 2.1). No amplicons are produced from the potato RNA extract through direct PCR amplification (Fig. 2.1(a), lane 1, and Fig. 2.1(b), lane 1), and no amplicons are produced from the *E. coli* RNA extract through RT-PCR amplification (Fig. 1(a), lane 2, and Fig. 2.1(b), lane 2). Stabilities of 18S rRNA, *nad2* mRNA, and PVX are analyzed with the potato leaves incubated at 4 °C and at room temperature for different periods. Results show that 18S rRNA, *nad2* mRNA, and PVX are detectable in tissues incubated at 4 °C at all six time points (Fig. 2.2(b), (d), and (f)), but the concentration of the product from *nad2* mRNA decreased sharply, as estimated, by decreasing stain intensity after incubation for 10 d (Fig. 2.2(d), lane 6). 18S rRNA and PVX are also detectable in tissues incubated at room

temperature at each time point (Fig. 2.2(a) and (e)); however, *nad2* mRNA was not detectable after incubation for more than 8 d (Fig. 2.2(c), lanes 5 and 6). Agarose formaldehyde electrophoresis shows that RNA samples from tissues stored at room temperature, especially for more than 8 d, displayed a higher level of RNA degradation than those from tissues stored at 4°C.

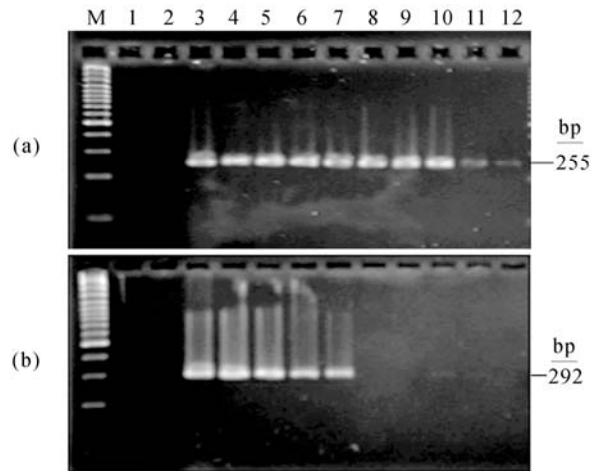


Fig. 2.1. Detection of 18S rRNA and *nad2* mRNA by RT-PCR. Primer pair's 18SF/18SR (a) and PotatoNad2F/PotatoNad2R (b) are used separately. Lane M: DNA marker; lane 1: RNA from potato leaf tissue without reverse transcription; lane 2: *Escherichia coli* strain DH5 α RNA; lanes 3 to 12: Amplification products of potato RNA diluted, 100, 101, 102, 103, 104, 105, 106, 107, 108 and 109, respectively

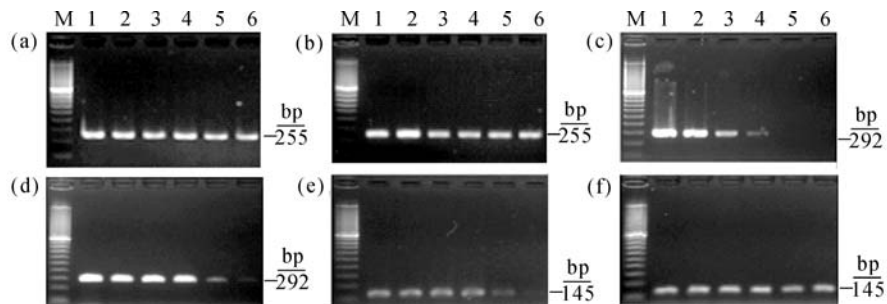


Fig. 2.2. Detection of 18S rRNA, *nad2* mRNA, and *Potato virus X* (PVX) by RT-PCR. The primer pairs are 18SF/18SR ((a) and (b)), PotatoNad2F/PotatoNad2R ((c) and (d)), and PVXF/PVXR ((e) and (f)). (a), (c), and (e): Potato leaves kept at room temperature; (b), (d), and (f): Potato leaves incubated at 4 °C. Lane M: 100-bp DNA ladder; Lanes 1 to 6: Potato leaf tissue samples incubated for 0, 2, 4, 6, 8 and 10 d, respectively

Since 18S rRNA displayed a much higher detection sensitivity than *nad2* mRNA and similar degradation kinetics in leaf tissues to PVX RNA, we believe it is a better internal control for virus detection of tissue samples. Therefore, 18S

rRNA was selected as the internal control to optimize the multiplex RT-PCR system for detecting five potato viruses.

2.2.2 *The Optimized System for Simultaneous Detection of Potato Viruses with Multiplex RT-PCR*

When the RT product, synthesized from the mixture of the five viruses, is amplified separately by PCR with 18S rRNA and each virus-specific primer pair of the five viruses, amplicons of the expected size for PVA (116 bp), PVX (145 bp), PVY (166 bp), PLRV (208 bp), PVS (342 bp), and 18S rRNA (255 bp) can all be detected in a single PCR (Fig. 2.3). Thus, the RT product can be obtained for first strand cDNA from all five viruses and 18S rRNA. Next, by using the RT product as a DNA template for the subsequent optimization assays of multiplex PCR, major reaction components for multiplex PCR, including DNA polymerase, MgCl₂, dNTPs and primer concentrations are systematically optimized. Optimal results were achieved when the reaction mixture consisted of 0.1 U/μl *Taq* HS DNA polymerase and 4.0 mmol/L MgCl₂. Optimum thermocycling results are achieved using 35 cycles of 94 °C for 30 s, 58 °C for 30 s, and 72 °C for 25 s. Virus mixtures containing zero, one, two, three, four, or five different viruses are analyzed by this optimized protocol. Amplicons of the expected size are successfully produced in all tested virus mixtures (Fig. 2.4).

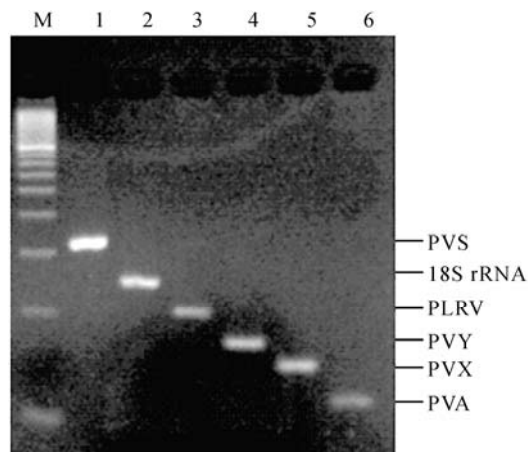


Fig. 2.3. Detection of five viruses and 18S rRNA from a mixture of individually infected leaf tissues by RT-PCR using virus-specific primer pairs
Lane M: 100 bp DNA ladder; Lane 1: PVSF/PVSR; Lane 2: 18SF/18SR; Lane 3: PLRVF/PLRVR; Lane 4: PVYF/PVYR; Lane 5: PVXF/PVXR; Lane 6: PVAF/PVAR. Amplification products corresponding to individual viruses and the 18S rRNA are indicated on the right

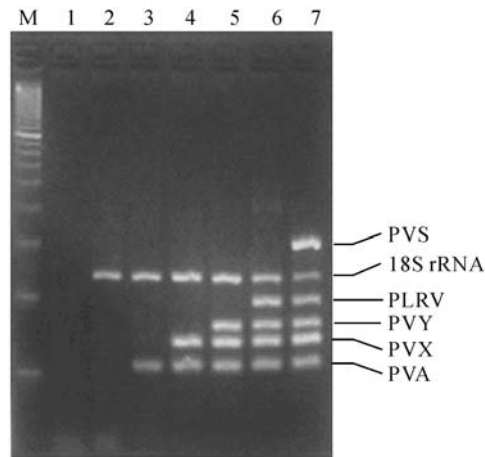


Fig. 2.4. Detection of different virus combinations by multiplex RT-PCR
 Lane M: 100-bp DNA ladder; Lane 1: water control; Lane 2: 18S rRNA; Lane 3: 18S rRNA and *Potato virus A* (PVA); Lane 4: 18S rRNA, PVA, and *Potato virus X* (PVX); Lane 5: 18S rRNA, PVA, PVX, and *Potato virus Y* (PVY); Lane 6: 18S rRNA, PVA, PVX, PVY, and *Potato leaf roll virus* (PLRV); Lane 7: 18S rRNA, PVA, PVX, PVY, PLRV, and *Potato virus S* (PVS). Amplification products corresponding to individual viruses and the 18S rRNA are indicated on the right

2.2.3 Sensitivities of Multiplex RT-PCR and DAS-ELISA in Detecting Potato Viruses

The sensitivity of the optimized multiplex RT-PCR and DAS-ELISA are compared by detecting PVX in serial concentrations of PVX virions, which are diluted with healthy leaf sap. The multiplex RT-PCR protocol detected as little as 0.5 pg of PVX without any nonspecific amplicons (Fig. 2.5(a)). The sensitivity of this protocol is 100 times higher than that of DAS-ELISA (Fig. 2.5(b)).

Based on the optimized multiplex RT-PCR system, 20 field potato samples have been tested by multiplex RT-PCR in comparison with DAS-ELISA. DAS-ELISA detected PVY in 1 sample and PVS in 13 samples. PVA, PVX, and PLRV were not detected in any sample with DASELISA. Multiplex RT-PCR confirmed the presence of PVY and PVS in samples detected by DAS-ELISA. However, multiplex RT-PCR was able to detect PVX in one sample and PVS in another sample that was not detected by DAS-ELISA. The two samples were confirmed to be infected with PVX and PVS, respectively, by single virus RT-PCR.

In conclusion, to be an internal control for potato virus detection, 18S rRNA is better than *nad2* mRNA in terms of detection sensitivity and degradation kinetics. A host RNA molecule used as an internal control in a virus-detection system should have similar degradation kinetics to viral RNA in host tissues. Smith et al.

has found that rRNA from mouse brain tissues had similar degradation properties to viral RNA and was more suitable as an internal control than *actin* mRNA. Plant NADH dehydrogenase mRNA has been used regularly as an internal control in virus-detection systems. By comparing 18S rRNA with *nad2* mRNA from potato leaf tissues, it has been shown that amplification of 18S rRNA is 105 times greater in sensitivity than that of *nad2* mRNA. In experiments, both 18S rRNA and PVX were amplified from tissue samples incubated at 4 °C and at room temperature for up to 10 d, but *nad2* mRNA was not detectable from the samples incubated at room temperature for more than 8 d, indicating the degradation kinetics of 18S RNA is more similar to PVX RNA than that of *nad2* mRNA.

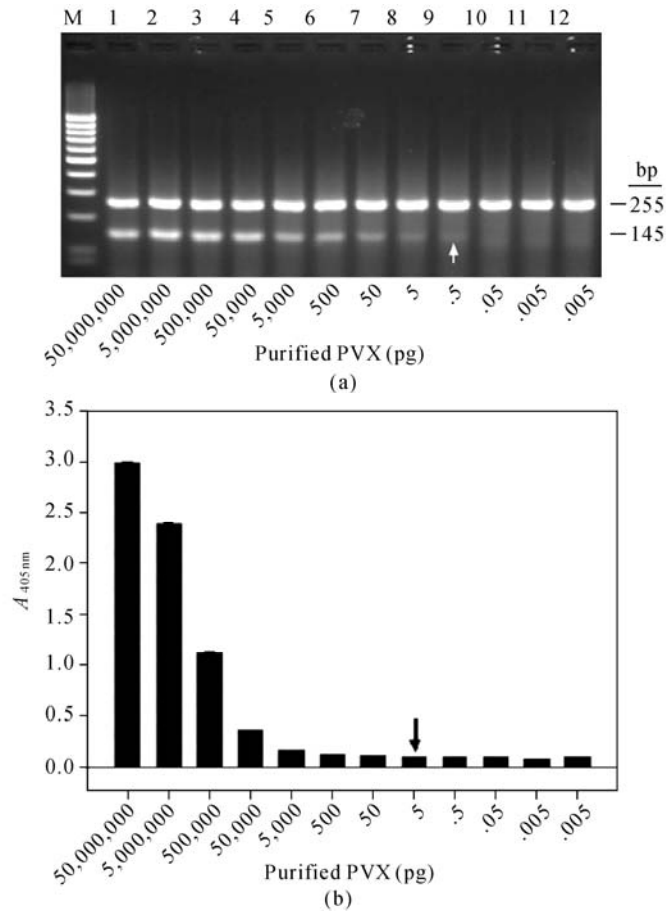


Fig. 2.5. Sensitivities of multiplex RT-PCR and DAS-ELISA for *Potato virus X* (PVX) detection in serial dilutions of virions (a) Multiplex RT-PCR; (b) DAS-ELISA. In both assays, tenfold serial dilutions of PVX virions were prepared by diluting 50 μg purified PVX virions with healthy potato leaf sap. Average absorbance value ($A_{405\text{ nm}}$) and standard error are presented in (b). The detection limits of both methods are indicated with arrowheads

2.3 Detection of Cucumber Mosaic Virus Subgroups and Tobamoviruses Infecting Tomato

The tomato, *Lycopersicon esculentum* Mill., named as the reservoir of many plant viruses, is an important economic crop all over the world. In Eastern China, it is mostly consumed as a fresh vegetable. With an increasing demand, it has become a daily vegetable grown all the year. That brings about the accumulation of diseases including viral diseases caused by CMV, ToMV and several Gemini viruses etc. Viral diseases often lead to losses of yield and fruit quality in different degrees depending on growing conditions. Generally, green house cultivated tomato and summer tomato crops are less infected, while tomato crops growing in the open field and autumn tomato crops are more severely infected. CMV, ToMV, PVX, PVY, TSWV and ToRSV have been found as the main epidemic viruses in many places (Labate et al., 2007). *Cucumovirus*, *Tobamovirus* and *Geminivirus* are of increasing importance for their occurrence in China and other Asian countries. Viruses infecting tomato in China were surveyed repeatedly over the last decades, and CMV and ToMV were considered as the most important viruses in this crop. To our knowledge, single or mixed infection of the two viruses above is a devastating threat to the field tomato in eastern China, where the tomato is grown on a large scale.

CMV sometimes isolates the infected tomato with additional 333–405 nt RNA as satRNA, and the presence of satRNAs can modify the symptoms in tomato plants caused by CMV. Based on present reports, CMV subgroup I used to predominant in the tropics and subtropics, whereas subgroup II is more frequently found in temperate regions (Haase et al., 1989). Since the first two isolates of CMV subgroup II were identified from the tomato in China (Feng and Yang, 2000), more subgroup II isolates have been detected in neighboring areas (Yu et al., 2005).

On the other hand, genomic recombination of CMV has been noticed in many areas. Analysis of CMV collected from Spain showed that the frequency of reassortants among subgroups IA, IB, or II was about 5%, and that of recombinants between these groups was 17%. Recombinants at RNA3 were significantly more frequent than recombinants at RNAs 1 and 2 (Broadbent, 1976).

As the typical species of *Tobamoviruses*, TMV, is closely related to ToMV. As a distinct strain of TMV, ToMV was separated from TMV early in 1971 according to the serological relationship and nucleotide sequence. Although the two viruses have been historically considered synonymously, the predominant virus in tomatoes worldwide is considered to be ToMV (Pfitzner, 2006). Mixed infection of CMV and ToMV in tomatoes has been reported frequently. A severe necrosis disease due to mixed infection of the above two viruses arising in eastern China was noticed in 2007. The typical symptoms displayed during the fruit season were top necrosis, plant stunt and fruit distortion, combined with brown necrosis strikes among stems and leaf stalks, which developed into the death of the whole plant (Chen et al., 2007). This damage occurred more severely when high temperatures

prevailed. To understand the occurrence of CMV and differentiate *Tobamoviruses* in tomatoes is basically sufficient for epidemiological investigations aiming to manage the principal viruses. Hence, an accurate, reliable and effective method for routine diagnosis of the above viruses is desirable.

Several methods have been described to identify plant viruses and many CMV isolates are characterized using RT-PCR, TAS-ELISA and immunocapture RT-PCR methods (IC-RT-PCR) (Rizos et al., 1992; Sharman et al., 2000; Yu et al., 2005). In addition, with a combination of virus specific antibody capture and primer specificity, a multiplex IC-RT-PCR assay for differentiation of TMV and ToMV was described (Jacobi et al., 1998). However, to understand more complex epidemiology of viruses infecting the tomato, simultaneous detection is still unavailable, which would allow us to distinguish all the above viral species and subgroups.

Thus, using 18S rRNA as an internal control, a multiplex RT-PCR method that can detect and differentiate CMV I and CMV II with satRNA, quickly and simultaneously, as well as for TMV and ToMV, is now introduced as follows. It also utilizes the detection method to exam viral epidemiology in tomato crops.

2.3.1 Multiplex RT-PCR for Simultaneous Detection of Strains of CMV and ToMV in Tomato

The multiplex RT-PCR system has been optimized, using ToMV and a strain of CMV from different subgroups with or without satellite.

- **Primer Sequences Suggested for Detecting Tomato Viruses**

The cDNA clones of viral strains used for simultaneous detection and their GenBank accession numbers are given in Table 2.2. And the sequences of primers used in the multiplex reverse-transcription polymerase chain reactions are listed in Table 2.3.

Table 2.2 Viral strains used in multiplex RT-PCR for simultaneous detection of tomato viruses

Clone of virus	Accession number
CMV-Fny	D10538
CMV-Tsh	EF202597
ToMV	GQ280794
TMV	GQ280795
Sat RNA	EF363688
18SrRNA	GQ280796

Table 2.3 Sequence of primers used in multiplex RT-PCR for simultaneous detection of tomato viruses

Virus	Code No.	Primer sequence (5'-3')	Position	Product size (bp)
CMV	CMVII F	CTACGTTTATCTTCC	970–984	704
	CMVII R	AACCGGTGATTTACCATCGC	1655–1674	
CMV	CMVI F	GCCACCAAAAATAGACCG	1484–1502	593
	CMVI R	ATCTGCTGGCGTGGATTCT	2057–2076	
TMV	TMV F	CGATGATGATTCGGAGGC	5664–5681	512
	TMV R	GAGGTCCARACCAAMCCAG	6157–6175	
ToMV	ToMV F	CATCTGTATGGGCTGAC	5746–5762	421
	ToMV R	GAGGTCCARACCAAMCCAG	6148–6166	
satRNA	satRNA F	GTTTTGTTTGTGGAGAGTTGCG	1–22	385
	satRNA R	GGGTCCTGTAGAGGAATGTGACATT	369–385	
18S rRNA	18S F	GAGAAACGGCTACCACATCCA	399–419	255
	18S R	CGTGCCATCCCAAAGTCCAAC	633–653	

- **Multiplex RT-PCR System and Protocols for Detecting Tomato Viruses**

The optional concentration of each primer pair is used as the following: CMV-II F/R, 10 pmol/L; CMV-I F/R, 1.25 pmol/L; TMV F/R, 5 pmol/L; ToMV F/R, 3.5 pmol/L; satRNA F/R, 1.25 pmol/L and 18S rRNA F/R, 1.25 pmol/L. As the positive control, the template concentration of each cDNA clone is adjusted empirically, which is CMV-II, 1.5 ng/μl; CMV-I, 11.5 ng/μl; TMV, 3 ng/μl; ToMV, 2 ng/μl; satRNA, 1.8 ng/μl; and 18S rRNA, 1 ng/μl.

In the multiplex RT-PCR system, total RNAs from 100 mg fresh leaf tissues is extracted, alternatively, portions of leaf tissues are kept under -80°C but are recommended to be used within six months without repeated freezing and thawing. The extraction is carried out by using TRizol Reagent (Canadian Life Technologies, Canada) following the manufacturer's protocol and dissolved in 35 μl of diethyl pyrocarbonate-treated (DEPC) water.

An optimized multiplex RT-PCR system is recommended as follows. Considering the different efficiency in amplification and the size of fragments, the final concentration of viral antisense primer is as follows: CMV-II 4 pmol/L, CMV-I 1 pmol/L, TMV (ToMV) 6 pmol/L, satRNA 1 pmol/L. For the abundance of 18S rRNA in total RNA, its concentration is 1 pmol/L.

The recommended reaction mixture consisted of 2U *Taq* DNA polymerase, 100 μmol/L dNTPs and 2.0 mmol/L MgCl_2 in a total volume of 50 μl. The optimal multiplex PCR reaction is conducted with one cycle at 94°C for 3 min, followed by 35 cycles at 94°C for 30 s, 52°C for 30 s, 72°C for 105 s, and an additional cycle at 72°C for 10 min.

The experimental detection results are shown in Figs. 2.6, 2.7 and 2.8.

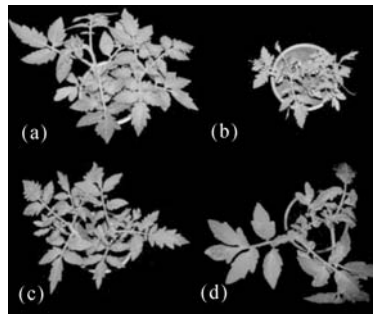


Fig. 2.6. Typical symptom in tomato induced by greenhouse infection of viruses
(a) Mock inoculation with buffer; (b) Linear; (c) Mosaic; (d) Necrosis on up-inoculated leaves of tomatoes

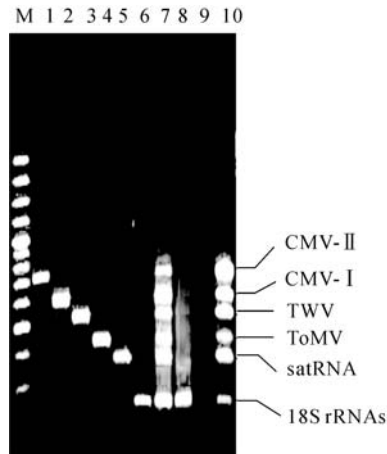


Fig. 2.7. Detection of viruses from a mixture of leaf tissues with individually infected viruses using simplex or multiplex RT-PCR
Lane M: 100 bp DNA ladder; Lane 1: CMV-IIF/R; Lane 2: CMV-IF/R; Lane 3: TMV F/R; Lane 4: ToMV F/R; Lane 5: SatRNA F/R; Lane 6: 18S rRNA F/R; Lane 7-10: Mixed primer pairs; Lane 8-10: Multiplex PCR control (healthy leaf tissue, ddH₂O, six cDNA clones respectively). 0.1 g of leaf tissue was used for each

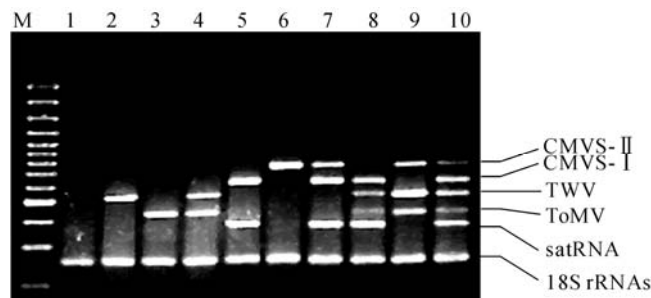


Fig. 2.8. Detection of virus combinations from mixing infected leaf tissues using multiplex RT-PCR
Lane M: 100-bp DNA ladder; Lane 1: Healthy leaf tissue; Lane 2: TMV; Lane 3: ToMV; Lane 4: TMV and ToMV; Lane 5: CMV-I+satRNA; Lane 6: CMV-II; Lane 7: CMV-I+satRNA, CMV-II; Lane 8: TMV, ToMV and CMV-I+satRNA; Lane 9: CMV-II, TMV and ToMV; Lane 10: All the viruses

Sensitivities of multiplex RT-PCR and DAS-ELISA: The sensitivities of multiplex RT-PCR are found out using a 10-fold dilution of mixture viral RNA with total RNA extract from a healthy tomato leaf, while the detected limit of ELISA is determined using 10-fold dilution of virions of CMV-Fny diluted with extract from a healthy tomato leaf. The multiplex RT-PCR showed positive results until 10^{-6} (≈ 1 pg) for CMV-Fny (Fig. 2.9), while the positive result of ELISA was 10^{-3} (≈ 1000 pg) (Fig. 2.10).

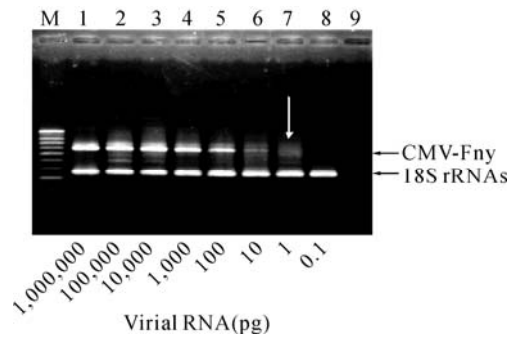


Fig. 2.9. Sensitivity of multiplex RT-PCR for detecting CMV
 Lane M: 100 bp marker; Lanes 1–8: RT-PCR products of virial RNA of a tenfold serially diluted in total RNA of a healthy plant; Lane 9: Blank. The detection limit of multiplex RT-PCR is indicated with arrowhead

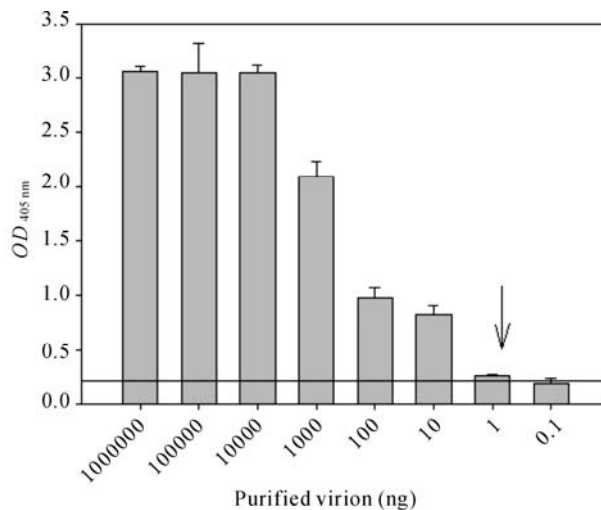


Fig. 2.10. Sensitivity of ELISA for detecting CMV
 Absorbance value ($A_{405\text{ nm}}$) and standard error are presented. The detection limit of ELISA is indicated with arrowhead. The line shows the two fold A -value of health, which interprets the positive results

2.3.2 *Field Detection of Tomato Viruses by Multiplex RT-PCR*

The field tomato leaf tissues with symptoms of mosaic, local necrotic, or stunted growth, were collected in 2007 and 2008. 159 samples were analyzed by multiplex RT-PCR and ELISA. Using ELISA, PVX was detected in one sample and PVY in one sample. TMV and ToMV, as well as CMV I and CMV II can be detected by ELISA, but there is cross reaction between TMV and ToMV, also between CMV subgroup I and CMV subgroup II. Using multiplex RT-PCR, viruses were detected in 128 samples, including some mixed infection of viruses (Table 2.4). No virus was detected by multiplex RT-PCR in some samples. In our judgement, that may be on account of a low concentration of the test virus, or because of other viruses, such as PVX and PVY detected by ELISA. Partial results of multiplex RT-PCR are shown in Fig. 2.11.

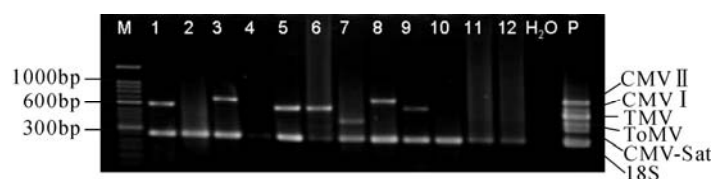


Fig. 2.11. Multiplex RT-PCR detection of field samples collected in China
Lane M: 100-bp marker; Lanes 1–12: Field samples; Lane 13: Blank; Lane 14: Six cDNA clones as the positive control

Table 2.4 Field occurrence of strains of CMV and ToMV detected by multiplex RT-PCR

Combination	Year		Total (159 samples)
	2007 (69 samples)	2008 (90 samples)	
CMV subgroup I	29	35	64
CMV subgroup II	9	4	13
TMV	1	0	1
ToMV	12	15	27
CMV subgroup I + ToMV	3	6	9
CMV subgroup II + ToMV	4	0	4
CMV subgroup I (satRNA)	5	2	7
CMV subgroup I (satRNA) + ToMV	3	0	3

2.3.3 *Identification of CMV Subgroups by Restriction Enzymes*

Restriction enzyme analysis: A method based on PCR and restriction enzyme analysis has been established to analyze the possibility of mixed infection by CMV strains of different subgroups and the natural reassortant between IA and II strains. Three primer pairs (Table 2.5), amplifying specific regions of CMV genomic RNAs, are designed according to nucleotide sequences of known CMV

isolates registered in GenBank. The expected sizes of RT-PCR products for different CMV subgroups are also shown in Table 2.5.

Table 2.5 Primers for RT-PCR amplification and restriction enzyme analysis

Primer	Positions ¹	Size ² (nt)	Nucleotide sequence ³
R1-599-F	168–188	599	5'-TCGTTGATAAGACAGCTCATG-3'
R1-599-R	743–762		5'-CCTTGGTCGTCAAACATCAT-3'
R2-513-F	2036–2056	513	5'-ACTCTCTGAYGAGTTYGGTAA-3'
R2-513-R	2531–2549		5'-CTCTCGCTGGGACTTTTGT-3'
R3-625-F	1408–1429	625/639	5'-CMACTMTTAACCACCCAACCTT-3'
R3-625-R	2021–2038		5'-GCCGTAAGCTGGATGGAC-3'

¹ Nucleotide positions of the primers in the genomic RNAs of Fny strain of CMV;

² Expected size of the resulting RT-PCR product;

³ Y= C or T, M = A or C

The relationship between restriction maps and different CMV subgroups is shown in Table 2.6. Digestion of the 600 bp DNA fragment corresponding to CMV RNA1 with *Cac8* I expects two restriction patterns: the 600 bp DNA fragments of subgroup I strains contain no *Cac8*I restriction site, while those of subgroup II give a pattern consisting of three fragments, approximately 45, 180 and 375 bp in size after digestion. Digestion of the 510 bp DNA fragment corresponding to RNA2 with *Cl*a I also expects two restriction patterns: the 510 bp fragments of subgroup I are digested into three fragments (approximately 40, 130 and 340 bp), while those of subgroup II contain no *Cl*a I restriction site. Digestion of the 625 bp/640 bp DNA fragment corresponding to RNA3 with *Msp* I expects three mainly restriction patterns. The 625 bp fragments of subgroup IA are digested into two fragments (approximately 290 and 335 bp), and those of subgroup IB produce four fragments (approximately 30, 95, 210 and 290 bp) except for strains Ix and Sd due to their high genetic diversity. However, the digestion of 640 bp fragments of subgroup II strains produce five fragments of about 30, 40, 125, 195 and 250 bp, respectively. Based on above analysis of different restriction patterns, RNAs 1, 2 and 3 of CMV strains can be classified into subgroup I or II.

Table 2.6 Correlation between the restriction maps and CMV subgroups

(a)				
Strains	Subgroup	Length	<i>Cac8</i> I site	Restriction map
Fny, Leg, Mf, Y	IA	599	0	599
Nt9, IA, Ix, Sd, Tfn	IB	598–599	0	599
LY, LS, Q, S, Trk7	II	596–599	2	45, 181, 373
(b)				
Strains	Subgroup	Length	<i>Cl</i> a I site	Restriction map
Fny, Leg, Mf, Y, O	IA	513	2	38, 132, 343
Nt9, IA, Ix, Sd, Tfn	IB	516	2	38, 132, 346
LY, LS, Q, R, S, Trk7	II	508–511	0	510

(c)

Strains	Subgroup	length	MspI site	Restriction map
Fny, Leg, Mf, Y, O	IA	623–625	1	288, 337
Nt9, IA, Tfn	IB	625	3	28, 97, 211, 289
Ix	IB	623	1	288, 335
Sd	IB	625	2	28, 288, 309
LY, LS, Q, R, Trk7	II	639	4	28, 40, 125, 197, 249

(d)

Strains	Subgroup	Length	MspI site	Restriction map
LY, LS, Q	II	867–870	5	28, 110, 126, 158, 197, 248
R, Trk7	II	875–877	5	28, 120, 126, 158, 197, 248

(a) The *Cac8*I restriction map of 599 bp fragment of CMV RNA1; (b) The *Call* restriction map of 513 bp fragment of CMV RNA2; (c) The restriction map of 625 bp fragment of CMV RNA3; (d) The restriction map of 870 bp fragment of RNA3 of CMV subgroup II strains

Different regions of genomic RNAs of CMV-Fny, CMV-LS and CMV-Tsh are amplified by RT-PCR (Fig. 2.12). For RNA1, RT-PCR products of Fny, LS and Tsh are all approximately 600 bp as expected size (Fig. 2.12(a)). For RNA2, about 510 bp fragments were obtained for all three tested strains (Fig. 2.12(b)). For RNA3, about 630 bp fragments were amplified for all three tested strains (Fig. 2.12(c)).

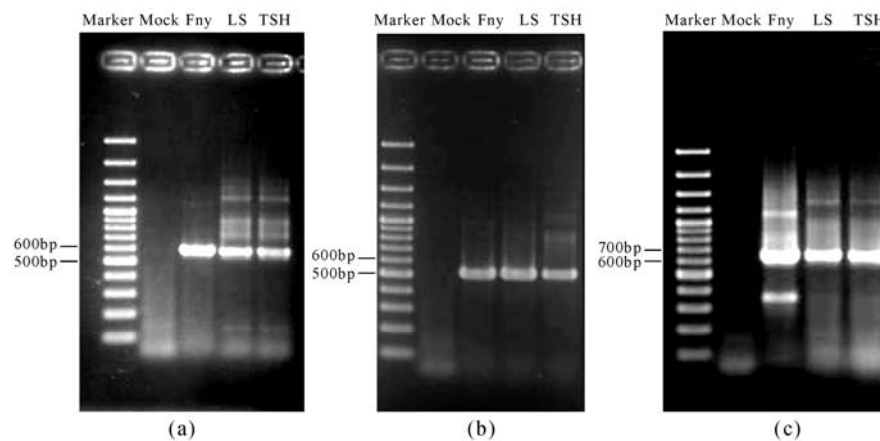


Fig. 2.12. Analysis of RT-PCR products of different regions of CMV genomic RNAs (Electrophoresis on 1.5% agarose gel)
 (a) 599 bp RNA1 fragments; (b) 513 bp RNA2 fragments; (c) 625 bp RNA3 fragments

Cac8 I digestion results of the 600 bp fragment corresponding to RNA1 revealed that Tsh RNA1 shared the same pattern with LS (Fig. 2.13(a)). This pattern is the same as the expected restriction pattern of subgroup II strains. For the 510 bp fragments, the digestion results (Fig. 2.13(b)) showed that Tsh and Fny

produced the same restriction pattern, which is the representation of subgroup I strains. For the 630 bp fragments, Tsh and LS produced the same restriction pattern specific for subgroup II strains (Fig. 2.13(c)). No mixed restriction pattern is found for all three fragments of CMV-Tsh. These restriction patterns demonstrated that RNA1 and RNA3 in the CMV-Tsh-infected tomato plant are derived from one or two subgroup II strain(s), while RNA2 in the CMV-Tsh-infected tomato plant is derived from a subgroup I strain. The five diseased tomato plants, sampled from the same planting area as the CMV-Tsh-infected tomato plant, present consistent restriction patterns with the CMV-Tsh-infected tomato plant.

The use of final identification of CMV genomic RNAs with restriction enzyme analysis of RT-PCR products is given in Fig. 2.13.

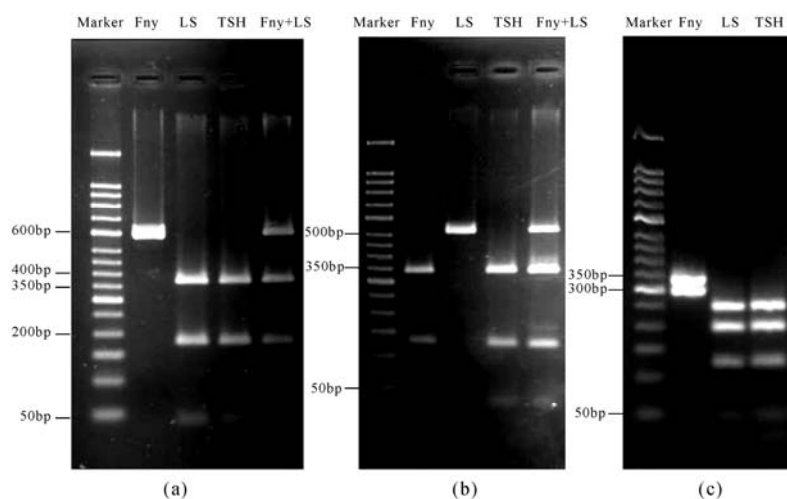


Fig. 2.13. Restriction enzyme analysis of RT-PCR products of CMV genomic RNA (Electrophoresis on 3% agarose gel)
 (a) 599 bp RNA1 fragments digested by Cac8I; (b) 513 bp RNA2 fragments digested by Call; (c) 625 bp RNA3 fragments digested by MspI

The restriction enzyme analysis results, along with sequence analysis results, can provide direct evidence as to whether a particular CMV is a naturally occurring reassortant between CMV subgroup IA and II strains or not.

2.4 A Novel Glass Slide Hybridization for Detecting Plant RNA Viruses and Viroids

A majority of plant viruses of economic importance are RNA viruses or viroids of RNA characters. When large numbers of samples have to be handled, DAS-ELISA is most widely used for the detection. Since viroids produce no specific protein, the serological test, applied so widely to viruses, can not be used for their

diagnosis. For this reason, nucleic acid hybridization on the membrane, RT-PCR and even electrophoresis with some modifications are developed for the detection of viroids. But up to now, most of the approaches to the application of nucleic acid hybridization for the diagnosis of plant viral diseases involve the use of filter hybridization, with a nylon membrane as the most popular matrix for immobilizing nucleic acids.

2.4.1 Preparation of Highly Sensitive Fluorescent-labeled Probes

Initially, nucleic acid hybridization was used to obtain hybrids between RNAs and DNAs in solution. Now the method is an important component of many techniques of molecular biology. Membrane hybridization methods exploit high specificity of molecular hybridization for detecting rare molecules in complex mixtures. Membrane dot-blot hybridization was firstly applied to *Potato spindle tube viroid* (PSTVd) detection. After that, the method with some modifications was successfully applied to detection of plant RNA and DNA viruses. When compared with a nylon membrane, a glass slide used for immobilization of nucleic acids in DNA microarray systems has unique merits, including covalent immobilization of DNA, durability to high temperature and high ionic strength, minimum hybridization volume and, in particular, parallel hybridization capacities. Presently, membrane hybridization with radioactive ³²phosphorous labels is still used widely, although some non-radioactive report systems have been developed.

In this section, a newly developed method modifying conventional RNA dot-blot hybridization is introduced. By replacing ³²phosphorous labels with CY5 labels and by replacing membranes with positive-charged glass slides, the modified RNA dot-blot hybridization method is named “RNA glass slide hybridization” and its application for detecting plant RNA viruses and a viroid is successful. The optimum efficiency of RNA binding onto surfaces of activated glass slides is simply achieved by utilizing aminosilane-coated glass slides as a solid matrix and using 5× SSC as a spotting solution. Combined with a CY5-labeled DNA probe prepared through PCR amplification, the optimized glass slide hybridization could detect as little as 1.71 pg of viral RNAs. The sensitivity of the modified method is four times that of dot-blot hybridization on a nylon membrane with a ³²P-labeled probe. The absence of a false positive within the genus potyvirus [*Potato virus A*, *Potato virus Y* (PVY) and *Zucchini yellow mosaic virus*] demonstrated that this method is of high specificity. Furthermore, PSTVd is also specifically detectable with this new method, demonstrating the extensive application of this method to plant viroid diagnosis. The primers used to prepare fluorescently labeled DNA probes described in this section are given in Table 2.7.

Table 2.7 List of primers used to prepare fluorescently labeled DNA probes

Virus	Abbreviation	Accession No.	Sequence (5'-3')*	Position	Product (bp)
CMV	CMV-L	AF533968	TGTGGGTGACAGTCCGTAAAG	566–584	277
	CMV-R		AGATGTGGGAATGCGTTGGT	841–822	
TMV	TMV-L	AY360447	TCACKACTCCATCKCAGTTYGTGTT	538–562	223
	TMV-R		GGGTCTARTACCGCATTGTACCTGT	760–736	
PVA	PVA-L	AY360381	TTTCTATGAGATCACTGCAACCACT	1–25	116
	PVA-R		TGACATTTCCGTCCAGTCCAA	116–96	
PVY	PVY-L	AY423428	ATACTCGRGCAACTCAATCACA	1–22	166
	PVY-R		CCATCCATCATAACCCAAACTC	166–145	
ZYMV	ZYMV-L	AY074809	CCAACGCTGCGACAAATAATG	493–513	287
	ZYMV-R		TGCCGTTTCAGTGCTTCGC	779–761	
PSTVd	PSTV-L	AY360446	GGGAAACCTGGAGCGAACTG	96–115	116
	PSTV-R		CGAGGAAGGACACCCGAAGA	192–211	

2.4.2 Effect of Spotting Solutions on Spot Quality

On newly surface-cleaned and aminosilane-activated glass slides, three types of spotting solutions have been compared in terms of overall fluorescent intensity and spot morphological homogeneity. Hybridization results showed that RNAs spotted in SSC solution yielded much higher signal intensities than those spotted in FF-SSC or DF-SSC (Fig. 2.14(a) and (b)). Increasing concentrations of formamide and DMSO in the solutions FF-SSC and DF-SSC reduced signal intensities, indicating that high concentrations of these two denaturants were unbeneficial to immobilizing RNA on the surfaces of the aminosilane slides. Also, SSC concentration can affect the hybridization signal intensity. RNA samples spotted in 5× SSC yielded significantly higher signal intensities than those spotted in 1× SSC or 3× SSC did ($P < 0.0085$). However, there was no significant difference between 1× SSC and 3× SSC in overall fluorescent intensities ($P = 0.9133$). Spot homogeneity is one of the critical criteria for evaluating spot quality. Inconsistent deposition of RNAs in many spots has been observed (Fig. 2.14(a)). In order to digitally analyze spot homogeneity, the CV of signal intensities was calculated for each spot produced by SSCs 1×, 3×, and 5×. The highest homogenous spots were yielded by using 5× SSC (lower CV values) as compared to 1× SSC and 3× SSC (Fig. 2.14(c)). Taken together, 5× SSC has been found to be the optimum RNA spotting solution tested.

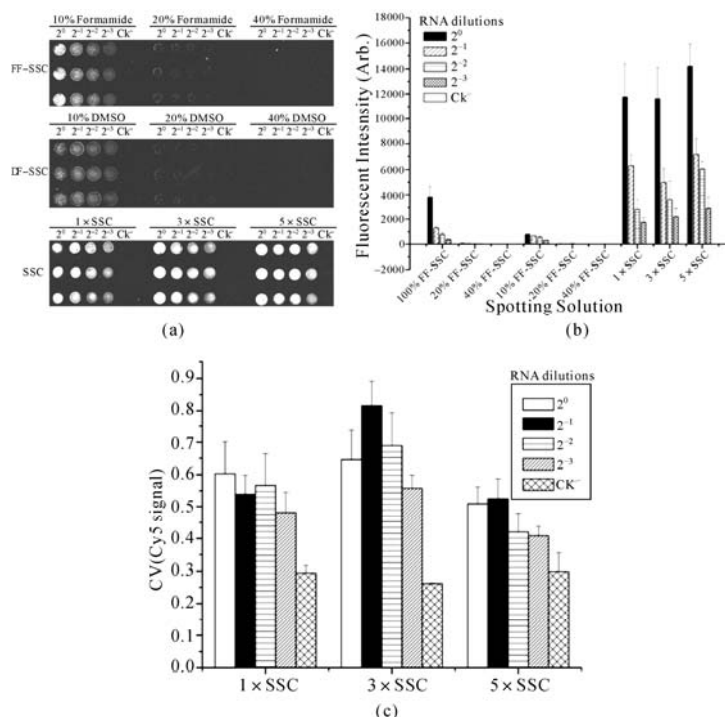


Fig. 2.14. Spot quality assessment of different spotting solutions

(a) Images of two-fold serial dilutions of TMV RNA spotted in three different solutions after hybridization with the CY5-labeled cDNA probe. These three concentrations [10%, 20%, and 40% (v/v)] of the denaturants (formamide and DMSO) in FF-SSC and DF-SSC were tested, and indicated on the upper. Three concentrations (1x, 3x, and 5x) of SSC in the solution SSC alone were tested, and indicated on the upper. The concentrations of SSC and formaldehyde in FF-SSC and DF-SSC were constant, 5x and 7% (v/v), respectively; (b) The average and standard deviation of the background-subtracted CY5 signals obtained from the spots of the TMV RNA dilutions for each spotting solution shown in (a); (c) The average CVs and standard deviations of the signal intensities obtained for CY5 based on all of the spots for the SSC spotting solution

2.4.3 Effect of Glass Surface Chemistries on Efficiencies of RNA Binding

Three types of glass slides with different chemical modifications (aminosilane, poly-L-lysine and aldehyde) have been tested in terms of capability of binding RNA onto their surfaces. RNA samples immobilized onto aminosilane slides generally yield stronger signals than those immobilized onto poly-L-lysine slides or aldehyde slides (Fig. 2.15). The overall signal intensities produced from aminosilane slides are significantly different from those produced from the other two types of slides ($P = 0.0001$). Fig. 2.15 showed that 7,000.00 pg (2.33 $\mu\text{g}/\mu\text{l}$) of

TMV RNA yielded much lower signal intensities on all the types of slides than the corresponding 3,500.00 pg (1.16 $\mu\text{g}/\mu\text{l}$) of TMV RNA did, demonstrating that 3,500.00 pg RNA almost reached the saturated quantity of RNA binding for all these three types of slides. It has also been found that the decreased signal intensity from 3,500.00 pg to 7,000.00 pg TMV RNA on the aminosilane slide is much less than those on the other two types of slides, demonstrating that the former probably have a strong capability of binding a high concentration of RNA. Taken together, glass slides coated with aminosilane are more suitable for RNA binding than those coated with either poly-L-lysine or aldehyde.

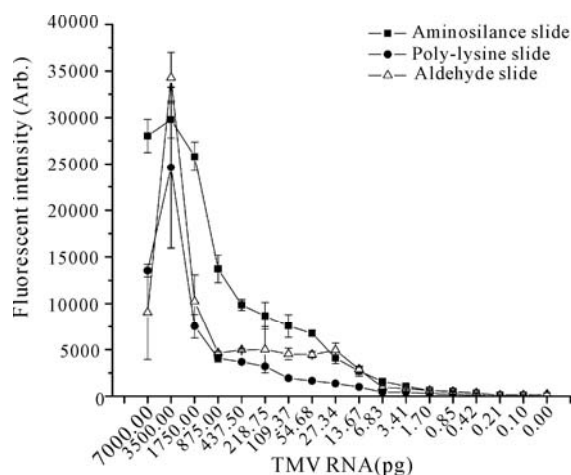


Fig. 2.15. Effect of different types of activated glass slides on RNA binding efficiency. The average and standard deviation of the background-subtracted CY5 signals obtained from spots of TMV RNA dilutions for each slide

2.4.4 Detection Limits of Glass Slide Hybridization and Nylon Membrane Hybridization

Detection limits of glass slide hybridization and nylon filter hybridization have been compared by detecting TMV RNA in serial dilutions. In the experimental condition, nylon membrane hybridization could detect 6.83 pg of TMV RNA (Fig. 2.16(a)). CY5-labeled DNA probes synthesized through either PCR amplification or random-priming labeling reaction are used to probe TMV RNA in its serial dilutions, and the five RNA samples extracted from healthy plant tissue gave a signal value of 13.46 ± 3.87 [Mean (F635 median-B635) \pm standard deviation], when hybridized with the PCR labeling probe. The signal value was 34.13 ± 16.26 when they hybridized with the random-priming labeling probe. According to these two signal values and the criterion described above, the cutoff values for the PCR labeling probe and the random-priming labeling probe were calculated to be 25.07

and 82.91, respectively. By comparing the cut-off values with the corresponding signal values of TMV RNA dilutions, the detection limit of glass slide hybridization with the PCR labeling probe was determined for 1.71 pg of TMV RNA, four times as sensitive as the nylon filter hybridization (Fig. 2.16(b)). However, the detection limit of glass slide hybridization with the random-priming labeling probe is 13.67 pg of TMV RNA, half as sensitive as the nylon filter hybridization (Fig. 2.16(c)).

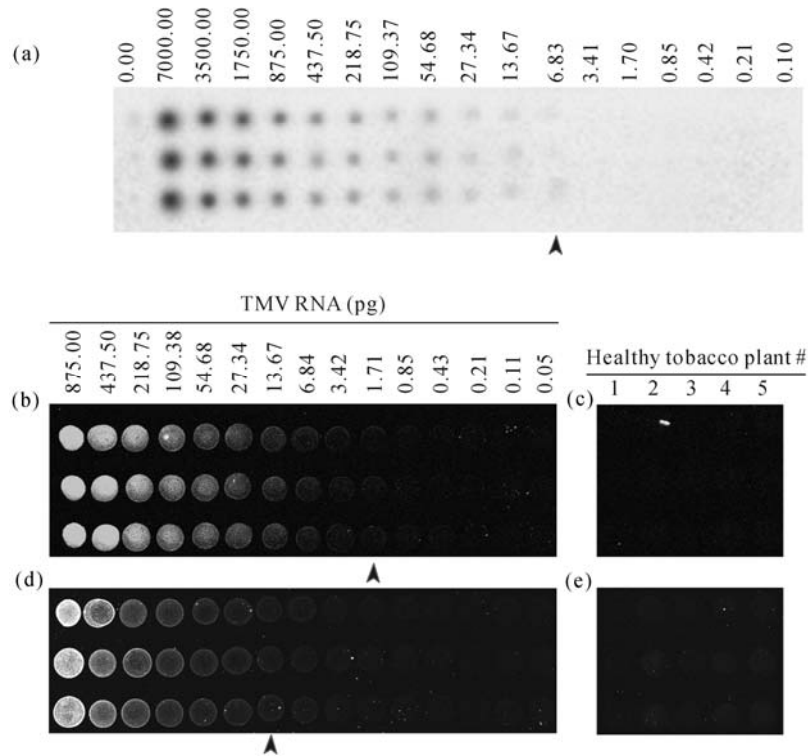
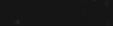
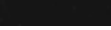


Fig. 2.16. Detection limits of two hybridization methods for detecting TMV RNA in serial dilutions (a) Nylon membrane hybridization with a ³²P-labeled DNA probe; (b) and (c) Glass slide hybridization with a CY5-labeled DNA probe prepared through PCR amplification; (d) and (e) Glass slides hybridization with a CY5-labeled DNA probe prepared through random-priming labeling reaction. In both assays, twofold serial dilutions of TMV RNA were prepared by diluting purified TMV RNA with total RNA from healthy tobacco leaf. Five healthy RNA samples were used to calculate the cut-off values for positiveness (c) and (e). Detection limits of both methods are indicated with arrowheads. Quantities of TMV RNA and the five healthy RNA samples are indicated on the upper

2.4.5 Specificity of Glass Slide Hybridization

To examine the specificity of glass slide hybridization, RNA samples, extracted from leaves infected singly with TMV [12 dpi], Q6-CMV (12 dpi), N6-CMV (6 dpi), PVY (60 dpi), ZYMV (30 dpi) and PSTVd (12 dpi), are spotted onto surfaces of aminosilane slides. The printed slides are then hybridized individually with six CY5-labeled probes: p-TMV, p-CMV, p-PVA, p-PVY, p-ZYMV, and p-PSTVd, being specific for TMV, CMV, PVA, PVY, ZYMV, and PSTVd, respectively. The hybridization results are shown in Table 2.8.

Table 2.8 Detection of RNA viruses and viroid in single infection by glass slide hybridization

Probes	Position on the glass slide [Mean (F635 median-B635)±standard deviation]**						Healthy control
	Q6-CMV	N6-CMV	TMV	PVY	ZYMV	PSTVd	
p-CMV	 2582.0±353.4*	 3943.4±789.2*	 8.4±2.8	 5.8±4.2	 9.4±23.5	 2.7±7.3	 5.4±3.2
p-TMV	 10.0±7.7	 15.5±11.2	 34342.6±409.0*	 2.0±5.6	 12.4±11.2	 10.2±4.3	 8.2±2.5
p-PVY	 18.4±15.1	 7.6±7.5	 12.6±6.1	 444.0±51.1*	 23.0±10.8	 10.8±19.3	 12.3±6.8
p-ZYMV	 17.4±26.9	 5.4±4.1	 7.2±14.2	 3.0±4.7	 2052.0±4.3.4	 14.8±12.4	 7.2±5.6
p-PSTVd	 17.6±14.9	 44.8±37.1	 32.6±37.5	 44.2±13.0	 16.8±16.4	 17199.0±2312.4*	 20.0±15.2
p-PVA	 7.4±7.0	 6.4±12.2	 0.4±4.5	 8.3±3.7	 9.4±23.5	 2.6±7.3	 6.5±5.6

* indicates the fluorescent values exceed the mean of the healthy control plus three standard deviations, and are regarded as positive;

** indicates these figures (on the above in grids) are the hybridization images, and these numbers (on the lower in grids) are the signal values corresponding to their hybridization images

A criterion is set to evaluate the specificity of the glass slide hybridization. A sample is regarded as positive if its signal value produced by its target probe exceeds the mean of the healthy control plus 3 times standard deviations, and is regarded as false positive if its fluorescence value produced by a un-targeted probe exceeds the mean of the healthy control plus 3 times standard deviations. Results have shown that the RNA samples hybridized with their target probes produced rather strong hybridization signals. No false positive has been found, even within the genus potyvirus (PVA, PVY, and ZYMV). In most cases, fluorescence values between the samples and the untargeted probes are less than 10, but some are in the range of 20 to 50. This case is regarded as the fluctuation of negative background according to the above described criterion. Both CMV isolates (Q6, N6) present rather strong hybridization signals with the CMV-specific probe (p-CMV). Besides plant viruses, glass slide hybridization detects PSTVd specifically. Thus, glass slide hybridization possesses rather high specificity.

2.4.6 Detection of PVY and PSTVd from Field Potato Samples

The ultimate validation of any diagnostic method involves testing samples of unknown identity. In this assay, 40 potato leaf samples were tested using both glass slide hybridization and nylon filter hybridization. Each RNA sample was spotted onto aminosilane slides and nylon membranes at 3 nl and 6 µl per dot, respectively. The printed glass slides were hybridized separately with CY5-labeled probes specific for PVY and PSTVd, whilst the prepared nylon membranes were hybridized separately with ³²P-labeled probes specific for PVY and PSTVd. The hybridization results are shown in Fig. 2.17. Utilizing the criterion for assessing the detection limit and specificity, the cut-off values of glass slide hybridization for PVY and PSTVd were calculated to be 64.8 and 53.7, respectively. By comparing the cut-off values with the fluorescent signal values of 40 samples tested, eight samples were found to be infected with PVY and PSTVd by glass slide hybridization (Fig. 2.17(a) and (b)). The result of PVY detection was consistent with that of nylon membrane hybridization (Fig. 2.17(c)). However, there was slight discrimination concerning PSTVd detection between glass slide hybridization and nylon filter hybridization (Fig. 2.17(b) and (d)). The samples IV-3 and IV-4 presented a faint hybridization signal by nylon filter hybridization, but they were regarded as negative by glass slide hybridization. Further investigation was performed by inoculating the crude saps of these two ambiguous samples on tomato plants. However, PSTVd-induced disease symptoms were not observed on the inoculated plants (Data not shown). Taken together, glass slide hybridization had a similar efficiency to nylon filter hybridization for the detection of PVY and PSTVd from field samples.

In conclusion, glass slide hybridization, using CY5-labeled probes to detect target RNA molecules immobilized on the surface of aminosilane slides, is a feasible method for the detection of plant RNA viruses and viroids in a large number of plant samples. In the developed glass slide hybridization procedure, the amount of RNA attached to glass slides that is available for hybridization is one critical factor. It was determined to a great extent by glass slide modification chemistries and spotting solutions. In conventional nucleic acid spot hybridization procedures, positive-charged nylon membranes are usually used to bind RNA through electrostatic interaction. In glass slide cDNA microarray systems, activated glass slides are usually positive-charged, such as aminosilane slide and poly-L-lysine slide. The aminosilane slide had a stronger capability of binding cDNA than the poly-L-lysine slide or the aldehyde slide (Zhu et al., 2001). Theoretically, RNA can be immobilized on surfaces of positive-charged glass slides under electrostatic interaction. The aminosilane slide is found to efficiently immobilize RNA, and had higher RNA binding efficiency than the poly-L-lysine slide or the aldehyde slide. In glass slide DNA microarray systems, 3× SSC and 50% DMSO are the most common spotting solutions (Ye et al., 2001). It is also found that the presence of the denaturants (formamide and DMSO) in DF-SSC and FF-SSC is unbeneficial to binding RNA onto the surface of aminosilane slides, and the binding efficiency of RNA molecules decreased with the increasing

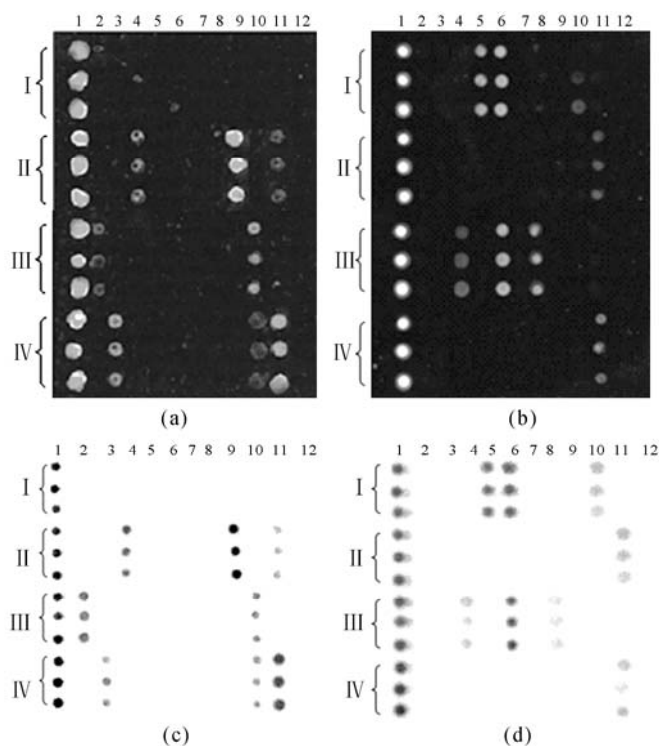


Fig. 2.17. Detection of PVY and PSTVd in field potato samples by two hybridization methods (a) and (b) Glass slide hybridization; (c) and (d) Nylon filter hybridization; (a) and (c) PVY detection; (b) and (d) PSTVd detection. I, II, III, and IV: Three replicative spots each sample; Column 1 (in (a) and (c)): PVY-infected potato as positive control; Column 1 (in (b) and (d)): PSTVd-infected potato as positive control; Column 12: Healthy potato as negative control; Columns 2–11 (I, II, III, and IV): Field potato samples

concentration of DMSO or formamide (Fig. 2.14(a) and (b)). It seems that these two denaturants blocked interaction of RNA molecules with aminosilane in some way. In physical terms, formamide and DMSO both increase the viscosities of the spotting solutions FF-SSC and DF-SSC, and reduce the rates of evaporation, depending on their concentrations. The SSC solution evaporates quickly, even 5× SSC. However, high concentrations of formamide and DMSO (20% and 40%) make FF-SSC and DF-SSC evaporate with difficulty over a short period. Unfortunately, RNA molecules are inclined to become degraded when they are exposed in liquid solutions for a long time. The decreased binding efficiencies of RNA molecules with increasing concentrations of formamide and DMSO were most likely due to RNA degradation.

Random-priming labeling reaction is used widely for preparation of ^{32}P -labeled DNA probes in conventional nucleic acid spot hybridization. The CY5-labeled DNA probe prepared by the labeling method detected 13.67 pg TMV RNA, which was a half sensitivity of the ^{32}P -labeled DNA probe. However, the detection sensitivity of the established glass slide hybridization increased by 8

times using the CY5-labeled DNA probe prepared by PCR method, when compared with the CY5-labeled DNA probe prepared by the random-priming labeling method. ELISA is popular in routine diagnostic laboratories due to its easy operation and interpretation. However, the ELISA test, in the case of viruses, is limited to viral coat proteins; thus, it cannot be applied to viroid diagnosis because viroids produce no specific protein. Up to now, dot-blot hybridization is used widely for detecting viroids. This is a highly sensitive method when compared with polyacrylamide gel electrophoresis (PAGE), and requires less time to finish a diagnosis than bioassay. Glass slide hybridization had an equivalent efficiency to nylon membrane hybridization for detecting PSTVd from field samples. Furthermore, it takes less than 8 hours to finish a whole diagnosis by glass slide hybridization, which is more time-saving than nylon membrane hybridization. Besides the application of viroid detection, glass slide hybridization has three other advantages, when compared with conventional RNA spot hybridization. First, it is easier to judge the positive or negative by digital analysis. Second, a glass slide can potentially allow the testing of a very large number of samples on one slide, and be able to spot the same samples onto multiple slides with high-speed robots, such that multiple viruses can be tested. Finally, glass slide hybridization does not involve dangerous chemicals or procedures.

However, glass slide hybridization has a significant disadvantage. It is strictly for use with RNA samples of relatively high purity, which can be quite laborious and was the main barrier to the detection of a large number of samples. In contrast, an obvious advantage of conventional nucleic acid spot hybridization is that little RNA sample preparation is required, and a crude sap can be applied to the nylon membrane, thus making it very suitable for testing a large number of samples. For the reasons given above, it is recommended to apply a simplified “tissue blot assay” to the crude leaf sap directly, with fresh tissues on the glass slides to avoid most of the fluorescent background. That means, in the case of leaf tissue, that leaves can be rolled and sharply cut before direct spotting onto the glass. The modified application can save time and reagents, while most of the background coming from extraction solutions can be avoided.

2.5 Quantitative Determination of CMV Genome RNAs in Virions by Real-time RT-PCR

Determining the expressed discrepancies in genes during a virus infection and in virions will bring a more direct understanding, not only for the packaging, disassembling of virions and virus replication and movement, but also for virus interaction with hosts and other factors, including other viruses and co-infected sub-viral agents. When the quantitative changes in different genes of a virus can be read, more detailed mechanisms concerning the above aspects can be described in more detail. Before that, the amounts of viral genomic RNAs can be quantified by electrophoresis, Northern blot hybridization and RT-PCR. However, the above

methods vary in their usefulness for accurate quantification, being either time consuming, laborious, insensitive, or having large variations in results. Because of the lack of a reliable methodology, few RNA viruses have been definitively quantified for their copy numbers and relative amounts of the genomic RNAs or genes.

A newly developed real-time RT-PCR approach is introduced and its first application to determine the genomic RNAs of an ssRNA virus is laid out. The accurate quantification property of such an assay could be useful to monitor viral replication kinetics, such as the changes in copy number ratios between genomic RNAs in the progress of an infection, the response to antiviral therapy, and the evaluation of viral tolerance levels in new breeding programs.

Presently, there are two general real-time PCR approaches, depending on specific or non-specific fluorescent reporting chemistries. Both approaches display similar levels of sensitivity. The use of a specific probe-based assay such as *TaqMan* requires high complementarities for probe binding, which might result in failure to detect a high sequence variability in the probe-binding region, while non-specific assays using intercalating dyes such as SYBR Green I are found to be more flexible, and of lower cost for detecting nucleic acid targets characterized by sequence variability. Since variations occur quite frequently in an RNA virus, SYBR Green I assay is especially useful for RNA viruses. SYBR Green I is a minor groove DNA binding dye with a high affinity for double-strand DNA (dsDNA) and exhibits fluorescence enhancement upon binding to dsDNA. The accumulation of amplified DNA is measured by determining the increase in fluorescence over time, and this is followed by confirmation of results by melting curve analysis. Thus, real-time RT-PCR with SYBR Green I dye is recommended here for quantification ORFs of viral genomic RNAs, using CMV as a model.

As a newly set-up method, the development of a real-time RT-PCR (SYBR Green I) assay, which allows accurate quantification of CMV genomic RNAs, is to be introduced. Copy number ratios in CMV virions are calculated and compared with assays by lab-on-a-chip and northern blot hybridization.

Primers used for quantification of Fny-CMV ORFs by real-time RT-PCR are listed in Table 2.9. Using full-length viral RNA transcripts and RNAs extracted from virions, cDNAs are synthesized.

Table 2.9 Primers used for quantification of Fny-CMV ORFs by real-time RT-PCR

ORF	Primer sequence (5'→3')	Range (position)
RNA 1		
1a ORF	1a-F, GGAGAGGAATGGGACGTGATATC	72 bp (1598–1669)
	1a-R, CAAAACCTTCCCATCGGTAACAG	
RNA 2		
2a ORF	2a-F, ATGAGCTCCTTGTCGCTTTTG	76 bp (361–436)
	2a-R, TTATTAACGCAGGGCACCAT	
2b ORF	2b-F, CGGCGGAAGACCATGATTT	61 bp (2681–2741)
	2b-R, CCTTCCGCCCATTCGTTAC	

(To be continued)

(Table 2.9)

ORF	Primer sequence (5'→3')	Range (position)
RNA 3		
3a ORF	3a-F, CTGATCTGGGCGACAAGGA	154 bp (453–606)
	3a-R, CGATAACGACAGCAAAACAC	
CP ORF	CP-F, CGTTGCCGCTATCTCTGCTAT	71 bp (1661–1731)
	CP-R, GGATGCTGCATACTGACAAACC	

2.5.1 Optimization of Real-time RT-PCR and the Specificity

Real-time RT-PCR has been optimized progressively by varying the concentrations of primers and concentration of SYBR Green I. As optimized, PCR was carried out in a 96-well plate in a reaction volume of 25 μ l containing 12.5 μ l Premix *EX Taq*TM (2 \times , TaKaRa, Dalian, China), 0.5 or 1 μ l SYBR Green I nucleic acid fluorescent dye (50 \times , TaKaRa, Dalian, China), 2 μ l template cDNA, and the forward and reverse primers at final concentrations of 0.2 μ mol/L. The thermal profile for PCR was 95 °C for 10 s, followed by 40 cycles of 95 °C for 10 s and 60 °C for 30 s. It was found that 0.5 μ l of SYBR Green I is optimal for the reaction. Increasing the concentration of SYBR Green I in the reaction mixture often results in an error reading of the fluorescent signals from the amplified DNA. Also, 0.2 μ mol/L of each forward and reverse primer can be used as the optimum concentration, which gives the highest reporter fluorescence and the lowest C_t value.

A consequent test has showed that real-time RT-PCR amplification of Fny-CMV ORFs with each primer set listed in Table 2.9 produced the expected amplicon. The predicted RT-PCR product is well confirmed by agarose gel electrophoresis with complete specificity. Dissociation curve analysis has also demonstrated that each of the tested primer sets can amplify a single PCR product with a distinct T_m value.

2.5.2 Quantification of CMV Genomic RNAs by RT-PCR and Comparison of the Quantification with Lab-on-a-Chip and Northern Blot Hybridization Assays

As the first attempt to qualify the relative ratio of genomic RNAs of CMV as a tripartite ssRNA virus, all of the five ORFs including 1a, 1b, 2a, MP and CP, are amplified clearly and reproducibly by real-time RT-PCR (Fig. 2.18). The assay proves to be highly reproducible, as demonstrated by low C_t standard deviation values between triplicates and a high correlation coefficient of the standard curves (R^2 0.99) (Fig. 2.19). Based on respective C_t values, the copy number of each

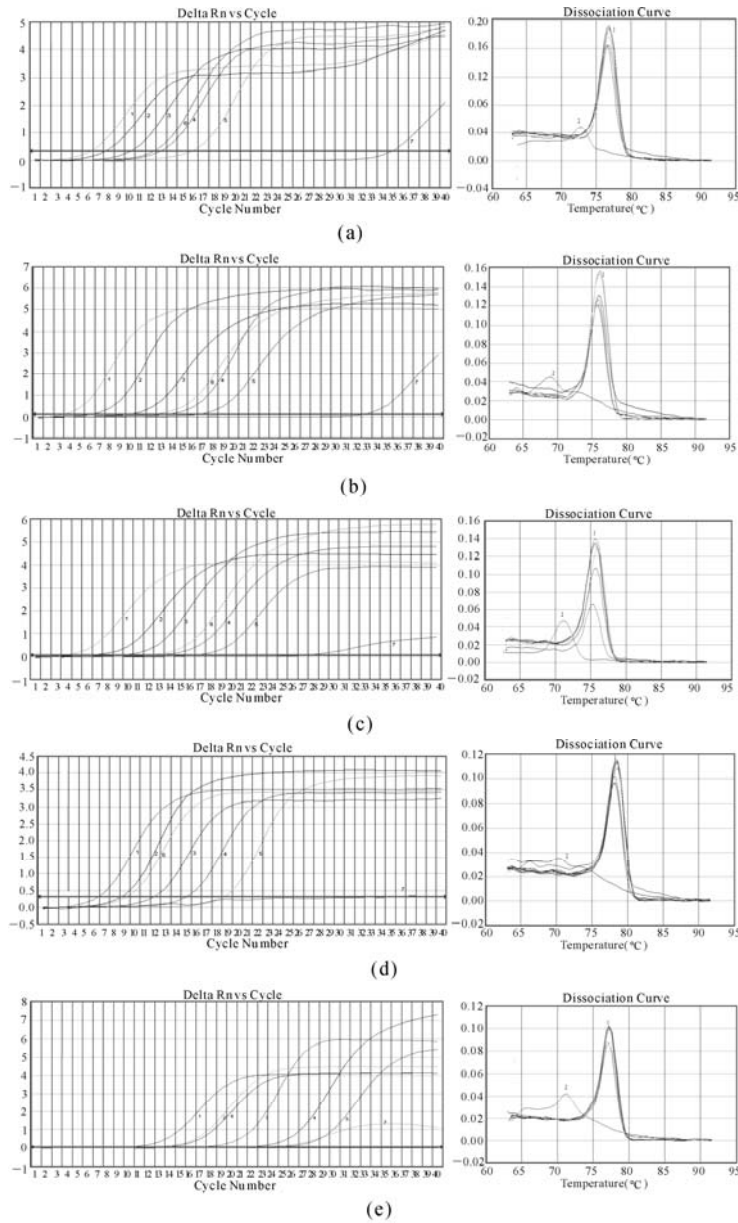


Fig. 2.18. Real-time RT-PCR amplification and dissociation curves of Fny-CMV ORFs in virions (a) 1a, ORF; (b) 2a, ORF; (c) 2b, OFR; (d) 3a and ORF; (e) CP ORFs. Left: Representative optic graph for the number of cycles versus the number of fluorescence units for each sample used to calculate the C_i value; 1–5: 10-fold serially diluted standard samples; 6: RNA extracted from virions; 7: PCR-negative control. Right: corresponding dissociation curve analysis, with the results represented by a graph of number of fluorescent units versus temperature; (1) The T_m value of each amplicon; (2) PCR-negative control

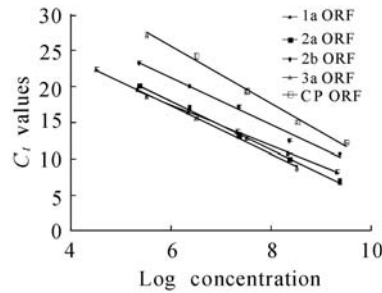


Fig. 2.19. Standard curves for the copy number of standard samples versus C_t values. The error bars indicate the standard deviations obtained in three independent experiments. 1a ORF: $Y = -2.825426X + 34.424$; 2a ORF: $Y = -3.396X + 38.452$; 2b ORF: $Y = -3.31X + 41.104$; 3a ORF: $Y = -3.346X + 37.417$; CP ORF: $Y = -3.93X + 49.155$

Fny-CMV ORF is calculated with intra-group coefficient variations (CVs) of 0.76%–6.24% and inter-group CVs of 2.51%–11.37%. Copy numbers of Fny-CMV RNAs 1 and 3 in virions have been represented by the amounts of 1a ORF and 3a ORF, and RNA 4 is obtained by subtracting the amounts of 3a ORF from those of CP ORF (Table 2.10).

Table 2.10 Quantification of Fny-CMV ORFs in virions by real-time RT-PCR

ORF	Average C_t value ^a	Copies per μ l
RNA 1		
1a ORF	12.25±0.11	$(4.47±0.5) \times 10^7$
RNA 2		
2a ORF	12.00±0.10	$(4.87±0.33) \times 10^7$
2b ORF	13.00±0.06	$(5.57±0.25) \times 10^7$
RNA 3		
3a ORF	9.61±0.09	$(1.60±0.09) \times 10^8$
CP ORF	13.26±0.12	$(4.20±0.11) \times 10^8$

^a The values are presented as Mean±SD for three independent experiments

Some differences between the copy number of 2a ORF and that of 2b ORF have been obtained ($(4.87±0.33) \times 10^7$ vs. $(5.57±0.25) \times 10^7$, $CV = 9.57\%$), but they are in the range of inter-group CVs, indicating an absence of RNA 4A in Fny-CMV virions. Therefore, the copy number of RNA 2 can be represented by the average amounts of 2a ORF and 2b ORF, and the copy number ratios between Fny-CMV RNAs 1, 2, 3, and 4 in virions are determined as being 1.00:1.17(±0.11):3.58(±0.20):5.81(±0.31).

Real-time RT-PCR quantification for the genomic RNAs of CMV has been confirmed by conventional methods. Thus, using RNAs extracted from virions, the ratios of CMV genomic RNAs are analyzed in parallel by Lab-on-a-Chip and Northern blot hybridization assays. The results of Lab-on-a-Chip are shown in Fig.

2.20. Based on the electropherogram, the relative concentrations of Fny-CMV RNAs 1, 2, 3 and 4 are presented, and the copy number ratios between them are deduced to be 1.00:1.23(± 0.08):3.68(± 0.15):5.79(± 0.65). The results of Northern blot hybridization of CMV genomic RNAs have been shown in several other reports, but a conclusion has never been reached. In the parallel above, due to different hybridization efficiency, RNA1, RNA2 and RNA3 standard samples with equal concentration yield a different hybridization intensity. Thus, when the relative concentration of each virus RNA is calculated, its hybridization intensity is divided by the intensity of the corresponding standard sample to eliminate this difference, and the copy number ratios between Fny-CMV RNAs 1, 2, 3 and 4 have been determined as being 1.00:1.20(± 0.10):4.03(± 1.07):6.19(± 2.51).

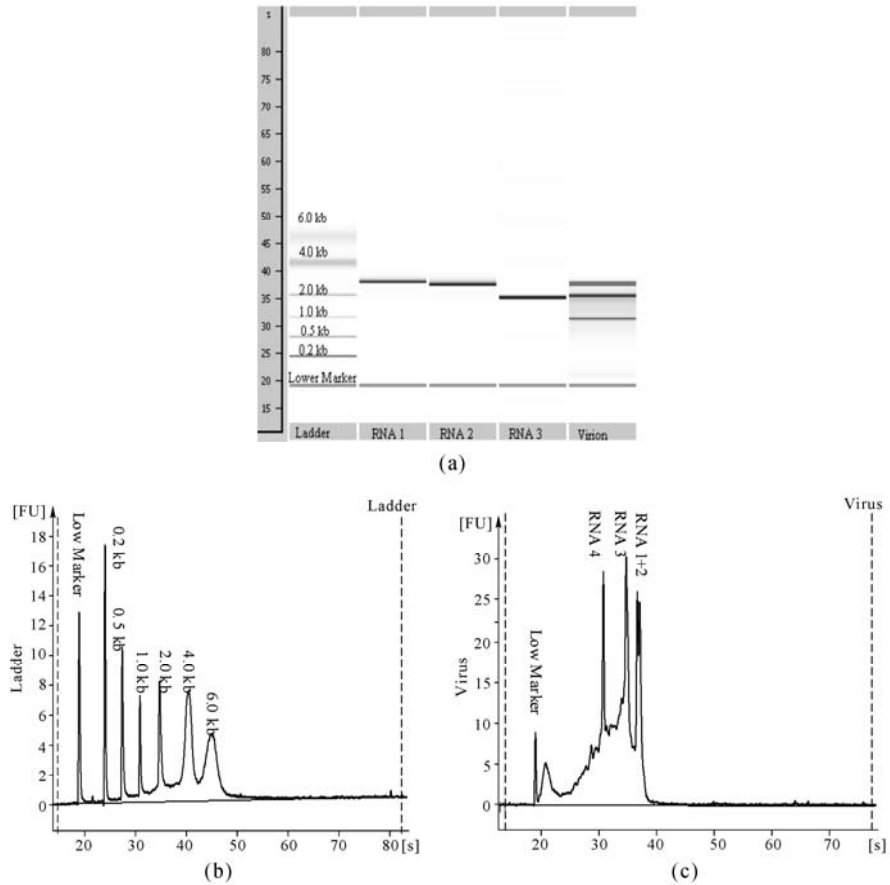


Fig. 2.20. Quantification of Fny-CMV RNAs in virions by Lab-on-a-Chip (a) Gel result, RNA 6000 ladder (0.2, 0.5, 1.0, 2.0, 4.0, and 6.0 KB respectively) (Ambion, Austrin, USA) was used; (b) Corresponding electropherogram of RNA ladder; (c) Corresponding electropherogram of Fny-CMV RNAs extracted from virions. Lower markers are internal standards and are used to align the ladder analysis with the individual sample analysis

The copy number ratios of Fny-CMV genomic RNAs in virions determined by real-time RT-PCR, Lab-on-a-Chip and Northern blot hybridization are compared in Table 2.11, revealing the largest variations of Northern blot hybridization.

Table 2.11 Comparison among the ratios of Fny-CMV genomic RNAs in virions qualified by real-time RT-PCR, Lab-on-a-Chip and Northern blot hybridization

RNA	Copy number ratio		
	Real-time RT-PCR	Lab-on-a-Chip	Northern blot hybridization
RNA 1	1.00	1.00	1.00
RNA 2	1.17±0.11	1.23±0.08	1.20±0.10
RNA 3	3.58±0.20	3.68±0.15	4.03±1.07
RNA 4	5.81±0.31	5.79±0.65	6.19±2.51

Thus, genomic RNA1, RNA2 and RNA3 of CMV-Fny strain is calculated as about 1:1.2:3.6. It is the first time to find that as tripartite +ssRNA virus, CMV genomic RNAs do not encapsidate in the same ratio, and the smaller the genomic RNA is, the more it is packaged into virions.

The real-time RT-PCR assay offers a sensitive and rapid method for high throughput detection and quantification of Fny-CMV genomic RNAs. Even though the relative RNA ratio could be determined theoretically by RNA hybridization and electrophoresis, this has never been said with confidence about the ratio of viral RNAs, ORFs and other portions of the virus genome, both in the virion and during the infection. The accurate quantification property of this assay could be useful for monitoring viral replication kinetics, such as the changes in copy number ratios between genomic RNAs in the progress of an infection, the effects of satellite RNA on the helper virus, the response to antiviral therapy and the evaluation of viral tolerance levels in new breeding programs.

Utilizing the reliable high throughput quantification method, other viruses with more than one partite genome can be determined for a better understanding of encapsidation and replication. With new research techniques, it is time to see if a mono-partite virus, such as a potyvirus is expressed and accumulated at the same level. And it is also time to see if there are more gene expressing straightedges, such as more subgenomic RNAs. For the reasons given above, more about the reality of virus replication and interaction with hosts is expected to be made clear.

More questions need to be answered before a conclusion is obtained for the expression of different genomic RNAs and gene fragments of an RNA virus. For example, the ratio of CMV genomic RNAs could be altered when infecting different hosts, at different infection times and even the conditions under complex infection with other viruses, mostly influenced by co-existent satellite RNAs in the case where this virus is severed as the helper virus.

2.6 Accurate and Efficient Data Processing for Quantitative Real-time PCR

As a newly developed method, real-time PCR is becoming a preferred method for the quantification of minute amounts of nucleic acids. With a high degree of sensitivity and a large dynamic range, it has greatly benefited many aspects of biological research, including plant virology. However, the full potential of this technology has not yet been realized, partially because of the limitations of the calculation methods that currently predominate. Northern blotting is a conventional approach for quantifying genes of ssRNA viruses due to the simple linear relationship between the intensity of each band and its quantity. However, Northern blotting often fails to provide reliable results because the hybridization rates are different for each probe.

The large quantities of numerical data produced by real-time PCR are generally analyzed by basic software tools provided with the PCR fluorescent thermal cyclers, which quantify the unknown samples either relatively or absolutely by comparing them with the standard DNA or a reference gene. These two groups of methods are based on the same assumptions, namely that amplification efficiencies of target genes are approximately equal to the standard DNA or the reference genes, and that the amplification efficiency is constant throughout the PCR. However, as noted by many researchers, this is often not the case in practical applications and it is believed to be a non-negligible source of biased results.

To circumvent the amplification efficiency problem, several new mathematical models have appeared for analyzing PCR data. By investigating the raw PCR fluorescence value measured per cycle of each reaction, these models directly predict the theoretical fluorescence value at cycle 0 (F_0). As the basic principle underlying real-time PCR is the fluorescence intensity proportional to DNA content, once F_0 is determined, the changes in amount of the target gene can be represented by the changes in F_0 values. However, using only F_0 values is inadequate when the definitive copy numbers are required or when expression levels, actually represented by the accumulation levels, of different genes are compared. The reason for this is that the calibration factor (CF) of the target gene, which relates fluorescence to DNA molecular content in real-time RT-PCR, is unknown. Nevertheless, these problems can be solved through amplification of the template, with known copy numbers as control.

Three models have been chosen to quantify the definitive copy numbers of CMV genomic RNAs using raw fluorescence data of real-time PCR, and equations can be proposed to compare their expression levels in virions or *in planta*. By quantifying and comparing the expression levels of three genes (*1a*, *2a*, and *MP*) of CMV, which are used to represent the accumulation levels of CMV genomic RNAs 1, 2 and 3, respectively, different strains of CMV and at different stages of infection, the accumulation levels of RNAs and their ratios are compared as follows.

2.6.1 Quantification of CMV RNAs in Virions with Standard Curves

In this process, the PCR data are initially analyzed using Sequence Detection Software (PE Applied Biosystems), and result in the assignment of a threshold cycle (C_t) value to each reaction. For each target gene, a standard curve is created based on the linear relationship between the C_t values of standard samples and the logarithm of the starting copy numbers, which are derived from the concentration of standard samples by Eq.(1):

$$N = C / (K \times 330 \times 1.6601 \times 10^{-18}), \quad (1)$$

where N is the copy number per μl , C is the concentration per sample ($\mu\text{g}/\mu\text{l}$), K is the length of each target gene (bases), and 1.6601×10^{-18} is the conversion constant between Dalton and μg .

For the unknown samples, copy numbers of each gene are provided by the software, according to the mean of the standard curve and their respective C_t values.

The standard curves of *1a*, *2a* and *MP* genes are constructed over a range of five orders of magnitude, using the wild-type Fny-CMV and four intraspecies hybrid viruses, FCb7^{2b}-CMV, FRad35^{2b}-CMV, FBX^{2b}-CMV, and FNa^{2b}-CMV which are generated as described in Table 2.12, while the viral RNA templates are extracted from inoculated tobacco seedlings at 30 dpi, or the virions purified from fresh leaf tissues. As shown in Fig. 2.21, these standard curves demonstrate a well-built linear relation ($R^2 > 0.99$) between the C_t values and the log-copy numbers of CMV genes. The standard deviations in C_t values are depicted as error bars, which are found to range from a minimum of 0.04 to a maximum of 0.79 cycles.

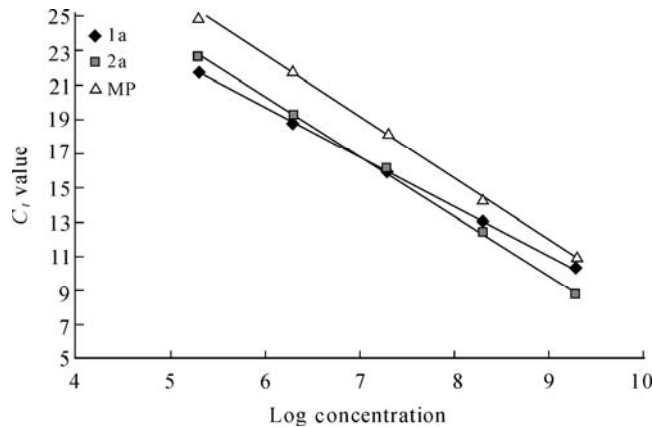


Fig. 2.21. Standard curves of CMV genes

The average C_t values were plotted versus log concentration of standard samples of CMV *1a*, *2a* and *MP* genes. The error bars indicate the standard deviations obtained from three independent experiments. *1a*: $Y = -2.866X + 36.862$ ($R^2 = 0.995$); *2a*: $Y = -3.459X + 41.008$ ($R^2 = 0.997$); *MP*: $Y = -3.595X + 44.312$ ($R^2 = 0.998$)

Based on the constructed standard curves, copy numbers of CMV RNAs 1, 2 and 3 in five types of virions can be calculated. The lowest accumulation levels are found in FRad35^{2b}-CMV virions, and the highest levels in FNa^{2b}-CMV virions (Fig. 2.22(a)). The accumulation ratios present in Fny-CMV, FCb7^{2b}-CMV, FRad35^{2b}-CMV, FBX^{2b}-CMV, and FNa^{2b}-CMV virions are calculated to be 1:1.34:2.36, 1:1.37:2.17, 1:1.39:1.47, 1:0.80:2.20 and 1:1.38:1.65, when the virions are extracted from tobacco leaf tissues at 30 dpi.

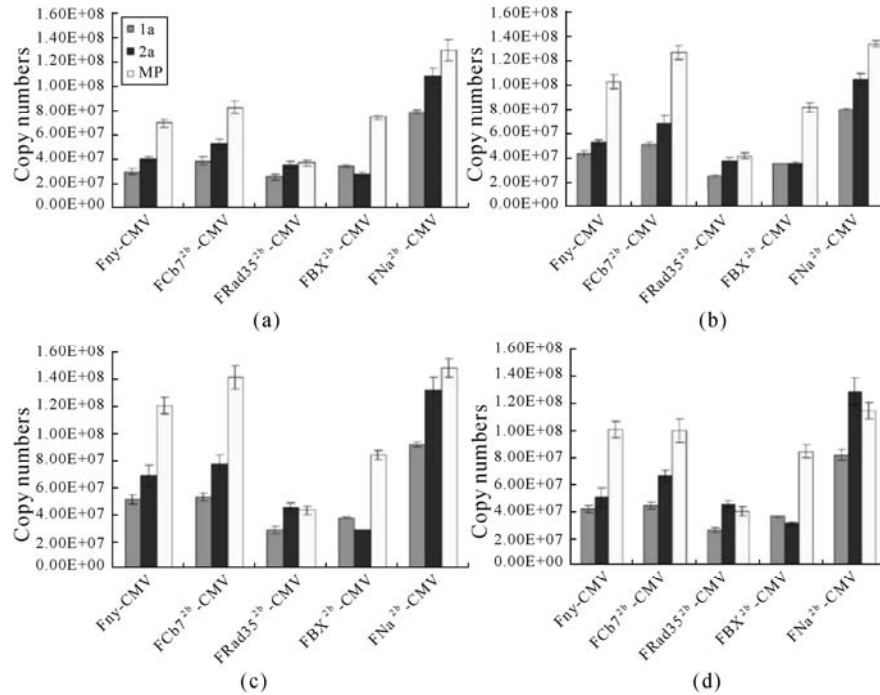


Fig. 2.22. Quantification of the copy number of CMV genes in virions. Copy numbers of each gene in five types of virions were calculated by standard curves method (a), sigmoidal curve fitting (b), LinRegPCR (c) and DART program (d), based on the C_t values for standard curve method or F_0 values of all the other calculation methods. Real-time PCR experiments were repeated three times, and variations between the results of the three experiments were reported as the standard deviation (\pm SD)

2.6.2 Quantification of CMV RNAs in Virions by SCF

In this process, the PCR fluorescence data of each amplicon are exported to an Excel workbook for analysis. Using Origin 7.5, the fluorescence readings of individual PCR amplifications are fitted to the nonlinear regression function given by Eq.(2):

$$F_c = \frac{F_{\max}}{1 + e^{(C_{1/2} - C)/k}} + F_b, \quad (2)$$

where C is the cycle number, F_c is the reaction fluorescence at cycle C , F_{\max} is the maximal fluorescence during the reaction, e is the natural logarithm base, $C_{1/2}$ is the cycle at which reaction fluorescence reaches half of F_{\max} , k is the slope of the sigmoid curve and F_b is the background reaction fluorescence. In contrast to C_t values in the standard curve method, the initial quantity of target gene (N_0) is represented directly by F_0 values in the SCF method, given by a simple derivation of Eq. (2) when $C = 0$:

$$F_0 = \frac{F_{\max}}{1 + e^{C_{1/2}/k}}. \quad (3)$$

When the fluorescence dataset of each amplicon is fitted to Eq.(2), a series of r^2 , F_{\max} , $C_{1/2}$ and k values is generated and F_0 values are obtained. The minimum-calculated F_0 value, being produced by the criterion recommended by Rutledge, is used to reflect the initial target quantity. Once the F_0 value is determined, it can be converted to N_0 by Eq.(4):

$$N_0 = (CF_{\text{SCF}} \times F_0 \times 9.1 \times 10^{11}) / As, \quad (4)$$

where CF_{SCF} is the SCF-based calibration factor, expressed as the number of nanograms of double-stranded DNA per SYBR Green I fluorescence unit (ng/FU), As is the amplicon size in base pairs and 9.1×10^{11} is the number of single base pair molecules per nanogram. It should be noted that CF_{SCF} determines the absolute accuracy or "exactness" of the quantitative scale in SCF methods, and it can be determined straightforwardly by the F_0 value of standard samples of known concentration, based upon rearrangement of Eq.(4):

$$CF_{\text{SCF}} = (N_p \times As) / (F_0 \times 9.1 \times 10^{11}), \quad (5)$$

where N_p is the predicted copy number of the target gene in standard samples. As long as the CF_{SCF} value of a specific gene is determined, the calculation of N_0 values of this gene in an unknown sample simply requires the knowledge of the F_0 value, which can be derived from the raw fluorescence data based on Eq.(3).

As the starting procedure for quantitative assessment, the calculated F_0 values of a series of diluted standard samples are examined, with the same CMV strains. As shown in Fig. 2.23(a), the relationship between F_0 and the initial concentration of 2a gene is precisely linear with a correlation coefficient of 0.992 and $R^2 > 0.999$. Similar results are obtained for 1a and MP genes. Based on these F_0 values, the average CF_{SCF} are determined to be 61.2, 65.8 and 68.3 ng/FU for 1a, 2a and MP genes, respectively (as shown in Table 2.12).

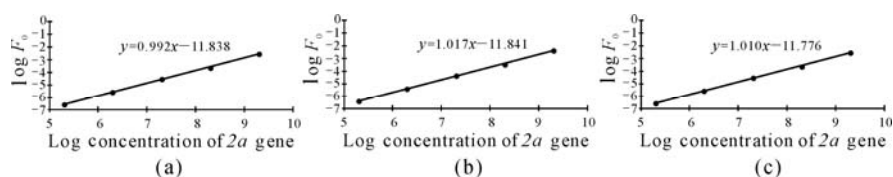


Fig. 2.23. The concentration of *2a* gene presented by F_0 values

The linear regression analysis generated by plotting the log of copy number of *2a* gene versus log of F_0 , which was determined by sigmoidal curve fitting (a), LinRegPCR (b) and DART program (c). The nearly perfect linear relationship ($R^2 \geq 0.999$) indicates that F_0 directly reflects the concentration of *2a* gene. The results correspond to triplicate experiments

Table 2.12 Correlation of reaction fluorescence values to mass of standard RNAs representing CMV genomic RNAs 1, 2, and 3

Predicted	1a (72 bp)			2a (76 bp)			MP (154 bp)		
	CF_{SCF}^b	CF_{LinReg}^c	CF_{DART}^d	CF_{SCF}^b	CF_{LinReg}^c	CF_{DART}^d	CF_{SCF}^b	CF_{LinReg}^c	CF_{DART}^d
N_0^a									
2E+09	64.6	44.2	40.8	65.0	40.0	39.5	75.2	43.6	46.0
2E+08	54.4	39.7	32.4	70.8	41.7	43.7	65.6	47.7	48.3
2E+07	67.6	42.0	38.0	66.3	46.7	44.5	65.0	54.0	41.3
2E+06	61.8	50.4	48.4	65.5	46.5	35.8	64.2	44.7	52.8
2E+05	57.8	43.2	47.1	61.6	45.6	48.8	71.7	49.4	56.9
Average	61.2	43.9	41.3	65.8	44.1	42.5	68.3	47.9	49.1
$\pm CV^e$	$\pm 8.62\%$	$\pm 9.14\%$	$\pm 15.93\%$	$\pm 4.98\%$	$\pm 6.98\%$	$\pm 11.79\%$	$\pm 7.11\%$	$\pm 8.63\%$	$\pm 12.28\%$

^aPredicted input amount of target molecules based upon dilution of standard RNA samples quantified via A_{260} ;

^bSigmoidal curve-fitting (SCF)-based calibration factor (ng/FU);

^cLinear regression PCR program (LinReg PCR)-based calibration factor (ng/FU);

^dData Analysis for real-time PCR program (DART)-based calibration factor (ng/FU);

^eAverage \pm coefficient of variation

Using the determined CF_{SCF} values, the copy numbers of CMV RNAs 1, 2 and 3 in virions are calculated by Eq.(4) (Fig. 2.22(b)). As expected, the results are similar to those obtained by the standard curve method, and their ratios are determined to be 1:1.22:2.40, 1:1.35:2.52, 1:1.49:1.66, 1:0.99:2.30 and 1:1.31:1.67.

2.6.3 Quantification of CMV RNAs in Virions by LinReg PCR and DART Programs

The exported PCR data can also be analyzed by described LinRegPCR 7.5 program or by the DART-PCR version 1.0 program. The LinRegPCR method is based on the basic exponential formula of PCR amplification:

$$X_c = X_0 \times E^c, \quad (6)$$

where X_c is the concentration of the template at cycle c , X_0 is the initial concentration of the template and E is the amplification efficiency ranging from 1 to 2. This equation can be expressed linearly in terms of fluorescence by taking the logarithm of both sides:

$$\log F_c = \log F_0 + \log E \times C, \quad (7)$$

where F_c and C are measured fluorescence data and cycle number, respectively. For each amplification curve, the log-linear part of the PCR is automatically determined by the program with the default option to contain from four to six points with the highest R^2 value. Once these points are determined, they are fitted to a regression line and the initial fluorescence F_0 then directly calculated as $10^{\text{intercept}}$.

The DART program is also based on Eq.(6), but with another reformulation:

$$F_0 = F_c \times (E)^{-C}, \quad (8)$$

where F_c is the fluorescence at the threshold cycle. As described by Peirson et al. (14), using the raw fluorescence data, this program can calculate the individual C_t , average E values and the resulting F_0 values automatically and rapidly.

For both LinReg and DART programs, once the F_0 value of each gene in a series of diluted standard samples is obtained, their respective CF_{LinReg} and CF_{DART} value can be determined by Eq.(5). The N_0 values of CMV 1a, 2a and MP genes in unknown samples can then be calculated in the same way as for the SCF method.

Once the N_0 values of CMV genes are obtained, their relative expression levels in the same RNA samples can be compared directly:

$$Rati_{A/B} = N_{0A} / N_{0B} = \frac{CF_A \times F_{0A} \times As_B}{CF_B \times F_{0B} \times As_A}. \quad (9)$$

However, when their copy numbers in different samples are compared, the variances in amounts of total RNA should be taken into account, which can be represented by changes in the F_0 values of the reference gene (18s rRNA) between samples. Therefore, the above formula was rearranged to:

$$Rati_{A \text{ sample 1} / B \text{ sample 2}} = \frac{N_{0A \text{ sample 1}} \times N_{0B \text{ sample 2}}}{F_{0 \text{ Refsample 1}} / F_{0 \text{ Refsample 2}}}. \quad (10)$$

With the above strains of CMV as model samples, when the experimentally derived fluorescence readings of the same real-time PCR procedure are treated by the LinReg PCR and DART programs, a good linear relationship can also be found between the F_0 values and the concentration of standard samples of 2a gene,

as the results show in Fig. 2.23(b) and (c).

Using the LinReg PCR program, the average CF_{LinReg} values are determined to be 43.9, 44.1 and 47.9 ng/FU for *1a*, *2a* and *MP* genes (Table 2.12). These values are lower than those obtained by SCF. However, as shown in Fig. 2.23(c), such a decrease in CF values has no significant effect on the final calculated results. The copy number ratios of RNAs 1, 2 and 3 in Fny-CMV, FCb7^{2b}-CMV, FRad35^{2b}-CMV, FBX^{2b}-CMV, and FNa^{2b}-CMV virions are thus determined to be 1:1.35:2.39, 1:1.46:2.69, 1:1.60:1.51, 1:0.75:2.26 and 1:1.43:1.62.

With the DART program, CF_{DART} values of *1a*, *2a*, and *MP* genes are determined to be 41.3, 42.5 and 49.1 ng/FU, which are very close to the CF_{LinReg} values (Table 2.12). Their variations (15.93%, 11.79% and 12.28% for *1a*, *2a* and *MP* genes), although significant, indicate that the DART approach has an acceptable level of reproducibility over the five magnitudes of target concentration. Similarly, the copy numbers of CMV RNAs in five types of virions are calculated and their ratios are determined to be 1:1.20:2.43, 1:1.50:2.26, 1:1.71:1.53, 1:0.86:2.34 and 1:1.57:1.40 (Fig. 2.22(d)).

2.6.4 Determination of the Suppression Effect of Satellite RNA on CMV Accumulation in Plant Tissues Using N_0 Values

Using Eqs.(9) and (10), the different accumulation levels of CMV RNAs 1, 2 and 3 in tobacco tissues have been detected at 4 dpi. As the results show in Fig. 2.24, the average accumulation level ratios are calculated to be 1:0.98:1.16 in CMV-Fny infection. While in CMV-Fny-T1sat infection, in the case of a satellite RNA which reduces the symptom induced by wild-type CMV on tobacco plants, the ratios changed to 1:1.49:6.27 and the accumulation levels of RNAs 1, 2 and 3 are 8.27, 5.45, and 1.53 folds lower than that of CMV-Fny infection. These ratios indicate that at this time point, the accumulation of all CMV genomic RNAs in tobacco are suppressed by T1sat, but the suppression effect on RNAs 1 and 2, which are responsible for replication, is more apparent than on RNA 3, which is more related to encapsidation of the virions.

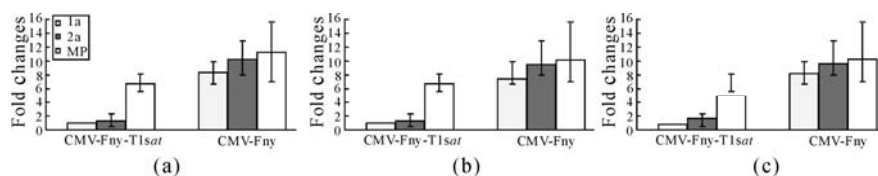


Fig. 2.24. Relative comparison of the expression levels of CMV RNAs *in planta*. The expression levels of CMV RNAs 1, 2 and 3 were determined by sigmoidal curve fitting (a), LinRegPCR (b) and DART program (c). The amount of RNA 1 in CMV-Fny-T1sat infection was set at 1 and the other RNAs were quantified relative to it. 18s rRNA was used as an endogenous control to normalize the data for differences in input total RNA between samples. The error bars indicate the standard deviations obtained from three independent experiments

The results demonstrate that using the N_0 values, a relative comparison between genes can be easily performed in the same sample or between different samples. When the relative ratios determined by these various methods are compared, the higher levels of accuracy of SCF and the LinReg PCR program are indicated by the smaller variations.

2.7 Methodology

In this section we introduce primers design and specificity tests in RT-PCR, comparison of 18S rRNA and nad 2 mRNA as internal controls, optimization of multiplex RT-PCR, comparison of sensitivities for multiplex RT-PCR and DAS-ELISA, and glass slide hybridization.

2.7.1 Primers Design and Specificity Tests in RT-PCR

Primers used for simplex and multiplex RT-PCR for CMV amplification can be designed using DNASTAR-lasergene (DNASTAR, USA) and Primer Premier 5.0 (Premier Biosoft International, USA), based on sequence published in GenBank. The primer pairs for CMV satRNA and that for 18S rRNA, which were used as the internal control and universal in *N. tabacum* (AJ236016) and tomato (X51576), are both used as described in Chapter 1. Highly conserved and variable regions between TMV and ToMV were determined with the alignments of sequence by Cluster X. Specific sense primers were designed to differentiate the two viruses in the variable regions, and the degenerated antisense primer was designed in a commonly conserved region of coat protein gene. For CMV-I and CMV-II, alignments were carried out and the specific antisense and sense(s) primers were designed among the coat protein gene for differentiating them.

In order to confirm the specificity of the primers and establish fundamental conditions for amplifying all the target fragments simultaneously, simplex and multiplex PCRs with cDNA clones templates should be carried out. PCRs are performed in a thermocycler (Biometra, Germany) (or else by) using *Taq* DNA polymerase (Beijing BioDev-Tech, China) or whatever else is recommended, according to the manufacturer's instructions. It is suggested the PCR products be visualized by electrophoresis in 2.0%–2.5% agarose gels stained with ethidium bromide when primer specificity is tested.

Single PCR should be performed in a volume of 25 μ l reaction mixture consisting of 19.25 μ l sterile- H_2O , 2.5 μ l 10 \times PCR buffer (100 mmol/L Tris-HCl (pH 8.3), 500 mmol/L KCl, 15 mmol/L $MgCl_2$), 1 μ l dNTPs (2.5 mmol/L each), 0.5 μ l forward and reverse primer (10 μ mol/L each), 0.25 μ l *Taq* (5 U/ μ l) and 1 μ l cDNA. The PCR reaction should be carried out, it is suggested, as follows: 94 $^{\circ}C$ for 2 min, followed by 35 cycles of 94 $^{\circ}C$ for 30 s, 52 $^{\circ}C$ for 30 s, 72 $^{\circ}C$ for 45 s,

with an additional cycle of 72°C for 10 min. Small alterations can be applied in different labs and cDNA clones are needed to test the specificity of different primer combinations. Multiplex PCR was performed with all the sets of primers using the mixture of the different cDNA templates. Several parameters, such as primer concentration, template concentration, annealing temperature and elongation times (from 30 to 150s) should be tested to optimize conditions for the simultaneous amplification of target fragments. PCR products should undergo electrophoresis in 2.0%–2.5% agarose gels.

Healthy and infected tomato leaf tissues (100 mg) frozen below –80°C are used to extract total RNA, using TRIzol reagent (Invitrogen, USA) following the manufacturer's protocol and dissolved in 35 µl of diethyl pyrocarbonate-treated (DEPC) water. First strand complementary DNA (cDNA) is synthesized with specific antisense primers in 10 µl volume using AMV reverse transcriptase (TaKaRa, Dalian) according to the manufacturer's instructions. 1 µl RT product as template is consequently a suggested test in a 25 µl volume PCR.

For measuring the sensitivity of PCR and multiplex RT-PCR, purified viral RNA of CMV should be serially diluted with extracts of healthy tomato leaf tissue. Dilutions, ranging from 1 to 1×10^{-7} µg/µl viral RNA, are subject to RT-PCR.

2.7.2 Comparison of 18S rRNA and *nad2* mRNA as Internal Controls

Sequences of 18S rRNA from *S. tuberosum* (X67238), *N. tabacum* (AJ236016), and *Lycopersicon esculentum* (X51576) are available in Genbank for use to design 18S rRNA-specific primers 18SF/18SR. A sequence of the NADH dehydrogenase subunit II (*nad2* gene) from *S. tuberosum* (X93575) is used to design the PotatoNad2 primer. The *nad2* gene contains three exons, a, b, and c, separated by two introns. The forward primer (PotatoNad2F) crosses the splice junction of exons a and b. The last two 3' nucleotides of this primer are homologous to the first two nucleotides of exon b. The reverse primer (PotatoNad2R) is located entirely within exon b. To compare the sensitivities of 18S rRNA and *nad2* mRNA as internal controls, total RNA is extracted from potato leaf tissue as described above and digested with DNase I (TaKaRa Biotechnology, Dalian, China) according to the manufacturer's instructions. The RNA extract is diluted in a tenfold series with RNA extract from *E. coli* strain DH5α. First strand cDNA is synthesized from these dilution samples using a 9-mer random primer and then amplified separately with primer pair's 18SF/18SR and PotatoNad2F/PotatoNad2R. To investigate the effect of tissue degradation on 18S rRNA and *nad2* mRNA, fresh leaves of potato infected with PVX are divided into 12 equal sections by weight and wrapped in plastic bags. Six sections of these tissues are placed at room temperature, while the other six are placed at 4 °C. On day 0, 2, 4, 6, 8, and 10, one section from each incubation temperature was transferred into a freezer maintained at –70 °C. At the end of the final incubation, total RNA is extracted

from all sectioned samples and digested with DNase I (TaKaRa, Dalian) according to the manufacturer's instructions. The quality of all RNA samples was examined by agarose formaldehyde electrophoresis. First-strand cDNA can be synthesized from these RNA samples with a 9-mer random primer and amplified with primer pairs PVXF/PVXR, 18SF/18SR, and PotatoNad2F/ PotatoNad2R separately, under conditions optimized separately.

2.7.3 Optimization of Multiplex RT-PCR

On the basis of conserved regions of coat proteins, the forward and reverse primers for specific viruses could be designed by using the software of Primer Premier 5.0 (Premier Biosoft, USA). First-strand cDNA was synthesized from viral RNA with a virus-specific reverse primer in 20- μ l reactions using AMV reverse transcriptase (TaKaRa, Dalian) according to the manufacturer's instructions. PCR was performed in a thermocycler (Biometra, Germany) using *Taq* Hot Start (HS) DNA polymerase (TaKaRa, Dalian, China) according to the manufacturer's instructions. A 25- μ l PCR reaction mixture consisted of 18.25 μ l double-distilled water, 2.5 μ l of 10 \times PCR buffer (100 mM Tris-HCl, pH 8.3, 500 mM KCl, 15 mM MgCl₂), 2 μ l dNTPs (2.5 mM each), 1 μ l forward and reverse primer (5 μ M each), 0.25 μ l *Taq* HS (5 U/ μ l), and 2 μ l RT product. PCR reaction should be conducted with one cycle of 94 °C for 3 min followed by 35 cycles of 94 °C for 30 s, 58 °C for 30 s, 72 °C for 25 s, and an additional cycle of 72 °C for 5 min. The PCR products are visualized by electrophoresis in 3.5% agarose gels stained with ethidium bromide. All target DNA fragments of the five viruses, 18S rRNA, and *nad2* mRNA were subsequently cloned and sequenced. PCR conditions can be justified according to the results observed.

A mixture of the all the target viruses (5–7 as maximum in one tube test) is to be prepared by mixing equal weights of leaf tissues individually infected with each virus. Viral RNA is extracted from the mixture as described above. Protocol for the multiplex RT reaction is identical with the single virus assays described above, except that the reaction mixture included virus specific reverse primers (0.5 μ mol/L each) for the five viruses and the 18S rRNA reverse primer (0.1 μ mol/L). The RT product is amplified separately by PCR with 18S rRNA, and each virus-specific primer pair of the five viruses, to ensure that the RT product contained first-strand cDNA from all five viruses and 18S rRNA. Subsequently, multiplex PCR is carried out with all target primer pairs and 18SF/18SR in a single reaction. Multiplex PCR reactions are optimized by a series of assays by variation of DNA polymerase, dNTPs, MgCl₂, and primer concentrations, as well as variations in annealing temperature, extension time and cycling numbers.

2.7.4 *Comparison of Sensitivities for Multiplex RT-PCR and DAS-ELISA*

DAS-ELISA performed in 96-well microtiter plates using commercial reagents according to the instructions of the manufacturer (Advanced Diagnostics, USA) for comparison tests. The test results are measured at 405 nm with a spectrophotometer (SpectraMax Plus384, Molecular Devices). A sample is regarded as positive if its absorbance value exceeded the mean value of the healthy controls by 3 standard deviations.

To compare the sensitivity of the multiplex RT-PCR with that of DAS-ELISA, tenfold serial dilutions of PVX samples can be prepared by diluting 50 µg purified PVX virions with healthy potato leaf sap. For multiplex RT-PCR, healthy potato leaf sap is prepared by grinding healthy potato leaf tissue with TRIzol reagent (Invitrogen, USA). For DASELISA, leaf sap was prepared by grinding healthy potato leaf tissue with SB1 buffer (1× phosphate-buffered saline, pH 7.4, containing 0.2% powdered egg albumin [wt/vol], 1% polyvinylpyrrolidone [wt/vol], 0.13% sodium sulfite [wt/vol], 0.02% sodium azide [wt/vol], and 1% Tween 20 [wt/vol]).

2.7.5 *Glass Slide Hybridization*

Viral cDNA clones and primers: Clones separately inserted with cDNA fragments of CMV, PVA, PVY, ZYMV and TMV had been previously described (Du et al., 2006; Chen et al., 2003). Full-length cDNA of PSTVd was amplified by RT-PCR using primers PSTVF (5' GGGAAACCTGGAGCGAACTG 3') and PSTVR (5' CGAGGAAGGACACCCGAAGA 3'), and cloned to pGEM-T easy vector (Promega, USA) according to the manufacture's instructions. The sequence data have been submitted to the GenBank databases under accession number AY360446. These clones were used as PCR templates for preparing fluorescently labeled DNA probes. Virus- and viroid-specific primers for fluorescently labeling PCR were designed using the software of Primer Premier 5.0 (Premier Biosoft International, USA) and synthesized (Table 2.1).

Isolation of nucleic acid: Fresh leaf tissue (0.1 g) was frozen in liquid nitrogen and normally ground with mortar and pestle. Total RNA was extracted using TRIzol reagent (Invitrogen, USA). Prior to precipitation of total RNA, supernatant was further extracted with an equal volume of chloroform. Extraction of TMV RNA from purified TMV virions was the same as described above. RNA concentration was determined by OD₂₆₀ measurement.

Nylon membrane hybridization with ³²P-labeled DNA probes: RNA samples were mixed with 3 volumes of the denaturing solution, which consisted of 66.7% (v/v) formamide, 9.8% (v/v) formaldehyde and 1.3× SSC. The samples were incubated at 65 °C for 5 min, immediately put on ice for 3 min, and then made to a

final concentration of 3× SSC. They were dispensed onto the Zeta-probe nylon membranes as three replicates at 1 µl or 6 µl per dot (Bio-Rad Laboratories, USA). RNAs were fixed on the membrane by baking at 80 °C for 1 h. Hybridization was performed according to a previously described procedure (Chen et al., 2007).

Glass slide hybridization with CY5-labeled DNA probes: Preparation of the printed slides: RNA samples were mixed with 3 volumes of 4× SSC (pH 8.0). The mixture was incubated at 65 °C for 5 min, quenched on ice for 3 min and then spotted onto surfaces of aminosilane slides (CEL Associates, Inc., USA) as three or five replicates at 3 nl per spot with a manual Glass Slide Arrayer (VP478A, V&P Scientific, USA). The printed slides were placed in a humid petri dish and incubated at 65 °C for 30 min. After baking for 1 h at 80 °C, the slides were rinsed in 0.1% SDS for 2 min and subsequently cleaned, by washing with diethyl pyrocarbonate-treated distilled water.

(1) Preparation of CY5-labeled probes. CY5-labeled probes were prepared by PCR, incorporating CY5-dCTP (Amersham Biosciences UK Ltd., UK) into newly-synthesized DNA fragments. Twenty-five microliters of PCR mixture contained the following components: 1× PCR buffer [10 mmol/L Tris-HCl (pH 8.3), 50 mmol/L KCl, 1.5 mmol/L MgCl₂], 0.2 mmol/L (each) of dATP, dTTP and dGTP, 0.02 mmol/L dCTP, 0.01 mmol/L CY5-dCTP, 0.25 µmol/L (each) of forward and reverse primers, 0.05 U/µl *rTaq* DNA polymerase [TaKaRa Biotechnology (Dalian) Co., Ltd.] and 0.05–0.5 ng/µl recombinant plasmid. PCR was performed with one cycle of 94 °C for 3 min, then 35 cycles of 94 °C for 20 s, 56 °C for 25 s, 72 °C for 15–25 s, and an additional cycle of 72 °C for 5 min. The PCR product was precipitated by the addition of 2 volumes of ethanol and 1/10 volume of 3 mol/L ammonium acetate. The CY5-labeled DNA was then collected by centrifugation and dissolved in formamide hybridization solution [50% (v/v) formamide, 5× SSPE, 2× Denhardt's solution, 0.1% (w/v) SDS]. The concentrations of the probes were usually around 20–40 ng/µl.

(2) Hybridization to printed slides. To block the remaining binding sites, the printed slide was pre-hybridized with 12.5 µl of formamide hybridization solution containing 20 µg salmon sperm DNA in an array cassette (HybChamberGene Machines, USA) at 42 °C for 30 min. The coverslip was then washed off by gently shaking the slide in 0.1× SSC, and the slide was dried by brief centrifugation. Prior to hybridization, the prepared probe was denatured at 94 °C for 5 min, and immediately put on ice for 3 min. The denatured probe (12.5 µl) was pipetted onto the slide and a coverslip was placed over the probe. Hybridization was performed in the array cassette at 42 °C for 2 h. The slide was washed in pre-heated 2× SSC/0.1% SDS at 42 °C for 5 min, and then in pre-heated 0.5× SSC/0.1% SDS at 42 °C for 5 min, and finally in 0.1× SSC at room temperature for 5 min. The slide was dried by brief centrifugation and stored in a light-proof slide box at room temperature.

(3) Scanning and analysis. The hybridized slides were scanned with a GenePix Personal 4100A scanner (Axon Instruments, Inc., USA), and the resulting 16 bit TIFF images were analyzed using GenePix Pro 5.0 software (Axon Instruments, Inc.). All slides were scanned using the same PMT Gain of 650 for CY5. The

background-subtracted median pixel intensities were used as a measure of overall spot intensity. The coefficient of variation (CV) of pixel intensity was calculated by dividing the standard deviation of the pixel intensity by the mean pixel intensity based on all of the pixels within a given spot. The measure was used to assess spot morphology homogeneity. Median pixel value was used to calculate the standard deviation and the mean of spot replicates.

Effect of spotting solutions on spot quality: To obtain the optimum spot quality of RNA on surfaces of aminosilane glass slides, three types of solutions were tested as spotting solutions. One solution consisted of saline sodium citrate (SSC) alone, which was used as a spotting solution in DNA microarrays (DNA chips). Three concentrations (1×, 3×, and 5×) of the solution were evaluated. The second solution, named FF-SSC, consisted of formamide, formaldehyde and SSC, which was commonly used as a spotting solution in the conventional nucleic acid spot hybridization. The third solution, named DF-SSC, consisted of dimethyl sulfoxide (DMSO), formaldehyde and SSC. Three concentrations [10%, 20%, and 40% (v/v)] of formamide and DMSO in spotting solutions FF-SSC and DF-SSC were assayed. However, concentrations of formaldehyde and SSC in these two solutions were constant, 7% (v/v) and 5×, respectively. Twofold serial dilutions of TMV RNA, prepared by diluting purified TMV RNA with total RNA from healthy tobacco leaves, were applied to each treatment of one of these three spotting solutions. Total RNA from healthy tobacco leaves was used as a negative control. Glass slide hybridization was performed as described above.

Effects of glass surface chemistries on efficiencies of RNA binding: Three types of surface-modified slides, including aminosilane, poly-L-lysine and aldehyde slides) (CEL Associates, Inc.) were tested. Twofold serial dilutions of TMV RNA, prepared by diluting purified TMV RNA with 5× SSC, were spotted onto surfaces of these three types of slides. The printed slides were hybridized as described above.

Detection limits of glass slide hybridization and nylon membrane hybridization:

To compare the detection limit of glass slide hybridization with that of nylon membrane hybridization, twofold serial dilutions of TMV RNA were prepared by diluting purified TMV RNA with total RNA extracted from healthy tobacco leaves. The dilutions were spotted on aminosilane slides and nylon membranes at 3 nl and 1 µl per dot, respectively. Meanwhile, five independent RNA samples isolated from healthy tobacco leaves were added together to calculate cutoff values. CY5-labeled probes were prepared through incorporating CY5-dCTP into newly-synthesized DNAs during either PCR amplification described as above or random-priming labeling reaction. The latter was performed using a random primer labeling kit according to manufacture's instructions [TaKaRa Biotechnology (Dalian) Co., Ltd.] with a slight modification. The ³²P-dCTP was replaced with CY5-dCTP in the reaction recipes. Glass slide hybridization and nylon filter hybridization were performed as described above. A criterion was set to access the detection limit of the glass slide hybridization. The criterion is that a sample was regarded as positive if its fluorescent signal value exceeded the mean value of the healthy controls by 3 times standard deviations.

References

- Balaji B, Bucholtz DB and Anderson JM (2003) *Barley yellow dwarf virus* and *Cereal yellow dwarf virus* quantification by real-time polymerase chain reaction in resistant and susceptible plants. *Phytopathology* 93(11): 1386-1392.
- Bariana HS, Shannon AL, Chu PWG, et al. (1994) Detection of five seedborne legume viruses in one sensitive multiplex polymerase chain reaction test. *Phytopathology* 84: 1201-1205.
- Barker JM, McInnes JL, Murphy PJ, et al. (1985) Dot-blot procedure with [³²P]DNA probes for the sensitive detection of avocado sunblotch and other viroids in plants. *J Virol Methods* 10(2): 87-98.
- Bertolini E, Olmos A, Martinez MC, et al. (2001) Single-step multiplex RT-PCR for simultaneous and colourimetric detection of six RNA viruses in olive trees. *J Virol Methods* 96(1): 33-41.
- Boonham N, Walsh K, Smith P, et al. (2003) Detection of potato viruses using microarray technology: towards a generic method for plant viral disease diagnosis. *J Virol Methods* 108(2): 181-187.
- Broadbent L (1976) Epidemiology and control of *Tomato mosaic virus*. *Annual Review of Phytopathology* 14: 75-96.
- Bystricka D, Lenz O, Mraz I, et al. (2005) Oligonucleotide-based microarray: a new improvement in microarray detection of plant viruses. *J Virol Methods* 128(1-2): 176-182.
- Chamberlain JS, Gibbs RA, Ranier JE, et al. (1988) Deletion screening of the Duchenne muscular dystrophy locus via multiplex DNA amplification. *Nucleic Acids Res* 16(23): 11141-11156.
- Chen SN, Chen JS, Wu P, et al. (2007) Characterization of viruses causing necrosis diseases on tomato. *Acta Phytopathologica Sinica* 37(4): 377-382.
- Cheung VG, Morley M, Aguilar F, et al. (1999) Making and reading microarrays. *Nat Genet* 21(1 Suppl): 15-19.
- Chizhikov V, Wagner M, Ivshina A, et al. (2002) Detection and genotyping of human group A rotaviruses by oligonucleotide microarray hybridization. *J Clin Microbiol* 40(7): 2398-2407.
- Delanoy M, Salmon M and Kummert J (2003) Development of real-time PCR for the rapid detection of episomal *Banana streak virus* (BSV). *Plant Dis* 87: 33-38.
- Deyong Z, Willingmann P, Heinze C, et al. (2005) Differentiation of *Cucumber mosaic virus* isolates by hybridization to oligonucleotides in a microarray format. *J Virol Methods* 123(1): 101-108.
- Dyson N (1991) Immobilization of nucleic acids and hybridization analysis. In: *Essential Molecular Biology: A Practical Approach* (Brown TA Ed.), IRL Press, Oxford, II: 111-114.
- Feng LX and Yang CR (2000) The identification of subgroup of CMV from tomato in China by DAS-ELISA. *Acta Horticulturae Sinica* 27(6): 418-422.
- Gal-On A, Kaplan I and Palukaitis P (1995) Differential effects of satellite RNA on the accumulation of *Cucumber mosaic virus* RNAs and their encoded proteins in tobacco vs zucchini squash with two strains of CMV helper virus. *Virology* 208(1): 58-66.
- Haase A, Richter J and Rabenstein F (1989) Monoclonal antibodies for detection and

- serotyping of *Cucumber mosaic virus*. *Phytopathology* 127: 129-136.
- Hauser S, Weber C, Vetter G, et al. (2000) Improved detection and differentiation of poleroviruses infecting beet or rape by multiplex RT-PCR. *J Virol Methods* 89(1-2): 11-21.
- Hsu YH, Annamalai P, Lin CS et al. (2000) A sensitive method for detecting *Bamboo mosaic virus* (BaMV) and establishment of BaMV-free meristem-tip cultures. *Plant Pathology* 49(1): 101-107.
- Hull R and Al-Hakim A (1988) Nucleic acid hybridization in plant virus diagnosis and characterization. 6(9): 213-218.
- Ito T, Ieki H and Ozaki K (2002) Simultaneous detection of six citrus viroids and *Apple stem grooving virus* from citrus plants by multiplex reverse transcription polymerase chain reaction. *J Virol Methods* 106(2): 235-239.
- Jacobi V, Bachand GD, Hamelin RC, et al. (1998) Development of a multiplex immunocapture RT-PCR assay for detection and differentiation of tomato and *Tobacco mosaic tobamoviruses*. *J Virol Methods* 74(2): 167-178.
- Labate JA., Grandillo S, Theresa F, et al. (2007) Tomato. *In: Genome Mapping and Molecular Breeding in Plants* (Kole C, Ed.), Springer-Verlag, Berlin Heidelberg, pp. 1-125.
- Lee GP, Min BE, Kim CS, et al. (2003) Plant virus cDNA chip hybridization for detection and differentiation of four cucurbit-infecting tobamoviruses. *J Virol Methods* 110(1): 19-24.
- Li J, Chen S and Evans DH (2001) Typing and subtyping influenza virus using DNA microarrays and multiplex reverse transcriptase PCR. *J Clin Microbiol* 39(2): 696-704.
- Mackay IM, Arden KE and Nitsche A (2002) Real-time PCR in virology. *Nucleic Acids Res* 30(6): 1292-1305.
- McInnes JL, Habili N and Symons RH (1989) Nonradioactive, photobiotin-labelled DNA probes for routine diagnosis of viroids in plant extracts. *J Virol Methods* 23(3): 299-312.
- Menzel W, Jelkmann W and Maiss E (2002) Detection of four apple viruses by multiplex RT-PCR assays with coamplification of plant mRNA as internal control. *J Virol Methods* 99(1-2):81-92.
- Nakahara K, Hataya T, Hayashi Y, et al. (1998) A mixture of synthetic oligonucleotide probes labeled with biotin for the sensitive detection of *Potato spindle tuber viroid*. *J Virol Methods* 71(2): 219-227.
- Nie X and Singh RP (2000) Detection of multiple potato viruses using an oligo(dT) as a common cDNA primer in multiplex RT-PCR. *Journal of Virological Methods* 86(2): 179-185.
- Nie X and Singh R P (2001). A novel usage of random primers for multiplex RT-PCR detection of virus and viroid in aphids, leaves, and tubers. *J Virol Methods* 91(1): 37-49.
- Nie X and Singh RP (2002) A new approach for the simultaneous differentiation of biological and geographical strains of *Potato virus Y* by uniplex and multiplex RT-PCR. *J Virol Methods* 104(1): 41-54.
- Owens RA and Diener TO (1981) Sensitive and rapid diagnosis of *Potato spindle tuber viroid* disease by nucleic acid hybridization. *Science* 213(4508): 670-672.
- Pfützner AJP (2006) Resistance to *Tobacco mosaic virus* and *Tomato mosaic virus* in Tomato. *In: Natural Resistance Mechanisms of Plants to Viruses* (Loebenstein G,

- and Carr JP, Eds.), Springer, Netherlands, pp. 399-413.
- Rizos H, Gunn LV, Pares RD, et al. (1992) Differentiation of *Cucumber mosaic virus* isolates using the polymerase chain reaction. *J Gen Virol* 73(Pt 8): 2099-2103.
- Roossinck MJ (2001) *Cucumber mosaic virus*, a model for RNA virus evolution. *Molecular Plant Pathology* 2(2): 59-63.
- Salazar LF (1996) *Potato Viruses and Their Control*. Centro Internacional de la Papa, Peru.
- Sharman M, Thomas JE and Dietzgen RG (2000) Development of a multiplex immunocapture PCR with colourimetric detection for viruses of banana. *J Virol Methods* 89(1-2): 75-88.
- Thompson JR, Wetzel S, Klerks MM, et al. (2003) Multiplex RT-PCR detection of four aphid-borne strawberry viruses in *Fragaria* spp. in combination with a plant mRNA specific internal control. *J Virol Methods* 111(2): 85-93.
- Valasek MA and Repa JJ (2005) The power of real-time PCR. *Adv Physiol Educ* 29(3): 151-159.
- Wang RF, Beggs ML, Robertson LH, et al. (2002) Design and evaluation of oligonucleotide-microarray method for the detection of human intestinal bacteria in fecal samples. *FEMS Microbiol Lett* 213(2): 175-182.
- Wilson WJ, Strout CL, DeSantis TZ, et al. (2002) Sequence-specific identification of 18 pathogenic microorganisms using microarray technology. *Mol Cell Probes* 16(2): 119-127.
- Ye RW, Wang T, Bedzyk L, et al. (2001) Applications of DNA microarrays in microbial systems. *J Microbiol Methods* 47(3): 257-272.
- Yu C, Wu J and Zhou X (2005) Detection and subgrouping of *Cucumber mosaic virus* isolates by TAS-ELISA and immunocapture RT-PCR. *J Virol Methods* 123(2): 155-161.
- Zhu B, Jin F, Zhao J, et al. (2001) Manufacture of complementary DNA arrays on amino-modified slides. *Prog Biochem Biophys* 28(1): 121-124.
- Zhu JY, Zhu SF, Liao XL, et al. (2003) Detection of *Tomato ringspot virus* by real-time fluorescent RT-PCR one step assay. *Acta Phytopathol Sinica* 33: 338-341.

Infectious Clones and Chimerical Recombination of *Cucumber Mosaic Virus* and its Satellite RNAs

3.1 Introduction

Through gene manipulation techniques, we can obtain nucleic acids materials such as RNA or DNA principles corresponding to a certain virus. And these nucleic acids materials replicate and assemble into virions or produce virus-induced symptoms by being inoculated hosts (host plants, cultured host cells, etc.). We call these nucleic acids materials infectious clones. And this technique is a virus rescue technique. Generally, to study the interaction between two viruses or to recognize the interaction between a particular virus and its host plant and to investigate the function of the viral gene, an infectious clone of the viruses is the critical and basic step. It is relatively easy to do this for *Cucumber mosaic virus* (CMV) and other *Bromoviridae* viruses, of which the segments of genomic RNAs are less than 4,000 nt, with quite a lot of reports related to the pseudo-recombination between CMV and other cucumoviruses and even viruses from other genes (see examples in Section 3.3).

The qualification of infectious viruses, including infectious materials such as RNAs, is another key factor in recognizing virus-virus interaction or virus-host interaction. Infectious RNAs can be determined by measuring the concentration of RNA when infectious RNAs are transcribed from plasmids. In the authors' opinion, T7 promoter is more functional than 35S system for obtaining reliable viral RNAs or direct infection by cDNA. In the case of tobamoviruses, a carefully diluted and measured virion can be used to initiate the infection, since the viruses are stable and of high concentration in leaf tissues. It is not suggested the transcribed RNAs should be kept long during and after determining the concentration. A biological assay to control the viral concentration is essentially suggested for all the tests.

Cross-protection is the protection conferred on a host by infection with one strain of a virus that prevents infection by a closely-related strain of that virus. This was first reported by McKinney (McKinney, 1929), who observed that

tobacco plants systemically infected by a “green” strain of TMV were protected from infection by another strain that induced yellow mosaic symptoms. This phenomenon often occurs between closely-related viruses (Culver, 1996; Lu et al., 1998; Yukio and Yuichiro, 2003; Ziebell et al., 2007). A CMV mutant lacking the 2b gene was shown to efficiently cross-protect against a challenge with wild-type CMV-Fny in two species of *Nicotiana* (Ziebell et al., 2007). Initial infection with a mutant named CgYD of crucifer *tobamovirus* Cg which is analogous to L₁₁A, an attenuated strain of *Tomato mosaic virus*-L (ToMV-L), can provides protection against a challenge with wild-type crucifer *tobamovirus* Cg in *Arabidopsis thaliana* Col-0 plants (Yukio and Yuichiro, 2003). An attenuated strain of *zucchini yellow mosaic virus* (ZYMV), obtained from a virulent ZYMV, significantly reduced the impact of ZYMV during field experiments (Kosaka et al., 2006). A number of mechanisms have been proposed to account for this phenomenon, including (1) the pre-existing CP interacts with that of the second virus and inhibits its uncoating so that the second virus cannot multiply, (2) competition of host cells, intracellular replication sites, host translational apparatus and/or other host factors indispensable for the virus to establish an infection, (3) induction of host resistance by which replication of the second virus is suppressed, and (4) the first virus prevents the long-distance movement of the second virus (Beachy, 1999; Sherwood and Fulton, 1982). Currently, the most popular hypothesis is RNA silencing, in which closely-related sequences are degraded in a sequence-specific manner (Ratcliff et al., 1997; Voinnet, 2001; Yukio and Yuichiro, 2003). But tomato plants (cv. Hezuo) can be protected against virion-purified RNA of ToMV-N5 to the same degree when compared to the use of the ToMV-N5 virion as the second challenge by initial CMV-Fny infection. It indicated that the CP from CMV-Fny inhibiting the uncoating of ToMV-N5 is probably not the route of interference between CMV-Fny and ToMV-N5 (see detail description below).

3.2 *Cucumber Mosaic Virus*-mediated Regulation of Disease Development Against *Tomato Mosaic Virus* in the Tomato

A *Tomato mosaic virus* isolate ToMV-N5 causes systemic necrosis on the tomato cv. Hezuo 903: A necrosis strain of ToMV has been found between 2005–2008 in Shanghai, eastern China, on account of its co-infection with CMV. The typical symptoms of the synergy displayed during the fruit season are top necrosis, plant stunt and fruit distortion, combined by brown necrosis strikes among stems and leaf stalks, which develop into the dying off of the whole plant, when the temperature rises above about 28°C. A *Tomato mosaic virus* (ToMV) isolate, namely ToMV-N5, for this necrosis strain has been obtained by three cycles of single-spot isolation on *N. glutinosa*. Sequence determination of this necrosis strain has found only some single nucleic acid, with some single amino acid mutated. In a greenhouse test, when ToMV-N5 is inoculated, chlorosis spots and necrosis spots consequently appear on the inoculated leaf at 4–6 dpi, and then the necrosis extends to the upper systemic leaves, when tomato cv. Hezuo 903 plants

are inoculated on the first true leaves at the 2- to 3-true-leaf stages. Apical necrosis followed by necrotic streaks on stems and plant death can be observed from 7–10 dpi. The rank of necrosis depends on complicated factors including temperature, the leaf stage for inoculation and the inoculation position. When tomato plants are inoculated after the 4-true-leaf stage or inoculated on the cotyledon, no necrosis at the apex can be observed, and the disappearance of apical necrosis can also be monitored when tomato seedlings are inoculated below 20°C, but a high inoculation temperature is found to give faster necrosis (Table 3.1). On other tomato varieties such as cv. Zhongsu 4, ToMV-N5 causes only mild mosaic or mottle symptoms like other ToMV S1, which causes only mild mosaic or mottle on cv. Hezuo 903 and also other tomato varieties tested (Fig. 3.1). Thus, inoculation of ToMV-N5 on the first true leaf at the 2- true-leaf stage of tomato cv. Hezuo 903 below 25°C was used for the following studies.

Table 3.1 Effects of temperature on ToMV-N5 infection on tomato cv. Hezuo 903

temperature	necrosis occur time	No. necrosis/no. inoculated plants
20°C	5 dpi	2/20
25°C	5 dpi	13/20
30°C	5 dpi	20/20
35°C	4 dpi	19/19



Fig. 3.1. Symptom development induced by ToMV-N5 on tomato cv. Hezuo 903 on different inoculation leaves. (a) Mock-inoculation; (b) Inoculated on the cotyledon; (c) Inoculated on the first true leaf. Tomato seedlings were inoculated at their 3-to 4-true-leaf stage and the experiments were observed under 25°C and the plants were photographed at 18 dpi

3.2.1 ToMV-N5 Initiated Necrosis on Tomato Can be Protected by Previous Inoculation with Wild-type CMV

CMV-Fny, can infect tomato cv. Hezuo 903 systemically. In tomato cv. Hezuo 903 plants inoculated with CMV-Fny alone, mild mosaic starts to appear at 5–7 dpi, followed by plants stunting and a typical mosaic appears which gradually develops into leaf deformation within 15 dpi, in the middle and younger leaves. Under mechanical inoculation conditions, CMV-Fny induces no symptoms at an early stage and then causes mild yellowing at a later stage in the older leaves (the first and second true leaves). Plants that have been pre-inoculated with CMV-Fny and later (after 7 d) challenged with ToMV-N5 express combinations of symptoms for both CMV-Fny and ToMV-N5, but symptoms induced by ToMV-N5 appeared to be localized only in the inoculated leaves and no necrosis can be observed in most plants (Fig. 3.2). An obvious CMV-Fny-mediated reduction of symptom development tomato cv. Hezuo 903 to ToMV-N5 is observed (Table 3.1). Interference collapsed when both viruses were inoculated simultaneously (Fig. 3.3(a)). It is found that the interval between the first inoculation by wildtype CMV and second inoculation by ToMV can obviously affect the extent of cross-protection between CMV-Fny and ToMV-N5. At seven days post CMV-Fny infection, tomato seedlings are found to be protected completely from top necrosis but there are still ToMV mediated yellowing of leaves on the lower parts of the seedlings. At nine days post CMV-Fny infection, tomato cv Hz903 seedlings are found to be protected almost completely from any symptom, including top necrosis and chlorosis. Furthermore, ToMV-N5 single infections always show growth stagnation because of the necrotic phenotype whereas, according to the plant's height measurement, the growth of CMV-Fny and ToMV-N5 double infections just slow down (Fig. 3.4). To clarify whether the coat protein (CP) produced by replication of CMV-Fny, inhibition of uncoating of the ToMV-N5, ToMV-N5 virion-purified RNA has been used as the second virus. Here, interference occurs to the same degree as when compared to using the ToMV-N5 virion as the second challenge. It shows that ToMV-N5 initiated necrosis on tomato cv. Hz 903 can be protected by previous inoculation with wild-type CMV but a necessary time interval is essential for the plant to gain resistance.

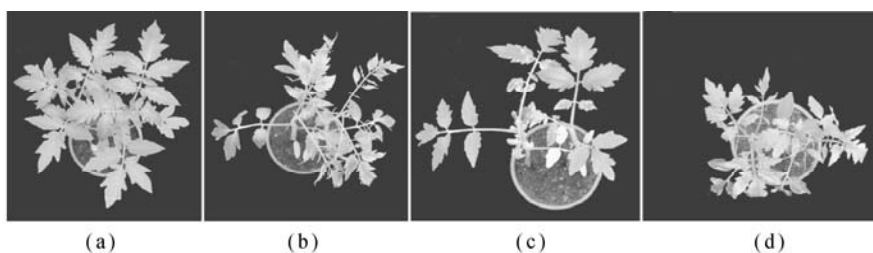


Fig. 3.2. Symptoms induced on tomato seedlings by pro-inoculation with CMV-Fny and ToMV-N5 alone or in combinations. (a) Mock-inoculation; (b) CMV-Fny; (c) ToMV-N5; (d) ToMV-N5 inoculation 7 d post CMV-Fny. Symptoms were recorded at 18 dpi with ToMV-N5

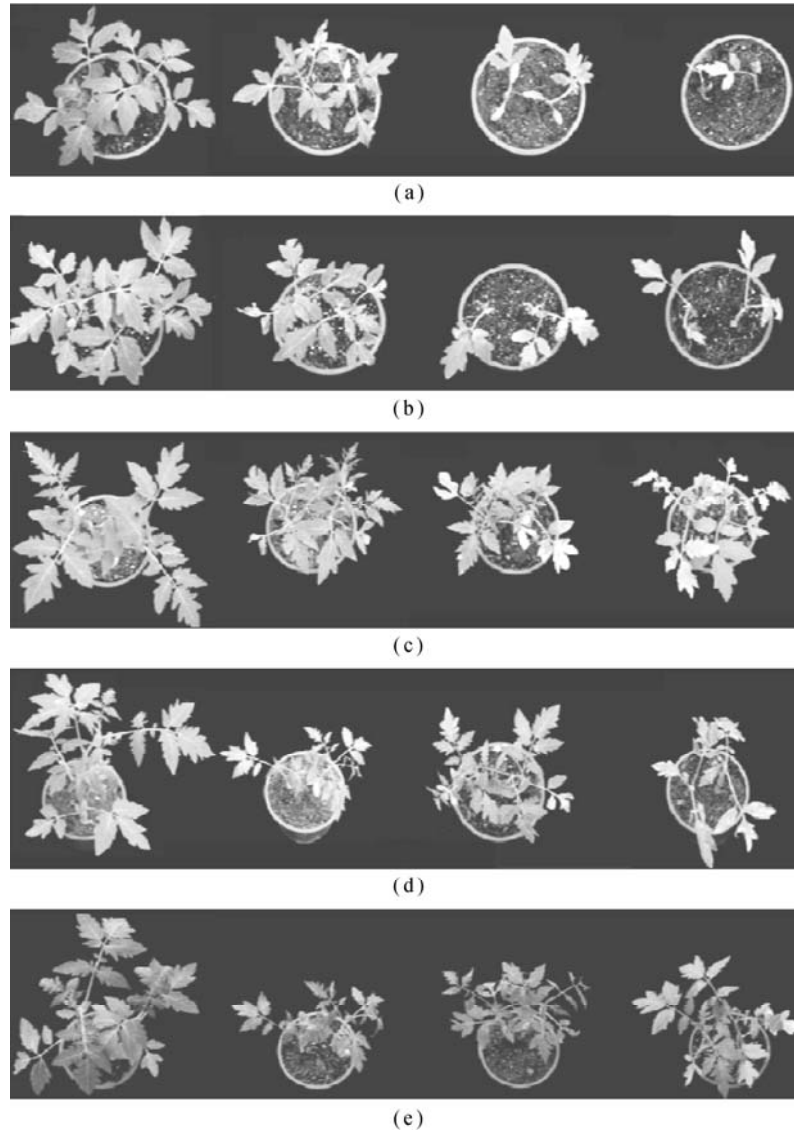


Fig. 3.3. Symptom on seedlings of tomato cv. Hezuo 903 inoculated with ToMV-N5 in different intervals post CMV inoculation. (a) ToMV-N5 inoculated at 0 d post inoculation of CMV-Fny; (b) ToMV-N5 inoculated at 3 d post CMV-Fny inoculation, (c) ToMV-N5 inoculated at 5 d post CMV inoculation; (d) ToMV-N5 inoculated at 7 d post CMV inoculation; (e) ToMV-N5 inoculated at 9 d post CMV inoculation. From left to right: mock-inoculated plants, CMV-Fny singly infected, CMV-Fny plus ToMV-N5 double infection and ToMV-N5 single infection. Plants are photographed 10 d post the inoculation with ToMV-N5

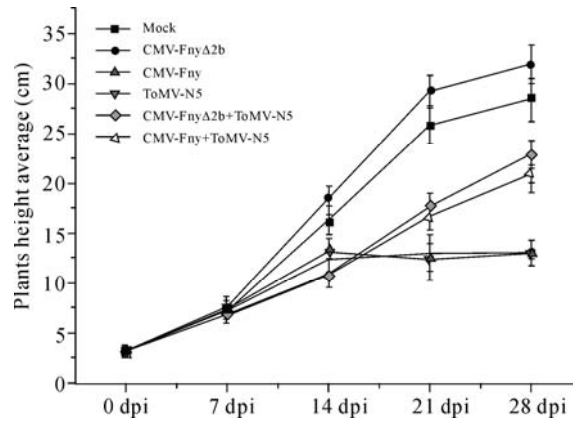


Fig. 3.4. The over time growth of tomato cv. Hezuo 903 presented by heights of seedlings under single- and double-inoculation of ToMV-N5 and CMV strains. ToMV-N5 was inoculated 7 d post inoculation of CMV strains and the experiment was carried out at 25–30°C under greenhouse conditions

3.2.2 *ToMV-N5 Initiated Necrosis on Tomato Cannot be Protected by Previous Inoculation with CMVΔ2b*

The infection of wildtype CMV-Fny with the 2b gene deleted does not show any symptoms but the seedlings appear to become stimulated for vegetative growth (bigger and taller), compared with mock-inoculated plants (Fig. 3.5).

Under the same inoculation conditions, when plants are serially inoculated with CMV-Fny with the 2b gene deleted (CMV-FnyΔ2b) and ToMV-N5, the seedling reaction proves to be similar in appearance to ToMV-N5 single-infections (Table 3.2). It shows that the complex infection by ToMV after CMV-FnyΔ2b yielded typical top necrosis caused by ToMV-N5 and there is no protection of this symptom, but at the same time the stimulation effects by CMV-FnyΔ2b infection are still expressed.

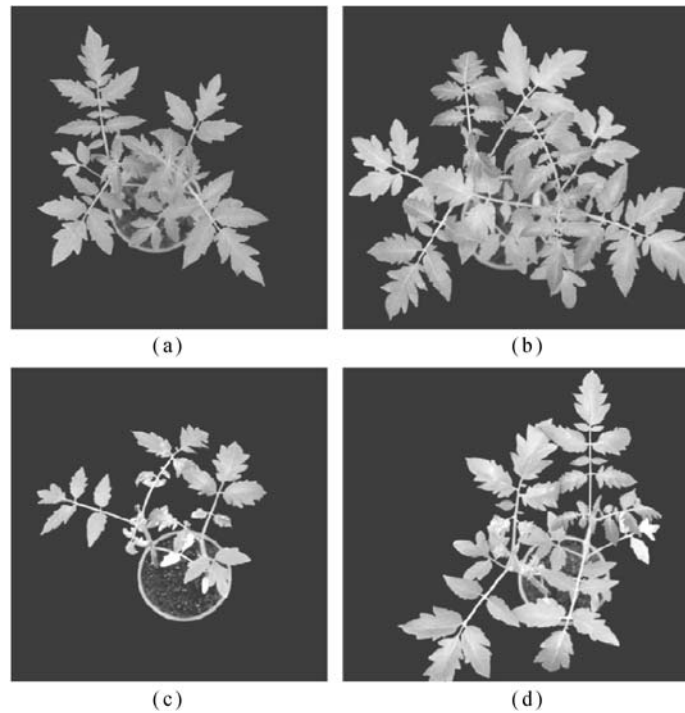


Fig. 3.5. Symptoms on seedlings of tomato cv. Hezuo 903 by inoculation

Table 3.2 Symptoms on seedlings of tomato cv. Hezuo 903 inoculated singly with ToMV-N5 or complexly with CMV or PVX

Viruses	The first true leaf	Systemic leaves
ToMV-N5	ChS, YI, NS	ChS, YI, NS, AN, D
CMV-Fny	L	LD
CMV-Fny +ToMV-N5	ChS, NS	YI, LD
CMV-Fny Δ 2b	L	L
CMV-Fny Δ 2b+ToMV-N5	ChS, NS	ChS, NS, YI, AN, D
PVX	L	M
PVX+ToMV-N5	ChS, NS	SM, NS, YI, AN, D

ToMV and PVX were inoculated at 7 dpi of CMV strains. AN = apical necrosis; Ch = chlorotic; ChS = chlorotic spots; YI: Yellow leaf; D = death of the plant; L = latent (symptomless) infection; LD = leaf deformation; SM = system mosaic; NS = necrotic spots

3.2.3 *ToMV-N5-initiated Necrosis on Tomato Cannot be Protected by Previous Inoculation with Potato Virus X*

Just like wildtype CMV, potato virus X (PVX) is a typical +ssRNA virus and it causes typical foliage mosaic in *Solanouse* crops, by accumulating high viral RNAs in leaf tissues. To clarify whether the protection phenomenon in tomato cv.

Hezuo 903 is mediated specifically by CMV-Fny, the interaction between PVX and ToMV-N5 has been comparably studied. PVX-BJ can infect tomato plants successfully and induce systemic mosaic symptom, but the pre-inoculated plants prove to be a failure against a challenge from ToMV-N5, even though the time interval between inoculations is extended to nine days and over.

It shows that the top necrosis initiated by ToMV-N5 infection can be cross-protected by wildtype CMV but not commonly by other +ssRNA viruses such as PVX, and the 2b gene of CMV as a post transcriptional gene regulation suppressor is essential for such induced protection.

3.2.4 CMV-initiated Protection against ToMV-N5 is Related to the Replication and Accumulation of Challenging Virus

It is found that the reduction in necrosis symptoms could be correlated to accumulation of CMV and/or ToMV-N5. Measured by real-time RT-PCR quantification, CMV-Fny Δ 2b can only be detected in the inoculated leaves, with none or quite little accumulation being detected in the non-inoculated systemic leaves. At 14 dpi and 21 dpi, CMV-Fny accumulation is not affected by co-infection with ToMV-N5 in systemic leaves, but the real-time RT-PCR values have shown that ToMV-N5 accumulation is significantly suppressed by pre-infection with wildtype CMV-Fny at 7 dpi and then becomes hardly detectable at 14dpi in the systemic leaves (Fig. 3.6). Half-leaf assays for testing the infectious viral components shows consistent results with real-time RT-PCR quantification. When *Nicotiana glutinosa* as a local lesion host of ToMV-N5 and the systemic mosaic host of CMV is used, and the right and left half of the same leaf are inoculated respectively, with equal sap extracted either from ToMV-N5 single infection or CMV-Fny plus ToMV-N5 double infection at 7 dpi (after ToMV-N5 infection), the number of lesions on the right is significantly more than those on the left. This intuitive result is consistent with that for viral RNA detection. A much lower level of ToMV-N5 accumulation in double infection with CMV-Fny at 7 dpi (after ToMV-N5 infection) is observed.

It has been known that the suppressor of the systemic post-transcriptional gene silencing (PTGS) response of PVX is a 25 kD movement protein (p25). CMV 2b protein is known as an important silencing suppressor by inhibiting the activity of the RNA mobile silencing signal. It can be speculated that the 2b protein may be an important determinant involved in CMV-mediated regulation of disease development caused by ToMV in tomato cv. Hezuo 903. The 2b protein may have some role in inhibiting the host response from interfering with virus infection, such as programmed death of the tissues and dependence on the interval between the first and second inoculation which to some extent support this point.

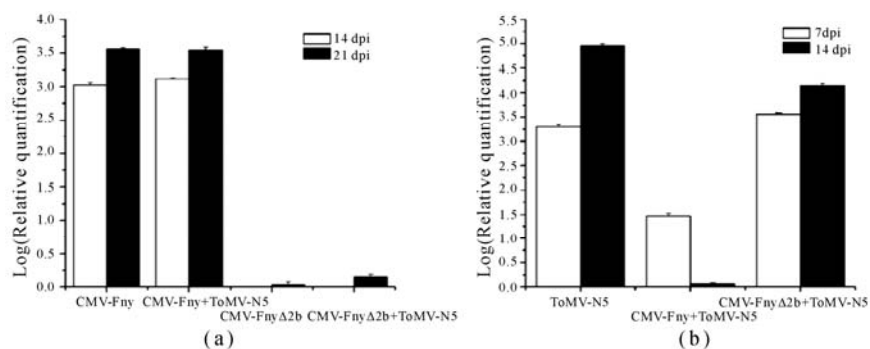


Fig. 3.6. Quantitative detection of CMV-Fny and CMV-FnyΔ2b compared with ToMV-N5 in single and double infected tomato plants. (a) CMV-Fny and CMV-FnyΔ2b are detected at 14 dpi and 21 dpi of the two viruses; (b) ToMV-N5 is quantitatively detected (C+T and CΔ2b +T) in tomato plants at 7 dpi and 14 dpi of this virus. Real-time RT-PCR is carried out with CMV CP-specific and ToMV CP-specific primers, respectively. Data were a mean of base-10 logarithm of relative quantification values. The value for each histogram represents the average of sample duplicates prepared from three leaf disks of the second leaves (one per leaf) of three plants. Vertical bars represent standard errors

3.3 Pseudo-recombination between Subgroups of *Cucumber Mosaic Virus* Demonstrates Different Pathotype and Satellite RNA Support Characters

A natural reassortant CMV-Tsh and its satRNA-Tsh were firstly detected in diseased tomato plants in Shanghai, eastern China (see Chapter 1). Sequencing analysis asserted that CMV-Tsh is a CMV subgroup IA RNA2 and subgroup II RNAs 1 and 3 (Chen et al., 2003). Infectious transcripts of CMV-Tsh RNA2 and RNA3 were successfully constructed. The replication, pathogenicity and relative accumulation properties of pseudo-recombinants by CMV-Fny (genomic RNA1, RNA2 and RNA3, named F1, F2 and F3 respectively) and CMV-Tsh (genomic RNA2 and RNA3, named T2 and T3 respectively), were proved to be built up in comparison with the wildtype CMV-Fny (F1F2F3), with the satRNA-Tsh maintaining characters.

3.3.1 Wildtype and Pseudo-recombinants and with or without satRNA Induce Different Symptoms on *N. glutinosa*

When infectious genomic RNAs of CMV, including RNA1, 2 and 3 of CMV-Fny, and RNA2 and 3 of CMV-Tsh, are co-inoculated onto *N. glutinosa* with or without SatRNA-Tsh, all the viruses are found to be pathogenic to this host plant. As

shown in Fig. 3.7, when the inoculation is kept under 22–28°C, typical mosaic symptoms are found on the newly-growing leaves of *N. glutinosa* seedlings inoculated by all the three pseudo-recombinant and CMV-Fny, from 5 to 7 dpi. F1F2T3 and F1T2T3 cause more severe symptoms than that of F1F2F3 (CMV-Fny) and F1T2F3, according to the degree of stunting, and yellowing. And these two viruses are found to cause top rosette and foliage necrosis on the lower part of the plants, whilst F1F2F3 and F1T2F3 cause no necrosis. The wild type CMV-Fny produces typical linear leaves on *N. glutinosa* but non-pseudo-recombinant viruses do. The addition of SatRNA-Tsh is found obviously attenuating all the pseudo-recombinant viruses and wild type CMV-Fny. The symptoms are noticeably reduced, but in comparison with healthy control seedlings, leaf chlorosis and stunting symptoms are obviously induced. No rosette symptom can be found but there are differences among the four viruses, but less severe necrosis symptoms are observed on seedlings inoculated with F1F2T3 and the degree of chlorosis is more apparent on seedlings inoculated with F1F2T3 and F1F2F3 (CMV-Fny). Observed at 35dpi, the symptom indecency is found in the decreasing order of F1F2T3, F1T2T3, F1F2F3 (CMV-Fny) and F1T2F3. Mosaic symptoms are mostly recovered from F1T2F3 inoculation but not for other treatments. The disease index for each treatment is observed and calculated at 7, 14, 21, 28 and 35 dpi, shown in Fig. 3.8. It is shown that among the four inoculations, F1F2T3 produces the most severe symptoms, but F1T2F3 produces the lightest symptoms.

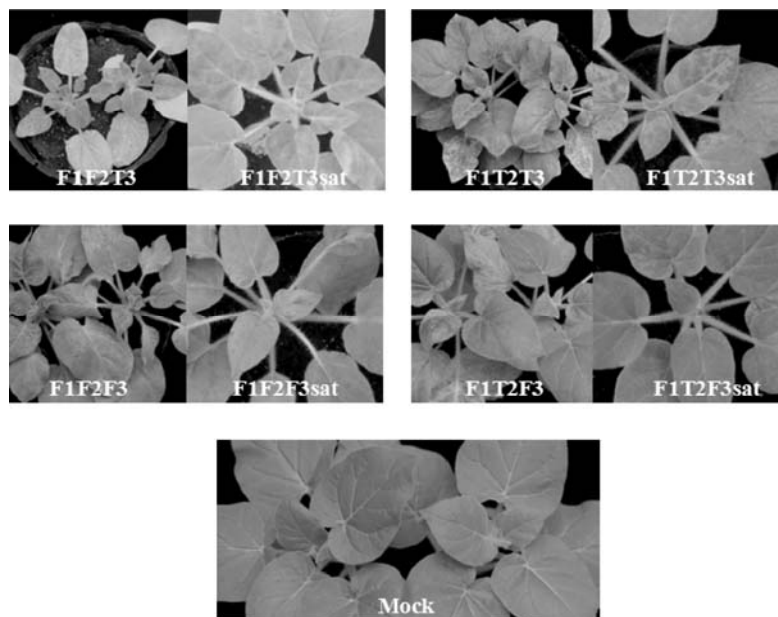


Fig. 3.7. Symptoms on *N. glutinosa* induced by wild type and pseudo-recombinant viruses with and without *satRNA-Tsh*. Mock-treated plants inoculated with distilled water. Photographs are taken 21 dpi

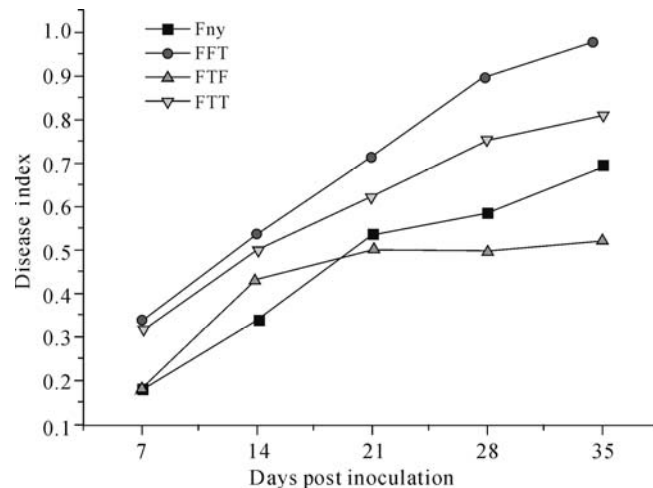


Fig. 3.8. Disease index on *N. glutinosa* under infection of the pseudo-recombinant viruses and CMV-Fny

Using activated viruses with five to seven days pre-inoculation on *N. glutinosa*, similar results are observed respectively, for all the four viruses. It is declared that all the three pseudo-recombinant and CMV-Fny are infectious to *N. glutinosa* and satRNA-Tsh could obviously attenuate the pathogenicity of CMV strains on this host plant.

3.3.2 Wildtype and Pseudo-recombinants with or without satRNA Induce Different Symptoms on *N. benthamiana*

When inoculated with virus pseudo-recombinants and CMV-Fny without satRNA on *N. benthamiana*, a similar tendency of symptom development can be observed on seedlings of all the four viruses, in the decreasing order of F1F2T3, F1T2T3, F1F2F3 (CMV-Fny) and F1T2F3. All the four viruses are found to induce necrosis and brought about leaf falling on the inoculated leaves. Yellowing foliage and stunt are the most typical symptoms on this host plant, but chlorosis is to a certain degree recorded on the inoculation of F1T2F3 and F1T2T3, as shown in Fig. 3.9. The attenuation effect is more apparent on *N. benthamiana* than that on *N. glutinosa* when satRNA-Tsh is induced to the genome of those four CMV strains, with neither necrosis nor yellow leaf symptom being observed. In comparison with those viruses without satRNA-Tsh, the viruses with satRNA-Tsh gave quite a lower reduction in plant growth. Mild mosaic could be inspected in all the inoculations and viruses could be transferred back to *N. glutinosa* seedlings from all the inoculated seedlings above.



Fig. 3.9. Symptoms on *N. benthamiana* induced by wildtype and pseudo-recombinant viruses with and without satRNA. Mock-treated plants inoculated with distilled water. Plants of *N. benthamiana* are photographed 21 dpi

Similar results can easily be obtained with both viruses directly transcribed from infectious RNAs and total RNAs extracted from leaf tissues of *N. glutinosa* systemically infected by the four viruses with or without satRNA. It is shown that virus pseudo-recombinants and wildtype CMV-Fny produced different symptoms on different host plants and satRNA-Tsh has a stronger attenuating effect on *N. benthamiana*.

3.3.3 Wildtype and Pseudo-recombinants with or without satRNA Induce Different Symptoms on Tomato Varieties

The induction of symptoms by inoculation virus pseudo-recombinants and wildtype CMV-Fny are found to be quite different, depending on tomato varieties, temperature and the condition with or without satRNA-Tsh. In most tomato varieties and inoculation cases, a similar tendency is found for the four viruses without satRNA as those on *N. glutinosa* and *N. benthamiana*, resulting in a decreasing order of F1F2T3, F1T2T3, F1F2F3 (CMV-Fny) and F1T2F3. The attenuation effect is observed on most tomato varieties, including tomato cv. Zhongsu 4 and cv. Zhongsu 2, and several cherry tomatoes. When tomato cv. Zhongsu 4 is inoculated at 7 dpi, mosaic symptoms appear on the newly growing leaves of seedlings inoculated with all the four pseudo-recombinant viruses but not on seedlings inoculated with satRNA-Tsh. At 21 dpi, symptoms in the seedlings inoculated with F1F2T3 were found to be the most severe, including severe stunting and chlorosis. While F1T2T3 causes severe symptoms including stunting, chlorosis and bubble-formed mosaic, F1F2F3 causes typical bubble-formed mosaic and stunting, while F1T2F3 only causes mild mosaic. At the same time, plants inoculated with four viruses with satRNA-Tsh only express slight mosaic

symptoms but no obvious deformation and stunting. It is suggested that Tsh-satRNA not only postponed the emergence of symptoms of the four recombinant viruses but also alleviated symptom expression in the tomato. As shown in Fig. 3.10(a), when tomato cv. Hezuo 903, a viral resistant hybrid is inoculated and the infected seedlings are kept under 25°C (mostly 20–25°C), all the three recombinant viruses and CMV-Fny are found to cause typical mosaic and stunting symptoms, whilst CMV-Fny produces more linear leaves. The addition of satRNA-Tsh generates an attenuating effect under normal green house temperatures, eg. 25°C. When the infected seedlings are grown over 30°C (mostly 35°C), the three recombinant viruses and CMV-Fny are found to produce more severe stunting and mosaic symptoms excluding necrosis, but the addition of satRNA-Tsh is found to produce heavy necrosis and plant death, except that F1T2F3sat could be recovered to a certain degree (Fig. 3.10(b)).

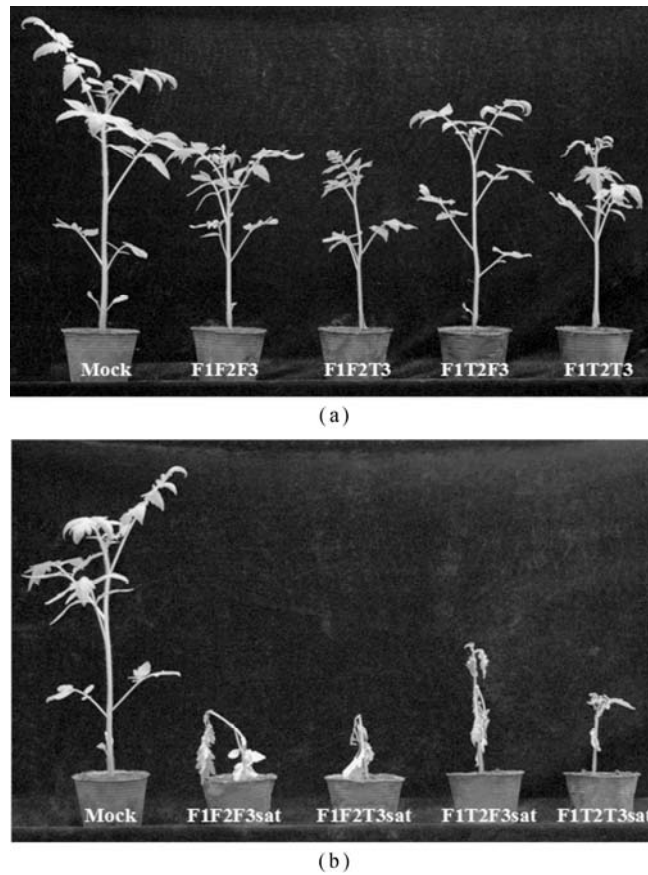


Fig. 3.10. Symptoms induced on tomato cv. Hezuo 903 infected with wildtype CMV-Fny and pseudo-recombinant viruses with or without satRNAs. (a) Helper viruses without satRNA; (b) Those with satRNA. The plants are grown at a temperature over 30°C, and they are photographed at 21 dpi

3.3.4 The Pathogenicity of Wildtype and Pseudorecombinants with or without satRNA-Tsh are Related to Viral Accumulation

As shown in Fig. 3.11, double-stranded RNA analysis shows that three pseudo-recombinant viruses, F1F2F3, F1T2F3 and F1T2T3 are successfully regenerated by pseudo-recombination RNA1 of Fny-CMV with full-length transcripts of Tsh-CMV RNA2 to yield F2, and RNA3 to yield F3, by extracting dsRNAs from systemic infected leaf tissues of *N. glutinosa*. All the four viruses including Fny-CMV as a control express similar ds-RNA patterns in agarose gel-electrophoresis, whilst satRNA-Tsh is found to be supported for replication with all the above four viruses, by adding the full-length transcript of this satRNA into the genome of the helper viruses. The appearance of high level ds-RNA in systemic tissues in *N. glutinosa* has brought a general reduction of genomic RNA accumulation of the helper virus, from which satRNA-Tsh is considered a potential attenuation factor for the above viruses.

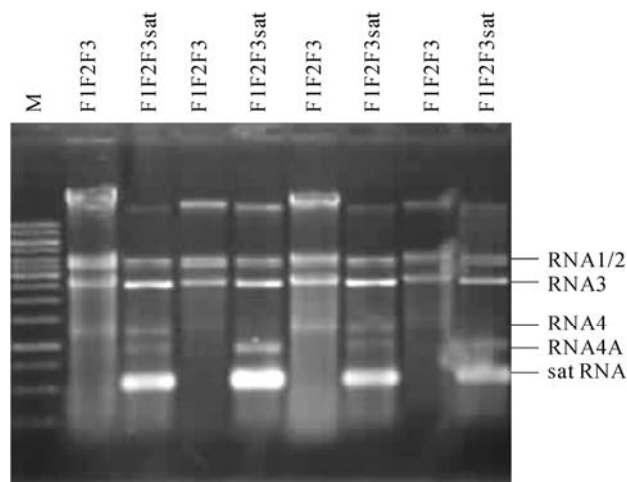


Fig. 3.11. Patterns of double-stranded RNAs from *N. glutinosa* inoculated with wildtype CMV-Fny and pseudo-recombinant viruses. The dsRNAs are extracted at 14 dpi

Both dsRNA and viral genomic progeny RNA showed the same accumulation tendency for helper virus reduction when satRNA is added. Thus, it could be considered that satRNA-Tsh attenuated the symptoms by depressing the accumulation of genomic RNAs in all the four viruses.

Again, as shown in Fig. 3.12, when determined with real-time RT-PCR assay, the relative accumulation of five CMV ORFs on systemic leaves of *N. glutinosa* at 14 dpi. shows some different inoculation treatment. Regarding genomic RNA1 (1a ORF), CMV-Fny yields the highest accumulation, implying that RNA2 and RNA3 (all of subgroup I strain) could well assist the replication of their own genomic RNA1. F1T2F3 with RNA2 from subgroup I but originally different from F2, give

a similar accumulation of RNA1, whilst F1T2T3 and F1F2T3 have obvious differences in their accumulation of genomic RNA1, indicating that their genomic RNAs are not so well adjusted in *N. glutinosa*. The change in RNA2 and RNA3 among those four viruses could not be well adjusted since primers for realtime PCR had been chosen only for adopting CMV-Fny genomic RNAs, but the relative accumulation of each pseudo-recombinant CMV ORFs 1a without satRNA-Tsh is 2.78–8.64 fold that of those with satRNA-Tsh on *N. glutinosa*, indicating that the satRNA could obviously decrease the replication and/or accumulation of the helper viruses. To a certain degree, the mechanism of satRNAs attenuation against CMV infection could be considered for the depression and reduction of genomic RNAs.

Recombination of virus strains (eg. those from different CMV subgroups) and the occurrence of *sat*RNAs may induce different pathogenicity of plant ssRNA viruses. We need to be careful to monitor the emergence of new strains from recombination/pseudo-recombination and the occurrence of *sat*RNAs, especially when the temperature and the agricultural system are changing.

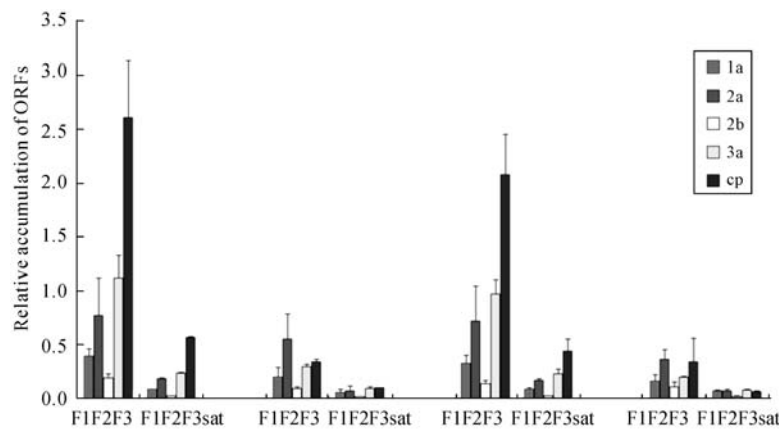


Fig. 3.12. Relative accumulation of five CMV ORFs detected in systemic leaves of *N. glutinosa* inoculated with wildtype CMV-Fny and pseudorecombinant viruses. Total RNAs are extracted at 14 dpi. The relative accumulation of each ORFs is analyzed by real-time reverse transcription-polymerase chain reaction amplified with specific pairs, and was repeated three times, with 18S rRNA used as the endogenous control. Relative quantization of data was carried out according to the comparative CT method ($2^{-\Delta\text{CT}}$), for example, the relative accumulation of F1F2F3 1a = $2^{-(\text{aver } 1a \text{ CT} - \text{aver } 18s \text{ CT})}$. The primer pairs and methods are described in Chapter 2

3.4 Synergy via *Cucumber Mosaic Virus* and *Zucchini Yellow Mosaic Virus* on *Cucurbitaceae* Hosts

Cucumber mosaic virus (CMV) and *Zucchini yellow mosaic virus* (ZYMV) are both principal viruses infecting cucurbitaceous crops, and their synergy has been

repeatedly observed. When crops are infected complexly by the two viruses, much more severe induction is always observed. Using a real-time reverse transcription–polymerase chain reaction procedure, the accumulation kinetics of these two viruses in single or complex infections are monitored at the molecular level, with the accumulations of open reading frames (ORFs) for 1a, 2a, 3a and coat protein (CP) of CMV and CP of ZYMV tested. In the single infection, CMV-Fny ORFs are found to accumulate to their maximums in cucumber or bottle gourd at 14 dpi, and gradually declined thereafter. ZYMV-SD CP ORF is found to reach the maximum accumulation at 14 and 28 dpi on cucumber and bottle gourd, respectively. However, when co-infected with CMV-Fny and ZYMV-SD, the maximum accumulation levels of all viral ORFs are delayed. CMV-Fny ORFs reach their maximums at 21 dpi on both hosts, and ZYMV-SD CP ORF reaches the maximum accumulation at 21 and 28 dpi on cucumber and bottle gourd, respectively. Generally, the accumulation levels of CMV-Fny ORFs in the co-infection are higher than those in the single infection, whereas the accumulation of ZYMV-SD CP ORF shows a reverse result. It is suggested that bottle gourd is more suitable than cucumber for synergy analysis of the two viruses, and new protocols to quantify the accumulation kinetics of CMV and ZYMV genomic RNA in either single or co-infection can lead us to a more detailed understanding of the interaction and the mechanism concerning disease synergy.

3.4.1 Assessment of Symptom and Synergic Interaction by Cucumber Mosaic Virus and Zucchini Yellow Mosaic Virus

Both seedlings of cucumber (*Cucumis sativus*) and bottle gourd (*Lagenaria siceraria*) infected with CMV-Fny, are found to present typical systemic mosaic, foliage distortion followed by flowering retardation, while the symptoms on bottle gourd are much more severe than those on cucumber, when observed at the same period of time, post inoculation. ZYMV-SD isolated, from Shangdong Province, China, produced much more severe effects on inoculated *Cucurbitaceae* plants. Systemic mosaic, yellowing, plant dwarfing and wilting, and obviously malformed leaves and fruits, were commonly present on several cultivars tested. But it also produced more severe symptoms on bottle gourd than on cucumber. CMV-Fny and ZYMV-SD co-inoculated plants are found to develop much more severe symptoms, including malformation, necrotic lesions, wilting and even the dying-off of the whole plant. The enhanced synergic interaction can be observed in quite a lot of species from *Solanaceae*, *Fabaceae* and *Cucurbitaceae*.

The severe symptom proved that these two viruses are synergic on *Cucurbitaceae* crops. Statistical data shows that, at 28 dpi, the disease index of single infection in three species of cultivars of bottle gourd are $34.98\% \pm 4.50\%$ and $37.12\% \pm 3.15\%$ for CMV-Fny and ZYMV-SD, respectively. However, the mean disease index is found to increase to $55.28\% \pm 3.01\%$ on those cultivars co-infected with two viruses, which is approximately 1.58 fold that of CMV-Fny

single infection and 1.50 fold that of ZYMV-SD single infection. The general calculations of disease indicated for bottle gourd (Yonghu 2) in single or complex infection at different stages of infection are listed in Table 3.3.

Table 3.3 Disease index of synergy and single infections by CMV and ZYMV ^a

Inoculum	Disease index (%) ^b				
	7 dpi	14 dpi	21 dpi	28 dpi	35 dpi
CMV-Fny	17.11	18.42	27.10	33.66	38.42
ZYMV-SD	34.21	36.84	38.63	37.60	40.00
Fny+SD	38.33	48.33	50.01	53.75	51.67

^a Three cultivars of bottle gourd (*L. siceraria*) were tested, but only the data tested for cv. Yonghu 2 were shown; ^b These for 30 tested seedlings

3.4.2 Accumulation Kinetics for CMV ORFs in Single or Complex Infection

Using optimized primer pairs, the amplification curves are found to be smooth and of good reproducibility, and each homogeneous RT-PCR produced a single, sharply-defined melting curve with a narrow peak. Thus, real time RT-PCR is reliable for reflecting viral genes quantitatively (Fig. 3.13). Based on this, the relative amounts of the CMV 1a, 2a, 3a and CP ORFs on cucumber (Jinyou 1) seedlings infected with CMV-Fny alone are quantified by real time RT-PCR. For CMV single infection, the accumulation of each CMV ORFs on cucumber plants is hardly detected at 7 dpi, but their accumulation reaches a peak rapidly at 14 dpi. But their accumulation is found to decline rapidly in the following days, when compared with complex infection. The accumulation of each CMV ORFs on cucumber plants co-infected with CMV-Fny and ZYMV-SD is detected as much higher than that of single infection at 7 dpi, but reaches a higher accumulation gradually, to peak at 21 dpi. The accumulation of CMV-Fny and ZYMV-SD ORFs declined gradually in the following weeks. However, compared with single infection, the accumulation of CMV-Fny 1a, 2a, 3a and CP ORFs is obviously higher in co-infection at 35 dpi. Thus, co-infection of CMV and ZYMV stimulates the early stage replication of CMV RNAs and postponed the decline of their accumulation levels (Fig. 3.14). At 35 dpi, the relative amounts of CMV-Fny 1a, 2a, 3a and CP ORFs in complex infection are 1.48, 2.24, 2.51, 0.99 folds that of a single infection, on cucumber plants.

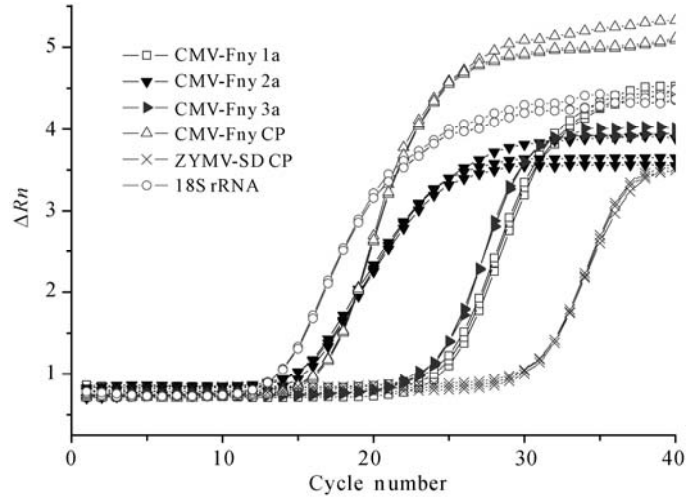


Fig. 3.13. Amplification curves of each detected ORFs in cucumber plants infected by complex of CMV-Fny and ZYMV-SD. A computer software program calculated a ΔRn using the equation $\Delta Rn = Rn^+ - Rn^-$, where Rn^+ is the fluorescence emission of the product at each time point, and Rn^- is the fluorescence emission of the baseline. Three repeats were assayed for each treatment

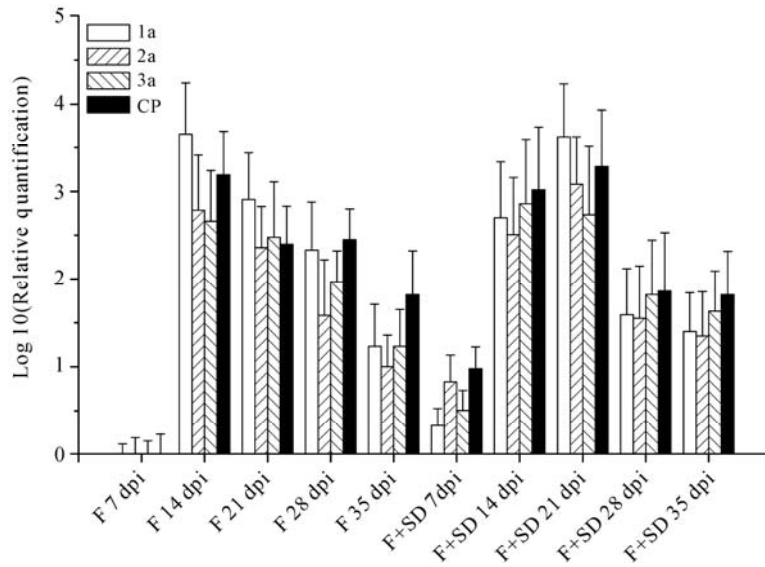


Fig. 3.14. Time courses of RNA accumulation for CMV-Fny 1a, 2a, 3a and CP ORFs from cucumber leaf tissue. Data are detected by real time RT-PCR for target RNAs (ORFs), when infected singly or doubly, set the logarithm (relative quantification) of CMV-Fny 1a, 2a, 3a, CP ORFs on cucumber plants at 7 dpi as zero. F and SD present CMV-Fny and ZYMV-SD, respectively. Data are mean of base-10 logarithm of relative quantification values; error bars represented the standard error

When the accumulation of the CMV 1a, 2a, 3a and CP ORFs on bottle gourd is assayed, it is found that ZYMV influences CMV accumulation more obviously. Early stage replication of CMV ORFs is stimulated in complex infection on bottle gourd at 7 dpi. The accumulation of CMV ORFs in a single infection increases rapidly but to a relatively low level, at 14 dpi, when compared with that of co-infection. And their accumulation levels are much higher in co-infection at 21 dpi, and decline gradually to a relatively high level at 35 dpi. At this time point, the relative amounts of CMV-Fny 1a, 2a, 3a and CP ORFs in complex infection are 15.14, 4.90, 3.16, 2.57 folds that of a single infection, on bottle gourd (Fig. 3.15).

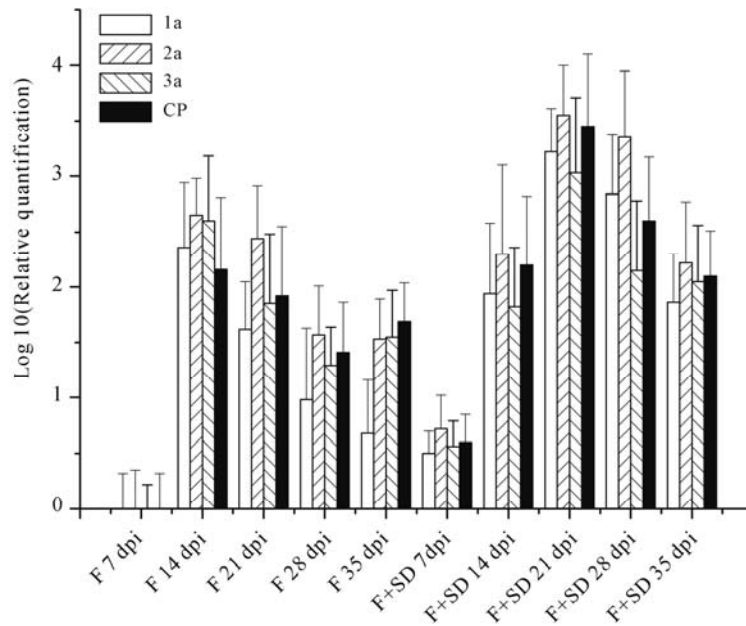


Fig. 3.15. Time courses of RNA accumulation for CMV-Fny 1a, 2a, 3a and CP ORFs from leaf tissue of bottle gourd. Data are detected by real time RT-PCR for target RNAs (ORFs), when infected singly or doubly, the logarithm (relative quantification) of CMV-Fny 1a, 2a, 3a, CP ORFs on bottle gourd at 7 dpi is set as zero. F and SD presented CMV-Fny and ZYMV-SD, respectively. Data are mean of base-10 logarithm of relative quantification values; error bars represented the standard error

That is to say, co-infection of ZYMV increases the replication and/or accumulation of CMV in both hosts.

3.4.3 Accumulation Kinetics of ZYMV CP ORF in Single or Complex Infection

During the testing period (~35 dpi), the relative amount of ZYMV CP gene is found to increase rapidly, and the loading level reached a maximum at 14 dpi in a single infection of the cucumber, but it increases slowly and reached the maximum at 21 dpi in a complex infection with CMV. However, on bottle gourd, the accumulation of ZYMV CP ORF is found to reach a maximum at 28 dpi in both single and complex infection, but the relative amount of ZYMV CP ORF in a complex infection is obviously lower than that of a single infection (Fig. 3.16). At 35 dpi, the relative amounts of ZYMV-SD CP ORF in a complex infection are 90% and 22% in a single infection, on cucumber and bottle gourd, respectively.

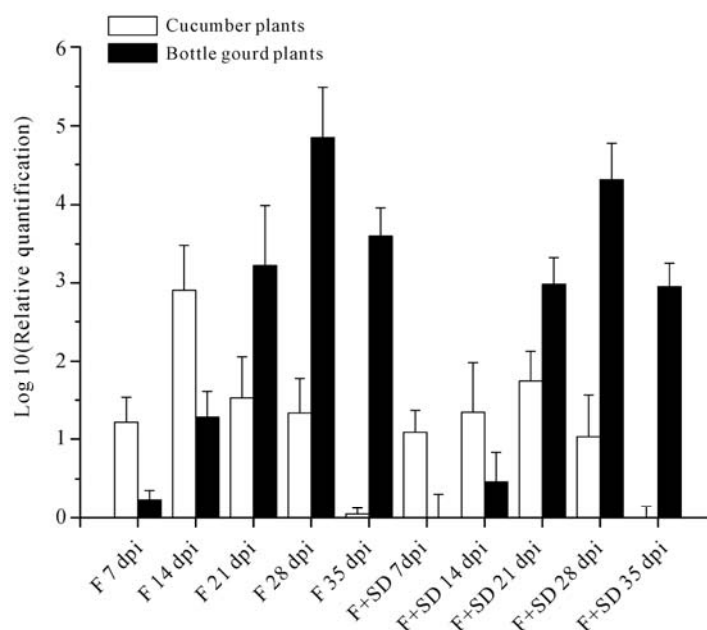


Fig. 3.16. Time courses of RNA accumulation for ZYMV-SD CP ORF at single or double infection on cucumber and bottle gourd. On cucumber plants, the logarithm (relative quantification) of ZYMV single inoculation at 35 dpi is set as zero. On bottle gourd, the log (relative quantification) of CMV and ZYMV complex inoculation at 35 dpi is set as zero. F and SD present CMV-Fny and ZYMV-SD, respectively. Data are mean of base-10 logarithm of relative quantification values; error bars represented the standard error

That is to say, co-infection of CMV reduced the replication and/or accumulation of ZYMV in both hosts.

It has been reported that when potyvirus co-infected the host with other viruses, the accumulation of the other viruses increased. However, the accumulation of potyvirus decreased (Poolpol and Inouye, 1986). In the case of CMV and ZYMV

co-infection, CMV CP accumulation increased in complex infection, and is about 2.03 times higher than that of single infection, but the accumulation of ZYMV CP gene ORF did not change obviously (Fattouh, 2003). The accumulation of ZYMV-SD CP ORF is found to be greatly suppressed in complex infection plants. Similar results have been reported on cucumber and zucchini squash plants but tested by Northern blotting (Wang et al., 2002; 2004). It is found that the accumulation of CMV-Fny RNAs increased on both hosts. Ratios of CMV ORFs are found to increase in the synergic interaction when hosts are co-infected with ZYMV. All of the above findings supported the conclusion that the accumulation of CMV could be enhanced by co-infection of ZYMV but the accumulation of ZYMV could be suppressed in co-infection with CMV, especially on bottle gourd, since a very significant enhancement of CMV-Fny is present on co-infected bottle gourd plants, which reaches 15.14 folds that of a single infection and obvious genomic RNA suppression of ZYMV is detected on co-infected bottle gourd plants.

Focusing on the synergy of the above two viruses, cross-protection has been used to control the large-scale events and mass epidemic viruses, mostly for related viruses. The attenuated strain of ZYMV-WK has been used widely as a bio-control agent in many areas in Europe and Japan (Cho et al., 1992; Walkey et al., 1992; Wang et al., 1987), but its interaction with CMV, as an epidemic virus in the same ecological position, has never been mentioned. Kosaka also reported the successful use of control viral infection and enrichment of resistant ability against the virus through inoculation of many attenuated strains of ZYMV on cucumber and some other plants (Kosaka and Fukunishi, 1997; Kosaka, Ryang, and Kobori, 2006). However, according to the comparison test described in this chapter, pre-inoculation with ZYMV brought the possibility of more CMV occurrence, and the accumulation of co-infected CMV could increase rapidly. It is also found that co-infection yields a lower accumulation of ZYMV, which agrees with the conclusion of others. So, using attenuated CMV may be more promising, since CMV also frequently occurs on *Cucurbitaceae* crops in China and the neighboring areas. At least it can be suggested that ZYMV as a bio-control agent should be used carefully when CMV existed as another principal virus, and an attenuated CMV could be safer than ZYMV or other potyviruses. Even so, it is important for doing ecological research on the influence of the large scale use of artificial attenuated strains.

3.5 Methodology

We introduce the interaction study on CMV and ToMV interaction, pseudo-recombination of CMV subgroups, synergy between CMV and ZYMV on *Cucurbitaceae*.

3.5.1 *The Interaction Study on CMV and ToMV Interaction*

- **Host Plant, Virus Strains and Inoculations**

Tomato (*Lycopersicon esculentum* Mill cv. Hezuo 903) plants were grown in an insect-proof greenhouse at 25 °C with a photoperiod of 14 h. (using supplementary lighting when required) and used for inoculation at the 2-true-leaf stage. Tomato (*Lycopersicon esculentum* Mill cv. Zhongshu 4) plants and *Nicotiana glutinosa* plants were used to maintain the viral cultures for inoculation of ToMV and CMV respectively. Purified virions of CMV-Fny (Rizzo and Palukaitis, 1990) and ToMV-N5 at 3 mg/ml or 15 mg/ml in 20 mol/L phosphate buffer (PB) were extracted from young leaves of source plants at 14 dpi, according to the method of Chen J. Y. (Chen et al., 2003). CMV-FnyΔ2b (Du et al., 2007) for inoculation was extracted from young leaves of source plants by grinding in 20 mol/L PB (1 g in 10 ml 20 mmol/L PB). The first inoculations with either CMV-Fny, CMV-FnyΔ2b, or PVX-BJ (5 μl/leave) of test plants were carried out mechanically by rubbing one cotyledon after dusting with Carborundum. 6–8 d after the first inoculation when the plants were in the 3-to 4-true-leaf stage, the plants were again inoculated with ToMV-N5 on the first true leaves (5 μl/leave). At the same time, ToMV-N5 single inoculation was carried out. First and second inoculations also were carried out by rubbing with 5 μl PB (20 mol/L) on the corresponding leaves as the control. For each treatment, at least 40 tomato seedlings of each species were inoculated.

- **Plant Response to Viral Infection**

Symptoms in the tomato were observed in the greenhouse Protection rate [No. protected/No. inoculated plants (%)] collected at 21 dpi with ToMV-N5. Values are mean ± standard deviation. At 0, 7, 14, 21, 28 dpi, plants height (stem length above the cotyledon) was measured. All the plants per each treatment were monitored for symptom phenotype analysis and height measurement.

- **Total RNA Extraction**

Three leaf disks (one per leaf; 9-mm diameter) were sampled from the second true leaves of three plants at 14 and 28 dpi (with CMV). Total RNAs were extracted using Trizol reagent (Takara, Dalian, China) and treated with DNase (Takara Dalian, China) according to the manufacturer's directions. The rapid progress of necrosis limits the period of sampling and leaves that can be harvested.

- **Primers Design and Quantitative Real-time RT-PCR**

Primers were designed using the primer Premier 5.0. Primers used for amplifying 18S RNA and CMV CP open reading frame (ORF) have been previously described. ToMV-N5 nucleotide sequences available in the GenBank database

were aligned and used to design the forward primer ToMV-F (5'-TTACTCAATCACTTCTCCATCGCAA-3') and the reverse primer ToMV-R (5'-GCTGTGTTTGAAACTGGTTACCTAA-3') to amplify a 113-bp fragment of the coat protein (CP) gene of ToMV-N5. Real-time RT-PCR reactions were performed in an ABI Prism 7000 (Applied Biosystems, California, USA) with three independent repetitions for all samples. A two-step amplification protocol was used for real-time RT-PCR as previously described: pre-denaturation at 95°C for 10 s followed by 40 cycles of denaturation at 95°C for 5 s and annealing/extension at 60°C for 31 s. Real-time RT-PCR assays were performed in 10- μ l reaction volume mixtures. Data were analyzed with ABI Prism 7000 sequence detection system software (Applied Biosystems, California, USA). Relative quantitation was calculated using $2^{-\Delta\Delta C_T}$ method (Livak and Schmittgen, 2001).

3.5.2 Pseudo-recombination of CMV Subgroups

• In Vitro Transcription of Infectious Clones of CMV and satRNA-Tsh

The infectious cDNA clones (pF109, pF209 and pF309) of CMV-Fny were provided by Dr. Peter Palukaitis. The infectious cDNA clones of CMV-Tsh genomic RNA2, RNA3 (GenBank accession number: EF202596 and EF202597) and satRNA-Tsh (GenBank accession number: DQ249297) were stored in our laboratory.

The CMV-Fny cDNA clones were linearized with PstI (Rizzo and Palukaitis, 1990), while CMV-Tsh RNA2 and CMV-Tsh RNA3 were linearized with PstI and SamI, respectively. The in vitro template of Tsh-satRNA was amplified from cDNA clones using primer T7-satF (5'-TAATACGACTCACTATAAGGTTTTGTTTGGWAG-3') and satR (5'-GGGTCCTGTAGAGGA-3'). Infectious RNAs were generated by in vitro transcription with T7 RNA polymerase (Promega) in the presence of the capanalogue m⁷GpppG (Promega). All full length RNAs were quantified by agarose gel electrophoresis before inoculation.

• Plant Seedlings and Viral Inoculation

Plants seedlings were grown in pots and maintained in growth chambers between 22°C and 28°C, with a 16 h light and 8 h darkness cycle. Seedlings of *N. benthamiana* and *N. glutinosa* were used as host plant at the 3-to 4-leaf stage. All the plants to be inoculated with transcripts were kept in the dark for 24 to 48 h and lightly dusted with carborundum before inoculation (Zhang et al., 1994). The RNA transcripts from the full-length cDNA clones of CMV-Fny RNAs 1, 2 and 3 and CMV-TshRNAs 2 and 3 were combined to form the parental RNA, F1F2F3(Fny), as well as the other three pseudorecombinants, F1F2T3, F1T2F3 and F1T2T3. Combined with satRNA-Tsh, F1F2F3sat (F1F2F3 with Tsh-satRNA), F1F2T3sat, F1T2F3sat and F1T2T3sat were formed. With or without satRNA-Tsh transcripts,

the inocula were prepared following the protocol described previously (Liao et al., 2007). Mock-treated plants were inoculated with inoculated buffer.

To detect the symptom induced in the tomato plants, the systemic infected leaves of *N. glutinosa* were used to inoculate onto the Carborundum-dusted first true leaves of tomato plant seedlings at the 2-true-leaf stage.

• Double-stranded RNA Extraction and Analysis

Systemic leaf tissues were collected from cultured *N. glutinosa* plant at 14 dpi. Double-stranded RNA extraction was done using the method as previously described, with some modifications. one percent agarose gel electrophoresis was done to detect the result of double-stranded RNA extraction.

• Northern Blot Hybridization and Real-time RT-PCR Testing

For Northern blot hybridization analysis, total RNA was extracted from systemic leaves of inoculated or mock-treated *N. glutinosa* plants using TRIzol reagent (Invitrogen) at 14 dpi. Universal probe for genomic RNAs1, 2 and 3 of CMV is 3 terminal oligonucleotide 5'-GACCATTTTAGCCGTAAGCTGGATGGACAA CCG-3'. Specific probe for *sat*RNA-Tsh is oligonucleotide 5'-CGCCAGTT CAACCGGAAACCGCTACGCTC-3'. The hybridization probes were prepared by end-labelling a DNA oligonucleotide with [γ -³²P] ATP using T4 polynucleotide kinase (Takara) before hybridization. Northern blot hybridization for viral progeny RNA analysis was performed using the protocol of Sambrook and Russell (2001).

For realtime RT-PCR analysis, total RNA was extracted from systemic leaves of inoculated or mock-treated *N. glutinosa* plants 14 dpi. We designed real-time RT-PCR Primers for amplifying 18S RNA and CMV-Tsh open reading frame as listed in Table 3.4. The Primers for CMV- Fny open reading frame were previously described (Feng et al., 2006). SYBR Green I dye used in the RT-PCR added the fluorescent signal from the amplified templates to accurate quantitation. Data were analyzed with ABI Prism 7000 sequence detection system software (Applied Biosystems, California, USA). Relative quantitation was calculated using 2^{-ΔC_t} method (Livak and Schmittgen, 2001).

Table 3.4 Primer pair for real-time RT-PCR

Primers	Primer sequence
CMV-Tsh 2a-F	5'-TCGCTGATGATTATGTTATTGAAGG-3'
CMV-Tsh 2a-R	5'-GGTTGGCGTTGGACATTTTT-3'
CMV-Tsh 2b-F	5'-TATGGTGGAGGCGAAGAAGCAGAG-3'
CMV-Tsh 2b-R	5'-GATAGAACGGTAGGAAACGGAACAG-3'
CMV-Tsh 3a-F	5'-TTGTAACGGTAGACATCTGTGACGC-3'
CMV-Tsh 3a-R CP-RRCP-R	5'-GCCCAACAGGGAGCAAAAAGG-3'
CMV-Tsh cp-F	5'-TCACATCTATTACCCTGAAACCGCC-3'
CMV-Tsh cp-R	5'-GCGCGAAACAAGCTTCTTATCATAG-3'
18s rRNA-F	5'GAGTCATCAGCTCGCGTTGAC-3'
18s rRNA-R	5'-CGGATCATTCAATCGGTAGGA-3'

3.5.3 Synergy between CMV and ZYMV on Cucurbitaceae

- **Plants and Viruses**

Seedlings of cucumber (*C. sativus* cv. Jinyou 1) and bottle gourd (*L. siceraria* cv. Yonghu 2), were grown in pots and maintained in a controlled growth chamber at 22–28°C, and 16 h daylight. Parallel to this treatment, a set of plants were grown in the field experiment. Twelve seedlings for each treatment were used for real-time PCR detection in pot testing, while 30 plants for each test were used for a disease index test in field testing. Isolates, CMV-Fny and ZYMV-SD, were pre-inoculated and maintained on seedlings of tobacco and bottle gourd respectively, and biologically assayed for their infectious virility. Seedlings of 2-true-leaf stage were mechanically inoculated on both cotyledons with CMV or ZYMV for the single infection test, and on one cotyledon with CMV and another cotyledon with ZYMV, respectively, for the mixed infection.

- **RNA Extraction and Real-time RT-PCR Amplification**

At 7 dpi, the 1st and 2nd systemic leaves were sampled. At 14, 21, 28 and 35 dpi, the 3rd and 4th, 5th and 6th, 7th and 8th, 9th and 10th systemic leaves were sampled, respectively. Our detecting experiment lasted for 35 dpi, and the seedlings were at 9–11 true-leaf-stage at the last sampling time for the pot-test. Four disks, about 0.1 g, were cut from three plants 7 to 35 dpi from the parallel systemically-infected new leaves. Total RNAs were extracted with TRIzol reagent (TaKaRa, Dalian, China), treated with DNase, and stored at –80°C. Seedlings inoculated with ddH₂O were used as mock treatment.

Primers targeting the ORFs of CMV 1a, 2a, 3a, CP and 18S rRNA used for PCR amplification were the same as our previous work [8]. A pair of primers for amplifying ZYMV-SD coat protein ORF (F-CATCGAGGTTGTTTGGTCTTGA, R-GCAGTGTGCCGTTTCAGTGTCT), were selected, expecting a 66 bp fragment product. A two-step amplification protocol was utilized for real-time RT-PCR as in our previous report, and reverse transcription was performed in a 10- μ l reaction mixture, including 1 μ g total RNAs extracted plant tissues.

- **Data Analysis**

To perform the relative quantification, 18S rRNA was used as an internal control to normalize the amount of CMV and ZYMV ORFs between treatments. The C_t values of CMV-Fny 1a, 2a, 3a, CP, and ZYMV CP ORFs were compared directly with 18S rRNA C_t and the results were presented by ratios of the target-specific signal to the internal reference. Relative quantification was performed by the $-\Delta\Delta C_t$ method. Thus, the fold changes in CMV and ZYMV (target gene) relative to the 18S rRNA was determined by:

$$\text{Fold change} = 2^{-\Delta\Delta C_t},$$

where $\Delta\Delta C_i = (C_{iTarget} - C_{i18S})_{Time\ x} - (C_{iTarget} - C_{i18S})_{Time\ 0}$. Time x was any time point and time 0 was the initial or original expression time of each gene. Relative quantification (RQ) of gene expression and the logarithm of RQ using the $2^{-\Delta\Delta C_i}$ method were considered as gold approaches (Livak and Schmittgen, 2001).

• Disease Index

Symptoms on hosts were observed at 7, 14, 21, 28 and 35 dpi. Based on the symptom expression, it was rated with 5 grades. Grade 0: with no obvious symptom. Grade 1: with light systemic mosaic or spot. Grade 2: typical systemic mosaic symptom on leaves. Grade 3: severe mosaic but without obvious malformation of the whole plant. Grade 4: severe mosaic with necrosis or plant dwarfing or dead. Based on host symptoms, the disease index was calculated as follows (Chen et al., 2003):

$$\text{Disease Index} = \frac{\sum (\text{Number of plants each grade} \times \text{Disease grade})}{\text{Total number of plants} \times \text{The highest grade}} \times 100.$$

References

- Beachy RN (1999) Coat-protein-mediated resistance to Tobacco mosaic virus: discovery mechanisms and exploitation. *Philos Trans R Soc Lond B Biol Sci* 354(1383): 659-664.
- Chen JY, Chen JS and Cai LH (2003) Molecular detection and pathogenic testing of two viruses infecting cucurbitaceous crops. *Acta Phytopathologica Sinica* 33: 449-455 (in Chinese).
- Cho J, Ullman D, Wheatley E, et al. (1992) Commercialization of ZYMV cross protection for zucchini production in Hawaii. *Phytopathology* 82: 1073.
- Culver JN (1996) Tobamovirus cross protection using a potexvirus vector. *Virology* 226(2): 228-235.
- Du ZY, Chen FF, Liao QS, et al. (2007) 2b ORFs encoded by subgroup IB strains of *Cucumber mosaic virus* induce differential virulence on *Nicotiana species*. *J Gen Virol* 88(Pt 9): 2596-2604.
- Fattouh F (2003) Double infection of a cucurbit host by *Zucchini yellow mosaic virus* and *Cucumber mosaic virus*. *Pakistan Journal of Pathology* 2: 85-90.
- Feng JL, Chen SN, Tang XS, et al. (2006) Quantitative determination of *Cucumber mosaic virus* genome RNAs in virions by real-time reverse transcription-polymerase chain reaction. *Acta Biochim Biophys Sin* 38(10): 669-676.
- Kosaka Y and Fukunishi T (1997) Multiple inoculation with three attenuated viruses for the control of cucumber virus disease. *Plant Disease* 81: 733-737.
- Kosaka Y, Ryang BS and Kobori TK (2006) Effectiveness of an attenuated *Zucchini yellow mosaic virus* isolate for cross-protecting cucumber. *Plant Disease* 90: 67-72.
- Livak KJ and Schmittgen TD (2001) Analysis of relative gene expression data using

- real-time quantitative PCR and the $2^{-\Delta\Delta C_t}$ method. *Methods* 25(4): 402-408.
- Lu B, Stubbs G and Culver JN (1998) Coat protein interactions involved in Tobacco mosaic tobamovirus cross-protection. *Virology* 248(2): 188-198.
- McKinney HH (1929) Mosaic diseases in the Canary Islands, West Africa and Gibraltar. *J Agricultural Research* 39(8): 557-578.
- Poolpol P and Inouye T (1986) Enhancement of *Cucumber mosaic virus* multiplication by *Zucchini yellow mosaic virus* in doubly infected cucumber plants. *Ann Phytopathol Soc Jpn* 52: 22-30.
- Ratcliff F, Harrison BD and Baulcombe DC (1997) A similarity between viral Defense and Gene Silencing in Plants. *Science* 276(5318): 1558-1560.
- Rizzo TM and Palukaitis P (1990) Construction of full-length cDNA clones of *Cucumber mosaic virus* RNAs 1, 2 and 3: generation of infectious RNA transcripts. *Mol Gen Genet* 222(2-3): 249-256.
- Sherwood JL and Fulton RW (1982) The specific involvement of coat protein in Tobacco mosaic virus cross protection. *Virology* 119(1): 150-158.
- Voinnet O (2001) RNA silencing as a plant immune system against viruses. *Trends in Genetics* 17(8): 449-459.
- Walkey Dga, Lecoq H, Collier R, et al. (1992) Studies on the control of *Zucchini yellow mosaic virus* in courgettes by mild strain protection. *Plant Pathology* 41(6): 762-771.
- Wang H, Gonsalves D, Providenti R, et al. (1987) Effectiveness of cross protection by a mild strain of *Zucchini yellow mosaic virus* in cucumber, melon and squash. *Plant Disease* 71: 491-497.
- Wang Y, Gaba V, Yang J, et al. (2002) Characterization of synergy between *Cucumber mosaic virus* and Potyviruses in cucurbit hosts. *Phytopathology* 92(1): 51-58.
- Wang Y, Lee KC, Gaba V, et al. (2004) Breakage of resistance to *Cucumber mosaic virus* by co-infection with *Zucchini yellow mosaic virus*: enhancement of CMV accumulation independent of symptom expression. *Arch Virol* 149(2): 379-396.
- Yukio K and Yuichiro W (2003) Cross-protection in *Arabidopsis* against crucifer tobamovirus Cg by an attenuated strain of the virus. *Molecular Plant Pathology* 4(4): 259-269.
- Zhang L, Handa K and Palukaitis P (1994) Mapping local and systemic symptom determinants of *Cucumber mosaic cucumovirus* in tobacco. *J Gen Virol* 75 (Pt 11): 3185-3191.
- Ziebell H, Payne T, Berry JO, et al. (2007) A *Cucumber mosaic virus* mutant lacking the 2b counter-defence protein gene provides protection against wild-type strains. *J Gen Virol* 88(Pt 10): 2862-2871.

Gene Function of *Cucumber Mosaic Virus* and its Satellite RNA Regarding Viral-host Interactions

4.1 Introduction

Gene replacement using wild viruses as reference strains, the artificial reassortant of viral genome segments from different viral strains and utilization of artificial mutations, are principle methods to investigate the function of viral genes. In combination with viral diagnosis techniques, especially quantitative measuring, the relationship between the viral gene function and the pathogenicity of a virus could be demonstrated from the divergence of pathogenicity of these manipulated viruses. To set up a useful system for gene function study, the infectious clone is of preliminary importance. In fact, transgenic study and newly-developed siRNA methods for complementary suppression studies are also effective ways to understand the gene function of plant viruses.

As a positive-sense tripartite RNA virus, *Cucumber mosaic virus* (CMV) has an advantage in the construction of infectious clones, since each genomic fragment can be modified independently. In natural conditions, numerous strains have been identified and characterized to date, reflecting the fast fitness of this virus to environmental factors such as host varieties, climate changes and variations in plant-growing systems. The function of most CMV genes has been well studied. Distributed among genomic RNA1, RNA2 and RNA3, there are five open reading frames (ORFs) in the CMV genome that encode five viral proteins, including proteins 1a encoded by RNA1, 2a and 2b encoded by RNA2, 3a (MP) and 3b (CP) encoded by RNA3. The protein 1a, 2a, 3a and CP are well-studied with regard to their functions in viral replication, movement and encapsidation. The 2b protein translated from the subgenomic RNA (RNA 4A) of RNA 2 has been identified relatively recently in Q-CMV-infected plants (Ding et al., 1994). Similarly, the homologous 2b protein is detected in Fny-CMV-infected hosts (Mayers et al., 2000). The 2b ORF is located at the 3' terminus of RNA 2 and partially overlaps with the 3' terminus of the 2a ORF (Ding et al., 1994). A 2b-like ORF is encoded by ilarviruses (Xin et al., 1998). However, species of the genera *Bromovirus* and *Alfalmovirus* do not contain equivalent ORF (Ding et al., 1994).

Studies to date have shown the CMV 2b protein to be a suppressor that interacts directly with AGO1 and weakens its cleavage activity in RNA silencing (Zhang et al., 2006), to inhibit the activity of the RNA mobile silencing signal (Guo and Ding, 2002), and to be a determinant of long-distance movement in the cucumber (Ding et al., 1995). Besides the above roles, the 2b protein has another important function as a pathogenicity determinant in solanaceous hosts. The mutant Q-CMV- Δ 2b, in which 2b ORF has been disrupted by inserting a termination codon in 2b ORF, is found to cause only mild symptoms in *Nicotiana glutinosa* plants, and is less virulent than the subgroup II wild-type Q-CMV (Ding et al., 1995). Similarly, the mutant Fny-CMV- Δ 2b, in which most (nt 2419–2713 of RNA 2) of the 2b ORF is deleted from the subgroup IA wild-type Fny-CMV, has been found to produce no symptoms in tobacco plants, while the wild-type Fny-CMV causes severe symptoms, including mosaic, stunting and leaf deformation (Soards et al., 2002). An interspecies hybrid virus, CMV-qt, in which the 2b ORF of Q-CMV has been replaced with that of the *Cucumovirus Tomato aspermy virus* (TAV), is found to be more virulent than the parental viruses (Q-CMV, TAV) in seven different host species, but do not infect the cucumber systemically (Ding et al., 1996). An intraspecies virus, CMV-qw, in which the 2b ORF of Q-CMV is substituted by that of subgroup IA strain WAII-CMV, is found to be more virulent than wild-type Q-CMV or WAII-CMV (Shi et al., 2002). All of the above findings support the initial conclusion that the cucumoviral 2b protein is a determinant of pathogenicity and controls symptom expression (Ding et al., 1995; 1996).

Based on the substitution of 2b genes from different isolates with variety of pathogenicity, and through analysis of encapsidation of viral RNAs, it is found that there is an apparent correlation between the virulence and the high level of encapsidated RNA 2 in virions of Fny-CMV, FCb7^{2b}-CMV or FNa^{2b}-CMV, explaining part of the mechanisms involved in 2b gene function.

Satellite RNAs (satRNAs) are molecular parasites that interfere in the pathogenesis of the helper viruses. In addition to the viral genomic RNAs, some CMV strains contain sat RNAs as additional RNAs associated with the virus genome. Up to date, over 100 CMV satRNA variants have been found associated with over 65 CMV isolates (Palukaitis and Garcia-Arenal, 2003). SatRNAs are completely dependent on their helper viruses for replication, encapsidation and dispersion, and do not encode any ORF, but tend to be highly structured. Despite their small size and poor protein product, CMV satRNAs may have dramatic effects on symptom expression induced by the helper virus, ranging from amelioration to severe exacerbation (García-Arenal and Palukaitis, 1999; Palukaitis and Garcia-Arenal, 2003; Roossinck et al., 1992; Simon et al., 2004). Specific nucleotide residues or structures of satRNAs determine the capability of modulating symptoms caused by helper viruses (Collmer and Howell, 1992; Masuta and Takanami, 1989; Palukaitis, 1988; Palukaitis and Roossinck, 1996; Sleat and Palukaitis, 1992).

In many hosts and for most strains of CMV, the presence of satRNA both attenuates the symptoms and the presence of CMV-satRNA usually reduces the titer of the helper virus, more so in *Solanaceous* than in cucurbit host plants, when tested qualitatively (Gal-On et al., 1995; Garcia-Arenal and Palukaitis, 1999;

Palukaitis and García-Arenal, 2003; Roossinck and Palukaitis, 1991; Simon et al., 2004). The phenotype reaction of the helper virus influenced by satellite RNA can be illustrated by Fig. 4.1. Some reports suggested that the effect of satRNA on the helper viruses could be related to the competitiveness of replication between the helper virus and satRNA (Rizzo and Palukaitis, 1990; Simon et al., 2004). The suppressive effect of satRNA on the accumulation of the CMV genomic RNAs and encoded proteins can be considered for its effect on accumulation of RNA1 and 2, relating to 1a and 2a protein, or the effect on accumulation of RNA3 and 4, relating to 3a and CP (Gal-On et al., 1995). Up to date, very limited reports have been documented for quantitative determination of the affection of satRNA on the genomic RNAs and genes of its helper virus, and less has been published on its effect on the 2b gene, which is correlated to virus distribution among plant organs and to symptom expression. When a relative accumulation of CMV genomic RNAs could be tested at present with or without satRNAs, the mechanism of satRNAs on their helper virus could be partially found out.

In this chapter, research into the function of the CMV 2b gene from different origins and the satellite RNA-mediated reduction in the accumulation of *Cucumber mosaic virus* genomic RNAs is analyzed, by using artificial mutation of this gene and quantitative analysis of ORFs.

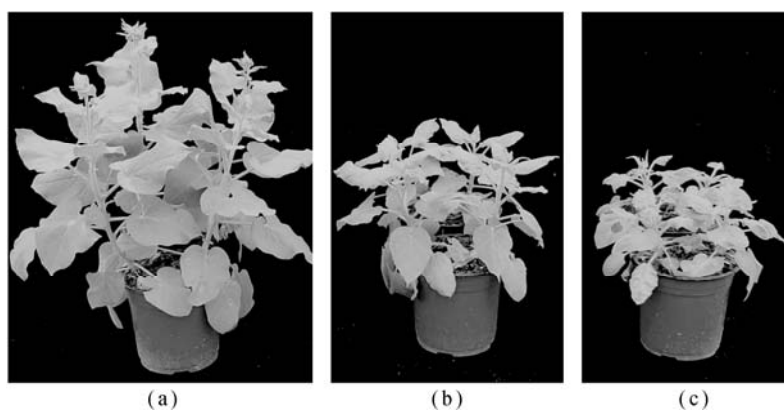


Fig. 4.1. Satellite RNA attenuation of symptoms produced by CMV on *Nicotiana glutinosa*. SatRNAs was pseudo-recombined into the genome of CMV-Fny and the symptom was recorded 21 days post inoculation. (a) Healthy seedlings; (b) Seedlings inoculated with CMV-Fny plus satRNAs; (c) Seedlings inoculated with CMV-Fny

4.2 The 2b Protein of *Cucumber Mosaic Virus* is a Determinant of Pathogenicity and Controls Symptom Expression

In recent years, CMV subgroup IB strains have been found widely distributed in China. Biological properties of differential virulence are possibly associated with their 2b proteins. The biological properties of the hybrid viruses can be compared

with each other and also with those of their parental viruses, when the 2b ORF of Fny-CMV is replaced with other isolates of different virulence.

4.2.1 Infectivity and Stability of Fny-CMV Derived Mutants

Based on the full length cDNA of RNA2 and the infectious clones of a wild type CMV strain, Fny-CMV, substitutions and mutations of CMV RNA2 and the interspecies viruses derived from artificial recombination are obtained. The origin and construction of wild-type Fny-CMV with its derivatives, Fny-CMV Δ 2aC81, FRad35^{2b}-CMV, FPGs^{2b}-CMV, FCb7^{2b}-CMV and FNa^{2b}-CMV, of which the 2b gene is changed are listed in Table 4.1. The structure diagrams of plasmid pFny209 and its derivatives for showing 2b substitution are given in Fig. 4.2. They have been generated by co-inoculating RNA transcripts onto seedlings of *N. glutinosa* at the 8-leaf stage. Independent assays show that all plants inoculated with the above viruses can produce typical mosaic symptoms on the upper systemic leaves. The six viruses are passaged once again through *N. glutinosa*. Virions have been purified from equal weights of infected leaves 14 d after passage. Viral RNAs are isolated from the purified virions and amplified by RT-PCR using the primer pair C2F1856/C123R. Results obtained from RT-PCR have shown that a DNA fragment of about 1.2 kb can be amplified in all viral RNA samples. All amplified DNA fragments are analyzed further by sequencing. No sequence variation has been observed in any RNA 2 of these intraspecies hybrid viruses, but the modified RNA 2 of Fny-CMV Δ 2aC81 reverted to the RNA 2 of wild-type Fny-CMV during inoculation and replication. The same reversion

Table 4.1 Constitution of RNA transcripts for wild-type Fny-CMV and derivatives with their 2b characters.

Virus construct	Transcription templates for			Derivation of 2b genes	Functional 2b genes [†]
	RNA 1	RNA 2	RNA 3		
Fny-CMV	pFny109*	pFny209*	pFny309*	Fny-CMV	Y
Fny-CMV Δ 2a81	pFny109	pFny209 Δ 2a81	pFny309	Fny-CMV	Y
Fny-CMV Δ 2b	pFny109	pFny209 Δ 2b	pFny309	— [‡]	N
Fny-CMV Δ 2bpro	pFny109	pFny209 Δ 2bpro	pFny309	Fny-CMV	N
FCb7 ^{2b} -CMV	pFny109	pFny209Cb7 ^{2b}	pFny309	Cb7-CMV	Y
FRad35 ^{2b} -CMV	pFny109	pFny209Rad35 ^{2b}	pFny309	Rad35-CMV	Y
FPGs ^{2b} -CMV	pFny109	pFny209PGs ^{2b}	pFny309	PGs-CMV	Y
FNa ^{2b} -CMV	pFny109	pFny209Na ^{2b}	pFny309	Na-CMV	Y
FCb7 ^{2b} CMV Δ 2bpro	pFny109	pFny209Cb7 ^{2b} Δ 2bpro	pFny309	Cb7-CMV	N

*Plasmids pFny109, pFny209, and pFny309 were previously constructed by Rizzo and Palukaitis (1990);

[†]Y indicates the functional 2b gene was present in the corresponding virus; N indicates the functional 2b gene was absent in the corresponding virus;

[‡]Indicates that the Fny-CMV Δ 2b virus does not contain any 2b ORF

situation has been found by Soards et al. (2002) for the same artificial mutation, but it did not happen to an equivalent derivative of Q-CMV (C1C2_{qt}C3) (Ding et al., 1996). Thus, the artificial mutations and recombination are useful systems to analyze CMV gene functions.

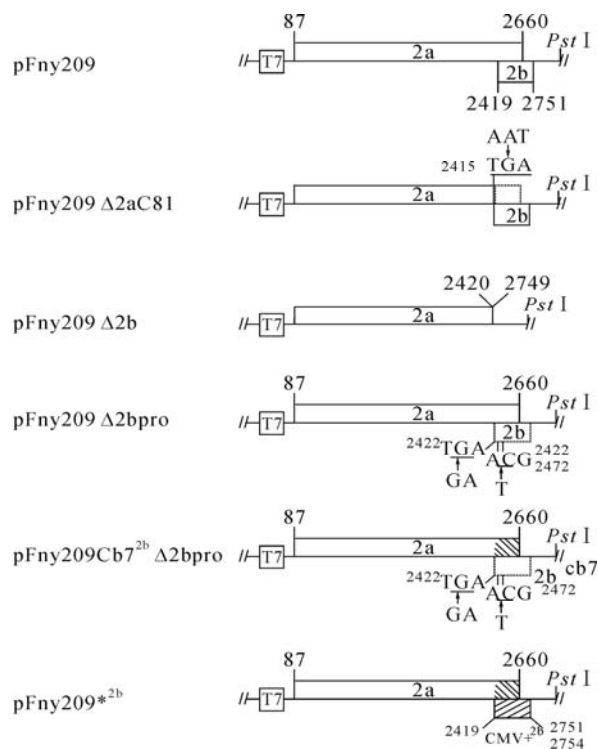


Fig. 4.2. Structure diagrams of plasmid pFny209 and its derivatives. Except for pFny209Δ2b, every plasmid contains either a wild-type 2b open reading frame (ORF) or a variant of 2b ORF in Fny-CMV RNA 2, as shown. These three nucleotides at nt 2415–2417 of Fny-CMV RNA 2 were substituted with a termination codon (TGA) to prevent the expression of the C-terminal overlapping part of the 2a ORF in plasmid pFny209Δ2a81. Coding sequence from nt 2421–2748 of RNA 2 representing most of Fny-CMV 2b ORF was deleted from plasmid pFny209, creating pFny209Δ2b. Nucleotide substitutions of either GA (nt 2422–2423) and T (nt 2441 and 2471) or GA (nt 2422–2423) and T (nt 2471) with TA and C nucleotides prevent the expression of the 2b ORF in pFny209Δ2bpro or pFny209Cb7^{2b}Δ2bpro, respectively. pFny209*^{2b}, representing four intraspecies hybrid clones, was constructed by precise replacement of the 2b gene in pFny209 with the 2b gene of Cb7-CMV, Rad35-CMV, Na-CMV or PGs-CMV. These coding sequences surrounded by dash lines in pFny209Δ2a81, pFny209Δ2bpro and pFny209Cb7^{2b}Δ2bpro present deletions in the ORFs only by single nucleotide substitutions. The nucleotides introduced to generate termination codons or alter ‘ATG’ codons were underlined. Arrows indicate the substituted nucleotides. In plasmid pFny209*^{2b}, there are two position numbers of stop codon, nt 2751 for pFny209PGs^{2b}, and nt 2754 for the other three intraspecies hybrid clones. All of the cDNA clones contained a modified T7 promoter [T7] at their 5' ends

4.2.2 Replacement of the 2b ORF Affected Capsidation of Viral RNA 2

The replacement of the 2b ORF directly results in changes in the nucleotide sequences of RNA 2 and RNA 4A, apart from changes in the 2b protein and the C-terminal part of the 2a protein. To analyze whether the replacement of the 2b ORF would affect the encapsidation of viral RNAs, virions of Fny-CMV, FRad35^{2b}-CMV, FPGs^{2b}-CMV, FCb7^{2b}-CMV and FNa^{2b}-CMV are purified from equal weights of leaf tissues. Virion RNAs are isolated from the purified virions, separated on an agarose gel, and then stained with ethidium bromide (Fig. 4.3(a)). The intensity of each viral RNA band is measured using GeneTool software (Syngene, USA), and the quantities of RNA 1, RNA 2 and RNA 4 relative to RNA 3 in each virus are thus calculated. RNA 3 in each virus is regarded as an internal reference; the relative quantity of RNA 3 in each virus is thus designated as 1. Although there are some differences in the relative quantities of RNAs 1 or RNAs 4 of the five viruses, this difference does not show a correlation with the degree of virulence (Table 4.2). By contrast, the difference in relative quantities of RNAs 2 of the five viruses is found to be well correlated with the degree of virulence. Fny-CMV, FCb7^{2b}-CMV and FNa^{2b}-CMV are all found to contain a very faint band with a migration faster than RNA 4, but FRad35^{2b}-CMV and FPGs^{2b}-CMV do not. A similar result concerning this band can be obtained by northern blot hybridization analyses (Fig. 4.3(b)). Although the RNA band has the same mobility to RNA 4A shows in total RNA from Fny-CMV-infected leaves of *N. glutinosa*, it cannot be verified as being RNA 4A. The quantities of RNAs 1, 2, and 4 relative to RNA 3 in each virus are compared, as shown in Fig. 4.3(c). The above analysis shows the successful regeneration of mutations and phenotype divergence of them. Thus, infectious clone based artificial mutation is a useful tool to investigate gene functions of a +ssRNA virus.

Table 4.2 Symptoms induced by various viruses on three *Nicotiana* species*

Virus	<i>Nicotiana glutinosa</i>	<i>Nicotiana benthamiana</i>	<i>Nicotiana tabacum</i>
Fny-CMV	Mos/LD/St	LD/St	sMos/LD
PGs-CMV	— [†]	— [†]	— [†]
Rad35-CMV	Mos/St	LD/YS	sMos/LD
Cb7-CMV	Mos/TN/St [‡]	LD/St	sMos/LD/St
Na-CMV	Mos/LD/St	LD/St	sMos/LD
FPGs ^{2b} -CMV	Mos	NoS	mMos
FRad35 ^{2b} -CMV	mMos	NoS	mMos
FCb7 ^{2b} -CMV	Mos/TN/St [‡]	LD/St	sMos/LD/St
FNa ^{2b} -CMV	Mos/LD/St	LD/St	sMos/LD

* Systemic symptoms: LD = leaf distortion; mMos = mild mosaic; Mos = mosaic; sMos = severe mosaic; St = stunting; TN = top necrosis; YS = yellow spot on systemic leaves; NoS = systemic infection but no obviously systemic symptom;

[†] Indicated that the PGs-CMV did not systemically infect *N. glutinosa* plants by mechanically inoculating with either crude sap or in vitro transcription products;

[‡] Although both FCb7^{2b}-CMV and Cb7-CMV caused top necrosis (TN) on *N. glutinosa*, FCb7^{2b}-CMV induced this symptom to appear about three to five days later than that induced by Cb7-CMV

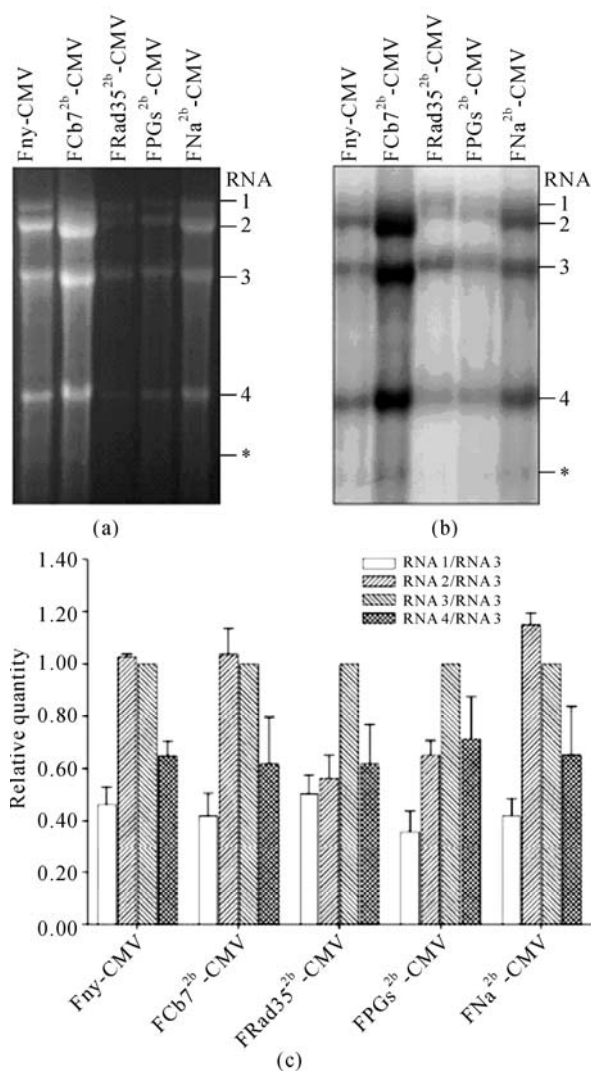


Fig. 4.3. Analysis of relative quantities of viral RNAs in virions of Fny-CMV and the intraspecies hybrid viruses purified from equal weights of infected leaf tissues. (a) Electrophoresis patterns of viral RNAs separated on 1.5% agarose gels in 1×TBE electrophoresis buffer; (b) Northern blot hybridization analysis of viral RNAs using the probeI-40 probe as described in the text; (c) The quantities of RNAs 1, 2 and 4 relative to RNA 3 in each virus as shown in (a). RNA 3 in each virus was regarded as an internal reference, thus the relative quantity of RNA 3 in each virus was defined as 1. The average and standard deviation of the relative quantity were obtained from three independent experiments. The positions of RNAs 1, 2, 3, and 4 are indicated on the left (a, b). *(a, b) indicates the position of an uncertain RNA band with the same mobility to RNA 4A

4.2.3 *Intraspecies Hybrid Viruses by Changing 2b Gene Induce Different Virulence*

When the virulence of the four intraspecies hybrid viruses and four parental viruses is comparably investigated by inoculating these viruses on three plants of *Nicotiana glutinosa*, *N. tabacum* and *N. benthamian*, respectively, the symptoms on these host species are found to be obviously diverging (Table 4.2). Of all the viruses, FCb7^{2b}-CMV and its parental virus Cb7-CMV are found to be the most virulent, both show high virulence on all host species tested, especially on *N. glutinosa*, where FCb7^{2b}-CMV and Cb7-CMV cause top necrosis early during infection and plant death later during infection. This is more severe than the disease caused by Fny-CMV. FNa^{2b}-CMV also is virulent in these plant species, showing similar virulence to its parental viruses Fny-CMV and Na-CMV. However, FRad35^{2b}-CMV causes only mild systemic symptoms or undetectable symptoms on these three host species, and is less virulent than its parental viruses Fny-CMV and Rad35-CMV. FPGs^{2b}-CMV, similar to FRad35^{2b}-CMV, shows little virulence in the three host species.

Although both FCb7^{2b}-CMV and Cb7-CMV cause top necrosis on *N. glutinosa*, FCb7^{2b}-CMV induces this symptom to appear about three to five days later than that induced by Cb7-CMV. A pseudo-recombinant virus F1P2F3, composed of Fny-CMV RNA 1 plus RNA 3, and PGs-CMV RNA 2, causes severe mosaic and leaf deformation on *N. glutinosa* at later stages of infection, which is more virulent than FPGs^{2b}-CMV. Similarly, differences in virulence are also observed between Rad35-CMV and FRad35^{2b}-CMV. These results suggest that the 2b protein played an important role in virulence, but it is not the only virulence determinant in these three subgroup IB strains.

4.2.4 *Divertive Virulence is Mediated by the 2b Protein Rather than by the C-terminal Overlapping Parts of the 2a Protein*

As stated above, the Fny-CMV Δ 2aC81 mutant is unstable and reverted to wild-type Fny-CMV after only one passage, so we could not directly rule out the possibility of the C-terminal part of the 2a protein of Fny-CMV affecting symptom expression and accumulation of viral progeny RNAs in host plants. To address this issue, Fny-CMV Δ 2b, Fny-CMV Δ 2bpro, and FCb7^{2b}-CMV Δ 2bpro, all of which could not express the 2b proteins, are generated by inoculation of *N. glutinosa* with viral RNAs transcribed in vitro from the corresponding cDNA clones. In addition, *N. glutinosa* plants are inoculated with Fny-CMV and FCb7^{2b}-CMV using RNAs transcribed in vitro from the corresponding cDNA clones. Both Fny-CMV Δ 2b and Fny-CMV Δ 2bpro are found to cause very mild mosaic symptoms in upper systemic leaves (Fig. 4.4), even by 30 dpi, and significantly reduced virulence, when compared with wild-type Fny-CMV. FCb7^{2b}-CMV Δ 2bpro also induced mild mosaic symptoms early in infection,

similar to Fny-CMV Δ 2b and Fny-CMV Δ 2bpro, although the infected plants then appeared symptomless later in infection. Northern blot hybridization analysis of viral progeny RNAs in systemically infected leaves shows that although RNA 3 of Fny-CMV can accumulate to a similar level to RNA 3 of Fny-CMV Δ 2b or Fny-CMV Δ 2bpro, the other four RNAs (RNAs 1, 2, 4, 4A) of Fny-CMV had higher accumulation levels than those of Fny-CMV Δ 2b or Fny-CMV Δ 2bpro, especially RNA 4 and RNA 4A. The difference in viral RNA accumulation profiles between FCB7^{2b}-CMV and FCB7^{2b}-CMV Δ 2bpro is similar to that between Fny-CMV and either Fny-CMV Δ 2bpro or Fny-CMV Δ 2b. It also could be observed that there is a similar profile of viral RNA accumulation among Fny-CMV Δ 2b, Fny-CMV Δ 2bpro and FCB7^{2b}-CMV Δ 2bpro. Taken together, these experiments show that the C-terminal overlapping part portions of the 2a protein from a subgroup IA strain or a subgroup IB strain did not affect symptom expression and accumulation of viral progeny RNAs in systemic leaves. Rather, the differential virulence is induced by the 2b proteins and not the C-terminal overlapping parts of the 2a proteins. No effects of the C-terminal overlapping part of the 2a protein of Q-CMV or V-TAV were observed in symptom expression of CMV in *N. glutinosa* (Ding et al., 1995; 1996).

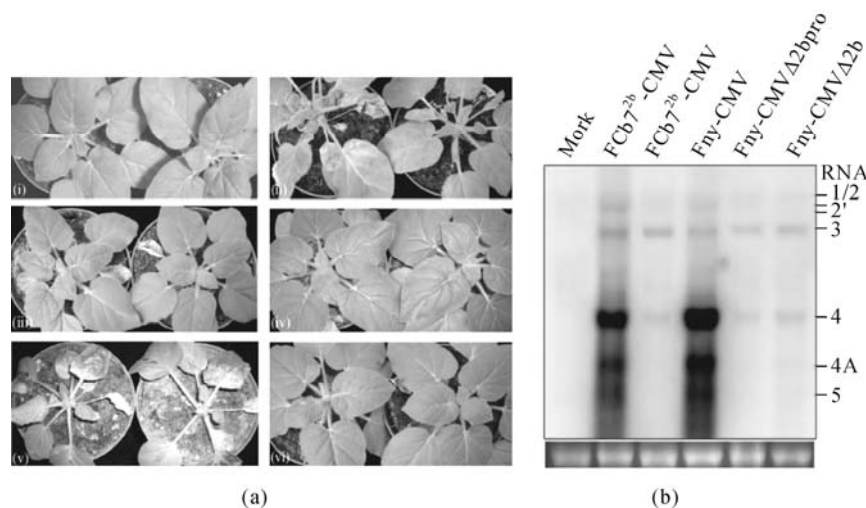


Fig. 4.4. Characterization of the various 2b gene mutants on *Nicotiana glutinosa*. (a) Symptoms induced by wild-type Fny-CMV (B), Fny-CMV Δ 2b (C), Fny-CMV Δ 2bpro (D), FCB7^{2b}-CMV (E) and FCB7^{2b}-CMV Δ 2bpro (F). Mock treated plants were inoculated with distilled water (A). Photographs were taken 3 weeks post-inoculation; (b) Northern blot hybridization analysis of the accumulated viral RNAs in systemically infected leaves of *N. glutinosa* plants singly inoculated with these five viruses. Viral progeny RNAs were hybridized with the probe-40 probe as described in the text. The inoculums corresponding to mock or each of these five viruses is indicated on the upper panel. The RNA samples loaded were visualized by ethidium bromide staining of 28S rRNA (lower panel). The positions of RNAs 1, 2, 3, 4, 4A, and 5 are indicated on the right, and the position of defective RNA 2 in Fny-CMV Δ 2b was indicated with 2' on the right

4.2.5 Virulence is Associated with the Accumulation of Viral Progeny RNAs Affected by 2b Protein

Shi et al. (2002; 2003) have found that the virulence mediated by the 2b gene is not correlated with the level of viral RNA accumulation and rate of long-distance viral movement in host plants. However, other studies suggest that the virulence is associated with either the accumulation level of viral progeny RNAs in systemic leaves (Ding et al., 1995, 1996) or the rate of both cell-to-cell and long-distance viral movement (Gal-on et al., 1994). To investigate whether the differential virulence of the four intraspecies hybrid viruses and wild-type Fny-CMV is associated with accumulation levels of viral progeny RNAs and/or rates of long-distance viral movement, viral RNAs are analyzed by northern blot hybridization using the probeI-40 probe, and their relative concentrations are shown in Fig. 4.5. No viral RNAs are detected for any of these viruses at 1 dpi. Viral RNAs are detected at 3 dpi, but only for FCb7^{2b}-CMV and FRad35^{2b}-CMV and not for Fny-CMV, FNa^{2b}-CMV or FPGs^{2b}-CMV. At 5 dpi, viral progeny RNAs of all the viruses are detectable readily. RNAs 1/2 of Fny-CMV, FCb7^{2b}-CMV and FNa^{2b}-CMV accumulated to a higher level than those of FPGs^{2b}-CMV or FRad35^{2b}-CMV. However, RNA 3 of FRad35^{2b}-CMV has a higher accumulation than RNA 3 of the other four viruses, and RNA 4 of FRad35^{2b}-CMV has an intermediate accumulation among all the viruses. Furthermore, RNAs 3, 4 and 4A of FCb7^{2b}-CMV have a relatively low accumulation among all the viruses. At 7, 14 and 28 dpi, the accumulation levels of most progeny RNAs of FPGs^{2b}-CMV and FRad35^{2b}-CMV are lower than those of Fny-CMV, FCb7^{2b}-CMV or FNa^{2b}-CMV (Fig. 4.5(a)-(d)), except for the accumulation level of RNA 3 of FRad35^{2b}-CMV, which is higher than RNA 3 of FNa^{2b}-CMV at 7 dpi. To determine whether there also is a similar difference in accumulation levels of viral progeny RNAs in the other two *Nicotiana* species, viral progeny RNAs, extracted from systemically infected leaves of *N. tabacum* at 28 dpi and *N. benthamiana* at 14 dpi, are analyzed by northern blot hybridization using the probeI-40 probe. Although accumulation levels of the progeny RNAs of Fny-CMV, FCb7^{2b}-CMV and FNa^{2b}-CMV are different to each other, all of them are higher than those of FPGs^{2b}-CMV or FRad35^{2b}-CMV in the other two host species. Taken together, the higher virulence caused by Fny-CMV, FCb7^{2b}-CMV and FNa^{2b}-CMV is associated generally with the high levels of accumulation of their progeny RNAs, but not with their rates of long-distance movement in the systemic leaves. Thus, when replication (RdRp determined by RNA1 mostly) and capsidation (coat protein function determined by RNA3) is consistent, CMV virulence can be obviously decided by replication/accumulation levels which are greatly determined by the 2b protein of this virus.

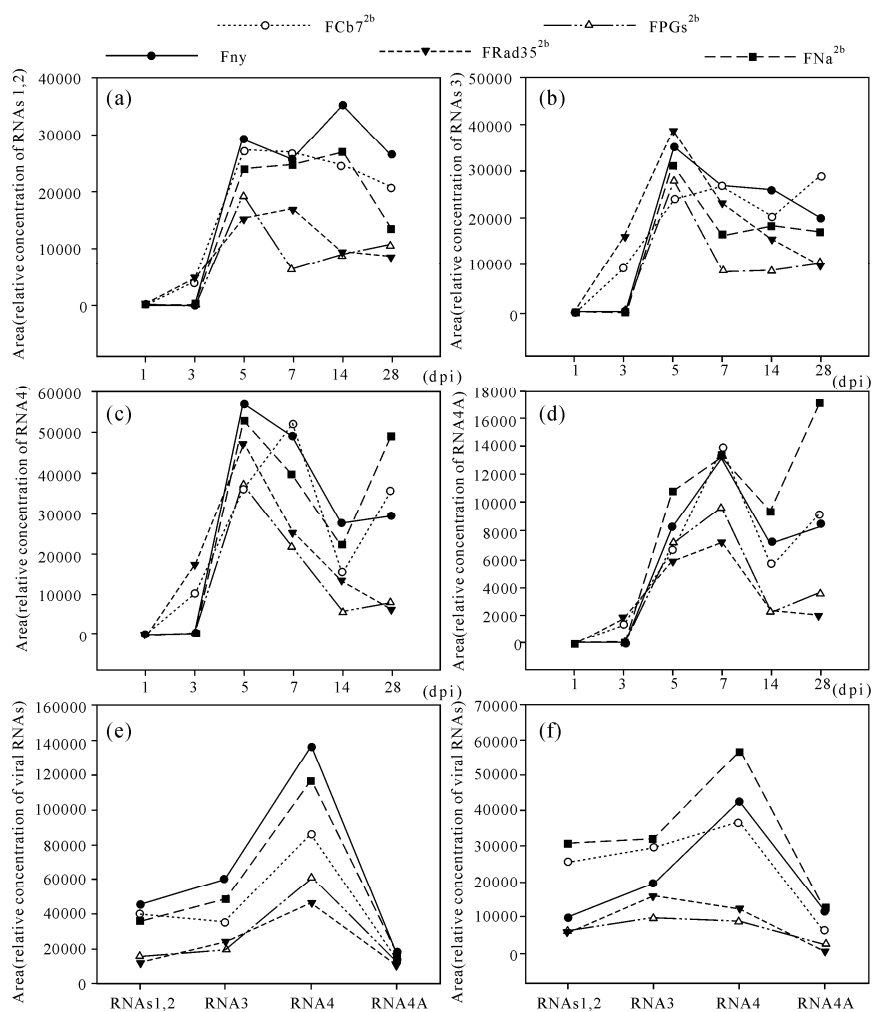


Fig. 4.5. Northern blot hybridization analysis of viral progeny RNAs of Fny-CMV and the four intraspecies hybrid viruses. The relative accumulation of viral RNAs in systemically infected leaves of *Nicotiana glutinosa* (a–d), *N. tabacum* (e) and *N. benthamiana* (f) are tested respectively. Relative concentrations of viral RNAs accumulating in *N. glutinosa* are shown for RNA 1/RNA 2 in panel (a), for RNA 3 in panel (b), for RNA 4 in panel (c) and for RNA 4A in panel (d). Total RNAs were extracted from systemically infected leaves of *N. glutinosa* at 1, 3, 5, 7, 14 and 28 dpi, of *N. tabacum* at 28 dpi, and of *N. benthamiana* at 14 dpi. Viral progeny RNAs were hybridized with the probeI-40 probe as described in the text. The inoculum corresponding to each of these five viruses is indicated on the upper what?. Relative quantities of the RNA samples loaded were normalized against their 28S rRNA. Relative concentration of viral RNAs in each RNA sample was calculated after normalization of loading quantities of these RNA samples against their 28S rRNA

CMV-encoded 2b protein has been identified to be a suppressor of post-transcriptional gene silencing (PTGS) (Brigneti et al., 1998). Suppression of PTGS by 2b protein correlated with its localization in the nucleus, and it is important for virulence determination (Lucy et al., 2000). Each of the four 2b proteins tested above has an arginine-rich nuclear localization signal: $^{22}\text{KRQRRRR}^{27}$ in the 2b proteins of Cb7-CMV and Rad35-CMV, $^{22}\text{KKQRRRR}^{27}$ in the 2b protein of PGs-CMV, and $^{22}\text{KQLRRRR}^{27}$ in the 2b protein of Na-CMV, presumably suggesting that the four 2b proteins could efficiently localize into the nucleus. Recently, Zhang et al. (2006) have found that the Fny2b protein interferes with microRNA (miRNA) pathways by direct interaction with AGO1, causing developmental defects in Arabidopsis. The interference in miRNA pathways posed by the Fny2b protein targeted some selectively but not all miRNAs (Lewsey et al., 2007). Although the LS2b protein from the mild strain (LS-CMV) is equally efficient as the Fny2b protein at suppressing PTGS (Lewsey et al., 2007), it and the Q2b protein from another mild strains (Q-CMV) had little effect on miRNA function and Arabidopsis development (Chapman et al., 2004; Lewsey et al., 2007), probably either due to the absence of a specific symptom-inducing functional domain in them (discussed in Lewsey et al., 2007), or due to their instability and low expression levels in vivo (discussed in Zhang et al., 2006). Potyviral HC-Pro protein, as one of the first identified suppressors of PTGS, has been shown to contain a symptom-inducing functional site or domain (Atreya and Pirone, 1993; Gal-On et al., 2000). The Fny2b protein and these four 2b proteins tested here share 70.0%–93.7% identity in their amino acid sequences. The obvious difference in the sequences suggests these four 2b proteins possess differential functional sites or domains involved in interrupting miRNA metabolism. Presumably, the 2b proteins of Cb7-CMV and Na-CMV, like the Fny2b protein, are more effective at interrupting miRNA metabolism than the 2b protein of either PGs-CMV or Rad35-CMV, by which Fny-CMV, FCb7^{2b}-CMV and FNa^{2b}-CMV all induced higher virulence than FPGs^{2b}-CMV or FRad35^{2b}-CMV in these three *Nicotiana* species tested. It has been shown that the high virulence of Fny-CMV, FCb7^{2b}-CMV and FNa^{2b}-CMV is concomitant with the high accumulation level of their viral progeny RNAs in systemically-infected leaves, which is probably a consequence of these viruses directing hosts to produce a cellular niche advantageous for their proliferation by altering the host miRNA metabolism (discussed in Zhang et al., 2006).

In summary, the different virulence resulting from replacement of the 2b ORFs is caused by the 2b proteins, rather than the C-terminal overlapping parts of the 2a proteins. The CMV 2b protein plays a most important role in symptom expression in *Nicotiana* species whether in a subgroup IA CMV strain or a subgroup IB CMV strain; the virulence of 2b proteins from subgroup IB strains varied, which correlated with the level of viral RNA accumulation, rather than the rate of long-distance viral movement.

4.3 Function of CMV 2b Protein and the C-terminus of 2a Protein in Determining Viral RNA Accumulation and Symptom Development

Symptom expression in plants induced by infection of viruses is a result of complex interactions between the host plant and the virus. Upon viral infection, host plants trigger antiviral defenses to moderate or inhibit viral infection (rev. by Soosaar et al., 2005; Voinnet, 2005). In contrast, many plant viruses identified to date encode functional suppressors to inhibit specific antiviral defenses (rev. by Li and Ding, 2006; Roth et al., 2004). The potyvirus HC-Pro, the tombusvirus p19, and the *Cucumber mosaic virus* (CMV) 2b are well-characterized suppressors involved in the induction of symptoms in viral infected plants (Cronin et al., 1995; Ding et al., 1995; Scholthof et al., 1995).

CMV is an economically important plant pathogen with a broad host range of more than 1,000 plant species (Palukaitis and García-Arenal, 2003). Numerous CMV strains have been identified and are characterized broadly into two subgroups, I and II, with further subdivision based on sequence variation within subgroup I, such as IA and IB (Palukaitis and García-Arenal, 2003). Most strains of CMV induce a generic light-green/dark-green mosaic; however, some strains induce other symptoms, such as chlorosis, stunting, epinasty, filiformism or necrotic lesions (Divéki et al., 2004; Shintaku et al., 1992; Suzuki et al., 1995; Szilassy et al., 1999). In a few cases, expression of such specific symptoms has been mapped to specific amino acids in the capsid, 1a or 2a proteins (rev. in Palukaitis and García-Arenal, 2003). Additionally, induction of symptoms such as mosaic and stunting has been attributed to the newly-identified 2b gene (Ding et al., 1995, 1996; Lewsey et al., 2007; Shi et al., 2002; Zhang et al. 2006). Using chimeric CMVs of various subgroup I strains, in which the 2b gene has been exchanged, can also determine 2b responsibility for symptom induction (Du et al., 2007). The molecular determinants of pathogenicity associated with the CMV 2b have not been clearly defined. However, elimination of the sequences encoding the KSPSE domain (amino acids 37–43) in the Q-CMV 2b protein was found to affect virus accumulation and the rate of systemic infection in the cucumber, while deleting the C-terminal 16 amino acids of Q-CMV 2b was shown to affect systemic infection and viral RNA accumulation in the cucumber (Ding et al., 1995). Moreover, Arg⁴⁶ of 2b protein from the spontaneous mutant CM95R is found to be associated with the induction of severe symptoms and the ability of the 2b protein to strongly bind siRNAs and suppress RNA silencing (Goto et al., 2007).

Differential virulence of cucumoviruses inducing their 2b genes has been repeatedly reported (Ding et al., 1995; Du et al., 2007; Shi et al., 2002; Soards et al., 2002). Inhibiting expression of 2b genes in CMV strains reduced virulence and viral accumulation (Ding et al., 1995; Du et al., 2007), while replacement of 2b genes in CMV with homologous or heterologous 2b genes usually resulted in changes in virulence (Ding et al., 1996; Du et al., 2007; Shi et al., 2002). These experiments demonstrated that the CMV 2b indeed participated and played an important role in inducing symptoms.

Transgenic and biochemical studies in *Arabidopsis* found that the 2b protein of Fny-CMV interfered with miRNA pathways by direct interaction with the AGO1 (Zhang et al., 2006) and targeted some miRNAs selectively, causing virus-like symptoms (Lewsey et al., 2007), but the 2b protein of either Q-CMV or LS-CMV do not (Chapman et al., 2004; Lewsey et al., 2007; Zhang et al., 2006). However, these effects on miRNAs might be attributable to a lack of viral siRNAs for the Fny-CMV 2b protein to interact with, as such effects on development have not been seen in transgenic plants in the presence of the replicating viral genome (Praveen et al., 2008). Although the 2b gene of Q-CMV has been identified as the virulence determinant for Q-CMV, constitutive expression of the 2b protein in *Arabidopsis* did not interfere with *Arabidopsis* development (Chapman et al., 2004; Lewsey et al., 2007). Recently, Diaz-Pendon et al. (2007) have shown that the *Arabidopsis* mutant *dcl2-dcl4* causes more severe symptoms after infection with Q-CMVΔ2b than did wild-type *Arabidopsis* after infection by wild-type Q-CMV, suggesting that the 2b gene is non-essential for Q-CMV to induce symptoms. Alternatively, induction of symptoms could be related to other CMV components.

A necrosis strain of CMV, Cb7-CMV has been found in Cruciferous crops in eastern China. It causes systemic necrosis in seedlings of *N. glutinosa*. The hybrid virus, FCb72b-CMV, generated by precise replacement of the 2b gene in Fny-CMV with the 2b gene of strain Cb7-CMV, causes systemic necrosis on both newly-developed and expanded leaves on this same host, as the parental virus does; however, another 2b-gene, hybrid virus, FRad35^{2b}-CMV, only induced mild mosaic symptoms as described in this chapter. The differential virulence between these hybrid viruses is to be compared to find out their roles in pathogenicity and virus accumulation, for a more detailed location of functional domains of the 2b gene.

4.3.1 The Systemic Necrosis-inducing Domain is Related to a 125-nucleotide Region of RNA 2

To delimit the determinant(s) of systemic necrosis induced by FCb7^{2b}-CMV, FRad35^{2b}-CMV is selected as a reference, both for its low virulence, causing only mild mosaic on *N. glutinosa*, and because its 2b gene has a high sequence identity (92.5% at the nucleotide level and 93.7% at the amino acid level) with the 2b of FCb7^{2b}-CMV. Chimeras are constructed between cDNA clones of RNAs 2 of FCb7^{2b}-CMV and FRad35^{2b}-CMV by exchange of sequences at nucleotide positions 2472, 2596, 2681 (as shown in Fig. 4.6). Each RNA transcript of these constructs is co-inoculated on *N. glutinosa* with RNA transcripts of pFny109 and pFny309, generating six chimeric viruses FCR2472, FRC2472, FCR2596, FRC2596, FCR2681, and FRC2681. And all the chimeric viruses are found to be replicated with successful infection. Sequencing of the 2b genes from the progeny RNAs has been obtained and shows that the chimeric 2b genes are all stable after one passage. The biological phenotypes of these six chimeras on *N. glutinosa* are summarized in Fig. 4.7. The chimeras FCR2681 and FCR2596, containing the

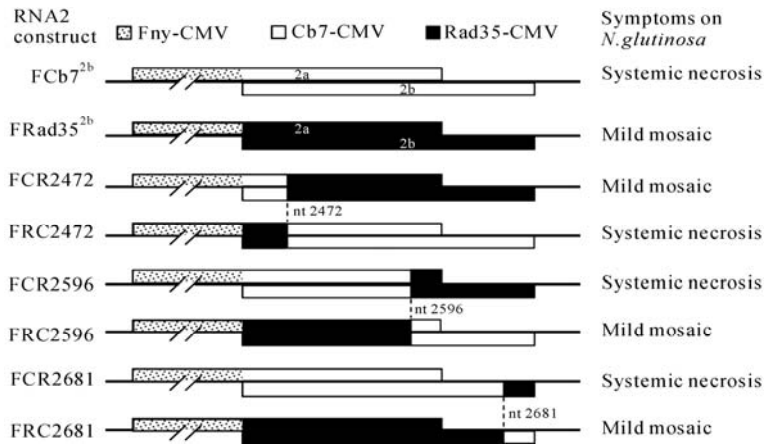


Fig. 4.6. Schematic diagram for constructing RNA 2 of FCB7^{2b}, FRad35^{2b} and FCB7^{2b}/FRad35^{2b} chimeric RNA 2. Chimeric viruses are obtained by adding RNA transcripts of each RNA 2 to co-inoculate with those of pFny109 and pFny309 on *N. glutinosa* i, and the symptoms induced are given in the right row. In each construct, sequences originating from CMV strains Fny, Cb7 and Rad35 are indicated by fill patterns in the 2a genes and 2b genes. The flanking lines indicate the 5' and 3' non-translated regions of Fny-CMV RNA 2. Exchange positions between RNAs 2 of FCB7^{2b} and FRad35^{2b} are indicated between two reciprocal constructs

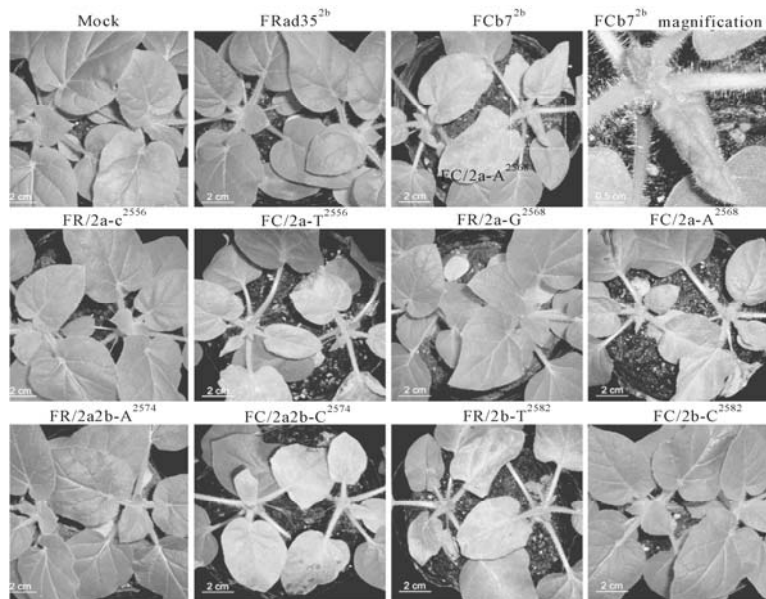


Fig. 4.7. Phytopathogenicity comparison of FCB7^{2b}, FRad35^{2b} and their point mutants in on *N. glutinosa*. Photographs of symptoms caused by FCB7^{2b}, FRad35^{2b} and their various point mutants indicated above each panel. Mock-treated plants were inoculated with distilled water. Photographs were taken 14 dpi. The photograph “FCB7^{2b} magnification” shows an enlargement of an area bordered by a rectangle in the adjacent panel containing FCB7^{2b}-infected plants

sequences of FRad35^{2b} RNA 2 from either positions 2681 to 2751 or 2596 to 2751 in a FCb7^{2b} background, respectively, induce systemic necrosis similar to FCb7^{2b}. By contrast, FCR2472, containing the sequence of FRad35^{2b} RNA 2 from positions 2472 to 2751 in an FCb7^{2b} background, causes only mild mosaic, similar to FRad35^{2b}. These results can demonstrate that the symptom-induction domain is delimited to the 125-nucleotide region of RNA 2 from positions 2472 to 2596. Differential symptom expression between FRC2472 and either FRC2596 or FRC2681 also reciprocally define this region responsible for induction of systemic necrosis or mild mosaic.

4.3.2 Effect of 2b Protein Amino Acid 55 on Viral Accumulation and Symptom Development

In the delimited region, FCb7^{2b} RNA 2 is found differed from FRad35^{2b} RNA 2 by four nucleotides at positions 2556 (Y= C or T), 2568 (R= G or A), 2574 (M= A or C) and 2582 (Y= T or C) (Fig. 4.8(a)). The first three differences result in changes at amino acid residues 824 (Leu or Phe), 828 (Ala or Thr), and 830 (Thr or Pro), respectively, of the 2a protein, and the last two differences result in changes of amino acid residues 52 (Leu or Phe) and 55 (Leu or Pro), respectively, of the 2b protein (Fig. 4.8(c)). It has been shown in this chapter that the nucleotide sequences of the 2b ORF and the 3' end of the 2a ORF of Cb7-CMV have little effect on symptom expression, suggesting that the necrosis determinant(s) should be expressed at the protein rather than at the nucleotide level. To determine which amino acid(s) is associated with the induction of the systemic necrosis, eight point mutants are generated by using the PCR-based, site-directed mutagenesis (Fig. 4.8(c)). Three FCb7^{2b}-derived mutants, FC/2a-T, FC/2a-A, and FC/2a2b-C, in which the nucleotides C at nt 2556, G at nt 2568, and A at nt 2574 of FCb7^{2b} RNA 2 have been substituted by nucleotides T, A, and C, respectively, show similar necrosis phenotype to FCb7^{2b}. Likewise, three reciprocal mutants FR/2a-C, FR/2a-G, and FR/2a2b-A, derived from FRad35^{2b}, all induce mild mosaic symptoms similar to FRad35^{2b}. These results demonstrate that the changes of the codons for these three differential amino acids in the 2a proteins and for the amino acid 52 in the 2b proteins have no obvious effect on symptom expression. However, the FC/2b-C mutant, in which the Leu⁵⁵ in the FCb7^{2b} 2b is changed to Pro⁵⁵ of the FRad35^{2b} 2b by substituting the nucleotide T at nt 2582 in the FCb7^{2b} RNA 2 to a C, induces only mild mosaic, whereas the reciprocal mutant FR/2b-T causes systemic necrosis. These observations are all consistent in demonstrating that the development of systemic necrosis after infection by FCb7^{2b} is associated with the amino acid Leu⁵⁵ of its 2b protein.

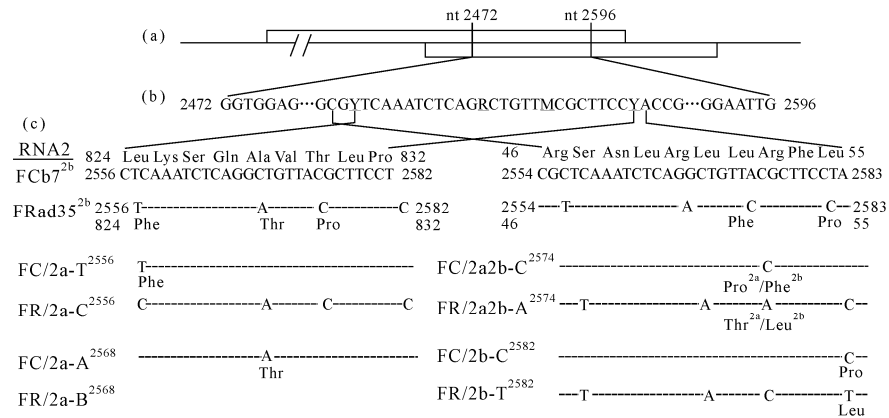


Fig. 4.8. Partial RNA 2 nucleotide sequence of FCb7^{2b} and FRad35^{2b} with their positions 2472-2596 as well as mutants illustrated. (a) Diagram representing RNA 2 of either FCb7^{2b} or FRad35^{2b}. In the diagram, the region bordered by nucleotides 2472 and 2596 responsible for induction of viral symptoms is indicated by two vertical dashed lines; (b) A merged nucleotide sequence representing the sequences of RNA 2 of FCb7^{2b} and FRad35^{2b} from positions 2472 to 2596. Four mixed nucleotides (Y=C or T, R=G or A, M=A or C, and Y=T or C), corresponding to the four differential nucleotides between FCb7^{2b} and FRad35^{2b}, are underlined. (c) The left side shows the partial 2a amino acid sequence and 2a ORF of FCb7^{2b}, FRad35^{2b} and their mutants, from positions 824 to 832, and their corresponding codon sequences from positions 2556 to 2582; the right side shows the 2b amino acid sequence and 2b ORF of FCb7^{2b}, FRad35^{2b} and their mutants, from positions 44 to 55 and their corresponding codon sequences from positions 2554 to 2583. In FRad35^{2b} and these eight mutants, sequences that are the same as FCb7^{2b} are shown by -; only those different from FCb7^{2b} are given, except for the mutated nucleotides in mutants FR/2a-C, FR/2a-G, FR/2a2b-A, and FR/2b-T

Previously, it has been shown that the virulence of FCb7^{2b}-CMV is associated with its high accumulation in the systemic leaves of *N. glutinosa*. To determine whether or not the changes in the amino acid 55 in the 2b proteins affected viral accumulation, northern blot hybridization has been done to analyze the viral RNAs, which are extracted 14 dpi from upper leaves of *N. glutinosa* plants singly infected with FCb7^{2b}, FRad35^{2b}, FC/2b-C, or FR/2b-T. The results show that FCb7^{2b} and FR/2b-T have similar accumulation levels of their progeny viral RNAs, much higher than those of FRad35^{2b} and FC/2b-C. Thus, the change in virulence mediated by aa 55 in 2b protein is associated with different levels of viral RNA accumulation. The presence of 2b Leu⁵⁵ brings a high level of viral RNA accumulation and results in higher pathogenicity of the virus.

4.3.3 Sequence Analyses of the 2b Proteins and the C-top of the 2a Proteins

For evaluating the contribution of Leu⁵⁵ in the induction of systemic necrosis, the encoded 2b protein sequences of CMV strains have been analyzed (Du et al., 2007;

Roossinck, 2002). Interestingly, only the 2b protein of Rad35-CMV is found to contain the amino acid Pro at position 55, while all other 2b proteins contain the amino acid Leu at this position (Fig. 4.9). Although systemic necrosis has not been reported for other strains of CMV strains, based on those strains examined in several laboratories, only the Cb7-CMV strain has been found to cause systemic necrosis on *N. glutinosa*. Therefore, it appears that Leu⁵⁵ of the 2b proteins is essential, but not sufficient for FCb7^{2b}-CMV or FR/2b-T to induce systemic necrosis on *N. glutinosa*, and the 2a or the 2b proteins of Cb7 and Rad35 presumably have other sequence(s) in common, but different from other strains that do not cause systemic necrosis in this host. A search has been made for site(s) common to the 2b proteins and the 2a proteins C-top of Cb7 and Rad35, but not in other strains. The analysis has showed that the 2b proteins of Cb7, Rad35 and Ix contained the amino acid Cys at position 37, which is not present in any other strains, while the amino acid Tyr was present at position 38 in the 2b proteins of Cb7, Rad35, PGs, Ix and all subgroup II strains, but absent in all other subgroup I strains. Analysis of the 2a protein C-top sequences shows that the amino acid Met at position 815, like the 2b Cys³⁷, only occurring in strains Cb7, Rad35 and Ix, and the amino acid Leu at position 816 has an identical occurrence in these strains to the 2b Tyr³⁸. This is because the 2b Cys³⁷ and the 2a Met⁸¹⁵ are both encoded by the nucleotide T at position 2527 of RNA 2, and both the 2b Tyr³⁸ and the 2a Leu⁸¹⁶ are encoded by the nucleotide T at position 2530 of RNA 2. Thus, the predicted common site(s) in the 2a C-top and 2b proteins could not be mutated independently.

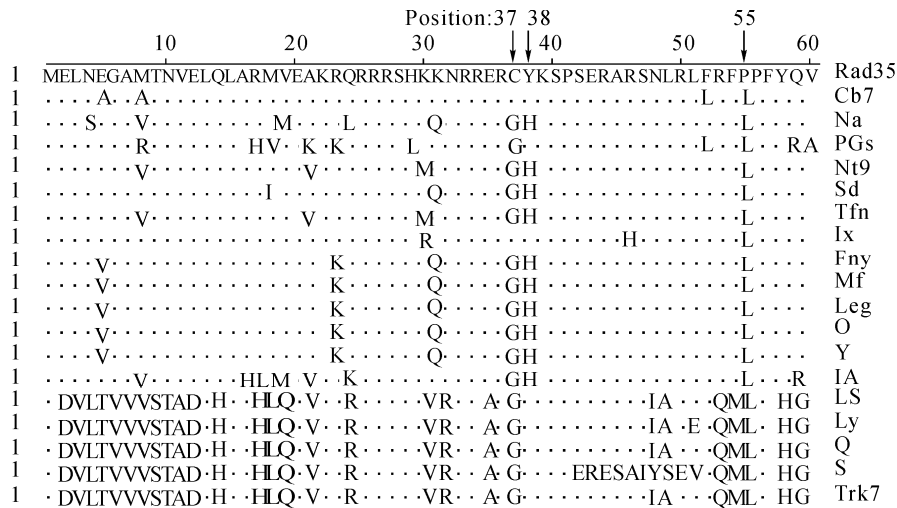


Fig. 4.9. Comparison of amino acid sequences of 2b proteins across CMV subgroups. Dot (.) indicates the residues that match Rad35. Black arrow indicates the position of the amino acids responsible for the differential symptoms between FCb7^{2b}-CMV and FRad35^{2b}-CMV. Red arrows indicate the positions of the amino acids in common for Cb7 and Rad35, but not for most of the other CMV strains

4.3.4 *Effect of the C-terminus of 2a Protein on Symptom Expression and Virus Accumulation*

To determine whether these predicted common sites are associated with the induction of systemic necrosis, it must be firstly assessed whether the Met⁸¹⁵/Leu⁸¹⁶ of the Cb7 2a protein C-top could potentially function in this phenotype, by introducing stop codons before these sequences in the 2a ORF, at nucleotide positions 2415–2417 and/or 2520–2522, in the plasmids designated pF2C-1TGA or pF2C-2TGAs. These sequence changes result in either one termination codon introduced after amino acid 811 of the 2a protein or two termination codons introduced after amino acids 776 and 811 of the 2a protein. A stop codon introduced at position 777 alone is found to be unstable (Du et al., 2007; Soards et al., 2002), which is why the downstream and dual termination sites are chosen. FCb72b-CMV2a811 (with one termination site) and FCb72b-CMV2a776 (containing two termination sites) are generated by co-inoculation of RNA transcript of either pF2C-1TGA or pF2C-2TGAs with RNA transcripts of pFny109 and pFny309, respectively. The nucleotide introduced to generate the termination codon at position 812 in the 2a ORF is silent in the 2b ORF, while the changes introduced at position 777 are upstream of the 2b gene. Sequence analyses shows that the two mutants are stable after at least one passage. Unexpectedly, both mutants have failed to induce systemic necrosis at 14 dpi, although they also exhibited obvious differences in virulence. FCb7^{2b}-CMV2a776 causes veinal chlorosis, and FCb7^{2b}-CMV2a811 causes severe mosaic on newly-developed leaves and yellow chlorosis on upper expanded leaves, and both of these mutant CMVs are much less virulent than FCb7^{2b}-CMV (Fig. 4.10(a)). The leaves showing yellow chlorosis after infection by FCb7^{2b}-CMV2a811 become necrotic later during infection, but the newly-developed, infected leaves do not. Northern blot hybridization analysis of viral progeny RNAs from systemically-infected leaves shows that FCb7^{2b}-CMV2a776 accumulated much less viral RNA than FCb7^{2b}-CMV. By contrast, FCb7^{2b}-CMV2a811 has similar accumulation levels for RNA 4A and only slightly lower accumulation levels for the other viral RNAs vs. FCb7^{2b}-CMV (Fig. 4.10(b)). These results show that the 2a protein C-top of FCb7^{2b}-CMV indeed participates in the process of inducing systemic necrosis and accumulating viral progeny RNAs when its 2b protein is present. In addition, the systemic necrosis phenotype in the upper expanded leaves and in the newly-developed leaves is controlled in different ways.

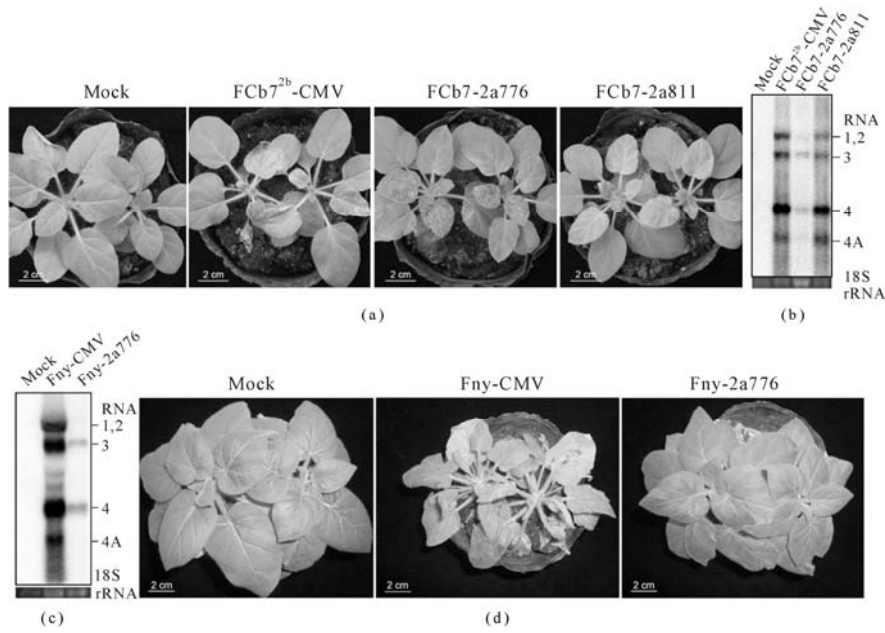


Fig. 4.10. Symptom expression and viral accumulation of FCb7^{2b}-CMV, Fny-CMV and their mutants in *N. glutinosa*. (a) and (d) Symptoms induced by the viruses indicated above each panel. Mock-treated plants were inoculated with distilled water. Photographs in (a) and (d) were taken at 14 and 35 dpi, respectively; (b) and (c) Northern blot hybridization analyses of the accumulated viral RNAs in systemically infected leaves of *N. glutinosa* plants infected singly by these viruses. The RNA samples loaded were visualized by ethidium bromide staining of 18S rRNA (low panel). The positions of RNAs 1, 2, 3, 4 and 4A are indicated on the right

Considering that the 2a protein C-top of FCb7^{2b}-CMV affected the expression of symptoms and accumulation of viral progeny RNAs, two stop codons have been induced into the positions of the 2a ORF of Fny-CMV, by generating pFny209-2TGAs (Fig. 4.11), and then Fny-CMV2a776 is generated by co-inoculating RNA transcript of pFny209-2TGAs with RNA transcripts of pFny109 and pFny309. The nucleotide introduced to generate the termination codon at position 777 is upstream of the 2b ORF, and the change at codon 812 in the 2a ORF again is silent in the 2b ORF. This mutant was stable after one passage, as determined by sequencing the progeny viral RNA. The Fny-CMV2a776 mutant could cause only mild mosaic symptoms on *N. glutinosa* even by 35 dpi, and shows significantly reduced virulence when compared with Fny-CMV. Northern blot hybridization analysis showed that accumulation of progeny RNAs of Fny-CMV2a776 is much lower than that of Fny-CMV. Taken together, 2a C-top of CMV can affect virulence and viral accumulation to a considerable extent in the absence of any specific effect mediated by the 2b gene.

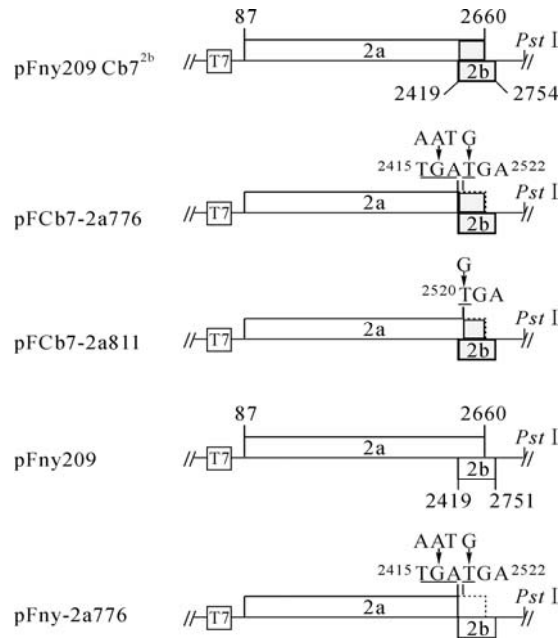


Fig. 4.11. Schematic diagram of sequence inserts in plasmids pFny209, pFny209Cb7^{2b} and their derivatives. pFny209Cb7^{2b} was constructed by replacing the 2b gene in the plasmid pFny209 with the 2b gene of Cb7-CMV. Plasmids pFC2-2TGAs and pFC2-1TGA were derived from pFny209Cb7^{2b}. In the pFC2-2TGAs, two termination codons were introduced by changing nucleotides AAT at 2415–2417 to TGA and nucleotide G to T at 2520, rendering the C-terminal overlapping part of Cb7 2a protein non-coding. In the plasmid pFCb2-1TGA, one termination codon was introduced by changing nucleotide G at 2520 to T, inhibiting expression of the C-terminal 55 amino acids of the Cb7 2a protein. pFny209-2TGAs, a derivative of pFny209, was constructed in the same way as the construction of the pFC2-2TGAs plasmid. The dotted rectangles indicate that the sequences are from Cb7-CMV. The region surrounded by dashed lines represents sequences that are no longer encoding. The nucleotides introduced to generate termination codons are underlined. Arrows indicate the substituted nucleotides. All the plasmids contain a modified T7 promoter at their 5' ends

Systemic necrosis is not a common disease phenotype induced by CMV. The hybrid virus FCb7^{2b}-CMV induced this phenotype on *N. glutinosa* (Du). The molecular determinants of the necrosis phenotype in FCb7^{2b}-CMV have been analyzed by using FRad35^{2b}-CMV as a reference strain (Du et al., 2008). It is found that the differences in symptoms induced by FCb7^{2b}-CMV vs. FRad35^{2b}-CMV are attributed to the different amino acids at position 55 of their corresponding 2b proteins, which correlates with changes in the level of viral RNA accumulation of the mutant viruses; even these sequence changes did not affect the sequence of the overlapping 2a protein. Thus, the effects can be attributed to the 2b protein. It seems unlikely that the addition of a Pro at position 55 of the Cb7 2b protein affected the local secondary structure, since sequence analysis of the 2b ORFs has shown that the residue at position 56 is also a Pro in all strains. The phenotypes also cannot be attributed solely to the Leu⁵⁵ in the Cb7

2b, as the 2b ORFs of all other strains of CMV contain a Leu at this position, indicating that the presence of Leu⁵⁵ alone in the 2b protein is insufficient to result in some interaction with the host causing systemic necrosis. Production of viral symptoms is a consequence of co-action of 2b protein and other CMV components. It is found that 2a C-top of subgroup IA strain Fny-CMV and IB strain Cb7-CMV play an important role in the process of inducing virulence and increasing viral RNA accumulation.

4.4 Satellite RNA-mediated Reduction in Accumulation of CMV Genomic RNAs in Tobacco Related to 2b Gene of the *Helper Virus*

The interaction between satellite RNA (satRNA) and CMV as a helper virus, provides a good model for recognizing sub-cellular communications for macromolecules. It has been found that in many hosts and for most strains of CMV, the presence of satRNA both attenuates the symptoms and the presence of CMV-satRNA usually reduces the titer of the helper virus, more so in *Solanaceous* than in cucurbit host plants, when tested qualitatively (Gal-On et al., 1995; García-Arenal and Palukaitis, 1999; Palukaitis and García-Arenal, 2003; Roossinck and Palukaitis, 1991; Simon et al., 2004). Some reports suggested that the effect of satRNA on the helper viruses could be related to the competitiveness of replication between the helper virus and satRNA (Rizzo and Palukaitis, 1990; Simon et al., 2004). When a reliable quantitative measurement has been set up, the suppressive effect of satRNA on the accumulation of the CMV genomic RNAs and encoded proteins can be considered for its effect on accumulation of RNA1 and 2, relating to 1a and 2a protein, or the effect on accumulation of RNA3 and 4, relating to 3a and CP. Up to date, only a very limited report has been documented for quantitative determination of the affection of satRNA on the genomic RNAs and genes of its helper virus, and less was reported and published on its effect on the 2b gene, which is correlated to virus distribution among plant organs and to symptom expression. Developing a sensitive method to quantitatively determine the low level of CMV 2b gene in the host plants world brings the chance to make a better retort to the above questions. Hereafter, the affection of satRNA on the accumulation CMV genomic RNAs and also the influence of deleting the 2b gene in viral RNA accumulation and symptom expression are to be introduced.

4.4.1 Symptom Expression on *N. Tabacum* Inoculated with *CMV-Fsat*

The full length cDNA clone, psatRs, obtained from a satRNA of 368 nt (Genbank accession number: AF451896), is originally from a CMV strain isolated from

Raphanus sativus. The artificial isolate, CMV-Fsat, is built with the infectious cDNA clones (pF109, pF209 and pF309) of CMV-Fny and the full length satRNA. A mixture of RNA *in vitro* transcripts from pF109, pF209 and pF309 is mechanically inoculated onto tobacco seedlings, to build CMV-Fny and a mixture of CMV-Fny RNAs plus satRs was inoculated to build CMV-Fsat. To be used as a control virus, CMV-Fny Δ 2b is constructed as per previously described in this chapter. As shown in Fig. 4.12, at the third day post inoculation (dpi), RT-PCR detection results show that CMV-Fny supported the replication of satRs in *Nicotiana tabacum* (tobacco) seedlings, and a high accumulation of satRs dsRNA in host plants suggested that CMV-Fny could be competent to serve as the helper virus of satRs. At 7 dpi, mosaic symptoms appeared on the newly growing leaves of seedlings inoculated with CMV-Fny but not on seedlings inoculated with CMV-Fsat, meaning a postponed affect of satRNA on symptom development. At 21 dpi, symptoms on the seedlings inoculated with CMV-Fny developed into severe mosaic, systemic deformation and stunt, while the plants inoculated with CMV-Fsat expressed only slight mosaic but without obvious deformation. This suggests that satRs postponed the emergence of symptoms induced by CMV-Fny and also attenuated symptom expression on tobacco seedlings.

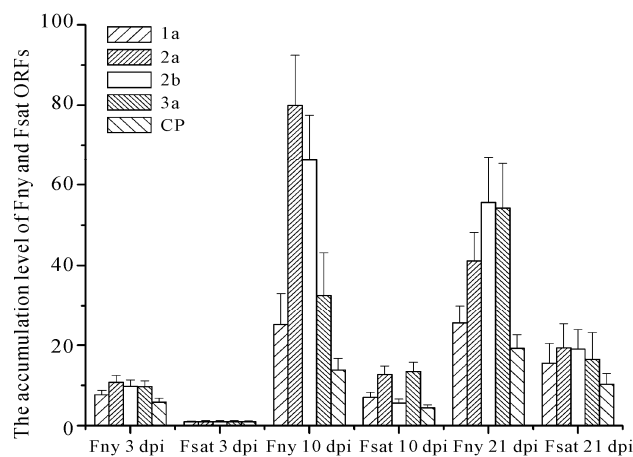


Fig. 4.12. The relative accumulation of ORFs for CMV-Fny and CMV-Fsat in systemic tobacco leaves at different inoculation time. Total RNA was extracted from the tissues of 4 host plants infected by CMV-Fny with or without satRs. The relative accumulation of each CMV-Fny gene was analyzed by Real-time RT-PCR amplified with specific pairs (Feng et al.), and the analysis of the accumulation of each gene was repeated three times. 18s rRNA was used as an endogenous control and relative quantization with data was performed according to the comparative C_t method ($2^{-\Delta C_t}$), for example, the relative accumulation of CMV-Fny 1a = $2^{-(\text{aver } 1a C_t - \text{aver } 18s C_t)}$. Because the relative accumulation of CMV-Fsat genomic RNAs was lowest at 3 dpi among the 6 samples, the relative accumulation of 1a, 2a, 2b, 3a and CP was normalized as 1 and the relative accumulation of the other sample genomic RNAs was calculated based on that of CMV-Fsat genomic RNAs at 3 dpi. The standard deviation was obtained in three repeats. The relative accumulation of different genes could not be compared because each Fny-CMV gene had different RT and PCR efficiency

4.4.2 Effect of satRs on the Accumulation of CMV-Fny Genomic RNAs

The relative accumulation of ORFs for CMV-Fny *1a*, *2a*, *2b*, *3a* and *CP* in systemic leaves was examined at 3 dpi, 10 dpi and 21 dpi by real-time RT-PCR. As shown in Fig. 4.12, the results indicated that the accumulation of CMV Fny genomic RNAs is clearly higher than those of CMV-Fsat. At 3 dpi, satRs begin to exert effects on CMV in host plants, resulting in lower accumulation of CMV-Fsat genomic RNAs. The degree of the accumulation of CMV Fny genomic RNAs affected by satRs is shown in Table 4.3. The accumulation level of CMV-Fny ORFs is found to be 5–10 fold higher than that of CMV-Fsat. The degree of depression of each ORF by satRs is significantly different, at a tendency of $2a > 2b > 3a > 1a > CP$. At 10 dpi, the accumulation level of CMV ORFs is still depressed by satRs, but the degrees are reduced with the exception of *2b*, in which the degree of depression was higher than 3 dpi. The depressing degree by satRs is $2b > 2a > 1a > 3a > CP$. At 21 dpi, the suppression effect of satRs on the accumulation of CMV ORFs is found to have clearly declined. The accumulation of *1a*, *2a*, *2b*, *3a* and *CP* for CMV-Fny is found to be 1.6-, 2.1-, 2.9-, 3.3- and 1.9-fold higher than that of CMV-Fsat, respectively. In the newly growing leaves, there is an especially low accumulation of satRs and CMV genomic RNAs, and the accumulation of CMV-Fny *1a*, *2a*, *2b*, *3a* and *CP* is 11.6-, 24.3-, 37.6-, 3.9- and 7.0-fold higher, respectively, than that of CMV-Fsat. Thus, satRs depress the accumulation of CMV RNAs, and the effect of satRs on the accumulation of the *2b* gene is relatively significant. The attenuation of symptoms in CMV-Fsat infected plants is due to low accumulation of CMV genomic RNAs.

Table 4.3 The degree of the accumulation of CMV-Fny genomic RNAs affected by satRs at different inoculation time

Viral genes	Accumulation degree		
	3 dpi	10 dpi	21 dpi
1a	7.6*	3.6	1.6
2a	10.8	6.28	2.1
2b	9.8	11.8	2.9
3a	9.7	2.4	3.3
CP	5.8	3.1	1.9

*. accounted as the relative accumulation of CMV-Fny *1a* gene versus that of CMV-Fsat, and the data of the relative accumulation of CMV-Fny and CMV-Fsat was obtained from Fig. 4.12.

4.4.3 Symptom Expression on the Host Plants Inoculated with CMV-Fny Δ 2b

Mixtures of RNA transcripts from pF109, pF209 Δ 2b and pF309 (to build CMV-Fny Δ 2b) and RNA transcripts for CMV-Fny Δ 2b plus satRs (to build

CMV-Fny Δ 2bsat) are mechanically inoculated on the tobacco seedlings, respectively. At 10 dpi, neither the host plant inoculated with CMV-Fny Δ 2b nor inoculated with CMV-Fny Δ 2bsat is found to express obvious symptoms, but RT-PCR detection of the CP gene and satRs in systemic leaves suggested that CMV-Fny Δ 2b could systemically infect tobacco, and CMV-Fny with 2b (partial 2a) gene deleted, still supported the replication and accumulation of satRs in host plants. At the same time, RNA2 of CMV-Fny Δ 2b, extracted from systemic leaf tissue, is amplified with RT-PCR and sequenced, the result showing that the RNA2 Δ 2b is not repaired. At 21 dpi, both host plants inoculated with CMV-Fny Δ 2b and also CMV-Fny Δ 2bsat appeared slightly mosaic (Fig. 4.13), but no further attenuation of the CMV-Fny Δ 2b symptoms could be observed when satRs had been added. It shows that the addition of satRNA could not express the same attenuating function when the 2b gene of the helper virus does not exist.

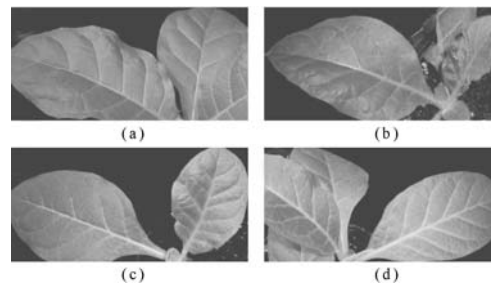


Fig. 4.13. Symptoms on the seedlings of *N. tabacum* infected with CMV-Fny and CMV-Fny Δ 2b with or without satRs at 21 dpi. (a) Mock; (b) CMV-Fny; (c) CMV-Fsat; (d) CMV-Fny Δ 2b

4.4.4 Accumulation of CMV-Fny Δ 2b Genomic RNAs and the Effect of satRNAs

The accumulation of CMV-Fny Δ 2b genomic RNAs and satRs in inoculated leaves has been examined at 3 dpi and 10 dpi. As shown in Table 4.4, at 3 dpi the relative accumulation level of CMV-Fny Δ 2b ORFs in the inoculated leaves is only 0.5%–5% of that for CMV-Fny. At 10 dpi, the accumulation levels of CMV-Fny Δ 2b genomic RNAs are still much lower than those of CMV-Fny, but their absolute amounts are obviously increased in comparison with those at 3 dpi. It suggests that attenuation of symptom expression on host plants by 2b gene deletion is related to low replication and/or accumulation of CMV genomic RNAs. At 3 dpi, the accumulation of CMV-Fny Δ 2bsat genomic RNAs in the inoculated leaves is at a similar level to CMV-Fny Δ 2b, which indicates that no suppression effect on the replication and/or accumulation of CMV-Fny Δ 2b ORFs is caused by adding satRs. At 10 dpi, even though the accumulation of CMV-Fny Δ 2b ORFs has increased, the presence of satRs shows no obvious decrease in the accumulation of CMV-Fny Δ 2b ORFs in the inoculated leaves. It suggests that satRs exerted no

obvious effect on the replication and/or accumulation of CMV genomic RNAs when the 2b gene is knocked off. At 10 dpi, the accumulation levels of CMV-Fny Δ 2bsat genomic RNAs in systemic leaves are found to be nearly equal to those of CMV-Fny Δ 2b. Thus, satRNAs show no effect on the replication and/or accumulation of CMV genomic RNAs when the 2b gene is not functioning.

Table 4.4 The relative accumulation of ORFs for CMV-Fny and CMV-Fny Δ 2b with or without satRs

Viral genes	CMV-Fny		CMV-Fny Δ 2b		CMV-Fny Δ 2bsat	
	3 dpi	10 dpi	3 dpi	10 dpi	3 dpi	10 dpi
1a	8.10±0.29	7.89±0.12	0.039±0.008	1.11±0.10	0.032±0.008	1.03±0.05
2a	3.78±0.10	1.98±0.03	0.063±0.002	1.42±0.45	0.055±0.015	1.15±0.14
2b	57.08±2.57	30.91±0.87	0	0	0	0
3a	0.28±0.03	0.23±0.007	0.012±0.001	0.14±0.02	0.011±0.003	0.10±0.03
CP	31.50±0.76	16.16±0.77	0.18±0.07	2.33±0.11	0.16±0.003	2.32±0.33

The relative accumulation of ORFs was detected from the inoculated leaves at 3 and 10 dpi, respectively. Total RNA was extracted from the tissues of 4 host plants infected by CMV-Fny or CMV-Fny Δ 2b with or without satRs. The relative accumulation of each CMV-Fny gene was analyzed by Real-timeRT-PCR amplified with specific pairs (Feng et al.), and the analysis of the relative accumulation of each gene was repeated three time. 18s rRNA was used as an endogenous control and relative quantization with data was performed according to the comparative C_t method ($2^{-\Delta C_t}$), for example the relative accumulation of CMV-Fny 1a = $2^{-(\text{aver } 1a C_t - \text{aver } 18s C_t)}$. The standard deviation was obtained in three repeats

CMV-Fny Δ 2b caused only slight mosaic symptoms in host plants, similar to that of CMV-Fsat, and the accumulation of CMV-Fny Δ 2b genomic RNAs is much lower than that of CMV-Fny. It shows that the efficiency of systemic infection of CMV-Fny declined greatly when the 2b gene is deleted. So the deletion of the 2b gene had a similar effect on CMV-Fny genomic RNAs replication and/or accumulation as adding satRs. The 2b gene of different cucumoviruses has been shown to have a major effect on long distance movement of CMV as well as on the degree of virulence and the host range (Feng et al., 2006; Moriones et al., 1992; Shi et al., 2003; Wang et al., 2002). These effects are believed to relate to the ability of the 2b protein to inhibit various defense reactions, such as suppressing the RNA silencing mechanism and interfering with the salicylic acid-mediated defense response (Brigneti et al., 1998; Guo and Ding, 2002; Kong et al., 1995; 1997; Li et al., 1999; Shi et al., 2003). But, to date, no report has focused on the ability of CMV to support satRNA when the 2b gene is deleted. Regarding the low accumulation of genomic RNAs in CMV-Fny Δ 2b, the relative accumulation of CMV genomic RNAs was not further reduced by satRNA.

4.4.5 Accumulation of CMV-Fny Genomic RNAs in the Inoculated Leaves and the Effect of satRNAs

It is important to find out whether the low accumulation of CMV-Fsat genomic RNAs in systemic leaves is due to low accumulation in the inoculated leaves. The accumulation of CMV-Fny and CMV-Fsat ORFs in the inoculated leaves is thus tested at early stages. At 2 dpi, the relative accumulation levels of CMV-Fny 1a, 2a, 2b, 3a and CP are found to be 2.2-, 2.1-, 4.6-, 1.8- and 3.5-fold those of CMV-Fsat, respectively (Table 4.5). At 3 dpi, the relative accumulation levels of CMV-Fny 1a, 2a, 2b, 3a and CP are found to be 2.3-, 3.4-, 3.8-, 2.2- and 2.2-fold those of CMV-Fsat, respectively. It suggests that satRs also mediated a reduction in genomic RNAs accumulation in the inoculated leaves. But, in the inoculated leaves, the replication and/or accumulation of CMV-Fny genomic RNAs is less obviously influenced by satRs, compared to that in systemic leaves. When replicons are removed from the inoculated leaf tissue to systemic organs, the replication/accumulation levels are not determined by the original replicons but by the systemic mechanisms. Thus, satRNA reduction of the helper genomic RNAs could be regarded as temporary affects.

Table 4.5 The relative accumulation of ORFs for CMV-Fny and CMV-Fsat in the inoculated leaves at the early infection stage

Viral genes	2 dpi		3 dpi	
	CMV-Fny	CMV-Fsat	CMV-Fny	CMV-Fsat
1a	1.69±0.12	0.76±0.08	8.10±0.29	3.58±0.28
2a	0.53±0.03	0.25±0.06	3.78±0.10	1.08±0.11
2b	4.26±0.30	0.93±0.10	57.08±2.57	14.88±0.88
3a	0.07±0.01	0.04±0.007	0.28±0.03	0.13±0.01
CP	3.64±0.12	1.03±0.26	31.50±0.76	14.76±0.88

It has been widely reported that the presence of satRNA modifies the pathogenesis of CMV, mostly resulting in attenuation of the symptoms. When the 2b gene of CMV-Fny (CMV-FnyΔ2b) is deleted with part of the 2a gene lacking, CMV-FnyΔ2b can still infect tobacco plants, and the inoculated host plants appeared to have slight mosaic symptoms. Many reports indicate that the inactivity of the CMV 2b gene by directed mutation of a single nucleotide acid or by gene deletion did not lead to a decrease in the accumulation of CMV genomic RNAs in protoplast, and that neither the C terminal 41 amino acids of the 2a protein nor the 2b protein of CMV was required for replication (Moriones et al., 1992; Soards et al., 2002; Wang et al., 2002). Quantitatively determining the different ORFs of CMV in the inoculated and systemic leaf tissues has shown for the first time indubitable replication of CMV in both leaf tissues when the 2b gene is deleted. The detection also reflects the support of satRNA replication by CMVΔ2b, even though the accumulation levels of both CMV genomic RNAs and satRNA are low. The addition of satRs to CMV-FnyΔ2b cannot show a further

decrease in the accumulation of CMV-Fny Δ 2b genomic RNAs. The effect of satRs on CMV-Fny genomic RNAs replication and/or accumulation in the inoculated leaves is less obvious than in systemic leaves. This suggests satRNAs jammed the systemic infection of CMV-Fny in tobacco.

4.4.6 The Effect of satRNAs on Long-distance Movement of CMV-Fny Genomic RNAs

To determine whether the reduction in CMV-Fsat genomic RNAs is due to the effect of satRs on viral long-distance movement, the accumulation of CMV-Fny genomic RNAs in systemic leaves and inoculated leaves should be compared. At 3 dpi, the efficiency of long-distance movement for CMV-Fny is obviously higher than that of CMV-Fsat in host plants. As shown in Table 4.6, the movement efficiency of CMV-Fsat 1a, 2a, 2b, 3a and CP is tested as less than 20%, 21%, 21%, 16% and 27% that for CMV-Fny. But at 10 dpi, the efficiency of long-distance movement between CMV-Fny and CMV-Fsat is similar.

Table 4.6 The long distance-movement efficiency of CMV-Fny and CMV-Fsat at different inoculation times

Viral genes	3 dpi		10 dpi		21 dpi*	
	Fny	Fsat	Fny	Fsat	Fny	Fsat
1a	0.25 [#]	0.05	0.48	0.78	0.020	0.002
2a	0.19	0.04	0.91	0.62	0.025	0.001
2b	0.14	0.03	0.64	0.40	0.008	0.001
3a	0.19	0.03	0.60	0.56	0.004	0.004
CP	0.22	0.06	0.74	0.85	0.021	0.007

* The long distance-movement efficiency at 21 dpi was the relative accumulation of genomic RNAs in the newly growing leaves vs that in the first systemic leaves, since the original inoculated leaves were dying away;

[#] The long distance-movement efficiency was accounted as the relative amount of 1a ORF in systemic leaves versus that in the inoculated leaves.

The presence of satRNA modifying the pathogenesis of CMV has been reported widely. Depending on the strains of the helper virus, satRNA and species of hosts, the effect of the satRNA on virus-induced symptoms can be none, enhanced or attenuated (García-Arenal and Palukaitis, 1999; Palukaitis and García-Arenal, 2003; Roossinck and Palukaitis, 1991; Simon et al., 2004). It seems that satRNAs attenuated the symptoms induced by CMV-Fny, and depressed CMV-Fny genomic RNAs accumulation in tobacco. The effect of satRNAs on CMV-Fny genomic RNAs accumulation in the inoculated leaves is not much less obvious than that in systemic leaves. At 21 dpi, the accumulation of CMV-Fny genomic RNAs has been found to have declined, but that of CMV-Fsat is still increasing. When the accumulation of CMV-Fny ORFs with or without satRNAs, both in inoculated leaves and systemic leaves, is compared, it has been

shown that the efficiency of long-distance movement of CMV-Fny is greatly affected by satRNAs.

The 2b gene of different cucumoviruses has been shown to have a major effect on long-distance movement of CMV as well as on the degree of virulence and on the host's range (Ding et al., 1995; 1996; Ji and Ding, 2001; Shi et al., 2002; Soards et al., 2002). These effects are believed to be due to the ability of the 2b protein to inhibit various defense reactions, such as by suppression of the RNA silencing mechanism (Brigneti et al., 1998; Guo and Ding, 2002) and by interference with the salicylic acid-mediated defense response (Ji and Ding, 2001).

In summary, the attenuation of CMV, by adding satRs or deletion of the 2b gene, is due to the low accumulation of CMV genomic RNAs, but the degree of satRNA affection to different genes can be obviously different, and it can be put forward that satRs might function in a way antagonistic to the function of the 2b gene, resulting in a decrease in the accumulation of CMV-Fny.

4.5 Methodology

We introduce methodology used in this chapter.

4.5.1 *Plants, Viruses and Plasmid Constructs*

Several *Nicotiana* species, including *N. glutinosa*, *N. tabacum* and *N. benthamiana*, are usually used as host plants, seedlings are grown in a greenhouse at 21–26°C. Some parental CMV isolates are used besides wild-type Fny-CMV (Rizzo and Palukaitis, 1990): Cb7-CMV, Na-CMV, Rad35-CMV and PGs-CMV, isolated from tomato, zucchini, radish and *Pinellia ternata*, respectively. *Pinellia ternata* is a traditional Chinese medicinal plant in Araceae. This crop has been cultivated only since the 1980s. CMV is seldom detected in wild medicinal plants, but a new CMV strain is commonly observed in cultivated plants, and the new strain can not be transmitted mechanically neither among pinellia plants nor to *Nicotiana* species. Four intraspecies hybrid clones, pFny209Cb7^{2b}, pFny209Na^{2b}, pFny209PGs^{2b} and pFny209Rad35^{2b}, derivatives of pFny209, are constructed by separately replacing the 2b gene of Fny-CMV with the 2b genes of Cb7-CMV, Na-CMV, PGs-CMV and Rad35-CMV, respectively (illustrated in Fig. 4.2). The four intraspecies hybrid clones are constructed using three overlapping PCR fragments I, II and III. Fragments I and III flank Fny-CMV ORF 2b (nt 2419–2751) and contain nt 1856–2420 and nt 2749–3050 respectively. The two fragments, I and III, are obtained by separate PCRs using pFny209 as the template and primer pairs C2F1856/C2R2420 and C2F2749/C123R, respectively (Table 4.7). Fragments II-Cb7^{2b}, II-Na^{2b}, II-PGs^{2b} and II-Rad35^{2b} represent coding region sequences of 2b ORFs in Cb7-CMV, Na-CMV, PGs-CMV and Rad35-CMV, respectively. The five fragments are obtained by separate PCRs using primer pairs

Cb7^{2b}F/Cb7^{2b}R, Na^{2b}F/Na^{2b}R, PGs^{2b}F/PGs^{2b}R and Rad35^{2b}F/Rad35^{2b}R, and full-length cDNA clones of RNAs 2 of Cb7-CMV, Na-CMV, PGs-CMV and Rad35-CMV as PCR templates respectively. The fragments I, II, and III are mixed and used as a template for a final amplification with primer pair C2F1856/C123R. The resultant fragments are subsequently digested with restriction endonucleases *Pst*I and *Hind*III, and then cloned into pFny209 previously digested with restriction endonucleases *Pst*I, *Eco*RI and *Hind*III.

The pFny209Δ2aC81 plasmid, a derivative of pFny209, in which 81 codons from the C-terminus of 2a ORF is rendered non-coding by substitutions at nt 2415–2417 (AAT→TGA), is constructed by an overlap-extension PCR using a pair of completely complementary mutagenic primers C2F2398Δ2a81/C2R2398Δ2a81. The pFny209Δ2b plasmid, a derivative of pFny209, in which most (nt 2421–2748) of the 2b gene is deleted, is constructed by an overlap-extension PCR using a pair of partially complementary primers C2F2749/C2RΔ2b. pFny209Δ2bpro plasmid (Fig. 4.2), a derivative of pFny209, in which 2b ORF was made non-coding by substitutions at nt 2422–2423 (GAA→TGA), and at nt 2441 and nt 2471 (ATG→ACG), was constructed by two overlap-extension PCRs using two pairs of partially complementary mutagenic primers, C2F2398Δ2b/C2R2770 and C2F2444/C2R2466 (Table 4.7). pFny209Cb7^{2b}Δ2bpro, a derivative of pFny209Cb7^{2b}, in which the Cb7-CMV-encoded 2b ORF is made non-coding by substitutions at nt 2422–2423 (GAA→TGA), and at nt 2471 (ATG→ACG), is constructed by two overlap-extension PCRs using two pairs of partially complementary mutagenic primers, C2F2398Δ2b/C2R2770, and Cb7Δ2bpro-F/Cb7Δ2bpro-R. All constructed plasmids are sequenced before use.

Table 4.7 Primers used for constructing mutant cDNA clones of RNA 2

Primers [*]	Primer sequence (5'-3') [†]	cDNA clone
Cb7 ^{2b} F	TCCAACAAACAGCGAAAAGAATT↑ATGGAATT GAACGCAGGCG (Fny-CMV RNA2 nt 2396–2418) (Cb7-CMV RNA2 nt 2414–2432)	pFny209Cb7 ^{2b}
Cb7 ^{2b} R	AGATGCGGAAGGGGAGGTT↑TCAAAACGCCCC TCCGC (Fny-CMV RNA2 nt 2752–2770) (Cb7-CMV RNA2 nt 2732–2749)	pFny209Cb7 ^{2b}
Rad35 ^{2b} F	TCCAACAAACAGCGAAAAGAATT↑ATGGAATT GAACGAAGGCG (Fny-CMV RNA2 nt 2396–2418) (Rad35-CMV RNA2 nt 2413–2431)	pFny209Rad35 ^{2b}
Rad35 ^{2b} R	AGATGCGGAAGGGGAGGTT↑TCAGAACGTACCT TCCGCC (Fny-CMV RNA2 nt 2752–2770) (Rad35-CMV RNA2 nt 2731–2748)	pFny209Rad35 ^{2b}
PGs ^{2b} F	TCCAACAAACAGCGAAAAGAATT↑ATGGAATT GAACGAGGCG (Fny-CMV RNA2 nt 2396–2418) (PGs-CMV RNA2 nt 2409–2427)	pFny209PGs ^{2b}

(To be continued)

(Table 4.7)

PGs ^{2b} R	AGATGCGGAAGGGGAGGTT↑TCAAAACACG	pFny209PGs ^{2b}
	CCCTCCGCC	
	(Fny-CMV RNA2 nt 2752–2770) (Rad35-CMV RNA2 nt 2723–2741)	
Primers *	Primer sequence (5'-3') [†]	cDNA clone
Na ^{2b} F	TCCAACAAACAGCGAAAGAATT↑ATGGAATT	pFny209Na ^{2b}
	GAGCGAAGGCG	
	(Fny-CMV RNA2 nt 2396–2418) (Na-CMV RNA2 nt 2414–2432)	
Na ^{2b} R	<i>AGATGCGGAAGGGGAGGTT↑TCAAAACGACCCT</i>	pFny209Na ^{2b}
	<i>TCCGCC</i>	
	(Fny-CMV RNA2 nt 2752–2770) (Na-CMV RNA2 nt 2732–2749)	
C2F1856	GGCTGAGTTTGCCTGGTGTATG	(Fny-CMV Multiple clones RNA2 nt 1856–1878)
C2R2420	ATAATCTTTCGCTGTTTGTGGGA	(Fny-CMV Multiple clones RNA2 nt 2397–2420)
C2F2749	TGAAACCTCCCCTTCCGCATCT	(Fny-CMV Multiple clones RNA2 nt 2749–2770)
C123R	AATT CTGCA GTGGTCTCCTTTTGGAGGCC	Multiple clones
	<i>PstI</i>	
	(Fny-CMV RNA2 nt 3032–3050)	
C2F2398Δ2aC81	TCCAACAAACAGCGAAAGTGATATG	pFny209Δ2a81
	(Fny-CMV RNA2 nt 2398–2421)	
C2RΔ2b	<i>AGATGCGGAAGGGGAGGTTTCA↑ATAATCTTTC</i>	pFny209Δ2b
	<i>GCTGTTTGTGGGA</i>	
	(Fny-CMV RNA2 nt 2749–2770) (Fny-CMV RNA2 nt 2397–2420)	
C2F2398Δ2b	CCAACAAACAGCGAAAGAATTATGTGATTG	pFny209Δ2bpro
	(Fny-CMV RNA2 nt 2398–2427)	
C2F2444	CAAACGTCGAACTCCAACCTGGCTCGTACGG	pFny209Δ2bpro
	(Fny-CMV RNA2 nt 2444–2473)	
C2R2466	AGCCAGTTGGAGTTTCGACGTTTGTTCGTTG	pFny209Δ2bpro
	(Fny-CMV RNA2 nt 2438–2466)	
Cb7Δ2bproF	GCAGCGACAAACGTCGAACTCCAACCTAGCTC	pFnyCb7 ^{2b} CMVΔ2bpro
	GTACGG	
	(Cb7-CMV RNA2 nt 2432–2468)	
Cb7Δ2bproR	GGAGTTCGACGTTTGTTCGCTGCGCCTGCGTT	FnyCb7 ^{2b} CMVΔ2bpro
	CAATCACAT	
	(Cb7-CMV RNA2 nt 2414–2453)	

* Primers C2R2770 and C2R2421Δ2a81 (not given) are completely complementary to C2F2749 and C2F2398Δ2a81, respectively;

† Primer sequences in italics are complementary to RNA 2, while those in Roman type correspond to RNA 1. Underlined nucleotides in six primers specify the mutations introduced into the three mutant cDNA clones; bold, in the primer C123R indicates the *PstI* site

The deletion of the 2b gene is performed by over-lapping PCR. The fragments I and II are amplified with two PCR primer pairs FnyΔ2bF1/FnyΔ2bR1, FnyΔ2bF2/FnyΔ2bR2, listed in Table 4.8, respectively. Two amplified fragments together are used as templates for a further amplification with the primer pair

Fny Δ 2bF1/Fny Δ 2bR2. The whole process of F209 Δ 2b construction is as shown in Fig. 4.14. The resultant fragment is digested with the *Bam*H I and *Pst* I and cloned into pF209 plasmid previously digested with the same enzymes. Colonies are subcultured and plasmids are isolated by standard procedures (Sambrook and Russell, 2001). The plasmid F209 Δ 2b is fully sequenced, to confirm the complete deletion of the 2b gene together with 41 amino acids from the C terminus of 2a protein.

Table 4.8

Gene	Primer pairs
Fny Δ 2b 1	Fny Δ 2bF1 ^a 5'-AATCGGATCCTAATACGACTCACTATAGTTTATTTACAAGAGCGTACGG-3' Fny Δ 2bR1 5'-AGATGCGGAAGGGGAGGTTTCAAATTCTTTCGCTGTTTGTGGA-3'
Fny Δ 2b 2	Fny Δ 2bF2 5'-TGAAACCTCCCCTTCCGCATCT-3' Fny Δ 2bR2 ^b 5'-AATTCTGCAGTGGTCTCCTTTTGGAGGCC-3'
satRNA	Sat F 5'-GTTTTGTTTGWTTGGAG-3' Sat R 5'-GGGTCCTGTAGAGGA-3'
18s rRNA	18s rRNAF1564 5'-TTCCTAGTAAGCGCGAGTCATCAGC-3' 18s rRNAR1630 5'-GCGACGGGCGGTGTGT-3'
CP gene	CP F 5'-GTGGGTGACGGTCCGTAA-3' CP R 5'-AGATGTGGGAATGCGTTGG-3'
satRs	satRsF F81 5'-GTAGCTGCATGGTGGTGGGAC-3' satRsRR210 5'-GCGGGGGCTCAAATGAAATG-3'

^a CCGATCC, *Bam*HI; TAATACGACTCACTATA, T7 promotor;

^b CTGCAG, *Pst*I

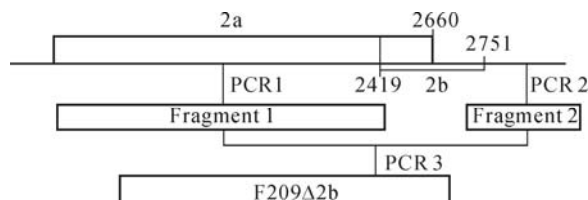


Fig. 4.14. Diagram of F209 Δ 2b construction strategy. PCR: polymerase chain reaction

Six chimeric DNA fragments containing the 2b gene are made between FCb7^{2b}-CMV and FRad35^{2b}-CMV through overlap-extension PCRs using three completely complementary primer pairs F2472/R2472, F2596/R2596 and F2681/R2681 at nucleotides 2472–2492, 2596–2606 and 2681–2701 of RNA 2, respectively (Table 4.9). These resulting fragments are digested with the restriction endonucleases *Pst*I and *Hind*III, and then cloned into pFny209 previously digested with the restriction endonucleases *Pst*I, *Eco*RI and *Hind*III, as described by Du et al. (2007), creating six RNA 2 constructs. PCR-based

site-directed mutagenesis (Higuchi et al., 1988) is performed to change each of the nucleotides at 2556, 2568, 2574 and 2582 of RNAs 2 of Fcb7^{2b}-CMV and FRad35^{2b}-CMV using mutagenetic oligonucleotides, creating four pairs of reciprocal mutants. In the same way, pFny209-2TGAs plasmid is constructed by substitutions at nt 2415–2417 (AAT→TGA) and at 2520–2522 (GGA→TGA) of pFny209 using the mutagenesis primer F209F2520 and the mutant Fny-CMV RNA 2 construct pFny209Δ2a81 described in this chapter. Both pF2C-1TGA and pF2C-2TGAs plasmids are derived from the plasmid pFny209Cb7^{2b} (Du et al., 2007). The former is made by changing nucleotide G at 2520 to T to generate a termination codon using a mutagenic primer Fcb7R2520, and the later is made by changing nucleotides AAT at 2415–2417 to TGA and nucleotide G at 2520 to T to generate two termination codons using the mutagenic primer Fcb7R2520 and the mutant Fny-CMV RNA 2 construct pFny209Δ2a81. All plasmid constructs should be sequenced prior to use.

Table 4.9 Primers used for constructing RNA 2 chimera and mutants of Fny-CMV

Primer	Primer sequence (5'-3')*	RNA 2 construct
F2472	GGTGGAGGCGAAGAGACAGAG	FCR2472
R2472	<i>CTCTGTCTCTTCGCCTCCACC</i>	FRC2472
F2596	GTAGATGGTTCGGAAGTATAGAGA	FCR2596
R2596	<i>TCTCTATCAGTTCGAAACCATCTAC</i>	FRC2596
F2681	CAGCGGAAGATGACCATGATT	FCR2681
R2681	<i>AATCATGGTCATCTTCCGCTG</i>	FRC2681
F2556T/2568G	GTCCCAGCGAGAGGGCGCG <u>T</u> TCAAATCT	FC/2a-T ²⁵⁵⁶
	CAG <u>G</u> CTG	FR/2a-G ²⁵⁶⁸
F2556C/2568A	GTCCCAGCGAGAGGGCGCG <u>C</u> TCAAATCT	FR/2a-C ²⁵⁵⁶
	CAG <u>A</u> CTG	FC/2a-A ²⁵⁶⁸
R2574C/2582T	<i>CGAACCATCTACTTGATAGAACGGT<u>A</u>GGAA</i>	FC/2a2b-C ²⁵⁷⁴
	<i>GCGG<u>A</u>AC</i>	FR/2b-T ²⁵⁸²
R2574A/2582C	<i>CGAACCATCTACTTGATAGAACGGT<u>G</u>GGAA</i>	FC/2b-C ²⁵⁸²
	<i>GCG<u>T</u>AAC</i>	FR/2a2b-A ²⁵⁷⁴
R2a2555	<i>CGCGCCCTCTCGCTGGGAC</i>	FC/2a-T ²⁵⁵⁶
		FR/2a-G ²⁵⁶⁸
		FR/2a-C ²⁵⁵⁶
		FC/2a-A ²⁵⁶⁸
F2b2583	ACCGTTCTATCAAGTAGATGGTTCG	FC/2a2b-C ²⁵⁷⁴
		FR/2b-T ²⁵⁸²
		FC/2b-C ²⁵⁸²
		FR/2a2b-A ²⁵⁷⁴
F209F2520	ACAGAATCGACG <u>T</u> GAAACGA	pFny-2a766
Fcb7F2520	GAAGAATCGACG <u>T</u> GAAACGA	pFcb7-2a766
		pFcb7-2a811

* Primer sequences in italics are complementary to RNA 2 while those in Roman type correspond to RNA 2. Underlined nucleotides in four primers specify the mutations introduced into the eight point mutants. Primer R2a2555 is completely complementary to 5'-end 19 nucleotides of F2556T/2568G or F2556C/2568A. Primer F2b2583 is completely complementary to 5'-end 25 nucleotides of R2574C/2582T or R2574A/2582C. Primers F209R2520 and Fcb7R2520 are completely complementary to the primers F209F2520 and Fcb7F2520, respectively

4.5.2 Plant Inoculation and Viral Progeny RNA Analysis

The viral RNA transcripts are quantified by agarose gel electrophoresis before inoculation and inoculated onto true leaves of test seedlings. These mock treated plants are inoculated with distilled water. Total RNA is extracted from CMV-inoculated plants or mock-inoculated plants using TRIzol reagent (Invitrogen, USA). Northern blot hybridization for viral progeny RNA analysis is performed using the protocol of Sambrook and Russell (2001). A CMV hybridization probe (probeI-40) is prepared by end-labeling a DNA oligonucleotide with γ -³²P-ATP using T4 polynucleotide kinase (Takara, Dalian), and this is used in the hybridization. The oligonucleotide sequence (5'-ACTGACCATT TTAGCCGTAAGCTGGATTGGACAACCCGTTTC-3') is completely complementary to a conserved sequence in the 3' end region of all genomic RNAs in all cucumoviruses (McGarvey et al., 1995). The virions of wild-type Fny-CMV and its intraspecies hybrids are purified from singly infected leaves of *N. glutinosa* plants at different times post-inoculation. Virion RNAs can also be extracted from the purified virions and analyzed by separation on a formaldehyde-containing agarose gel and by northern blot hybridization using the probeI-40 probe described above.

To obtain an infectious CMV with the addition of satellite RNA of this virus, full length RNA transcript of satRNA is obtained with T7 RNA polymerase (Promega, USA), and then co-inoculated with the infectious transcripts of plasmid pF109, pF209 and pF309. It is suggested to harvest and transmit the inoculated leaf area co-inoculated CMV genomic RNAs with satRNA to a larger amount of new plant seedlings when the infectious CMV-satRNA combination is to be used for more tests. The full-length satRNA transcript can also be mechanically inoculated onto a leaf part systemically infected with the helper virus in advance. Usually 4–7 dpi and more than one satRNA can be added into the genome of CMV, one by one or under mixed treatment. Seedlings of *Nicotiana* species are inoculated with Fny-CMV, Fny-CMV Δ 2b and other artificial recombinants at an equal concentration of their RNA transcripts. The systemic leaves (third from top leaf) are collected at 3 to 21 dpi, and total RNAs are extracted from equal weights of these collected leaves. The total RNAs are separated in a formaldehyde-containing agarose gel, and then blotted onto a nylon membrane (PALL). Accumulation of viral progeny RNAs of these viruses is analyzed by hybridization with the probe probeI-40 described above. The hybridized membrane is exposed to a storage phosphor screen (Molecular Dynamics, USA) for 4 hours, and the storage phosphor screen is scanned by a Typhoon 9200 (Amersham, USA).

Total RNA extraction and northern blot hybridization are carried out as described above. Hybridization signal intensities of viral RNAs in each RNA sample are calculated after normalization of loading quantities of these RNA samples against their 28S rRNA.

4.5.3 Quantifying the Accumulation of Viral RNAs in Leaf Tissue

The relative amount of CMV genomic RNAs and satRs in systemically infected tobacco seedlings is determined by a real time RT-PCR protocol used in our previous report (Feng et al., 2006). Total RNA is extracted from leaf tissues of CMV-inoculated plants or mock inoculated-plants, using TRIzol reagents (Invitrogen, USA). RNA integrity is electrophoretically verified by staining with ethidium bromide and judged by OD260/OD280 nm absorption. Total RNA (about 1 µg) is to be reverse transcribed with 100 U of Superscript II Plus RNase H-Reverse Transcriptase (Invitrogen, USA), using 100 µM random 6mers primers according to the manufacturer's instructions. All the real-time PCR primer pairs are used to assay the relative accumulation of each ORF for CMV and satRs according to the previous description in Chapter 2, and the real-time PCR reaction is to be performed with the PRISM[®]7000 (ABI, USA) or any equivalent. Relative quantization with data is performed according to the comparative C_t method ($2^{-\Delta C_t}$). The 18s ribosomal RNA extracted from the host plants is suggested as internal control.

References

- Ahlquist P, French R, Janda M, et al. (1984) Multicomponent RNA plant virus infection derived from cloned viral cDNA. *Proc Natl Acad Sci USA* 81(22): 7066-7070.
- Atreya CD and Pirone TP (1993) Mutational analysis of the helper component-proteinase gene of a potyvirus: effects of amino acid substitutions, deletions and gene replacement on virulence and aphid transmissibility. *Proc Natl Acad Sci USA* 90(24): 11919-11923.
- Brigneti G, Voinnet O, Li WX, et al. (1998) Viral pathogenicity determinants are suppressors of transgene silencing in *Nicotiana benthamiana*. *EMBO J* 17: 6739-6746.
- Chapman EJ, Prokhnovsky AI, Gopinath K, et al. (2004) Viral RNA silencing suppressors inhibit the microRNA pathway at an intermediate step. *Genes & Development* 18(10): 1179-1186.
- Collmer CW and Howell SH (1992) Role of satellite RNA in the expression of symptoms caused by plant viruses. *Annu Rev Phytopathol* 30: 419-442.
- Cronin S, Verchot J, Haldeman-Cahill R, et al. (1995) Long-distance movement factor: a transport function of the potyvirus helper component proteinase. *Plant Cell* 7(5): 549-559.
- Diaz-Pendon JA, Li F, Li WX, et al. (2007) Suppression of antiviral silencing by *Cucumber mosaic virus* 2b protein in Arabidopsis is associated with drastically reduced accumulation of three classes of viral small interfering RNAs. *Plant Cell* 19(6): 2053-2063.
- Ding SW, Anderson BJ, Haase HR and Symons RH (1994) New overlapping gene encoded by the *Cucumber mosaic virus* genome. *Virology* 198(2): 593-601.

- Ding SW, Li WX and Symons RH (1995) A novel naturally occurring hybrid gene encoded by a plant RNA virus facilitates long distance virus movement. *EMBO J* 14(23): 5762-5772.
- Ding SW, Shi BJ, Li WX, et al. (1996) An interspecies hybrid RNA virus is significantly more virulent than either parental virus. *PNAS* 93(15): 7470-7474.
- Diveki Z, Salanki K and Balazs E (2004) The necrotic pathotype of the *Cucumber mosaic virus* (CMV) ns strain is solely determined by amino acid 461 of the 1a protein. *Mol Plant Microbe Interact* 17(8): 837-845.
- Du ZY, Chen FF, Liao QS, et al. (2007) 2b ORFs encoded by subgroup IB strains of *Cucumber mosaic virus* induce differential virulence on *Nicotiana species*. *J Gen Virol* 88(Pt 9): 2596-2604.
- Feng JL, Chen SN, Tang XS, et al. (2006) Quantitative determination of *Cucumber mosaic virus* genome RNAs in virions by real-time reverse transcription-polymerase Chain reaction. *Acta Biochim Biophys Sin* 38(10): 669-676.
- Gal-On A, Canto T and Palukaitis P (2000) Characterisation of genetically modified *Cucumber mosaic virus* expressing histidine-tagged 1a and 2a proteins. *Arch Virol* 145(1): 37-50.
- Gal-On A, Kaplan I. and Palukaitis P (1995) Differential effects of satellite RNA on the accumulation of *Cucumber mosaic virus* RNAs and their encoded proteins in tobacco vs zucchini squash with two strains of CMV helper virus. *Virology* 208(1): 58-66.
- Gal-On A, Kaplan I, Roossinck MJ, et al. (1994) The kinetics of infection of zucchini squash by *Cucumber mosaic virus* indicate a function for RNA 1 in virus movement. *Virology* 205(1): 280-289.
- García-Arenal F and Palukaitis P (1999) Structure and functional relationships of satellite RNAs of *Cucumber mosaic virus*. In *Satellites and Defective Viral RNAs* (Vogt PK Jackson and AO, Eds.), Springer-Verlag, Berlin, pp: 37-63.
- Goto K, Kobori T, Kosaka Y, et al. (2007) Characterization of silencing suppressor 2b of *Cucumber mosaic virus* based on examination of its small RNA-binding abilities. *Plant Cell Physiol* 48(7): 1050-1060.
- Guo HS and Ding SW (2002) A viral protein inhibits the long range signaling activity of the gene silencing signal. *EMBO J* 21(3): 398-407.
- Higuchi R, Krummel B and Saiki RK (1988) A general method of in vitro preparation and specific mutagenesis of DNA fragments: study of protein and DNA interactions. *Nucleic Acids Res* 16(15): 7351-7367.
- Ji LH and Ding SW (2001) The suppressor of transgene RNA silencing encoded by *Cucumber mosaic virus* interferes with salicylic acid-mediated virus resistance. *Mol Plant Microbe Interact* 14(6): 715-724.
- Kong Q, Oh JW and Simon AE (1995) Symptom attenuation by a normally virulent satellite RNA of turnip crinkle virus is associated with the coat protein open reading frame. *Plant Cell* 7(10): 1625-1634.
- Kong Q, Wang J and Simon AE (1997) Satellite RNA-mediated resistance to *Turnip crinkle virus* in *Arabidopsis* involves a reduction in virus movement. *Plant Cell* 9(11): 2051-2063.
- Lewsey M, Robertson FC, Canto T, et al. (2007) Selective targeting of miRNA-regulated plant development by a viral counter-silencing protein. *Plant J* 50(2): 240-252.
- Li F and Ding SW (2006) Virus counterdefense: diverse strategies for evading the RNA-silencing immunity. *Annu Rev Microbiol* 60: 503-531.

- Li HW, Lucy AP, Guo HS, Li WX, et al. (1999) Strong host resistance targeted against a viral suppressor of the plant gene silencing defence mechanism. *EMBO J* 18(10): 2683-2691.
- Lucy AP, Guo HS, Li WX, et al. (2000) Suppression of post-transcriptional gene silencing by a plant viral protein localized in the nucleus. *EMBO J* 19: 1672-1680.
- Masuta C and Takanami Y (1989) Determination of sequence and structural requirements for pathogenicity of a *Cucumber mosaic virus* satellite RNA (Y-satRNA). *Plant Cell* 1(12): 1165-1173.
- Mayers CN, Palukaitis P and Carr JP (2000) Subcellular distribution analysis of the *Cucumber mosaic virus* 2b protein. *J Gen Virol* 81(Pt 1): 219-226.
- McGarvey P, Tousignant M, Geletka L, et al. (1995) The complete sequence of a *Cucumber mosaic virus* from Ixora that is deficient in the replication of satellite RNAs. *J Gen Virol* 76 (Pt 9): 2257-2270.
- Moriones E, Diaz I, Rodriguez-Cerezo E, et al. (1992) Differential interactions among strains of *Tomato aspermy virus* and satellite RNAs of *Cucumber mosaic virus*. *Virology* 186(2): 475-480.
- Palukaitis P (1988) Pathogenicity regulation by satellite RNAs of *Cucumber mosaic virus*: minor nucleotide sequence changes alter host responses. *Mol Plant Microbe Interact* 1(4): 175-181.
- Palukaitis P and Garcia-Arenal F (2003) Cucumoviruses. *Adv Virus Res* 62: 241-323.
- Palukaitis P and Roossinck MJ (1996) Spontaneous change of a benign satellite RNA of *Cucumber mosaic virus* to a pathogenic variant. *Nat Biotechnol* 14(10): 1264-1268.
- Praveen S, Mangrauthia SK, Singh P, et al. (2008) Behavior of RNAi suppressor protein 2b of *Cucumber mosaic virus* in planta in presence and absence of virus. *Virus Genes* 37(1): 96-102.
- Rizzo TM and Palukaitis P (1990) Construction of full-length cDNA clones of *Cucumber mosaic virus* RNAs 1, 2 and 3: generation of infectious RNA transcripts. *Mol Gen Genet* 222(2-3): 249-256.
- Roossinck MJ and Palukaitis P (1991) Differential replication in zucchini squash of a *Cucumber mosaic virus* satellite RNA maps to RNA 1 of the helper virus. *Virology* 181(1): 371-373.
- Roossinck MJ, Sleat D and Palukaitis P (1992) Satellite RNAs of plant viruses: structures and biological effects. *Microbiol Rev* 56(2): 265-279.
- Roth BM, Pruss GJ and Vance VB (2004) Plant viral suppressors of RNA silencing. *Virus Res* 102(1): 97-108.
- Sambrook J and Russell DW (2001) *Molecular Cloning: A Laboratory Manual*. Cold Spring Harbor Laboratory Press, Cold Spring Harbor, New York.
- Scholthof HB, Scholthof KB and Jackson AO (1995) Identification of *Tomato bushy stunt virus* host-specific symptom determinants by expression of individual genes from a potato virus X vector. *Plant Cell* 7(8): 1157-1172.
- Shi B, Miller J, Symons R, et al. (2003) The 2b protein of cucumoviruses has a role in promoting the cell-to-cell movement of pseudorecombinant viruses. *Mol Plant Microbe Interact* 16: 261-267.
- Shi BJ, Palukaitis P and Symons RH (2002) Differential virulence by strains of *Cucumber mosaic virus* is mediated by the 2b gene. *Mol Plant Microbe Interact* 15(9): 947-55.
- Shintaku MH, Zhang L and Palukaitis P (1992) A single amino acid substitution in the

- coat protein of *Cucumber mosaic virus* induces chlorosis in tobacco. *Plant Cell* 4(7): 751-757.
- Simon AE, Roossinck MJ and Havelda Z (2004) Plant virus satellite and defective interfering RNAs: new paradigms for a new century. *Annu Rev Phytopathol* 42: 415-437.
- Sleat DE and Palukaitis P (1992) A single nucleotide change within a plant virus satellite RNA alters the host specificity of disease induction. *The Plant Journal* 2(1): 43-49.
- Soards AJ, Murphy AM, Palukaitis P, et al. (2002) Virulence and differential local and systemic spread of *Cucumber mosaic virus* in tobacco are affected by the CMV 2b protein. *Mol Plant Microbe Interact* 15(7): 647-653.
- Soosaar JL, Burch-Smith TM and Dinesh-Kumar SP (2005) Mechanisms of plant resistance to viruses. *Nat Rev Microbiol* 3(10): 789-798.
- Suzuki M, Kuwata S, Masuta C, et al. (1995) Point mutations in the coat protein of *Cucumber mosaic virus* affect symptom expression and virion accumulation in tobacco. *J Gen Virol* 76 (Pt 7): 1791-1799.
- Szilassy D, Salanki K and Balazs E (1999) Stunting induced by *Cucumber mosaic cucumovirus*-infected *Nicotiana glutinosa* is determined by a single amino acid residue in the coat protein. *Mol Plant Microbe Interact* 12(12): 1105-1113.
- Voinnet O (2005) Induction and suppression of RNA silencing: insights from viral infections. *Nat Rev Genet* 6(3): 206-220.
- Wang Y, Gaba V, Yang J, et al. (2002) Characterization of synergy between *Cucumber mosaic virus* and Potyviruses in cucurbit hosts. *Phytopathology* 92(1): 51-58.
- Xin HW, Ji LH, Scott SW, et al. (1998) Ilarviruses encode a cucumovirus-like 2b gene that is absent in other genera within the bromoviridae. *J Virol* 72(8): 6956-6959.
- Zhang X, Yuan YR, Pei Y, et al. (2006). *Cucumber mosaic virus*-encoded 2b suppressor inhibits *Arabidopsis Argonaute1* cleavage activity to counter plant defense. *Genes Dev* 20(23): 3255-3268.

Plant MicroRNAs and Their Response to Infection of Plant Viruses

5.1 Introduction

In systemic infection, plant viruses bring disease symptoms that range from mild discoloration to severe developmental defects and death (Bazzini et al., 2007; Kasschau et al., 2003). In recent years, it has been demonstrated that small interfering RNAs (siRNAs) and microRNAs (miRNAs) play important roles in the process of host-pathogen interaction (Finnegan and Matzke, 2003; Voinnet, 2001). There is accumulating evidence that miRNAs function as an antiviral defense mechanism, therefore investigating the alteration of miRNAs expression profiles after virus infection provided a new insight into understanding the sophisticated virus-host plant interaction.

SiRNAs are generally derived from endogenous aberrant double-stranded RNAs (dsRNAs), or from exogenous agents such as viruses. They involve in post-transcriptional gene silencing (PTGS) and RNA-induced silencing complex (RISC) systems, to specifically detect and eliminate homologous dsRNAs and aberrant or mis-folded single-stranded RNAs (ssRNAs) (Chapman and Carrington, 2007). Therefore, siRNAs provide a natural defense against invasive nucleic acids, such as those produced during viral infection (Voinnet, 2005). However, many plant viruses have evolved a counter-defensive strategy in which viral proteins, referred to as PTGS suppressors, target different steps of the PTGS pathway, resulting in increased virus replication (Vance and Vaucheret, 2001).

MiRNAs are a group of naturally occurring, single-stranded non-coding RNAs of 19–25 nt that serve as post-transcriptional negative regulators of gene expression in both plants and animals, and a majority of them are found to be evolutionarily conserved (Carrington and Ambros, 2003). In plants, miRNA genes are transcribed by RNA polymerase II from independent transcriptional units, then processed by Dicer-like 1 (DCL1), hyponastic leaves 1 (HYL1), serrate (SE) proteins and HUA enhancer 1 (HEN1), to finally yield the mature miRNAs (Chen, 2005; Kurihara and Watanabe, 2004; Park et al., 2005; Zhang et al., 2006). Like siRNAs, most

plant miRNAs are also loaded into the RISC, target endogenous plant transcripts for degradation or translational repression in a sequence-specific manner. Thus, miRNAs play vital roles in regulating plant development, such as the formation of embryos, roots, vasculature and floral tissue, asymmetric cell division, signal transduction and environmental stress responses (Schwab et al., 2005).

To date, a total of 1,389 plant miRNAs across 20 species have been discovered and are deposited in Sanger miRNA Registry Database (<http://microrna.sanger.ac.uk>, Release 13.0; March 2009). However, most of them are identified only from species such as *Arabidopsis thaliana* (thale cress), *Oryza sativa* (Rice), *Sorghum bicolor* (Sorghum), *Zea mays* (Maize), *Glycine max* (Soybean), *Medicago truncatula* (beans) and *Saccharum officinarum* (sugarcane), the full-genome of which have been sequenced. Tomato (*Lycopersicon esculentum* L.) is a vegetable crop of significant economic importance worldwide. Nevertheless, only 26% of the genome has been sequenced, thus little is known about the experimental or computational identification of miRNAs in tomato, and even less is known about their target genes.

With a number of tomato miRNAs and some of their targets predicted computationally, the images showing the existence of tomato miRNAs are validated and identified by microarray for a general understanding. Based on such a general image of tomato miRNAs and their response to the infection of strains of CMV and other viruses, methods of quick determination for particularly interesting miRNAs and their targets are set up, to investigate their expression alterations after various virus infections are introduced below. Utilizing stem looped RT-PCR, the interference of CMV 2b protein and alleviated/aggravated satellite RNA on the host miRNA pathway are discussed. Different mechanisms of tomato miRNA response to the infection by CMV, TAV and ToMV are analyzed. The results presented here represent the most comprehensive investigation of the tomato miRNA on a genome scale thus far and provide much needed information for further study of the interaction between virus and host plants.

It could be highly supposed that the utilization of a high-thought identification method will provide new insight into recognizing virus infection in hosts, especially the explanation at a molecular level of the physiological or pathological phenomenon in plants. On the other hand, using plant viruses as stressing facets, understanding the realities and mechanisms of miRNA could be further achieved in different ways.

More miRNAs are found to be over expressed under infection by plant strains of and also a strain of ToMV, than those down regulated ones. It could be calculated that miRNA involvement in virus-plant interaction is found to be a complex and important response of the host. To survive infection by viruses and many other pathogens, host plants should have developed their multi-step defense system. The initiation of the expression of many miRNAs could be regarded as a general calling-up of many regulating genes, against the invading viruses. The high accumulation/expression of certain miRNAs could be regarded as the need to regulate/control those highly-transcribed target mRNAs, or the need to stop the function of their target gene which is involved in controlling some other genes, which again are required in antiviral activities.

Since plants have a hypersensitive response (HR), gene silencing at the transcription stage (GTR), post transcriptional gene regulation (PTGS) and many other antiviral-responses, and while viruses have developed gene silencing suppressors and other possible mechanisms, a general description of the mechanism for miRNA involvement has, nevertheless, not yet been described.

The general image of virus-host plant interaction described in the diagram might be not complete or correct in all cases, but the discovery of miRNA involvement in virus infection response will bring a broader understanding of the plant defense system.

5.2 Methodology

We introduce methodology used in this chapter.

5.2.1 Computational Prediction of miRNAs and Their Target Genes for Plant Species with Known Genome Sequences

- **miRNA Reference Set, Tomato EST, GSS, CoreNucleotide BACs and mRNA Sequences**

Taking the tomato (*Solanum lycopersicum* Mill.) as an example, to search potential tomato miRNAs, most of the total (about 900) miRNAs precursor sequences and their mature sequences previously described from *A. thaliana* and other plant species can be downloaded from the open miRNA Registry Database (<http://miRNA.sanger.ac.uk>). These miRNAs can be defined as a reference set. The repeat mature miRNA sequences should be removed and the remaining sequences (about 300) be kept, and thus they can be used as query sequences for BLAST search and for designing microarray probes. To search miRNA precursors, tomato nucleotide sequences can be downloaded from the NIH GenBank nucleotide databases (a total of about 600,000, including those in CoreNucleotide, EST and GSS). Additionally, BACs sequences can be obtained from ITSP sequencing data (ftp://ftp.sgn.cornell.edu/tomato_genome/). The genomes of several plant species and models are under sequencing, with more and more sequence data up-and-coming almost every month.

- **Prediction of miRNAs and Their Precursors**

The procedure described in (Xie et al., 2007; Zhang et al., 2006), modified for predicting potential tomato miRNAs, could be used as the general strategy (Fig. 5.1). To obtain the hits for sequences with a perfect match against known miRNAs, previously reported tomato sequences (CoreNucleotide, GSS, EST and BACs

sequences) need to be searched with all known non-redundant mature miRNA sequences identified or predicted from other plants. The repeat sequences, and those coding proteins, are then removed from the hit sequence. BLAST 2.2 (<ftp://ftp.ncbi.nih.gov/blast/>) and BLASTX (<http://www.ncbi.nlm.nih.gov/BLAST/>) can be used for the sequence search. The secondary structures of candidate sequences can be predicted using the web-based software Mfold 3.2 (<http://frontend.bioinfo.rpi.edu/applications/mfold/cgi-bin/ma-form1.cgi>). The candidate potential pre-miRNAs should meet all of the following criteria: a) The secondary structure of the candidate sequences should have the stem-loop structure and no loop or break in the mature miRNA sequences; b) miRNA should have less than six mismatches with the opposite miRNA* sequences; c) The mature miRNA and miRNA* site must be in one arm of the stem-loop structure; d) The candidate pre-miRNA sequence should have 30%–75% A+U contents; e) The predicted stem-loop candidates should have higher MFEIs and negative MFEs.

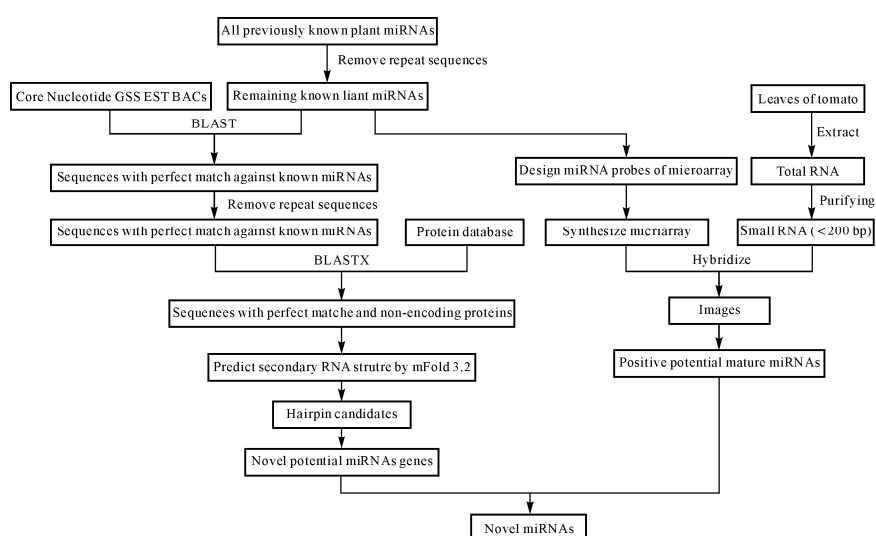


Fig. 5.1. Procedure for identifying potential plant miRNAs using homolog search compared with previously known plant species

• Prediction of miRNA Targets

Previous studies have proved that all miRNAs fulfill the function of post-transcriptional gene regulation by binding to the target mRNA sequences in one or more perfect, or near-perfect, complementary site(s), bringing convenience in predicting plant miRNA targets simply using a gene-homology search. The newly-identified miRNA can be used to search through their potential targets against the protein-coding nucleotide database from the GenBank with BLASTn. The number of allowed mismatches at complementary sites between miRNA sequences and potential mRNA targets is four or fewer, and no gaps can be allocated at the complementary sites.

5.2.2 Use Plant miRNA Microarrays to Identify Conservative miRNAs from New Host Plants

Based on the conservative characterization of plant miRNAs, those reported from other plant species by miRNA cloning and computational prediction can be used as probes to detect and identify uncovered miRNAs from new plant species, where the genomic sequencing information is limited. By controlling the detection signal, those who have positive hybridizations should be certain of the existence of particular miRNAs even though those who have negative or insignificant hybridizations could also possibly show the existence of miRNAs. As shown in Fig. 5.2, one single mismatch in the middle of miRNA probes can induce a completely negative hybridization result, but one to two mismatches at the terminal of miRNA probes can still bring positive hybridization results, but with quite reduced strength.

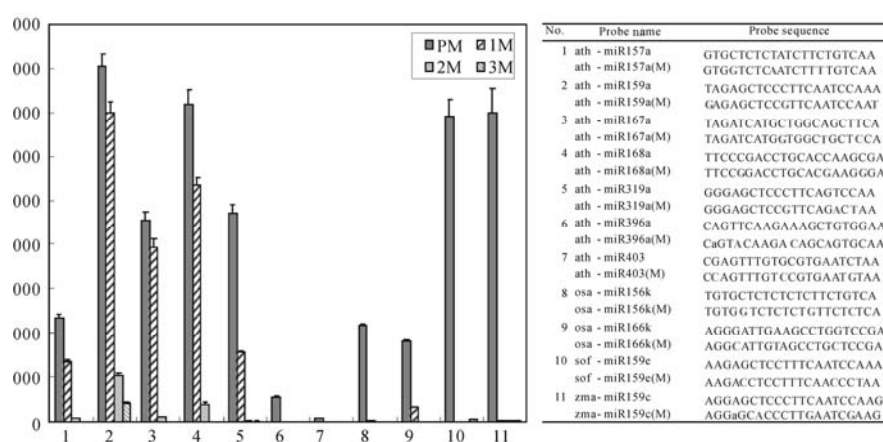


Fig. 5.2. Effect of mismatch numbers within microarray probes on signal intensity. Signals from hybridization from plant tissues with Cy5 labeling are presented. Each miRNA probes set contain perfect match (PM) probe, one mismatch (1M) probe, two mismatch (2M) probes, three mismatch (3M) probes. Data are presented as Median signal intensity plus standard deviation for 4 replicates of probes. Bold letter: the first mutated nucleotide; Bold letter with underline: the second mutated nucleotide; Bold italic letter with underline: the third mutated nucleotide. Mismatch results showed the reliability of positive hybridizations

• Design of Plant miRNA Microarray

In situ synthesis microfluidic chip (e.g. μ Paraflo™ microarray Atactic Inc., USA) or similar nuclei acid chips are recommended. μ Paraflo™ miRNA microarray contains 3,968 isolated reaction sites in a 1.4 cm² area and the total solution volume of the chip is 9.6 L. The probes synthesized consist of natural DNA and modified nucleotide residues to provide enhanced sensitivity for detecting miRNA sequences of low abundance. The miRNA and miRNA* sequences were extracted

from the miRbase Database, containing miRNAs and miRNAs*, including those from plant species such as *A. thaliana*, rice, sorghum, maize, soybean, *M. truncatula* and sugarcane. Except that a lot of small noncoding RNAs (sncRNAs) including U1 and U6, tRNA and ribosomal RNA sequences of these seven species and other species can be put as internal controls. Each probe was chemically modified to obtain a nearest neighbor hybridization melting temperature. A set of spiking-in RNAs is synthesized to control the chip quality. Each probe is triplicate or quadruplicate in one chip. Presently μ Paraflo™ plant miRNA microarray is commercially available (LC Sciences, Hangzhou, China).

- **Examination of miRNA Microarray**

The microarray experimental design should be a treatment-control comparison with six or more plants per group. At each time point, two microarray experiments with color reversal needed to be performed. For example, when plant virus inoculation is applied to a plant host, each independent experiment should use at least twelve plants (e.g. six virus-inoculated plants and six control plants). A total of eight to twelve hybridizations are to be performed.

Most commercialized microarrays have their own experimental system. Taking μ Paraflo™ miRNA microarray as an example, the microarray assays can be performed using a service provider (LC Sciences, Hangzhou, China, or others), or using a micro fluid hybridization station (see below). The assay can start with a 2 to 5 μ g total RNA sample, which was size-fractionated using a YM-100 microcon centrifugal filter (Millipore) and the small isolated RNAs (<300 nt) are 3'-extended with a poly(A) tail using poly(A) polymerase. An oligonucleotide tag is then ligated to the poly (A) tail for later fluorescent dye staining. Two different tags are to be used for the two RNA samples in dual-sample experiments. Hybridization is to be performed overnight on a μ Paraflo microfluidic chip using a micro-circulation pump (Atactic Technologies, USA). The pooled probe used for hybridization contains probes for over one hundred mature miRNAs and miRNA* with multiple controls including other small RNA (rRNA, tRNA, sncRNA and synthetic species) and the oligonucleotide miRNA probes with mutations. The detection probes should make three or four replications by *in situ* synthesis using photogenerated reagent (PGR) chemistry. The hybridization melting temperatures are balanced by chemical modifications to the detection probes. Hybridization was carried out using 100 μ l 6xSSPE buffer (0.90 mol/L NaCl, 60 mol/L Na₂HPO₄, 6 mol/L EDTA, pH 6.8) containing 25% formamide at 34°C. After hybridization, detection uses fluorescence labeling using tag-specific Cy3 and Cy5 dyes. Hybridization images are collected using a laser scanner (GenePix 4000B, Molecular Device, USA) and digitized using Array-Pro image analysis software (Media Cybernetics, USA). Data can be analyzed by first subtracting the background and then normalizing the signals using a LOWESS filter (Locally weighted Regression). The reported detected signals should meet with two criteria: greater than the background value plus 3x the background standard deviation and spot co-variance ($CV = \text{stdev} \times 100/\text{intensity}$) less than 50%. The mean and the spot to spot CV ($CV = \text{stdev} \times$

100/replicate mean) of each probe having a detected signal are calculated, and those having a CV less than 50% will be used in further analyses. Generation of comparison data sets from detectable signals include \log_2 transformation, gene centering and normalization. Hierarchical clustering is to be performed by average linkage and Euclidean distance metric. Differentially-expressed genes with a cutoff of 0.05 p -values are further analyzed by the ANOVA model.

- **Confirmation of miRNAs by Northern Blotting and Target mRNA by 3'-RACE (Rapid Amplification of cDNA Ends)**

Conventional northern blotting can be applied to confirm the expression of miRNAs from tissues of root, stem and leaf, but with some difficulties, since miRNAs are not always rich in total RNAs and they are not very stable. The 3'-RACE method can also be used to clone the target mRNAs as a kind of standard measurement.

5.2.3 Use Plant miRNA Microarrays to Identify Conservative miRNAs Response to Virus Infection

As a kind of stressing factor, a plant virus can obviously alter the miRNA expression in plant tissues. Consequently a test, qualitatively or quantitatively, of miRNA accumulation under certain conditions can be thus analyzed, by which means the reality of plant miRNAs can be further recognized. At the same time, examining the change in host miRNAs with regard to their target genes can help us to understand the mechanisms of virus-host interactions. Various aspects need to be considered regarding the above measurements. First of all, more attention should be paid to the divergences of individuals, such as plant and tissue origin. A necessary number of controls and repeats can be utilized to avoid such trouble.

- **Plant Seedlings, Virus Inoculation and RNA Extraction**

Seedling growth and virus inoculation are about the same as mentioned above (see Chapter 2). Crop varieties which are sensitive to virus infection and mechanically transmittable viruses are recommended. Viral strains producing obviously different symptoms can be used, and single or complex infection can both be used for such a challenge. RNA transcripts obtained from infectious clones are recommended for the above assay, especially for quantitative analysis such as microarray hybridization, real-time RT-PCR or northern blotting. For example, when miRNAs in tomato seedlings of healthy control and CMV inoculation are tested, the experiment design is a treatment-control comparison with six plants per group. At each time point, two microarray experiments with color reversal should be performed, each independent experiment using twelve plants (six CMV-inoculated plants and six control plants). A total of six to eight hybridizations are performed.

Tomato seedlings (cv. Hezuo903 or other varieties sensitive to CMV infection) are grown in a growth chamber at 21–26°C, with a 14 h light and 10 h darkness cycle or similar conditions. Seedlings of 6- to 8-true-leaf stage can be used for microarray detection and the 5th to 7th leaves are sampled. Total RNAs are extracted using TriZol reagent according to the producer's construction and small RNAs (<200 nt) can be size-fractionated by utilizing mirVana kit (Ambion, USA), while 0.2 g of fresh leaf tissue are used for each test.

Virus isolates generated from infectious RNA can be maintained on systemic hosts such as *Nicotiana tabacum*, and transferred 7–10 d before mechanically inoculating the first true leaves of 10 d old tomato seedlings. At 35 dpi, the upper systemical leaves of virus-inoculated plants or mock are harvested from pools of 12 to 18 plants. Total RNA can be extracted from leaf tissues using TRIzol reagent (Invitrogen, Carlsbad, USA), followed by RNase-free DNase treatment (Takara, Dalian, China). Small RNAs, less than 200 nt, are thus isolated using mirVana miRNA kits (Ambion, Austin, USA). Their concentrations are quantified by absorbance at 260 nm.

5.2.4 Quantitative Determination of miRNAs by Stem-loop Real-time RT-PCR

- **PCR Amplification of miRNAs Targets**

Up to date, just a few miRNA targets of plant species have been reported on a public database. To amplify mRNA sequences, full or partial sequences of miRNA are necessary. Using tomato genes, ARF8 and AGO1, a target of miR167 and miR168 respectively as examples, a conventional method is used by rapid amplifying of cDNA 3' ends (3'-RACE). Total RNA is firstly isolated from about 3g of fresh leaf tissues, and then poly (A)⁺mRNA is prepared with an *Oligotex*TM-dT30 <Super> mRNA Purification Kit (Takara, Dalian, China). The oligo (dT)₁₅ is used to primer cDNA synthesis with reverse transcriptase. This cDNA can then be subject to a first round of amplification procedure with the 3'-RACE out primer (5'-GTTTTCCAGTCACGACTTTTTTTTTTTTTTTTTT-3') and the gene-specific out primers, ARF8: 5'-ATGTGTTGGGAGGTCAGTGGGA-3' and AGO1: 5'-WGCTCATTAYCAYGTTYTKTGGG-3'. For the second round, 3'-RACE inner primer (5'-GTTTTCCAGTCACGAC-3') is used with the second set of gene-specific inner primers, ARF8: 5'-GGGGCAGATGTTTCGGTATTG-3' and AGO1: 5'-CACTTGTKCCCCCTGCWTATTA-3'. All of the gene-specific primers should be designed based on the homologous sequences, here of defined ARF8 or AGO1 genes in *Arabidopsis*, *Nicotiana* and *Solanum*. In each case, a unique gene-specific DNA fragment can thus been amplified. The PCR products are then gel purified, cloned to pMD18-T vector (TaKaRa, Dalian, China), transformed into competent cells of *Escherichia coli* DH5α, and three to five independent clones should be selected from each amplicon for DNA sequencing.

- **Primer Design for Real-time RT PCR**

For quantitative determination of miRNAs and to investigate the effects of virus infection on the expression of miRNAs and their target mRNAs, real-time RT-PCR is a kind of optional choice to present techniques. Because of their short size (20–29 nt) for mature miRNAs, stem-loop RT primers should be used. Gene-specific primers are to be designed using Primer Express version 2.0 (Applied Biosystems, USA). The mature miRNAs sequences can be downloaded from the miRNA Registry database (<http://miRNA.sanger.ac.uk>) and from previous publications (Zhang et al., 2008). Their stem-loop RT primers, forward primers and reverse primers can be designed according to the criteria mentioned by Chen et al. (2005) and Tang et al. (2006). For target mRNAs, the conventional gene-specific forward and reverse primers are easily designed, based on sequences obtained from clone (AGO1 and ARF8), or from public database (MYB and SCL). Primers should be validated using gel electrophoresis of PCR amplicons, and by the presence of one peak on the thermal dissociation curve generated by the thermal denaturing protocol, which followed each real-time PCR run. Beside this, the sequences of the miRNA amplicons should be further determined by subcloning the PCR product into TA cloning vectors (Takara, Dalian, China) according to the manufacture's protocols. Primers used for some miRNAs and their targets are given in Table 5.1 and Table 5.2, respectively.

- **Real-time Quantitative RT-PCR**

Firstly, the total RNA from 0.1 g of fresh tomato leaves is reversely transcribed to cDNA using stem-loop RT primers for miRNAs, or reverse primers for their target mRNAs. A 1 $\mu\text{mol/L}$ aliquot of DNase-treated total RNA is inoculated with 1 μl of a cocktail containing 10 $\mu\text{mol/L}$ of each gene-specific primer for miRNA or target mRNAs. The reaction is heated to 80°C for 5 min to denature the RNA, and then inoculate for 5 min at 60°C to anneal the primers. The reaction is cooled to room temperature and the remaining reagents (5 \times buffer, dNTPs, RNase inhibitor, M-MLV) are to be added according to the protocol and the reaction proceeds for 30 min at 16°C, followed by 60 cycles at 20°C for 30 s, 42°C for 30 s, 50°C for 1s, and finally 5 min at 85°C to inactivate the reverse transcriptase. The minus reverse transcription controls for each gene are treated identically as described above, except that the reaction is lacking the RNA targets. Then, the SYBR Green PCR is performed using protocols on an Applied Biosystem's 7,300 sequence Detection System. Briefly, 2.5 μl of cDNA template is added to 12.5 μl of the 2 \times SYBR green PCR master mix (Takara), 800 nmol/L of each primer and ddH₂O to 25 μl . The reactions are amplified for 10 s at 95°C, followed by 40 cycles at 95°C for 10 s and 60°C for 30 s. All reactions are run in triplicate, and the no template/no reverse transcription controls are included for each gene. The threshold cycle (C_T) values are determined automatically by the machine, and the fold changes of each gene are calculated using the equation $2^{-\Delta\Delta C_T}$, where $\Delta\Delta C_T = (C_{T \text{ target}} - C_{T \text{ 18S rRNA}})_{\text{SampleX}} - (C_{T \text{ target}} - C_{T \text{ 18S rRNA}})_{\text{Sample1}}$.

Table 5.1 Primers of some miRNAs used for stem-loop Realtime PCR

miRNA ID	Primer	Sequences
miR159	RT	GCGTGGTCCCGACCACCACAGCCGCCACGACCACG CTAGAGC
	Forward primer	CGTGCGTTTGGATTGAAGG
miR162	Reverse primer	TCCCGACCACCACAGCC
	RT	GCGTGGTCCCGCAGCACCTCAGCCGCCACGACCACG CCTGGATGC
miR164	Forward primer	CGCAGCGTCGATAAACCTCT
	Reverse primer	TCCGCAGCACCTCAGCC
miR165/166	RT	GCGTGGTCCACACCAGTTGACGGGCGACGACCAC GCTGCACG
	Forward primer	CACGATGGAGAAGCAGGGC
miR167	Reverse primer	CCACACCAGTTGACGGGC
	RT	CTCAGCGGCTGTCGTGGACTGCGCGCTGCCGCTGA GGGGGRATG
miR168	Forward primer	CTGTGTCGGACCAGGCTTC
	Reverse primer	GGCTGTCGTGGACTGCG
miR171	RT	GCGTGGTCCACACCACCTGAGCCGCCACGACCACG CTAGATCAT
	Forward primer	CGTGCGTGAAGCTGCCA
miR171	Reverse primer	TCCACACCACCTGAGCCG
	RT	CTCAGCGGCTGTCGTGGACTGGGTGCTGCCGCTGA GTTCCCGAC
miR171	Forward primer	CGTGTGTCGCTTGGTGCA
	Reverse primer	GGCTGTCGTGGACTGGGTG
miR171	RT	GCGTGGTCCACACCACCTGAGCCGCCACGACCACG CGATATTGG
	Forward primer	CGTGCGTGATTGAGCCGT
miR171	Reverse primer	TCCACACCACCTGAGCCG

Table 5.2 Realtime RT-PCR primers of target mRNAs for some miRNAs

mRNA	Primer	Sequences
MYB	Forward primer	TATTGAGATGCGGAAAGAGTTGC
	Reverse primer	ATCTGTTCTCCTGGTAATCTTGC
ARF8	Forward primer	TGGGAAAGGAAGAGGGCTGAA
	Reverse primer	GCGATCCAAGAGATGGCATT
AGO1-1	Forward primer	TGGATCAGTAACAAGCGGAGC
	Reverse primer	TTGAGAGCAGGAAGAGGTCTAACAG
AGO1-2	Forward primer	ATGGAACCAGAGACATCTGACGG
	Reverse primer	CCTTACAGCAGCACCAACACC
SCL	Forward primer	GATGGAGCTATGTTGTTGGGATG
	Reverse primer	CCACCAGGCTGTCCTTTCG

- **Calculation of PCR Efficiency**

PCR efficiency can be calculated as previously described (Feng et al., 2008) from the equation $E = 10^{-1/\text{slope}} - 1$. To experimentally determine PCR efficiency, 10-fold dilutions of RNA are diluted over 6-logs. The diluted RNA is amplified by real-time PCR using identical conditions established for gene expression analysis.

Plots are made of the log of the total RNA input versus the C_T values and the PCR efficiency is calculated from the slope of the line, using the equation described above. The actual concentration of the miRNA or mRNA template is not needed when determining the efficiency as it only depends on the slope of the line. The efficiency and range of detection for both miRNA and their targets are obtained and given in Table 5.3 and Table 5.4.

Table 5.3 Efficiency and range of stem-loop PCR for detecting seven miRNAs

miR	Avg. slope	Std. dev. slope	r^2	Avg. eff. (%)	Tm of amplicons (°C)	Range
miR159	-2.8143	0.463672	0.9864	126.6356	84.1	5
miR162	-3.0045	0.276223	0.9953	115.1959	85.5	7
miR164	-3.1715	0.223573	0.9993	106.6846	84.9	6
miR165/166	-2.9403	0.573949	0.9951	118.8272	84.6	6
miR167	-2.845	0.300743	0.9973	124.6435	84.3	6
miR168	-2.9968	0.369715	0.9976	115.6201	84.9	6
miR171	-2.9659	0.503369	0.9936	117.3531	84.3	6

Table 5.4 Efficiency and range of Realtime RT-PCR for detecting five miRNA targets

mRNA	Avg. slope	Std. dev. slope	r^2	Avg. eff. (%)	Tm of amplicons (°C)	Range
MYB	-2.6327	0.198001	0.9988	139.7939	79.4	6
ARF8	-3.3657	0.178519	0.9992	98.20519	83.1	5
AGO1-1	-3.0053	0.530545	0.997	115.152	86.0	5
AGO1-2	-3.0761	0.159519	0.9979	111.3912	86.3	6
SCL	-3.0707	0.299225	0.9978	111.6697	81.3	5

5.2.5 Design of Plant miRNA-array and Data Analysis

This study is to confirm the prediction work based on conservation and to detect other miRNAs expressed in tomato leaf tissue. A total of 294 non-redundant mature miRNA sequences from other species were used as microarray probes and each probe was repeated four times in one chip (CIBEX, Accession Number CBX55). The *in situ* synthesis miRNA microarray was customly synthesized by LC Sciences (Houston, Texan, USA), and strictly followed by their protocols (Gao et al., 2004). Poly-A tails were added to the small RNAs prepared above at the 3' ends using a poly(A) polymerase, and Cy3 gain was then ligated to the poly-A tails. The tagged RNAs were hybridized to the microfluidic hybridization chip. Hybridization images were scanned, using a GenePix 4000B microarray scanner (Molecular Devices, Sunnyvale, USA) at 445 nm. Data extraction and image processing were performed using ArrayPro™ image analysis software (Media Cybernetics, Silver Spring, USA). The maximum signal level of background

probes was set at 99.48. Normalization was performed by the LOWESS method to remove system-related variations. A miRNA detection signal threshold was defined as the maximum background signal plus three times background standard deviation, and a strong positive miRNA detection signal threshold was defined as 1,000 after normalization, approximately 1/13 of an expression level of 5S rRNA in leaf tissue.

5.2.6 Confirmation of miRNAs by Northern Blotting and Target mRNA by 3'-RACE

Northern blotting was applied to confirm the expression of several miRNAs from the tissues of root, stem and leaf simultaneously, and the 3'-RACE was used to clone a target mRNA. Conventional methods were utilized in both assays.

5.3 Tomato miRNAs Predicted from Known Genomic Sequences and Discovered by miRNA Microarray

Ever since the discovery of *lin-4*, which was determined to control the developmental timing in *Caenorhabditis elegans* (Lee et al., 1993), a rapidly-increasing number of miRNAs have been identified from extending species, including animals, plants and even viruses (<http://microrna.sanger.ac.uk/sequences/>). Increasing evidence suggests that plant miRNAs play vital roles in multiple essential biological processes, such as leaf morphogenesis and polarity (Palatnik et al., 2003), floral organ identity (Aukerman and Sakai, 2003; Chen, 2004), phase changes from vegetative growth to generative growth (Aukerman and Sakai, 2003; Chen, 2004), stress responses such as plant hormone (Mallory et al., 2005), virus stress (Kasschau et al., 2003), mineral nutrient and dehydration stress (Sunkar and Zhu, 2004).

Although over one thousand miRNAs have been identified from 9 plant species, only limited information has been obtained for the existence and function of miRNAs from the tomato (*Solanum lycopersicum* Mill.), which is an important model *Solanaceae* crop for floral development and fruit ripeness studies, even though some work has been done on this crop recently (Zhang et al., 2006; Itaya et al., 2008; Ori et al., 2007; Pilcher et al., 2007; Zhang et al., 2008). To date, over 150,000 tomato ESTs have been established in the tomato expression database. In addition, more than 28% of tomato genome sequencing from TIGR has been completed. The above conditions permit the predication of tomato miRNA by computational methods.

The conservative properties of miRNAs across kingdoms permit the prediction of their existence in unstudied species, by using themselves as detecting probes, even though special miRNAs should not be detected in this way. Using an

miRNA-detecting microarray with probes complementary to all the documented plant miRNAs, the predicted or unpredictable miRNAs could be detected from tomato tissues. The general image of tomato miRNA profiles will provide an imperative platform for investigating the mechanism response to virus infection.

5.3.1 Potential Tomato miRNAs Predicted Computationally According to Known Genomic Sequences

Fourteen tomato sequences with a perfect match with known plant miRNAs have been obtained from over 578,000 tomato sequences and all of the 14 sequences contained a non-repeat and non-protein-coding sequence. Based on the biogenesis criteria, only 12 miRNA candidates were retained, distributing in nine miRNA families, miR157, miR159, miR162, miR167, miR171, miR172, miR319, miR395 and miR399 (Table 5.5). Amongst these, four miRNAs were obtained from the GSS database, one miRNA from the ITSP BACs database and others were found from the EST database. All of the 12 miRNA candidates showed perfect stem-loop secondary structures simulated by mfold (Fig. 5.3). When we focused on confirming the potential tomato miRNAs, mature miRNAs and their precursors of miR319, miR171 and miR162 were firstly publicized by Ori et al. (2007), Pilcher et al. (2007) and Itaya et al. (2008). In addition, the mature miRNAs of miR159, miR162, miR166 and miR167 were cloned by *Pilcher's and Itaya's* group just recently (2007; 2008), but no information about their precursors was reported. This proved that our discovery could be validated by other methods. The only miRNA candidate not fitting the biogenesis criteria was a GSS sequence (gi: 84293419), which had a homology site to the mature miRNA (5'-UGACAGAAGAGAGAGACACA-3') in miR156 family but with an extra loop in the arm of the stem-loop secondary structure of the potential pre-miRNA.

Table 5.5 Tomato miRNAs predicted from known sequences of the genome.

miRNA	Sequence (5'-3')	Gene ID	Gene source	LM (nt)	LP (nt)	Side	A+U (%)	MFEs	MFEIs
miR157a	UUGACAGAAGAU AGAGAGCAC	117704089	EST	21	100	5'	64.00	43.40	1.21
miR157b	UUGACAGAAGAU AGAGAGCAC	84273338	GSS	21	84	5'	60.71	39.10	1.18
miR157c	UUGACAGAAGAU AGAGAGCAC	84236627	GSS	21	83	5'	61.45	40.20	1.26
miR159	UUUGGAUUGAAG GGAGCUCUA	116645971	EST	21	178	3'	62.92	73.60	1.12
miR162	UCGAUAAACCUC UGCAUCCAG	72276781	GSS	21	98	3'	53.06	33.70	0.73
miR167	UGAAGCUGCCAG CAUGAUCUA	117695324	EST	21	73	5'	64.38	27.30	1.05
miR172a	AGAAUCUUGAUG AUGCUGCAU	117691535	EST	21	106	3'	66.04	39.80	1.11
		4380108	EST					39.80	1.11
miR172b	AGAAUCUUGAUG AUGCUGCAU	72400226	GSS	21	135	3'	72.59	47.50	1.28
miR319	CUUGGACUGAAG GGAGCUCC	121822560	CoreNuc	20	169	3'	52.07	80.70	1.00
miR395	CUGAAGUGUUUG GGGGAACUC	118918463	CoreNuc	21	71	3'	52.11	33.50	0.99
miR399	UGCCAAAGGAGA GUUGCCCUA	117723706	EST	21	71	3'	57.75	33.40	1.11
miR171	UGAUUGAGCCGU GCCAAUAUC	C02HBa00 60J03.1	BACs	21	92	3'	60.04	36.00	0.98

Conserved miRNAs were predicted according to sequences from BAC, EST, GSS and CoreNucleotide. LM: Length of mature miRNAs; LP: Length of precursor; C: Content of A + U; MFEs: Minimal folding free energies; MFEIs: Minimal folding free energies

miR157a
 U - U -- U AAUUUCA AA
 UGACAGAAG AUAGAGACAC AAUGA UGA AUGCU UUC \
 ACUGUCUUC UAUCUCUCGUG UUACU ACU UACGA GGG U
 U G U UA C AAACGAC UU

miR157b
 U - G AU - UAAUU
 UGACAGAAG AUAGAGA CACGA AA UGAGGUGC G
 ACUGUCUUC UAUCUCU GUGUU UU AUUCCACG G
 U A A CC A UCGAA

miR157c
 U UA UAAC- UAAUU
 UGACAGAAGA GAGAGCACGAA GAGGUGC G
 ACUGUUUUUCU CUCUCGUGUUU UUCCACG G
 U UA CUUAA UACAA

miR159
 GA C AA U --- U U G C - UU U C UU AUU
 UGGAGCCUUCU AGUCCAA AAA AUC AACAA GGU AAAU GAGCU CUGAC UAUG GA CC CAG CCUAUCUA UAUG U
 AUUCUGAGGGA UUAGGUUU UAG UUGU CCA UUUU UUCGA GACUG AUAC UU GG GUU GGAUAGAU AUAC C
 AG U AC U UUC U U G U G UG U U -- AAA

miR162
 G C CC C CUGGAA - AUUAUA
 CUGGA GCAG GGU AUUGAUC GUUCC GCUG AAU \
 GACCU CGUC CCA UAGCUGG UAAGG CGAC UUA U
 A U AA C AAAA-- A CAACGCA

miR167
 U G AAA A A AUU
 UGAAGC GCCA CAUGAUCU CUU CCU UAA \
 ACUUCG UGGU GUACUAGA GAA GGA AUU U
 U - CUA C - AUA

miR172a
 UG A A AAA G --- UG A GA
 AUG GCAU AUCAAGAUUC CGUGA GUU CAAA U GUUAU UAAUU \
 UAC CGUA UAGUUCUAG GCACU CAA GUUU G CCGUA AUUAA U
 GU G A --- A AUC GU - AG

miR172b
 A A- AUUAAG A AAU GCUUUA GAA
 AUGUAGCAUCAAGAUUC UAC UGAAA AGGCA GGUUA AUGUA AUUU A
 UACGUUCGUAGUAGUUCUAAAG GUG ACUUU UCUGU CCAGU UAUAU UAAA U
 A AA AUUUA- A AC- AAUA-- AAG

miR319
 - UU CAC ACGA GU -- G AC UC AA ----| AU
 GAGCU CUUUAGUCCA AUGGGGA UAGG UCAAUUUG CU CCG UCAUUA CA UGUUGAGGU CUUG \
 CUCGA GAAGUCAGGU UGUCCUU GUUC AGUUGAAC GA GGC AGUAAGU GU ACGACUCCA GAGC A
 C GG UCA CGA- UG AU G GA GA CA CCGU* UA

miR395
 UG C U UU--- UU
 GAGUUUCCU A CGCUUCA UAGGGC AC C
 CUCAAGGGG U GUGAAGU GUCCUG UG G
 GU U C UAGUU UU

miR399
 U A A G- A UG UCA
 UAGGGC AC CUCU UUGGCAU CA CU A A
 AUCCCG UG GAGG AACCGUA GU GA U A
 U A A AA C GU UAU

miR171
 C C ---- - GUA AU
 GAUAUUGGC UGGUUA UCAGAC AAC AAAAU AACUAU U
 CUUAUAACCG GCCGAGU AGUUUG UUG UUUUG UUGGUA U
 U U CUUU C AG- AG

Fig. 5.3. Mature and precursor sequences with stem-loop structures predicted from tomato. The mature miRNAs are red colored. The actual size of the precursors may be slightly shorter or longer than represented. MiR319, miR171 and miR162 are reported by Ori et al. (2007), Pilcher et al. (2007) and Itaya et al. (2008), respectively

5.3.2 Potential Targets of Newly Predicted miRNAs and Their Function

The same procedure described above was used to predict potential miRNA targets in the mRNA database. Eighty-four potential target mRNA sequences were found to fit the criteria of Section 2.3 as miRNA targets, after homologues searching for nine conserved mature miRNA against 262,065 tomato mRNA sequences. When a potential target mRNA had detailed gene function annotation, it was not accepted. Otherwise, we presumed the function of the target mRNA through BLAST search. Consequently, 23 genes-coding proteins with known function were predicted as tomato miRNA targets, without validation experimentally (Table 5.6). The other 61 potential targets encoding unknown proteins were also detected.

Table 5.6 List of the potential targets of some conserved tomato miRNAs

miRNA	Targeted protein	Target function	Targeted sequence
miR157	Squamosa promoter binding-like protein	Transcription factor	AW933950, BE433988, BE435668, BM536323, DQ672601
miR159	GAMYB-like1	Transcription factor	EF175474*
	GAMYB-like2	Transcription factor	EF175475*, DU876962
miR167	AUXIN RESPONSE FACTOR 6 (ARF6)	Transcription factor	AW223741, BE434602, DB715336**
	AUXIN RESPONSE FACTOR 8 (ARF8)	Transcription factor	BI925927, BP902363
	p69 gene	Stress response	Y17278*
	p69 gene	Stress response	AJ005173*
	NADH dehydrogenase subunit 5	Metabolism	CD003107*
miR172	PHAP2A protein (Ap2A)	Transcription factors	BT013640
	PHAP2B protein (Ap2B)	Transcription factors	DU004888
miR319	GAMYB-like1	Transcription factor	EF175474*
	GAMYB-like2	Transcription factor	EF175475*, DU876962
	Zn finger protein	Transcription factor	BG791302
miR171	Scarecrow transcription factor family protein	Transcription factor	BT014581

*: The gene annotation obtained from the NCBI nucleotide database;

** : The sequence cloned by 3'-RACE

The largest group of miRNA targets contains 20 genes predicted to encode transcription factors, which control plant development and phase change from vegetative growth to reproductive growth. Amongst *SPL* genes encoding transcription factors were previously reported containing complementary sequences of miR156 in 3' UTR of *SPL* transcripts in *Arabidopsis* and rice (Wu and Poethig, 2006; Xie et al., 2006). The vegetative phase change in *Arabidopsis* was found to be regulated by increasing expression of *SPL*, which was a consequence of decreasing the level of miR156 (Wu and Poethig, 2006). Over-expression of miR156 has been found for protracting the expression of juvenile vegetative traits and delaying flowering of *Arabidopsis* (Wu and Poethig,

2006). The same results have been found in rice (Xie et al., 2006). Here, we presume that *SPL* in tomato contains a perfect complementary site against miR157, and *SPL* should be considered as the target of miR157 as well as the possible target of miR156, since miR156 has not yet been predicated in tomato due to the limited sequence data available.

Plant hormones play critical roles in regulating plant growth and development. GAMYB is a component of gibberellins (GA) signaling in cereal aleuronic cells of rice, and its transcripts have been found as the direct cleavage targets of miR159 (Achard et al., 2004; Tsuji et al., 2006). As transcription factors, GAMYB-related proteins were thought to be involved in the GA-promoted activation of LEAFY, and to regulate another development (Achard et al., 2004; Millar and Gubler, 2005). Analysis of mRNA expression profiles shows that *GAMYB* and *GAMYB-like* genes are regulated by miR159 in rice flowers. Thus, miR159 is considered to be a regulated homeostatic modulator of GAMYB activity (Achard et al., 2004; Tsuji et al., 2006). It seems that a similar miR159-GAMYB pathway should exist in the tomato. In addition, another complementary site was found directing to miR319 in *GAMYB* mRNA. It suggests that the level of GAMYB transcription could also be regulated by miR319.

ARF6 and ARF8 in *Arabidopsis* have been reported in regulating gynoecium and stamen development in immature flowers, and their transcripts are cleaved by miR167 (Ru et al., 2006; Yang et al., 2006). Mutations of *ARF6* or *ARF8* in the miR167 target sites were found to cause growth arrestment of ovule integuments, abnormal growth of anthers and failure to release pollen (Wu et al., 2006). And abnormal pollen was produced in miR167 over-expressing transgenic flowers (Ru et al., 2006; Wu et al., 2006). Thus, an miR167-mediated regulatory pathway is an important link of gene expression for promoting plant reproductive development through an auxin signal network. In our present work, homology transcripts of *ARF6* and *ARF8* were also found in the tomato, which could be considered as a common target of miR167 (Fig. 5.4).

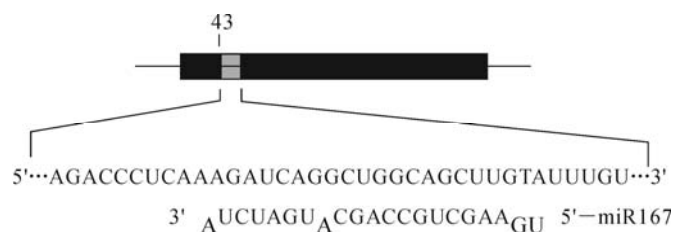


Fig. 5.4. Diagrammatic representation of target mRNA binding site by miR167. The putative miRNA (DB715336) interaction site is shown as a gray box, with the nucleotide position within the ORF indicated. The miRNA sequence and partial sequence of the target mRNA are shown in the expanded regions

In addition to *SPL*, *GAMYB*, *ARF6* and *ARF8*, other transcription factors presumably targeted by conserved miRNAs play important roles in virus stress. Infection of *Arabidopsis* by TuMV induced several developmental defects in vegetative and reproductive organs, while suppression of RNA silencing due to

TuMV-encoded RNA-silencing suppressor, P1/HC-Pro, was found to be a counter defensive mechanism enabling systemic infection by this virus (Kasschau et al., 2003). The suppressor was found to inhibit miR171-guided nucleolytic function by interfering with miR171 activity in directing cleavage of several mRNAs coding for Scarecrow-like transcription factors (Kasschau et al., 2003). Interference with miRNA-mediated developmental pathways, which share components with the antiviral RNA-silencing pathway, may partly be the mechanism for virus-induced disease (Kasschau et al., 2003). Similarly, there is a *scarecrow* transcript directly targeted by miR171 in the tomato, which suggests the potential mechanism for virus-induced disease in the tomato. Furthermore, we found that two homologues of transcription factors, PHAP2A protein (Ap2A) and PHAP2B protein (Ap2B), had at least one near-perfect complementary site with miR172, which was experimentally confirmed by Itaya et al. (2008) just recently, while some other studies of *Arabidopsis* showed that Ap2 could control the perianth identity (Aukerman and Sakai, 2003; Jack, 2004).

Other groups of target mRNAs contain miRNA targets presumptively coding a range of proteins which may play important roles in the aspects of stress response, metabolism and development. On the other hand, stress response intermediated by plant virus infection or other pathogens may bring a further understanding of miRNA. Previous reports revealed that the *P69* gene-encoding subtilisin-like proteases associate with the defense response (Jorda et al., 2000; Kavroulakis et al., 2006). Under pathogenic attack, P69 was able to assist the host to mount a defense response with the coordinated activation of a battery of defense-related genes (Jorda and Vera, 2000). At this point, tomato *P69* transcript may be the target of miR167. In addition to *P69*, we found that the transcript encoding NADH dehydrogenase subunit, as a part of tomato metabolism, could be considered as a presumptive target of miR167 in the tomato.

After comparison with the study of miRNAs in other plants, it was revealed that the relationships of miRNAs and their target mRNAs are conservative among the plant kingdom. Consequently, the 5'-RACE was one of the judicious choices to verify the prediction, and the result of proving miR172 target mRNA (Ap2) by Itaya et al. (2008) has been shown by prediction work (Zhang et al., 2008).

5.3.3 Confirmation of Tomato miRNAs Expression and Survey by Microarray

The current miRNA sequence database (miRBase) contains more than 1,389 mature plant miRNAs across 20 species, but few tomato miRNAs are accounted for in the literature and in the miRBase. A microarray suitable for detection of tomato miRNAs has been created based on the conservative character of plant miRNAs, using a flexible in situ parallel synthesis technology. The sample of the small nucleic acid property of miRNAs is basically used for hybridization in the microarray, and it shows that a single or more mismatches in the miRNA probe

will bring a negative signal and only those that have full conservative sequences among miRNAs are detectable (Fig. 5.5). Those miRNAs which have one mismatch at the ends could possibly be identified but with less strength of hybridization. A chip-to-chip hybridization also shows the reliability of microarray detection (Fig. 5.6).

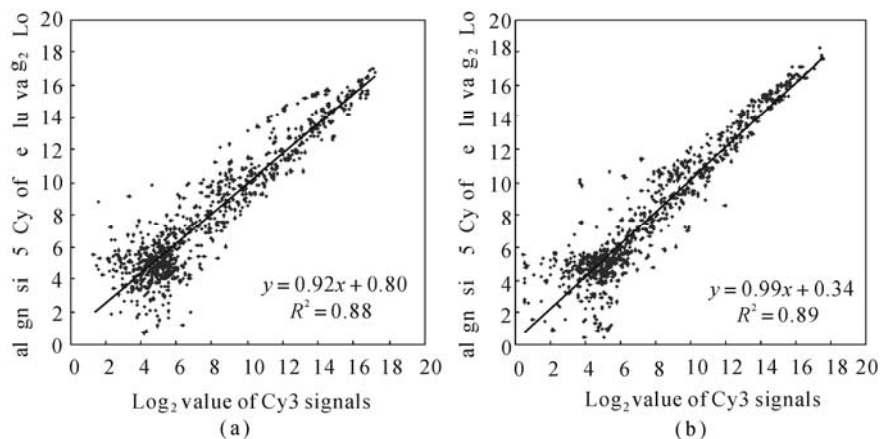


Fig. 5.5. Comparison of the same sample chip-to-chip hybridization results. Two samples (Mock and CMV inoculation) with each labeled with Cy3 and Cy5. The Cy3 and Cy5 pair co-hybridized to a chip. (a) The Mock-inoculated treatment; (b) The CMV inoculated treatment. Chip-to-chip hybridization results showed the reliability of microarray detection

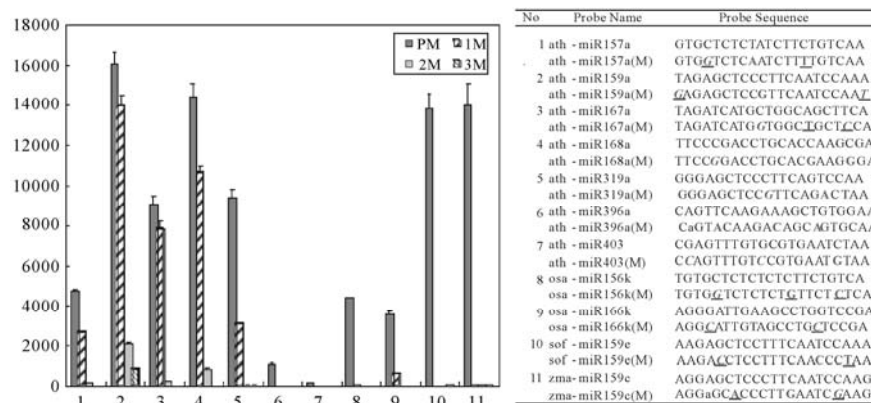


Fig. 5.6. Effect of mismatch numbers within probes on signal intensity. Signals from hybridization of healthy (Mock inoculated) tomato samples with Cy5 labeling are presented. Each miRNA probes set contains perfect match (PM) probe, one mismatch (1M) probe, two mismatch (2M) probes, three mismatch (3M) probes. Data are presented as Median signal intensity plus standard deviation for 4 replicates of probes. Bold letter: the first mutated nucleotide; Bold letter with underline: the second mutated nucleotide; Bold italic letter with underline: the third mutated nucleotide. Mismatch results showed the reliability of our detection method.

Using a microfluidic-microarray-based assay with probes complementary to all the known plant miRNAs, out of the 294 mature miRNAs reported in another nine plant species, 258 miRNAs distributed in 92 miRNA families were detected with positive expression in tomato leaf tissue (Table 5.7). Providentially, all the 12 predicted pre-miRNAs against 9 mature miRNAs were identified by the microarray, though the expression levels of miR395 and miR399 were significantly lower than for the other mature miRNAs (Fig. 5.7). Highly-expressed miRNAs, such as miR157, miR159, miR167 and miR319 in leaf, stem and root tissues can be easily confirmed by Northern blotting, but it's difficult to get positive hybridization results because of the length of small RNAs and/or stability limitations. The expression of miR157 was found to be the highest in tomato leaf tissue, which was approximately 132 times higher than that of miR395 in leaf tissue. Thus, the expression levels of tomato miRNAs were obviously different during the six to eight leaf stages of tomato seedlings. Among the other 246 mature miRNAs detected, the expression of 21 mature miRNAs in leaf tissue was higher than miR157 and 146 mature miRNAs were lower than miR395. The microarray results can be used for confirming the prediction and for effectively detecting the expression of mature miRNAs. The low expression of certain miRNAs might be caused by their timely expression characteristics in seedling development. Unfortunately, 246 mature miRNAs detected by microarray could not be found in sequencing prediction, due to the lack of tomato genome information at present.

Table 5.7 Mature miRNAs detected with microarray from tomato leaf tissue according to plant miRNAs reported from other species

No.	Probe ID ^a	Sequence (5'-3')	Family	No.	Probe ID	Sequence (5'-3')	Family
1	ath-miR156h	UUGACAGAAGAA AGAGAGCAC	miR156	13	osa-miR159a	UUUGGAUUGAAG GGAGCUCUG	miR159
2	gma-miR156b	UGACAGAAGAGA GAGAGCACA	miR156	14	osa-miR159f	CUUGGAUUGAAG GGAGCUCUA	miR159
3	ptc-miR156k	UGACAGAAGAGA GGGAGCAC	miR156	15	ptc-miR159f	AUUGGAGUGAAG GGAGCUCGA	miR159
4	ath-miR156a	UGACAGAAGAGA GUGAGCAC	miR156	16	osa-miR159d	AUUGGAUUGAAG GGAGCUCCG	miR159
5	ath-miR156g	CGACAGAAGAGA GUGAGCACA	miR156	17	osa-miR159e	AUUGGAUUGAAG GGAGCUCCU	miR159
6	sbi-miR156e	UGACAGAAGAGA GCGAGCAC	miR156	18	osa-miR159c	AUUGGAUUGAAG GGAGCUCCA	miR159
7	ath-miR157d	UGACAGAAGAU GAGAGCAC	miR157	19	ptc-miR159d	CUUGGAUUGAAG GGAGCUCCU	miR159
8	ath-miR157a	UUGACAGAAGAU AGAGAGCAC	miR157	20	ath-miR162a	UCGAUAAACCUC UGCAUCCAG	miR162
9	ath-miR159b	UUUGGAUUGAAG GGAGCUCUU	miR159	21	zma-miR162	UCGAUAAACCUC UGCAUCCA	miR162
10	ath-miR159a	UUUGGAUUGAAG GGAGCUCUA	miR159	22	osa-miR162b	UCGAUAAAGCCUC UGCAUCCAG	miR162
11	sof-miR159e	UUUGGAUUGAAA GGAGCUCUU	miR159	23	sbi-miR164c	UGGAGAAGCAGG ACACGUGAG	miR164
12	ath-miR159c	UUUGGAUUGAAG GGAGCUCCU	miR159	24	osa-miR164e	UGGAGAAGCAGG GCACGUGAG	miR164

(To be continued)

(Table 5.7)

No.	Probe ID ^a	Sequence(5'-3')	Family	No.	Probe ID	Sequence(5'-3')	Family
25	ptc-miR164f	UGGAGAAGCAGG GCACAUGCU	miR164	52	zma-miR171b	UUGAGCCGUGCC AAUAUCAC	miR171
26	ath-miR164a	UGGAGAAGCAGG GCACGUGCA	miR164	53	zma-miR171c	UGAUUUGAGCCGU AGAUUUGAGCCGC	miR171
27	ath-miR164a	UGGAGAAGCAGG GCACGUGCA	miR164	54	ptc-miR171c	AGAUUUGAGCCGC GCCAAUAUC	miR171
28	osa-miR164c	UGGAGAAGCAGG GUACGUGCA	miR164	55	zma-miR171c	UGACUGAGCCGU GCCAAUAUC	miR171
29	osa-miR164d	UGGAGAAGCAGG GCACGUGCU	miR164	56	ptc-miR171k	GGAUUGAGCCGC GCCAAUAUC	miR171
30	ath-miR165a	UCGGACCAGGCU UCAUCCCC	miR165	57	zma-miR171f	UUGAGCCGUGCC AAUAUCACA	miR171
31	ath-miR166a	UCGGACCAGGCU UCAUCCCC	miR166	58	ath-miR172a	AGAAUCUUGAUG AUGCUGCAU	miR172
32	sbi-miR166a	UCGGACCAGGCU UCAUCCCC	miR166	59	ath-miR172e	GGAAUCUUGAUG AUGCUGCAU	miR172
33	osa-miR166g	UCGGACCAGGCU UCAUCCUC	miR166	60	sbi-miR172a	AGAAUCUUGAUG AUGCUGCA	miR172
34	osa-miR166m	UCGGACCAGGCU UCAUCCCU	miR166	61	ath-miR172c	AGAAUCUUGAUG AUGCUGCAG	miR172
35	ptc-miR166n	UCGGACCAGGCU UCAUCCUU	miR166	62	osa-miR172c	UGAAUCUUGAUG AUGCUGCAC	miR172
36	osa-miR166k	UCGGACCAGGCU UCAUCCCU	miR166	63	sbi-miR172b	GGAAUCUUGAUG AUGCUGCA	miR172
37	osa-miR166i	UCGGAUCAGGCU UCAUCCUC	miR166	64	ptc-miR172g	GGAAUCUUGAUG AUGCUGCAG	miR172
38	ptc-miR166p	UCGGACCAGGCU CCAUCCUU	miR166	65	ath-miR172b*	GCAGCACCAUUA AGAUUCAC	miR172
39	osa-miR166e	UCGAACCAGGCU UCAUCCCU	miR166	66	ptc-miR172i	AGAAUCCUGAUG AUGCUGCAA	miR172
40	ptc-miR167h	UGAAGCUGCCAA CAUGAUCUG	miR167	67	ath-miR319c	UUGGACUGAAGG GAGCUCCU	miR319
41	ath-miR167a	UGAAGCUGCCAG CAUGAUCUA	miR167	68	ppt-miR319a	CUUGGACUGAAG GGAGCUCC	miR319
42	ath-miR167d	UGAAGCUGCCAG CAUGAUCUGG	miR167	69	ath-miR319a	UUGGACUGAAGG GAGCUCC	miR319
43	ath-miR167c	UUAAGCUGCCAG CAUGAUCUU	miR167	70	ppt-miR319c	CUUGGACUGAAG GGAGCUCC	miR319
44	osa-miR167d	UGAAGCUGCCAG CAUGAUCUG	miR167	71	osa-miR319a	UUGGACUGAAGG GUGCUC	miR319
45	ptc-miR167f	UGAAGCUGCCAG CAUGAUCUU	miR167	72	gma-miR319c	UUGGACUGAAAG GAGCUCCU	miR319
46	ath-miR168a	UCGCUUGGUGCA GGUCGGGAA	miR168	73	ath-miR396a	UCCACAGCUUU CUUGAACUG	miR396
47	osa-miR168a	UCGCUUGGUGCA GAUCGGGAC	miR168	74	ath-miR396b	UCCACAGCUUU CUUGAACUU	miR396
48	sof-miR168b	UCGCUUGGGCAG AUCGGGAC	miR168	75	osa-miR396d	UCCACAGGCUUU CUUGAACUG	miR396
49	osa-miR168b	AGGCUUGGUGCA GCUCGGGAA	miR168	76	ptc-miR396f	UCCACGGCUUU CUUGAACUG	miR396
50	ath-miR171b	UUGAGCCGUGCC AAUAUCACG	miR171	77	osa-miR398b	UGUGUUCUCAGG UCGCCCCUG	miR398
51	ath-miR171a	UGAUUGAGCCGC GCCAAUAUC	miR171	78	ath-miR403	UUAGAUUCACGC ACAAACUCG	miR403

^a: When a mature miRNA simultaneously appeared in two or more species, probe ID was defined as the first, and the priority list for naming miRNA homolog was in the following order, ath-miR, osa-miR, zma-miR, sbi-miR, mtr-miR, sof-miR, gma-miR, ptc-miR, ppt-miR

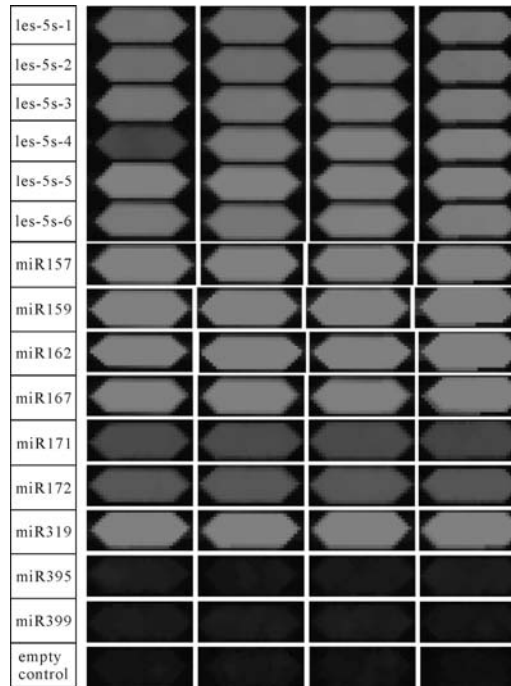


Fig. 5.7. Microarray signals showing miRNA accumulation in tomato leaf tissue indicating their expression differences

Regarding all known miRNAs documented from other plant species, the distribution of relative amounts of miRNAs detected from tomato leaf tissue are shown in Fig. 5.8.

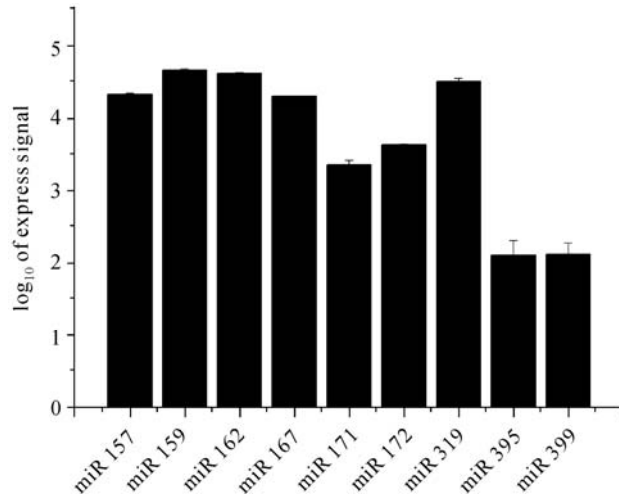


Fig. 5.8. Relative amounts of presently identified miRNAs detected from tomato leaf tissue

When the detection signals were enhanced, with the same microarray probes against 1,389 plant miRNAs registered in the Sanger Database, a total of 105 conserved plant miRNAs were detected from tomato leaf tissues in the 8 to 10 leaf stages. Regarding the specificity of microarray hybridization, the number of tomato miRNAs might exclude those miRNAs homologous with one or more nucleotides differing from the previous report sequences.

In conclusion, when considering factors such as development stages, organs, and the considerably-stressed conditions associated with plant growth, profiles of tomato miRNAs can be quite multifarious and more tomato miRNAs are waiting to be discovered. Finding more convenient miRNA detection methods, especially sensitive techniques for real-time quantitative determination for particular miRNAs, will bring a broader insight to the understanding of crop development and the host reaction to virus infection and other stressed conditions.

5.4 Mechanisms Involved in Plant miRNA Expression with Regard to Infection of ssRNA Viruses

In recent years, there has been accumulating evidence that miRNAs get involved in the defense mechanism in animals and plants. Therefore, investigating the alteration of miRNAs expression profiles after virus infection would provide new insights for understanding the sophisticated virus-host plant interaction. And at the same time, the reality of miRNA could be recovered in other tracks. The current miRNA sequence database (miRBase) contains more than 1,389 mature plant miRNAs across 20 species, and the number of novel miRNAs and the plant species studied for miRNA profiles are increasing speedily.

For the majority of known miRNA target codes for proteins with a known or suspected role in a range of developmental processes (Laufs et al., 2004; Mallory et al., 2004; Guo et al., 2005) as well as in response to nutrient homeostasis and environmental stress (Jones-Rhoades and Bartel, 2004; Sunkar and Zhu, 2004). Therefore, investigation of the changes in plant miRNAs expression profile after virus infection is not only an important aspect in the study of plant-pathogen interactions but also a noteworthy way to know more about the reality of miRNA response under stressed conditions.

Taking the tomato as the model host plant, from which few tomato miRNAs are accounted for in the literature and in the miRBase, miRNA expression justified by infection with *Cucumovirus* and *Tobamovirus* has been investigated. Tested by using an *in situ* parallel synthesis microarray, 85% of the detected tomato miRNAs showed significant expression alterations in tomato leaf tissues after infection with different viruses. The possible mechanisms between miRNA-interfering CMV and TOMV have thus been evaluated. Under large scale detection conditions, the comprehensive investigation of host miRNAs in virus infection on a genome scale can be studied.

5.4.1 Phenotype in Tomato Under Infection with CMV/satRNA Combinations and ToMV

Solanum lycopersicum cv. Hezuo903, a dominating local variety in East China, is used as testing plant. It is sensitive to infection of CMV and also ToMV, presenting stunt with typical systemic mosaic under CMV infection and mosaic or necrosis under ToMV infection according to viral strains. The viral strains used in this work are as follows: CMV-Fny as a typical subgroup I strain of this virus (Palukaitis and Garcia-Arenal, 2003); CMV-Fny-*Sat*T1 as CMV-Fny plus T1 satellite, which is identified as a necrosis satellite RNA of CMV when infecting the tomato (Liao et al., 2007; Feng et al., 2007); CMV-Fny-*Sat*Yn12 as CMV-Fny plus Yn12 satellite, which is identified as an attenuating satellite RNA of this virus (Liao et al., 2007); CMV-Fny Δ 2b, as a mutation of this virus but with the 2b coding sequence of CMV-Fny deleted (Du et al., 2007), and ToMV-N5 as a strain of ToMV which has been found to induce necrosis in certain tomato varieties (Chen et al., 2007).

In tomato seedlings (cv. Hezuo903), different phenotypes are found developed under infection by CMV-Fny, CMV-Fny Δ 2b, CMV-Fny-*sat*Yn12, CMV-Fny-*sat*T1 and ToMV-N5 (Fig. 5.9) Under experimental conditions, CMV-Fny infection causes systemic mosaic with mild leaf distortion and growth reduction, linear leaf and severe stunt appeared at the later stages. CMV-Fny Δ 2b infection causes slight mottle occasionally at the early developing stages but raised general growth-promotion, demonstrating an increase in plant height, leaf area, root length and number of lateral roots. The stimulation becomes more common and clearer in the later developing stages. The addition of *sat*Yn12 could alleviate the symptoms induced by CMV-Fny, with almost the similar height and leaf area to the mock infection. However, the symptoms are exacerbated in the CMV-Fny-*sat*T1 infection, with yellow spots and necrosis occurring on the inoculated leaves, and seedlings inoculated by it show more severe stunt and shrinkage than that caused by the helper virus alone. ToMV-N5 infection brings leaf death to the lower leaves and induces top necrosis at the early stages, but develops into limitation of growth or death of the whole plant, the appearance of which is fairly different from the typical systemic mosaic phenotypes induced by *Cucumovirus*.



Fig. 5.9. Symptoms induced by various virus infections on tomato seedlings at 35 dpi

5.4.2 Response of Tomato miRNA Expression to Virus Infection

It is not difficult to consider that miRNA expression changes with host development. For presenting a relatively firm picture of plant miRNA response to virus infection (accumulation/expression), time course detection of miRNAs in the tomato shows that when tomato seedlings are inoculated at two to three true-leaf stages, the differences between mock inoculation and CMV inoculation vary until 20 dpi. Thus, a period after this could be used to observe the most obvious and established changes (Fig. 5.10).

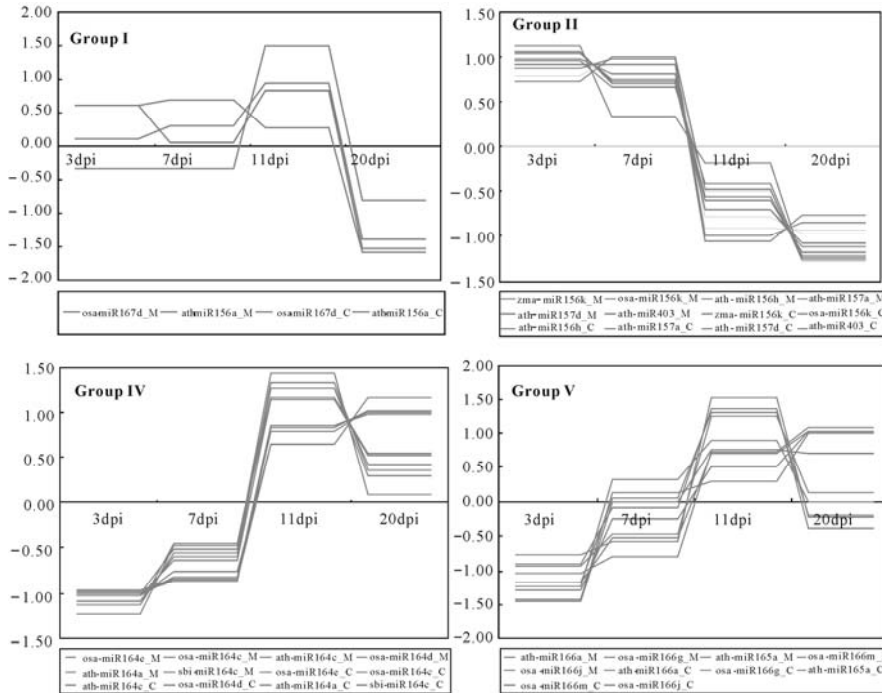


Fig. 5.10. Comparing expression pattern of miRNAs in groups between mock and CMV inoculated tomato. miRNAs in groups I (a) and II (b) showed no obvious difference, while miRNAs in groups IV (c) and V (d) showed distinct signature change at 20 dpi. The variation became constant until 30 dpi but some plants died off at 40 dpi (data not show here). Thus, we chose 35 dpi to determine the miRNA profile of different treatments

When the miRNA detection signal threshold was defined as 500 after normalization, 105 conserved miRNAs (38%) were found positive, expressed in tomato leaves tissues. These detected miRNAs were found to be distributed in 25 miRNA families, including miR156, miR157, miR159, miR160, miR162, miR164, miR165, miR166, miR167, miR168, miR170, miR171, miR172, miR319, miR390, miR394, miR395, miR396, miR397, miR398, miR399, miR403, miR408, miR474 and miR482. Amongst these, families of miR159 and miR171 contained the maximum

numbers of detected miRNAs in the tomato (12 miRNAs respectively). The remarkable and interesting tomato miRNAs involved in virus-infection and their expression levels are given in Table 5.8.

Table 5.8 Remarkable tomato miRNAs involved in virus-infection and their expression levels

Probe_ID ^a	CMV-Fny vs. Mock ^b	CMV-FnyΔ2b vs. Mock ^b	CMV-FnyYn12 vs. Mock ^b	CMV-FnyT1 vs. Mock ^b	ToMV-N5 vs. Mock ^b
ath-miR156a	0.32		0.41	0.57	0.33
ath-miR156g	0.30	0.64	0.40	0.61	0.33
ath-miR156h		0.65			
ath-miR159a		0.62			
ath-miR159b		0.62			
ath-miR159c		0.62			
ath-miR160a	0.32		0.52		
ath-miR164a	0.55		0.59		0.54
ath-miR164c	0.54		0.58		0.55
ath-miR165a	0.55		0.57		
ath-miR166a	0.52		0.54		
ath-miR167a					1.57
ath-miR167c					1.69
ath-miR168a				2.43	1.87
ath-miR171a	0.29		0.42		0.54
ath-miR171b	0.32		0.46	0.54	0.49
ath-miR172a	0.49		0.52	0.59	
ath-miR172b*		0.63		0.51	
ath-miR172c	0.42		0.46	0.52	
ath-miR172e	0.44		0.49	0.55	
ath-miR394a	0.29		0.32		
ath-miR395b	0.29		0.58	0.64	0.61
ath-miR398a	1.68			5.17	2.56
ath-miR398b	1.58		1.51	5.18	2.47
ath-miR399b	0.61			2.02	1.61
ath-miR403	2.25		2.78	3.32	2.02
ath-miR408	0.59			2.61	
gma-miR156b					0.60
gma-miR319c	0.37		0.35	0.08	0.05
mtr-miR171	0.40	2.13	0.64		
mtr-miR395g	0.43				0.50
mtr-miR399b		1.98			2.00
mtr-miR399d		2.05			2.02
osa-miR156l	0.40		0.54		0.46
osa-miR160e	0.37	1.74			
osa-miR162b			1.72		

(To be continued)

(Table 5.8)

Probe_ID ^a	CMV-Fny vs. Mock ^b	CMV-FnyΔ2b vs.Mock ^b	CMV-FnyYn12 vs.Mock ^b	CMV-FnyT1 vs.Mock ^b	ToMV-N5 vs.Mock ^b
osa-miR164d	0.59				0.58
osa-miR166g	0.65				
osa-miR166i	0.48		0.61		0.61
osa-miR166k	0.67				
osa-miR166m	0.65				
osa-miR167d				1.51	1.72
osa-miR168a	2.32		2.22	2.88	2.99
osa-miR168b	3.20		2.78	3.89	3.79
osa-miR171b	0.32		0.49		
osa-miR171i	0.52		0.56		0.65
osa-miR172c	0.48		0.54	0.64	
osa-miR319a	0.36	0.46	0.24	0.10	0.07
osa-miR396d	0.42		0.42	0.25	0.17
osa-miR397b	2.42		2.20	2.21	2.67
osa-miR398b	1.55	1.54	1.77	5.44	2.56
osa-miR408				2.70	
ptc-miR156k	0.60		0.49	0.20	0.16
ptc-miR159e	0.44		0.47	0.38	0.30
ptc-miR166p	0.63				
ptc-miR167f					1.76
ptc-miR171c	0.34		0.55		0.64
ptc-miR171j	0.46		0.52		
ptc-miR171k	0.35		0.57		
ptc-miR172g	0.52				
ptc-miR172i	0.54		0.61		
ptc-miR319i	0.38	0.46	0.29	0.23	0.18
ptc-miR396f	0.23	0.63	0.14	0.01	0.01
ptc-miR474a	0.33		0.22	0.23	0.24
ptc-miR474c	0.32		0.22	0.21	0.24
sbi-miR156e	0.33		0.38	0.45	0.27
sbi-miR164c	0.65			0.64	0.54
sbi-miR166a	0.53				
sbi-miR172a	0.54		0.64	0.52	
sbi-miR172b	0.57	1.72			
sof-miR168b	2.49		2.26	2.26	2.54
sof-miR408e			2.18	4.88	3.24
zma-miR171a	0.38		0.52		0.55
zma-miR171b	0.36		0.58	0.57	0.56
zma-miR171c	0.30		0.54	0.57	0.57
zma-miR171f	0.38		0.59	0.56	0.52

^a: The interesting genes were selected for this analysis if their expression levels were significantly different to Mock with *t*-test analysis (*p* value<0.05), fold change >1.5 and higher than 500 after normalization;

^b: the ratio of the miRNA expression level in virus-infected tomato compared to mock

To investigate the function of these interesting miRNAs, we blasted the tomato nucleotide database and predicted 523 presumable target mRNAs. However, it was complicated to find out the function annotation for most of them, thus only 118 target genes were kept remaining and their presumable function annotation was predicted (Table 5.9). As the result shows, most of the predicted miRNA targets are transcription factors, which control plant flower, leaf and height development and phase change from vegetative growth to reproductive growth.

Virus infections had significant influences on tomato miRNAs expression profiles (Fig. 5.11). Firstly, there were 13 mature miRNAs, 12.4% of the total detectable mature miRNAs, which were undetectable in the healthy tomato, but were expressed in the leaf tissues of virus-infected plants (Table 5.9). Secondly, the effects of different viruses on tomato miRNA expression profiles were different. In comparison with mock, the expression of 60, 15, 48, 38 and 48 mature miRNAs were significantly altered in CMV-Fny, CMV-Fny Δ 2b, CMV-Fny-*sat*Yn12, CMV-Fny-*sat*T1 and ToMV-N5 infected plants (fold changes > 1.5). CMV-Fny infection elicited the greatest alterations, and then the CMV-Fny-*sat*Yn12 and ToMV-N5 infection. CMV-Fny Δ 2b induced the fewest alterations, which agree with the morphological or physiological developments.

Table 5.9 List of the predicted potential targets of some conservative tomato miRNAs

miRNA	Targeted protein	Target function	Targeted genes
miR156	25S ribosomal RNA gene, 25S-18S intergenic spacer and 18S ribosomal RNA gene		DU011034
	succinate dehydrogenase subunit 3	Metabolism	CZ961748
	squamosa promoter binding protein-like protein mRNA	Transcription factor	BE435668, AW933950
	retrotransposon	Transcription factor	AQ367875, DU021064, DU065939, DU068263, DU850860, DU864426, DU871733, DU880883, DU905156, DU950704, DU093046, DU058166
miR159	<i>Solanum lycopersicum</i> microRNA miR319a/b precursor	Transcription factor	DU051444
	GAMYB-like1	Transcription factor	EF175474
	GAMYB-like2	Transcription factor	EF175475, DU876962
miR160	auxin response factor (ARF) mRNA	Transcription factor	BP880486, AW038480
miR164	salicylic acid-induced protein 19 gene	Metabolism	DB693703

(To be continued)

(Table 5.9)

miRNA	Targeted protein	Target function	Targeted genes
miR164	salicylic acid-induced protein 19 gene	Metabolism	DB693703
miR165	PHAVOLUTA(PHV)-like HD-ZIPIII protein mRNA	Transcription factor	DB685981, BI925551, DB696932
miR167	auxin response factor 6/8 p69 gene	Transcription factor Transcription factor	AW223741, BE434602, DB715336, BP902363 Y17278*, AJ005173*
miR171	scarecrow transcription factor family protein	Transcription factor	BT014581
miR172	PHAP2A protein (Ap2A) mRNA	Transcription factor	BM408872, BM410833, BM413247
miR319	GAMYB-like1	Transcription factor	EF175474
	GAMYB-like2	Transcription factor	EF175475, DU876962
miR394	F-box family protein mRNA	Transcription factor	DB683617
miR396	GROWTH-REGULATING FACTOR, GRF	Transcription factor	AW650985, BI925781, AW648434, AW035720, AW650563
miR398	cytoplasmic Cu-Zn superoxide dismutase (EC 1.15.1.1)	Metabolism	AW093126, AW622072, AW930621, BE432482, BE460699, AW038693, AW040225, AW093090, AW443525, AW932873, AI484868, AI485182, AI485174, AI485125, AI487399, AI489736, AI488828, AI489229, AI488403, AI488458, AI773204, AW621585, AI483263, AI490904, BG123682, BG127139, BG129242, BG129516, BG131296, BG132171, BG132265, BG135177, BG791287, BG791288, BI921824, BI922824, BI926766, BI928086, BI929979, BI933900, BM408699, BM411086, BM411709, BM412919, BM413419, BP886589, BP889475, BP889926, BP891061, BP892039, BP892118, BP893860, BP894623, BP894749, BP894787, BP896917, BW685053, BW685549, BW685770, BW685989, BW686004, BW686432, BW688154, BW689470, BW689976, BW690176, BW691600, BW692198, BW692300, EG552916, EG553304, EG553837, EG554001, DB723962, DB710946, ES890162, ES891124, ES892399, ES892798, ES894260, ES895359, AW030320

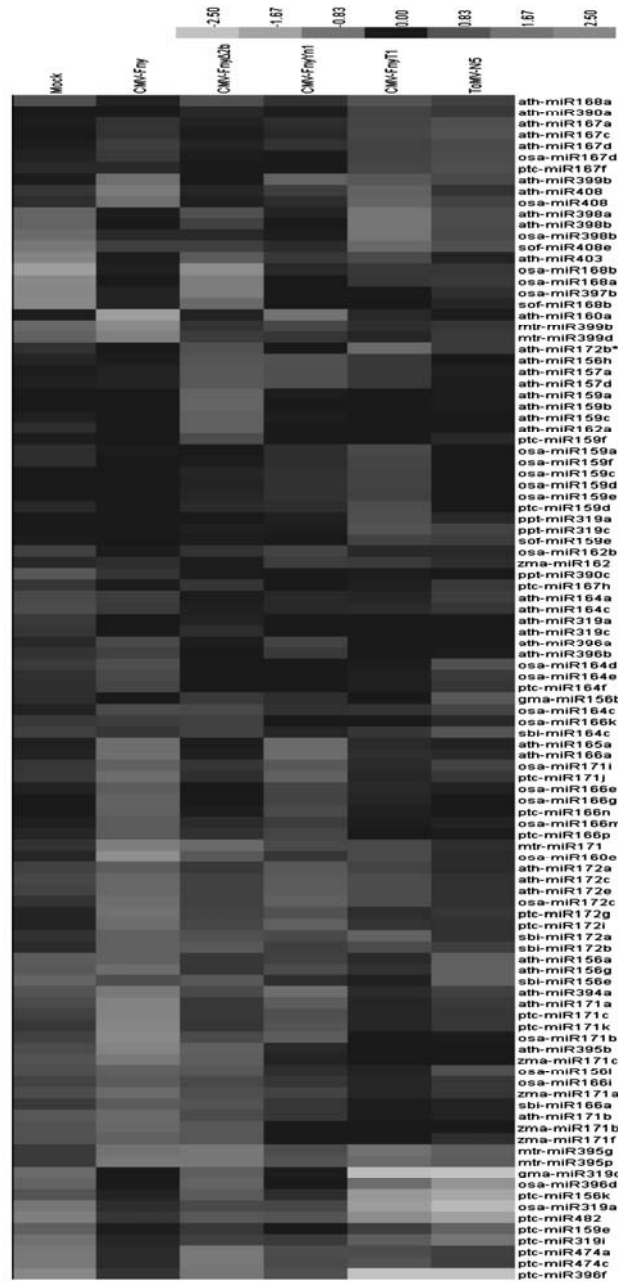


Fig. 5.11. The altered tomato miRNAs expression profiles after various virus infections. The following parameters for cluster analysis and methods are used: median center, \log_2 transform, Euclidean distance and average linkage. (a) All detectable miRNAs; (b) Genes are selected for this analysis if their expression level was significantly different to Mock with *t*-test analysis (p value <0.05), fold change >1.5 and higher than 500 after normalization

Because of the high throughput character of the microarray, its application to nucleic acid detection has major advantages, especially for quantitative comparison studies. With the increasing number of available plant genes sequenced, this technology has proven to be sensitive and highly reproducible in miRNA detection, and suitable for investigating the overall miRNA expression profiles (Axtell and Bartel, 2005). The miRNA microarray designed and synthesized according to the conservative characteristics of plant miRNAs are found to be well adopted to application upon novel species. Among the 1,389 plant miRNAs registered in the Sanger Database, many of them are reported conserved between species, often over wide evolutionary distances. For instance, certain miRNAs cloned or predicated from *Arabidopsis* have sets of identical matches in the genome of *Oryza sativa* (Rice) (Bonnet et al., 2004), and some miRNAs such as ath-miR166 are conserved in all lineages of land plants, including bryophytes, lycopods, ferns and seed plants (Floyd and Bowman, 2004; Reinhart et al., 2002). Apart from the conservative character of most plant miRNAs, some miRNAs are reported specific to certain species. For instance, the families of miR158, miR161, miR163, miR173 and miR447 have only been found as yet in *Arabidopsis* (Xie et al., 2005), and the families of miR435, miR437, miR438, miR439, miR440, miR441, miR442, miR443, miR444, miR445a and miR446 are proved to have evolved independently in *Oryza sativa* (Sunkar et al., 2005). Besides these, many miRNAs in the present miRNA database remain for further validation. For example, miR400, miR401, miR402, miR404, miR405, miR406 are only computer predicated (Sunkar and Zhu, 2004), and although miR407, miR408, miR413–miR420 are experimentally validated, they are more likely the endogenous siRNAs (Wang et al., 2004; Xie et al., 2005; Lu et al., 2006). Therefore, excluding those uncertain and species-specific miRNAs, the remaining 279 miRNAs are selected as the candidates for detecting the conserved miRNAs in the tomato.

5.4.3 *MiRNA Expression Profiles between CMV-Fny and CMV-Fny Δ 2b Infections*

As the 2b protein of CMV-Fny was the pathogenicity determinant in *Solanaceous* hosts, we compared the miRNA expression alterations in the presence or absence of the 2b gene firstly. As the results show in Fig.3(a), tomato miRNA expression profiles were significantly different between the two infections. In CMV-Fny infection, the expression of only eight miRNAs (belonging to the families of miR168, miR397, miR398 and miR403) increased by 1.55–3.20 folds, 16 miRNAs (distributed mainly in the families of miR156, miR159, miR167, miR399 and miR408) were unchanged, and the other 52 miRNAs decreased to 0.29–0.67 fold of mock infection. But at the same state, in CMV-Fny Δ 2b infection, the expression of six miRNAs belonging to the families of miR160, miR171, miR172, miR398 and miR399 increased by 1.54–2.13 folds, nine miRNAs belonging to the

families of miR156, miR159, miR319 and miR396 decreased by 0.45–0.63 fold, and the other 61 miRNAs were unchanged to mock. When the two profiles were compared, the expression of miR156, miR319, miR396 and miR398 showed similar alterations, but miR160, miR171 and miR172 were completely opposite.

It was straightforward to see that when CMV-Fny was compared with CMV-Fny Δ 2b infection, the significant differences between their miRNA expression profiles revealed that the 2b gene is critical in the interaction between virus and host system defense/resistance. When 2b gene is deleted, host plants would elicit the PTGS defense system through the siRNA pathway, to inhibit the replication and movement of viral RNAs, thus no typical symptoms could be observed (Lewsey et al., 2007). However, the mechanisms underlying development promotion induced by CMV-Fny Δ 2b infection remains unknown, and it might be correlated with the regulation role of CMV-Fny Δ 2b in the expression of certain plant genes. Tested by microarray hybridization, under CMV-Fny Δ 2b infection, the expression of miR156, miR159, miR319 and miR396 decreased, whereas miR160, miR171, miR172, miR398 and miR399 increased, when compared with mock inoculation. Among them, the targets of miR159 and miR319 are MYB and TCP genes, which regulate the development of tomato leaves. The target of miR160 is ARF8, which regulates the development of the lateral root through an auxin signaling pathway. Targets of miR156, miR171 and miR172 are related to the development of floral tissues and the phase change from vegetative to reproductive growth (Yang et al., 2006; Chuck et al., 2009). Targets of miR398 and miR399 are related to environmental stress response (Ru et al., 2006; Yang et al., 2006). However, the expression levels of miR162 and miR168, which play critical regulation roles in the miRNA pathway, have not shown significant expression alterations. The changes in both their target genes in further studies are needed to interpret the effect of CMV-Fny Δ 2b infection on the development of tomato seedlings.

5.4.4 *MiRNAs Expression Profiles Altered with Addition of satRNAs*

To investigate the interference of adding *satRNAs* to miRNAs pathway caused by CMV infection, the miRNAs expression profiles of tomato leave tissues infected by CMV-Fny, CMV-Fny-*satYn12* and CMV-Fny-*satT1* were compared. It shows that miR168, miR397, miR398 and miR403, which had higher expression levels under CMV-Fny infection, also showed a 1.51–5.44 fold increase either in CMV-Fny-*satYn12* and CMV-Fny-*satT1* infections. On the other hand, the expression of miR408, which decreased in CMV-Fny infection (0.59 fold of mock), was increased to 2.18–4.88 folds in the presence of *satYn12* and *satT1*. Besides these, the expression of miR162 was 1.72 folds higher than mock in CMV-Fny-*satYn12*, but unchanged in CMV-Fny and CMV-Fny-*satT1* infections. A similar phenomenon was also found for miR167, which was 1.51 folds of mock

in CMV-Fny-*satT1*, but unchanged in CMV-Fny and CMV-Fny-*satYn12* infections. These results indicate the expression of certain miRNAs was changed by the addition of *satRNAs*, which would aggravate or alleviate the symptoms induced by CMV-Fny infection.

In general, there were 29 miRNAs showing common expression changes among the three infections, which account for 48% of the total altered miRNAs in CMV-Fny infection, 60% in CMV-Fny-*satYn12* infection, and 76% in CMV-Fny-*satT1* infection. When the three infections were compared to each other, only the expression of one and three miRNAs were altered specifically in CMV-Fny-*satYn12* infection (*osa-miRNA162b*) and CMV-Fny-*satT1* infection (*ath-miRNA168a*, *osa-miRNA167d* and *osa-miRNA408*), respectively. The known functions of miR162 and miR168 concerned small RNA self-synthesis and metabolism (Xie et al., 2003). miR167 was predicted targeting auxin response factors 6/8 (*ARF6/8*), which has been reported in regulating gynoecium and stamen development in immature flowers through an auxin signal network (Ru et al., 2006; Yang et al., 2006). MiR408 was predicted targeting mRNAs which play important roles in the aspects of stress response.

Although *satYn12* and *satT1* had quite opposite effects on symptom development induced by CMV, fewer miRNAs were found specifically altered in both of their infections. However, the expression levels of some miRNAs were obviously changed in the presence of *satYn12* or *satT1*. For example, the expression levels of *ath-miR398b* were 1.58, 1.51 and 5.18 folds of mock in CMV-Fny, CMV-Fny-*satYn12* and CMV-Fny-*satT1* infections, showing that expression or accumulation of this miRNA significantly increased in the case of necrosis producing infection by *satT1*. The expression level of *ath-miR398b* is also obviously increased up to 2.5 folds, which supports its possible involvement in necrosis reaction. These results demonstrated not only that the scope of miRNAs is involved, but that the extent of their expression level is affected by different phenotype motivates.

5.4.5 A Comparison of miRNAs Expression Profiles between CMV and ToMV Infections

In ToMV-N5 infection seedlings, the expression of 17 miRNAs (distributed mainly in the families of miR167, miR168, miR398 and miR399) increased by 1.57–3.79 folds, 29 miRNAs (distributed mainly in the families of miR156, miR164, miR171, miR319, miR395, miR396 and miR474) decreased to 0.01–0.65 fold of mock, and another 30 miRNAs were unchanged by mock inoculation. When those of CMV-Fny were compared with ToMV-N5, the expression of 37 miRNAs were significantly changed in both infections, which account for 62% of the total altered miRNAs in CMV-Fny infection, and 80% in ToMV-N5 infection. However, the expression of 23 miRNAs were altered uniquely by CMV-Fny infection (including members in the families of miR160, miR165, miR166,

miR171, miR172, miR394 and miR408), and nine miRNAs were specific to ToMV-N5 infection (including members in the families of miR156, miR167, miR168, miR399 and miR408) (Fig.3(b)). This implies CMV and ToMV might function by different means against host defenses. Recent study has proved that the 2b suppressor of CMV functioned downstream of DICER and siRNA production, by blocking AGO1 cleavage activity, and by stopping the production of secondary siRNA in the infected plant cell (Zhang et al., 2006). The silence suppressor of ToMV is a 130 kD replicate and its silencing-suppression strategy has on no account been studied. Thus, further investigation is needed to determine its exact mode of action and to have a deeper understanding when similar/different pathways are studied compatibly.

When the cases of infection by CMV-Fny, CMV-Fny Δ 2b, CMV-Fny-*sat*Yn12, CMV-Fny-*sat*T1 and ToMV-N5 were compared to mock inoculation, the expression of miR156, miR159, miR319 and miR396 decreased in all of the five infections, while miR398 was found to have increased. Besides this, the expressions of miR168, miR397 and miR403 increased in CMV-Fny, CMV-Fny-*sat*Yn12, CMV-Fny-*sat*T1 and ToMV-N5 infection, but no obvious alterations were found in CMV-Fny Δ 2b infection. On the contrary, the expression of miR171 and miR395 decreased in other infections, but increased or were unchanged in CMV-Fny Δ 2b infection. Thus, this may bring a molecular physiological explanation for stimulation of tomato growth.

Different viruses may act at distinct steps in the gene-silencing mechanism, which results in different miRNAs expression profiles of host plants. CMV-Fny and ToMV-N5 are common severe viral pathogens occurring in the tomato, but the microarray data showed that their miRNAs expression profiles were rather different. The altered miRNAs have been reported to regulate the expression of genes *SBP-like*, *ARF*, *HD-ZIP*, *AGO*, *SCARECROW*, *F-box* and *UBC*, all of which are transcription factors and found to be involved in important biological metabolism processes. Therefore, their expression levels might result in different symptoms development in tomato seedlings.

In conclusion, the majority of miRNAs from an “unknown” new species to be studied can be “predicated” and identified with such a plant miRNA microarray based on the documented records of other species. Because of the high throughput character of the microarray, its application in nucleic acid detection has major advantages, especially for quantitative comparison studies. With the increasing number of available plant genes sequenced, this technology has proven to be highly sensitive and reproducible in miRNA detection, and suitable to investigate the overall miRNA expression profiles (Axtell and Bartel, 2005). To survey the conserved miRNAs expression profiles in the tomato and their expression after infection with viruses which bring different symptom development, 105 tomato miRNAs were detected/identified from tomato leaf tissues, and more miRNAs could be expected from different developing stages and other tissues. We can also see that virus infection could alter miRNAs expressions in both inducing and suppressing ways, but unlike the majority of foliage miRNAs, some other tomato miRNAs showed no differential expression upon virus infection.

A different virus may act at distinct steps in the gene-silencing mechanism, which results in different miRNAs expression profiles of host plants. CMV-Fny and ToMV-N5 are common severe viral pathogens occurring in the tomato, but the microarray data showed that their miRNAs expression profiles were rather different. The altered miRNAs have been reported to regulate the expression of genes *SBP-like*, *ARF*, *HD-ZIP*, *AGO*, *SCARECROW*, *F-box* and *UBC*, all of which are transcription factors and found to be involved in important biological metabolism processes. Therefore, they might result in different symptoms development in tomato seedlings.

5.5 Tomato miRNA Response to Virus Infection Quantified by Real-time RT-PCR

Virus infection in host plants often has an obvious influence on plant development. To identify the molecular mechanisms of gene expression and interaction through miRNA pathways, application of the novel miRNA quantification method is required. Using tomato inoculated by CMV and TAV as host plants, a stem-loop reverse transcription followed by SYBR Green PCR assay is to be introduced. The miRNAs and their targets with their amplification primers are listed in Table 5.10. For the seven tested tomato miRNAs, this quantification method showed high sensitivity, specificity and broad dynamic range. Precise quantification can be achieved with as little as 0.01 ng of total RNAs in most cases. Additionally, the mRNA targets can be quantified from the same RNA sample simultaneously, by conventional real-time PCR assay. In comparison with mock inoculation, accumulation levels of miRNAs and mRNA targets are found obviously altered, and their quantification by the above method indicated that the miRNA pathway is interrupted by inoculating CMV and TAV. The utilization of stem-loop RT-PCR will accelerate research on the relationship between virus infection and disease symptoms in plants. Efficient and reliable detection of miRNAs is the essential first step towards understanding their potential roles in virus plant interaction. By setting up a consensus system, whereby alteration of miRNA pathways involved in virus infection is determined, the stem-loop real-time RT-PCR protocol to quantitative determination of miRNAs, firstly proposed by Chen et al. (2005), has been successfully used to quantify the miRNAs profile in human disease-related study and other fields (Raymond et al., 2005; Schmittgen et al., 2008; Tang et al., 2006, Feng et al., 2009). The use of stem-loop RT primers in miRNA quantification assays has demonstrated higher specificity and sensitivity than conventional linear ones, due largely to additional base stacking and spatial constraint of the stem-loop structure (Chen et al., 2005; Anwar et al., 2006). The base stacking can improve the thermal stability and the efficiency of RT reaction, while the spatial constraint of the stem-loop structure may prevent it from binding miRNA precursors or double-stranded genomic DNA molecules and, therefore, eliminate the need for a special fraction of small RNAs from total RNAs. Thus, in

parallel with the conventional real-time RT-PCR assay, both mature miRNAs and their target mRNAs could be assayed from the same RNA sample simultaneously. This is important in plant and animal tissue, but more important for human tissue, where the amount of the sample is limited.

Table 5.10 Primers used for stem-loop real-time RT-PCR assay of several miRNAs

Target miRNA	Primer	Sequence
miR159	RT	GCGTGGTCCCGACCACCACAGCCGCCACGACCACGCT AGAGC
	Forward primer	CGTGCGTTTGGATTGAAGG
	Reverse primer	TCCCGACCACCACAGCC
miR162	RT	GCGTGGTCCCGCAGCACCTCAGCCGCCACGACCACGCC TGGATGC
	Forward primer	CGCAGCGTCGATAAACCTCT
	Reverse primer	TCCGCAGCACCTCAGCC
miR164	RT	GCGTGGTCCACACCAGTTGACGGGCGACGACCACGC TGCACG
	Forward primer	CACGATGGAGAAGCAGGGC
	Reverse primer	CCACACCAGTTGACGGGC
miR165/166	RT	CTCAGCGGCTGTCGTGGACTGCGCGCTGCCGCTGAGG GGGRATG
	Forward primer	CTGTGTCGGACCAGGCTTC
	Reverse primer	GGCTGTGCTGGACTGCG
miR167	RT	GCGTGGTCCACACCACCTGAGCCGCCACGACCACGCT AGATCAT
	Forward primer	CGTGCGTGAAGCTGCCA
	Reverse primer	TCCACACCACCTGAGCCG
miR168	RT	CTCAGCGGCTGTCGTGGACTGGGTGCTGCCGCTGAGT TCCCGAC
	Forward primer	CGTGTGTCGCTTGGTGCA
	Reverse primer	GGCTGTGCTGGACTGGGTG
miR171	RT	GCGTGGTCCACACCACCTGAGCCGCCACGACCACGC GATATTGG
	Forward primer	CGTGCGTGATTGAGCCGT
mRNA	Reverse primer	TCCACACCACCTGAGCCG
	Primer	Sequence
MYB	Forward primer	TATTGAGATGCGGAAAGAGTTGC
	Reverse primer	ATCTGTTCGTCCTGGTAATCTTGC
ARF8	Forward primer	TGGGAAAGGAAGAGGCTGAA
	Reverse primer	GCGATCCAAGAGATGGCATT
AGO1-1	Forward primer	TGGATCAGTAACAAGCGGAGC
	Reverse primer	TTGAGAGCAGGAAGAGGTCTAACAG
AGO1-2	Forward primer	ATGGAACCAGAGACATCTGACGG
	Reverse primer	CCTTACAGCAGCACCAACACC
SCL	Forward primer	GATGGAGCTATGTTGTTGGGATG
	Reverse primer	CCACCAGCTGTCCTTTCG

When comparing the SYBR Green-based stem-loop assay with the TaqMan assay, the latter requires the synthesis and optimization of a specific probe for each

of the miRNAs. On the other hand, the SYBR Green assay may be considered to lose a certain amount of specificity by eliminating the miRNA-specific probe, but it is more efficient by reducing the time and cost of developing method. Moreover, the SYBR Green stem-loop real-time RT-PCR analysis always displays a higher degree of sensitivity, specificity and wide dynamic ranges, which can easily detect miRNAs expression accurately at the 0.01 ng level of total RNAs. Stratford et al. (2008) also reported similar siRNA quantification results obtained using the TaqMan and SYBR Green assays. Experimentally, the SYBR Green assay was more convenient and efficient than SYBR Green assays, especially when large numbers of different miRNA sequences are tested. Primers used for stem-loop real-time RT-PCR assays of several miRNAs are given in Table 5.10.

5.5.1 Identification of Tomato ARF8- and AGO1-like Genes

A major challenge in understanding the biological function of miRNAs is to spot their target genes and their potential interactions. Using primers designed according to the reports from other plant species, one ARF8-like fragment of 686 bp and two AGO1-like fragments of 456 bp and 458 bp were amplified and sequenced from the tomato variety Hezuo903. These sequences were deposited in the GenBank under the accession numbers FJ222762, FJ222763 and FJ222764 respectively. For an expected ARF8-like sequence, it displayed 84.4% identity to tomato ARF8 recorded in the NCBI database (EF667342) and 56.3% to ARF6 from *Arabidopsis* (AF013467) at the amino acid level. Beside this, the complementary site against miR167 was recognized in FJ222762 at position 43–63 (Fig. 5.12), thus it was considered as a target of miR167 of the tomato. For the two AGO1-like sequences, they shared sequences identity of 73.2% to each other. Although no complementary sequences against miR162 were contained from the present database for the tomato genome, their putative translated protein showed high levels of identity (82.2%–93.2%) to AGO1 of *N. benthamiana* (DQ321489, DQ321488), and 74.0%–78.1% identity to AGO1 of *Arabidopsis* (NM.179453). Accordingly, the two obtained AGO1-like mRNA might actually represent alleles of a single AGO1-like gene in the tomato.



Fig. 5.12. Identification of tomato ARF8-like and AGO1-like genes. (a) Alignment of the translated ARF8-like protein (FJ222762) with *Arabidopsis* ARF6 (AF013467) and tomato ARF8 (EF667342); (b) Diagrammatic representation of putative miR167 interaction site in the sequence of ARF8-like gene. The putative interaction site is shown as a gray box, with the nucleotide position within the ARF8-like gene indicated. The miRNA sequence and partial sequence of the target mRNA is shown in the expanded regions. Four mismatched base pairings are shown; (c) Alignment of the two translated AGO1-like proteins with *Arabidopsis* AGO1 (NM179453) and two tobacco AGO1 (DQ321488, DQ321489)

5.5.2 Analytical Validation of Real-time RT-PCR for Amplification of miRNAs

The initial step in the real-time RT-PCR quantification assay is to validate the designed primers for each amplification fragment. Using the designed primers, all the reactions produced amplicons of expected size with no additional products, and their dissociation curves showed single peaks. As a further validation, these amplicons have been cloned, and the sequence data verified that 100% of the expected sequences could be specifically amplified, indicating that each

microRNA was amplified specifically by its primers.

To further test the sensitivity and accuracy of the assay, total RNAs obtained from 0.1 g leaf tissues are serially diluted 10-fold and subjected to real-time RT-PCR assay of each gene. The assays showed excellent linear relationships between the log concentrations of template RNA and C_T values (Fig. 5.13). All miRNA assays have slopes ranging from -2.81 to -3.17, with the PCR efficiencies within the acceptable range of 106.68% to 126.64% (Table 5.11). The dissociation temperatures ranged from 84.1 to 85.5°C, suggesting they were from target-specific amplifications.

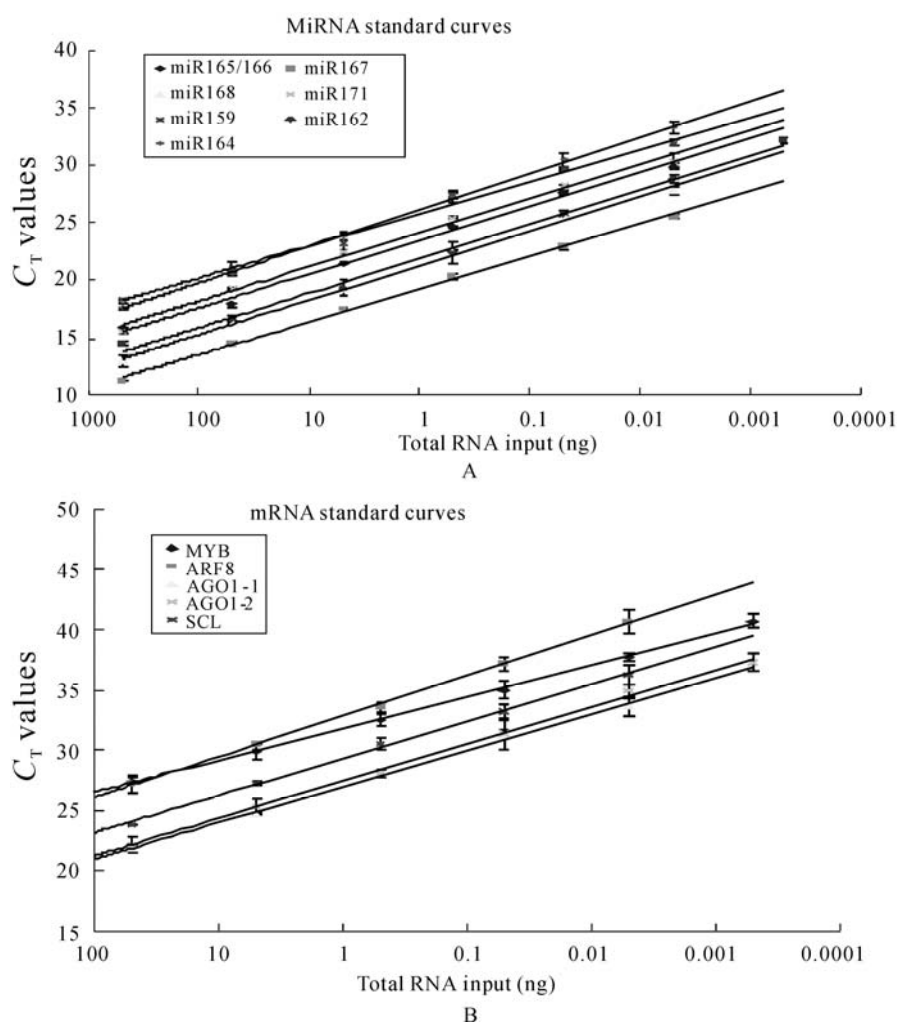


Fig. 5.13. Standard curves of studied miRNAs and target mRNAs. Correlation of total RNA input to the threshold of cycle (C_T) values for seven miRNA assays (a) and for five targets mRNAs assays (b). Total RNA input ranged from 0.0005 to 500 ng per RT reaction for miRNAs standard curves construction, and 0.0005 to 50 ng for mRNAs standard curves construction

Table 5.11 Efficiency of amplification for seven miRNAs and five target mRNAs in tomato.

Target	Avg. slope	Std. dev. slope	r^2	Avg. eff. (%)	T_m of amplification (°C)
miRNA					
miR159	-2.81	0.464	0.986	126.64	84.1
miR162	-3.01	0.276	0.995	115.20	85.5
miR164	-3.17	0.224	0.999	106.68	84.9
miR165/166	-2.94	0.574	0.995	118.83	84.6
miR167	-2.85	0.301	0.997	124.64	84.3
miR168	-3.00	0.370	0.998	115.62	84.9
miR171	-2.97	0.503	0.994	117.35	84.3
mRNA					
MYB	-2.63	0.198	0.999	139.79	79.4
ARF8	-3.37	0.179	0.999	98.21	83.1
AGO1-1	-3.01	0.531	0.997	115.15	86.0
AGO1-2	-3.08	0.160	0.998	111.39	86.3
SCL	-3.07	0.299	0.998	111.67	81.3

For the five target mRNAs, their real-time RT-PCR primers were also firstly validated by the amplicon size on agarose gel and then by dissociation curve analysis (dissociation temperatures ranged from 79.4 to 86.3°C). Using the serially diluted total RNAs, the slopes of the standard curves of these genes ranged from -2.63 to -3.37, indicating PCR efficiencies ranging from 98.21% to 139.79%. These results demonstrated that these real-time RT-PCR assays displayed dynamic ranges of at least five logs of magnitude and were capable of quantifying miRNAs and their target mRNAs.

5.5.3 *Quantification of Tomato miRNAs Expression by Stem-loop Real-time RT-PCR*

Taking the advantages of RT-PCR assays, the expression patterns of a limited number of miRNAs can be firstly determined by the time course, to reflect the reality of the miRNA function during plant development. Here, tomato seedlings inoculated with a strain of CMV and TAV from *Cucomoviruses* at 10, 20 and 30 dpi, respectively, are investigated for their miRNA expression. Although different phenotypes are elicited in tomato seedlings infected by the two viruses, CMV-Fny causes systemic mosaic with mild leaf distortion, whereas TAV-Bj induces stunting, reduced internodal distances, mosaic and pronounced lobing of leaves. Elevated levels of most of the 7 miRNAs tested are detected after viral infections (Fig. 5.14). Among these miRNAs, miR159, miR162, miR168 and miR171 showed

significant expression level changes, while the expressions of miR164, miR165/166, and miR167 were less affected.

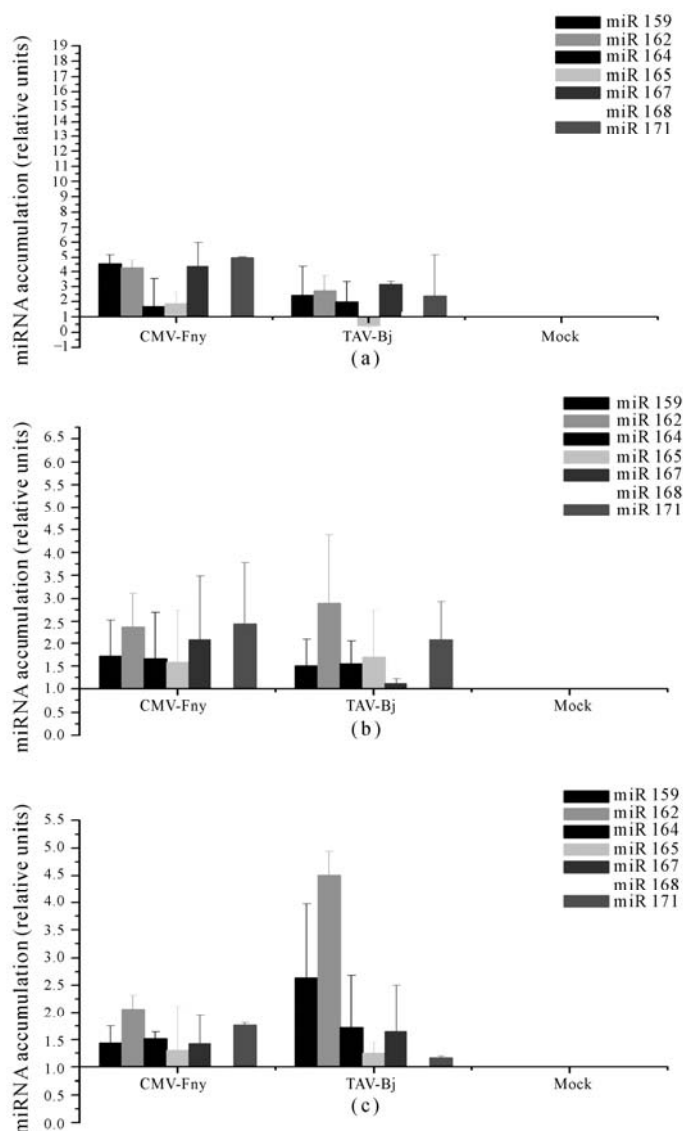


Fig. 5.14. Quantitative analyses of seven miRNAs using stem-loop real-time RT-PCR. (a) At 10 dpi; (b) At 20 dpi; (c) At 30 dpi. The expression level of each miRNA in mock was set as 1, and that in CMV-Fny and TAV-Bj infection was quantified relative to it, using the $2^{-\Delta\Delta C_t}$ method. 18S rRNA was chosen as an endogenous control. The results were obtained from three independent experiments, and the considerable error bars might result from the changed culture conditions, different host plants, different total RNAs isolation steps, etc.

Compared to the TAV-Bj-inoculated tomato seedlings, higher accumulation levels of miRNAs at 10 dpi in CMV-Fny infection were found. However, there were comparable levels found in both infections at 20 dpi, and higher levels of most miRNAs in TAV-Bj infection at 30 dpi. It indicates that CMV infection may bring a quicker response of host reaction but a slower response of host reaction occurs in TAV infection, and the interactions develop into more severe symptoms in TAV infection in the tomato. Besides these, the most significant increase was found in miR168 in CMV-Fny infection at 10 dpi (15.2 folds); whereas in TAV-Bj infection it was miR162 at 30 dpi (4.5 folds). These observations may be a result of the different effects of CMV-Fny and TAV-Bj infection on the expression of certain miRNAs.

5.5.4 Quantification of miRNAs Targets in Tomato under Cucumovirus Infection

Target mRNAs of miRNAs could be quantified in parallel together against their miRNA. To systematically analyze the effects of virus infection on miRNA pathways in the tomato, the transcript levels and accumulations of AGO1, ARF8, MYB and SCL6, as targets of miRNAs 168, 167, 159 and 171, respectively, are quantitatively determined by real-time RT-PCR. Under the experimental conditions described above, the expression levels of these target mRNAs are found generally to be variably enhanced, after CMV-Fny or TAV-Bj infections. Amongst these, ARF8 is the most severely affected, for it showed a significant and constitutive up-regulation in expression levels at all the three detection time points, while the effect of virus infection on MYB and AGO1 was severe at 10 and 20 dpi but moderate at 30 dpi, whereas the expression of SCL displayed the smallest change. Despite the different accumulation levels of miR162 and miR168 between CMV-Fny and TAV-Bj infections, no apparent differences between the two expressions of their target mRNAs are observed (Fig. 5.15). From these results, an increase in expression of the tested miRNAs is found and target mRNAs are common features after CMV-Fny and TAV-Bj infection.

It was found that CMV-Fny and TAV-Bj infection in tomato caused elevated levels of both miRNAs and their target mRNAs. According to the suggestion of Zhang et al. (2006), these results were due to the blocked cleavage activity of AGO1 by viral silencing suppressors through direct protein-protein interaction. In plants, the miRNA pathway is negatively regulated by miR162 and 168 through targeting *DCL1* and *AGO1* mRNAs, respectively. Such feedback regulation is important to achieve an appropriate balance of steady-state miRNA levels, which depend on miRNA production by *DCL1* and miRNA stabilization by AGO1 (Vaucheret et al., 2004). Thus, inhibition, by silencing suppressor, of miR162-guided cleavage of *DCL1* mRNA may result in higher *DCL1* protein levels, which, in turn, promotes additional maturation of miRNAs from pre-miRNAs. Meanwhile, the accumulation levels of target mRNAs are also

increased because their cleavage by AGO1 is blocked. This would explain why the overall levels of miRNAs and mRNAs increased after virus infection.

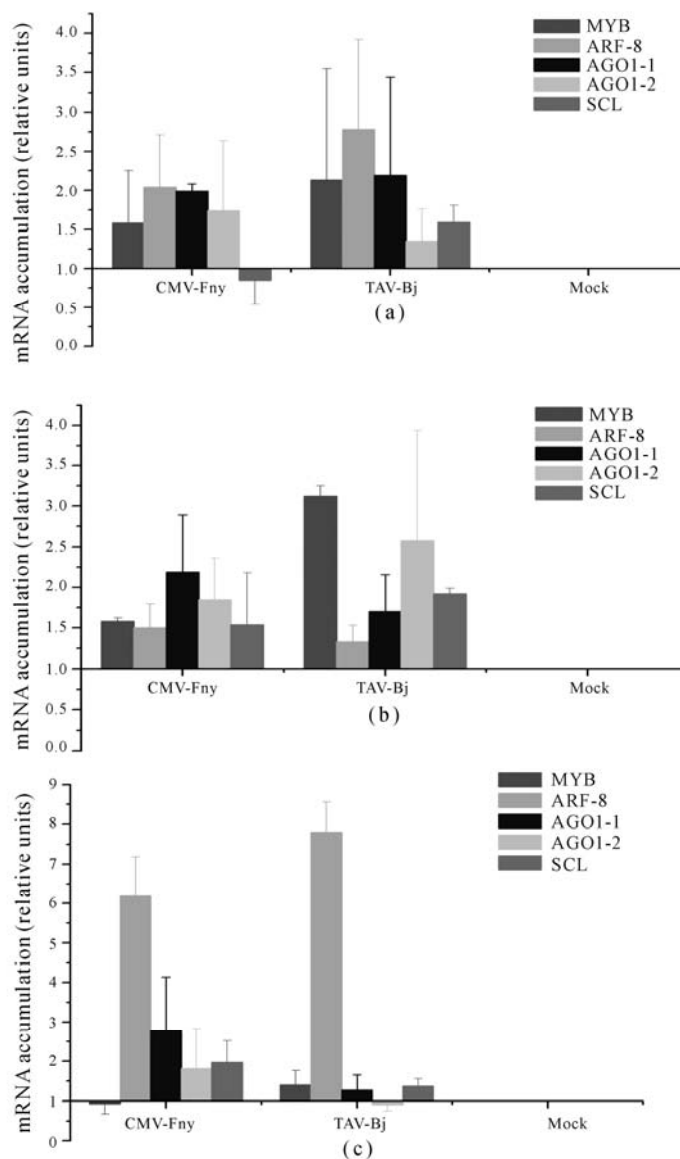


Fig. 5.15. Comparison of the expression levels of five mRNAs in CMV-Fny and TAV-Bj infected tomato leaves, using real-time RT-PCR. (a) At 10 dpi; (b) At 20 dpi; (c) At 30 dpi. The expression level of each mRNA was firstly normalized against 18s rRNA, and the relative abundance was quantified as described in Fig. 5.15 Both the transcript levels of AGO1-like-1 and AGO1-like-2 were determined by different primers. The results were the average of three independent experiments, and the considerable error bars might result from the reasons mentioned in Fig. 5.15

Different expression/accumulation levels of miRNAs in CMV-Fny and TAV-Bj infection at the three detection time points, could not rule out a direct correlation between the severity of the symptoms and the alteration in levels of the tested miRNAs, since the developmental anomalies elicited by virus infection result from a more complex biological process, in which both miRNAs and target mRNAs, as well as other regulatory factors, may be involved. The significant increase in expression levels of miR159, miR162 and miR168 after CMV-Fny infection is concordant with those reported by Zhang et al. (2006) in *Arabidopsis*. It could be calculated that the quicker response of tomato tissue to CMV infection brings less destruction/symptom to the host, while its slower response to TAV infection brings more severe damage/symptoms to the host, since both viruses belong to Cucumoviruses and their mechanisms in pathogenicity are comparable. It has been proved that although certain miRNAs displayed considerably different expression changes between the CMV-Fny and TAV-Bj infections, the expression changes of tested target mRNAs were very similar, suggesting a similar mechanism in perturbing miRNA pathways.

References

- Achard P, Herr A, Baulcombe DC, et al.(2004) Modulation of floral development by a gibberellin-regulated microRNA. *Development* 131(14): 3357-3365.
- Anwar A, August JT and Too HP (2006) A stem-loop-mediated reverse transcription real-time PCR for the selective detection and quantification of the replicative strand of an RNA virus. *Anal Biochem* 352(1): 120-128.
- Aukerman MJ and Sakai H (2003) Regulation of flowering time and floral organ identity by a MicroRNA and its APETALA2-like target genes. *Plant Cell* 15(11): 2730-2741.
- Bazzini AA, Hopp HE, Beachy RN, et al.(2007) Infection and co-accumulation of *Tobacco mosaic virus* proteins alter microRNA levels, correlating with symptom and plant development. *Proc Natl Acad Sci USA* 104(29): 12157-12162.
- Bonnet E, Wuyts J, Rouze P, et al.(2004) Detection of 91 potential conserved plant microRNAs in *Arabidopsis thaliana* and *Oryza sativa* identifies important target genes. *Proc Natl Acad Sci USA* 101(31): 11511-11516.
- Carrington JC and Ambros V (2003) Role of microRNAs in plant and animal development. *Science* 301(5631): 336-338.
- Chapman EJ and Carrington JC (2007) Specialization and evolution of endogenous small RNA pathways. *Nat Rev Genet* 8(11): 884-896.
- Chen C, Ridzon DA, Broomer AJ, et al.(2005) Real-time quantification of microRNAs by stem-loop RT-PCR. *Nucleic Acids Res* 33(20): e179.
- Chen X (2004) A microRNA as a translational repressor of APETALA2 in *Arabidopsis* flower development. *Science* 303: 2022-2025.
- Chen X (2005) MicroRNA biogenesis and function in plants. *FEBS Lett* 579(26): 5923-5931.
- Chuck G., Candela H and Hake S (2009) Big impacts by small RNAs in plant development. *Curr Opin Plant Biol* 12(1): 81-86.

- Feng J, Wang K, Liu X, et al.(2009) The quantification of tomato microRNAs response to viral infection by stem-loop real-time RT-PCR. *Gene* 437(1-2): 14-21.
- Feng J, Zeng R and Chen J (2008) Accurate and efficient data processing for quantitative real-time PCR using a tripartite plant virus as a model. *Biotechniques* 44(7): 901-912.
- Finnegan EJ and Matzke MA (2003) The small RNA world. *J Cell Sci* 116(Pt 23): 4689-4693.
- Floyd SK and Bowman JL (2004) Gene regulation: ancient microRNA target sequences in plants. *Nature* 428(6982): 485-486.
- Gao X, Gulari E and Zhou X (2004) In situ synthesis of oligonucleotide microarrays. *Biopolymers* 73(5): 579-596.
- Guo HS, Xie Q, Fei JF, et al.(2005) MicroRNA directs mRNA cleavage of the transcription factor NAC1 to down-regulate auxin signals for arabidopsis lateral root development. *Plant Cell* 17(5): 1376-1386.
- Itaya A, Bundschuh R, Archual AJ, et al.(2008) Small RNAs in tomato fruit and leaf development. *Biochim Biophys Acta* 1779(2): 99-107.
- Jack T (2004) Molecular and genetic mechanisms of floral control. *Plant Cell* 16 Suppl: S1-17.
- Jones-Rhoades MW and Bartel DP (2004) Computational identification of plant microRNAs and their targets, including a stress-induced miRNA. *Molecular Cell* 14(6): 787-799.
- Jorda L, Conejero V and Vera P (2000) Characterization of P69E and P69F, two differentially regulated genes encoding new members of the subtilisin-like proteinase family from tomato plants. *Plant Physiol* 122(1): 67-74.
- Jorda L and Vera P (2000) Local and systemic induction of two defense-related subtilisin-like protease promoters in transgenic *Arabidopsis* plants. Luciferin induction of PR gene expression. *Plant Physiol* 124(3): 1049-1058.
- Kasschau KD, Xie Z, Allen E, et al.(2003) P1/HC-Pro, a viral suppressor of RNA silencing, interferes with *Arabidopsis* development and miRNA unctioin. *Dev Cell* 4(2): 205-217.
- Kavroulakis N, Papadopoulou KK, Ntougias S, et al.(2006) Cytological and other aspects of pathogenesis-related gene expression in tomato plants grown on a suppressive compost. *Ann Bot (Lond)* 98(3): 555-564.
- Kurihara Y and Watanabe Y (2004) Arabidopsis micro-RNA biogenesis through Dicer-like 1 protein functions. *Proc Natl Acad Sci U S A* 101(34): 12753-12758.
- Laufs P, Peaucelle A, Morin H, et al.(2004) MicroRNA regulation of the CUC genes is required for boundary size control in *Arabidopsis* meristems. *Development* 131(17): 4311-4322.
- Lee RC, Feinbaum RL and Ambros V (1993) The *C. elegans heterochronic* gene lin-4 encodes small RNAs with antisense complementarity to lin-14. *Cell* 75(5): 843-854.
- Lewsey M, Robertson FC, Canto T, et al.(2007) Selective targeting of miRNA-regulated plant development by a viral counter-silencing protein. *Plant J* 50(2): 240-252.
- Lu C, Kulkarni K, Souret FF, et al.(2006) MicroRNAs and other small RNAs enriched in the Arabidopsis RNA-dependent RNA polymerase-2 mutant. *Genome Res* 16(10): 1276-1288.
- Mallory AC, Bartel DP and Bartel B (2005) MicroRNA-directed regulation of *Arabidopsis* AUXIN RESPONSE FACTOR17 is essential for proper development

- and modulates expression of early auxin response genes. *Plant Cell* 17(5): 1360-1375.
- Mallory AC, Dugas DV, Bartel DP, et al.(2004) MicroRNA regulation of NAC-domain targets is required for proper formation and separation of adjacent embryonic, vegetative, and floral organs. *Current Biology* 14(12): 1035-1046.
- Millar AA and Gubler F (2005) The *Arabidopsis* GAMYB-like genes, MYB33 and MYB65, are microRNA-regulated genes that redundantly facilitate anther development. *Plant Cell* 17(3): 705-721.
- Ori N, Cohen AR, Etzioni A, et al.(2007) Regulation of LANCEOLATE by miR319 is required for compound-leaf development in tomato. *Nat Genet* 39(6): 787-791.
- Palatnik JF, Allen E, Wu X, et al.(2003) Control of leaf morphogenesis by microRNAs. *Nature* 425(6955): 257-263.
- Palukaitis P and Garcia-Arenal F (2003) Cucumoviruses. *Adv Virus Res* 62: 241-323.
- Park MY, Wu G, Gonzalez-Sulser A, et al.(2005) Nuclear processing and export of microRNAs in *Arabidopsis*. *Proc Natl Acad Sci U S A* 102(10): 3691-3696.
- Pilcher RL, Moxon S, Pakseresht N, et al.(2007) Identification of novel small RNAs in tomato (*Solanum lycopersicum*). *Planta* 226(3): 709-717.
- Raymond CK, Roberts BS, Garrett-Engele P, et al.(2005) Simple, quantitative primer-extension PCR assay for direct monitoring of microRNAs and short-interfering RNAs. *RNA* 11(11): 1737-1744.
- Reinhart B, Weinstein EG, Rhoades MW, et al.(2002) MicroRNAs in plants. *Genes Dev* 16(13): 1616-1626.
- Ru P, Xu L, Ma H and Huang H (2006) Plant fertility defects induced by the enhanced expression of microRNA167. *Cell Res* 16(5): 457-465.
- Schmittgen TD, Lee EJ, Jiang J, et al.(2008) Real-time PCR quantification of precursor and mature microRNA. *Methods* 44(1): 31-38.
- Schwab R, Palatnik JF, Riester M, et al.(2005) Specific effects of microRNAs on the plant transcriptome. *Dev Cell* 8(4): 517-527.
- Stratford S, Stec S, Jadhav V, et al.(2008) Examination of real-time polymerase chain reaction methods for the detection and quantification of modified siRNA. *Anal Biochem* 379(1): 96-104.
- Sunkar R, Girke T, Jain PK, et al.(2005) Cloning and characterization of microRNAs from rice. *Plant Cell* 17(5): 1397-1411.
- Sunkar R and Zhu JK (2004) Novel and stress-regulated microRNAs and other small RNAs from *Arabidopsis*. *Plant Cell* 16(8): 2001-2019.
- Tang F, Hajkova P, Barton SC, et al.(2006) MicroRNA expression profiling of single whole embryonic stem cells. *Nucleic Acids Res* 34(2): e9.
- Tsuji H, Aya K, Ueguchi-Tanaka M, et al.(2006) GAMYB controls different sets of genes and is differentially regulated by microRNA in aleurone cells and anthers. *The Plant Journal* 47(3): 427-444.
- Vance V and Vaucheret H (2001) RNA silencing in plants--defense and counterdefense. *Science* 292(5525): 2277-2280.
- Vaucheret H, Vazquez F, Crete P, et al.(2004) The action of ARGONAUTE1 in the miRNA pathway and its regulation by the miRNA pathway are crucial for plant development. *Genes Dev* 18(10): 1187-1197.
- Voinnet O (2001) RNA silencing as a plant immune system against viruses. *Trends in Genetics* 17(8): 449-459.
- Voinnet O (2005) Induction and suppression of RNA silencing: insights from viral

- infections. *Nat Rev Genet* 6(3): 206-220.
- Wang XJ, Reyes JL, Chua NH, et al.(2004) Prediction and identification of *Arabidopsis thaliana* microRNAs and their mRNA targets. *Genome Biol* 5(9): R65.
- Wu G and Poethig RS (2006) Temporal regulation of shoot development in *Arabidopsis thaliana* by miR156 and its target SPL3. *Development* 133(18): 3539-3547.
- Wu MF, Tian Q and Reed JW (2006) *Arabidopsis* microRNA167 controls patterns of ARF6 and ARF8 expression, and regulates both female and male reproduction. *Development* 133(21): 4211-4218.
- Xie FL, Huang SQ, Guo K, et al.(2007).Computational identification of novel microRNAs and targets in *Brassica napus*. *FEBS Lett* 581(7): 1464-1474.
- Xie K, Wu C and Xiong L (2006) Genomic organization, differential expression, and interaction of SQUAMOSA promoter-binding-like transcription factors and microRNA156 in rice. *Plant Physiol* 142(1): 280-293.
- Xie Z, Allen E, Fahlgren N, et al.(2005) Expression of *Arabidopsis* MIRNA genes. *Plant Physiol* 138(4): 2145-2154.
- Xie Z, Kasschau KD and Carrington JC (2003) Negative feedback regulation of Dicer-Like1 in *Arabidopsis* by microRNA-guided mRNA degradation. *Curr Biol* 13(9): 784-789.
- Yang JH, Han SJ, Yoon EK, et al.(2006) Evidence of an auxin signal pathway, microRNA167-ARF8-GH3, and its response to exogenous auxin in cultured rice cells. *Nucleic Acids Res* 34(6): 1892-1899.
- Zhang B, Pan X, Cobb GP, et al.(2006) Plant microRNA: a small regulatory molecule with big impact. *Dev Biol* 289(1): 3-16.
- Zhang J, Zeng R, Chen J, et al.(2008) Identification of conserved microRNAs and their targets from *Solanum lycopersicum* Mill. *Gene* 423(1): 1-7.

Genomic Characterization of New Viruses with Double Stranded RNA Genomes

6.1 Introduction

In general, numerous dsRNAs, varying from 50bp to 5,000 bp in size can be easily extracted and harvested from 0.5 g to 10 g of fresh plant leaf tissue by using presently founded methodology (Chen et al., 2006; Dodds et al., 1984; Morris and Dodds, 1979).

The appearance of dsRNAs is mostly considered as the evidence of virus invaders, such as either a virus with a double-stranded genome, or the trace of replication of ssRNA viruses. It is commonly assumed that dsRNA is generated by viral RNA polymerases either as a replicating intermediate of the viral genome (RNA viruses) or as an erroneous product, due to converging bidirectional transcription (DNA viruses) (Jacobs and Langland, 1996; Kumar and Carmichael, 1998; Weber et al., 2006). Some have explained dsRNAs as the combination of a full-length negative stranded RNA template with their offspring strands during preparation and extraction. For viruses which have a double stranded genome, a relatively high concentration of unique size dsRNA segments is easy to understand. What is the function of these full-length double stranded RNAs during the replication of single stranded RNA viruses (even some DNA viruses)? Recognizing the origin and function of these dsRNAs is a key to thoroughly realizing the mechanisms of virus replication to date.

In recent years, the discovery of siRNA and miRNA gave more motivation to study dsRNAs, by which both siRNA and miRNA realize their function for preventing gene expression (Bartel, 2004; Bernstein et al., 2001; Fire et al., 1998). And in the author's experiences, larger dsRNAs up to 10 kbp and over (e.g., those dsRNAs for potyviruses) could be extracted with normal methodology. Among the commercialized reagents or documented protocols, few are related to the preparation of dsRNAs. In the case of the development of novel methods, smaller and larger dsRNA segments will be easily collected on a large scale; the study of dsRNAs will bring more exciting scientific progress.

Is dsRNA the most important forefather of our macromolecules? There is no doubt we can see the explicative role of dsRNA molecules, and it is more stable and reliable than ssRNA. Research results have provided the enzymatic activity of ssRNAs with dsRNAs zones (e.g., hairpin structure, stem-loop structure) (Doherty and Doudna, 2001; Lincoln and Joyce, 2009), and also the banding capacity of dsRNAs with proteins (Child et al., 2006; Fenner et al., 2007; Tian et al., 2004).

The need for so many dsRNA molecules to remain in eukaryotic cells may tell us their basic origination or function, and will possibly give us a key to enter a new world of biological investigation.

As said by Carter and De Clercq (1974), "Namely, each deviation from a perfect double-helical arrangement introduces the possibility for emphasizing one biological reactivity at the expense of another. This latter structure-activity property may partially account for the extreme apparent diversity, commonly encountered, in the presentations of virology illness". The significance of dsRNA structure in virus infection and replication was noticed long ago, but little evidence was drawn together until now. It is time to pay attention to those ignored macromolecules in general.

Like higher plants, fungi are commonly infected by viruses, but the genome of mycoviruses is of a double stranded property (Ghabrial and Suzuki, 2009; Hollings, 1978; Lemke and Nash, 1974; McCabe et al., 1999). Among their hosts, there are plant pathogenic fungi and endophytic fungi which coexist with plants that are widely infected by RNA viruses. Based on the present point of view, the reason for most plant viruses using a single stranded genome but fungal viruses mostly using a double stranded genome is seldom considered. In the author's view point, the existence of plant-infecting viruses with a dsRNA genome is greatly underestimated.

In the past few decades, some dsRNA viruses have been isolated from plant tissues. In this chapter, several plant-infecting double stranded RNA genomes are introduced, with regard to their occurrence, damage to plant hosts, origination relationship with mycoviruses, and with a special emphasis on their dsRNA/protein functions.

6.2 Novel dsRNA Viruses Infecting *Raphanus Sativus*

Crops from the family *Cruciferae*, such as rapeseed (*Brassica napus*), cabbage (*Brassica oleracea* L.), Chinese cabbage (*Brassica pekinensis*) and stem mustard (*Brassica juncea* var. Tsatsai), are found commonly to be infected by *Turnip mosaic virus* (TuMV) and CMV. And from tissues of the host plant infected by the CMV, dsRNAs are easily detected. As a worldwide-distributed vegetable crop, radish (*Raphanus sativus* L.) is an herbaceous plant belonging to the family *Cruciferae*, but originated independently from *Brassica* crops. And it is cultivated mainly for its enlarged hypocotyl and taproot, but it has been said that radish leaves are used for culinary and medicinal uses in some particular varieties. In

China, there is a saying “radish is a kind of small ginseng” which is hundreds of years old.

In the last few decades, the extract from a kind of red radish was found to have possible anti-virus and anti-tumor effects with the capability of inducing interferon *in vivo* (Wang et al., 1988; Xu and Li, 2001; Xu et al., 1987). Further studies have proved that the most possible active principles in the extracts are the double-stranded RNAs (dsRNA) contained in them. Two different views had been proposed for the origins of dsRNA from radish tissues, that is originating from normal cells or from virus-infected cells (Libonati et al., 1980).

Radish yellow edge virus (RYEV) was firstly described as a seed borne dsRNA virus found in Japan in 1979 (Natsuaki et al., 1979), with five dsRNA fragments detected from yellow edged radish plants when analyzed by polyacrylamide gel electrophoresis (Natsuaki et al., 1983), but there was few consequent reports and concern about this phenomenon. When a radish variety Yidianhong was firstly noticed for containing multi-segments of dsRNAs, in China, the discovery of common infection by dsRNA viruses from this crop became much noticed. During the past five years, more than five viruses, all of them dsRNA genomes, have been discovered in the variety Yidianhong, with all the spherical particles, and more novel viruses have also been detected in other varieties. Based on the genomic characterizations of dsRNA viruses infecting this plant and the involvement of more viruses occurring in the radish, new nomenclature and a classification should be considered and re-arranged.

6.2.1 Yellow Edge Symptoms and dsRNA Patterns in the Radish

Yellow edge symptoms are commonly observed across radish plants of different varieties grown in the field. The symptoms are not obvious at the seedling stages but become obvious in the developing stages before blossoming, in spring. Taking the Yidianhong variety as an example, yellow edges often appear, between the fourth and sixth leaf stages, and the symptoms appear firstly in the newly-growing leaves. The plants developing yellow spot, are obviously stunted with distortion at later stages, and give blossom and fruit when the symptoms become severe. At the blossoming stage, leaves on the lower parts become dry and die while the whole plant remains alive (Fig. 6.1).

To find out the occurrence and development of yellow edge symptoms, seeds of fourteen radish cultivars were collected from different areas in China, and then pot-cultivated in the greenhouse. During the early growing stages, the seedlings present few symptoms, such as light or dark green chlorosis, an occasional yellowing edge or edge chlorosis, leaf rolling and uneven leaves. Such symptoms disappear or are enhanced during plant development, but it is hard to tell the unhealthy plants from the healthy ones, and dsRNA segments are commonly identified from all those seedlings, with unclear dsRNA in some cases, occasionally (Table 6.1).

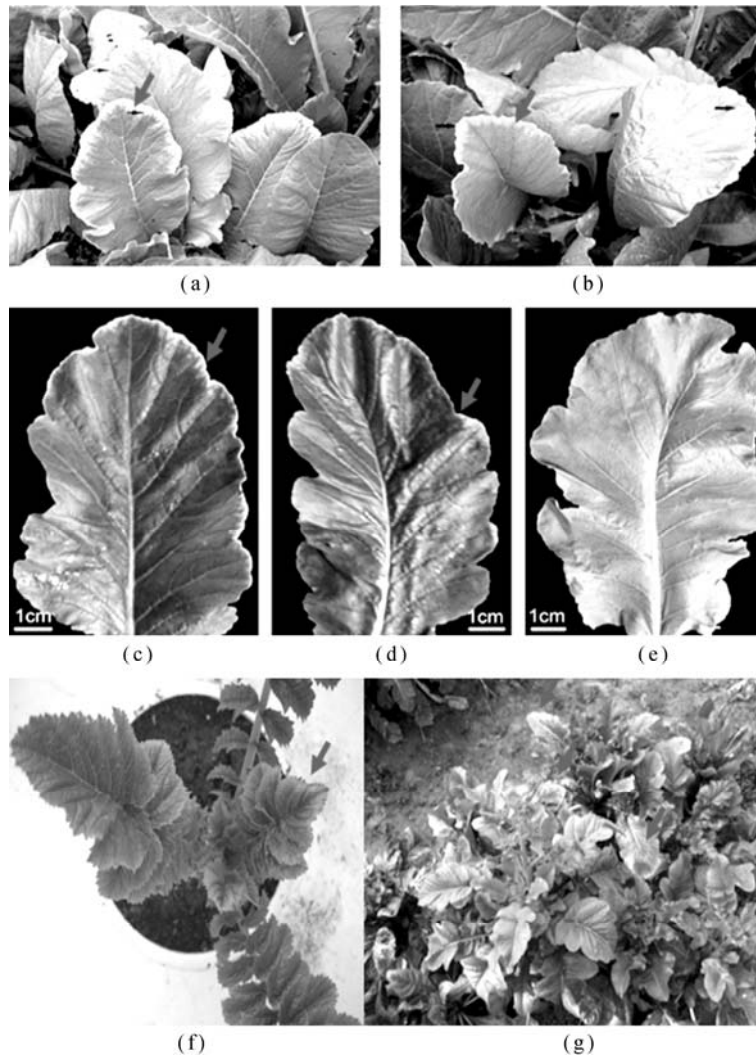


Fig. 6.1. Symptoms presented in radish variety Yidianhong, showing leaves with yellow edge symptoms. The yellow edges are arrowed (a–d), or normal appearance but with typical dsRNA segments detected (e); Field symptoms presented at blossoming stage (f) and yellow edges developed on pot-grown plants, but of Jingbai variety (g)

Table 6.1 Symptoms on seedlings of different radish cultivars grown in greenhouse with commercial seeds

No.	Radish cultivar	Location of seed production	Symptoms
1	<i>R. sativus</i> cv. Yidianhong	Hangzhou, Zhejiang Province	Apparently healthy, occasional yellow edges or chlorosis
2	<i>R. sativus</i> cv. Yuanbai	Hangzhou, Zhejiang Province	Yellowing edge or edge chlorosis, leaf rolling, occasional light uneven
3	<i>R. sativus</i> cv. Qiubai	Beijing	Apparently healthy
4	<i>R. sativus</i> cv. Sijihong	Mianyang, Sicuan Province	Light uneven, occasional mosaic
5	<i>R. sativus</i> cv. Daqingpi	Changcun, Jilin Province	Mild leaf rolling, light uneven
6	<i>R. sativus</i> cv. Nanpanzhou	Shantou, Guangdong Province	Unclear mosaic or mottle
7	<i>R. sativus</i> cv. Meidu	Hangzhou, Zhejiang Province	Unclear mosaic
8	<i>R. sativus</i> cv. Xiaoxue	Chongqing	Apparently healthy
9	<i>R. sativus</i> cv. Goubai	Hangzhou, Zhejiang Province	Unclear mosaic or mottle
10	<i>R. sativus</i> cv. Zhongsuhong	Beijing	Light mosaic, occasional green islands and leaf rolling
11	<i>R. sativus</i> cv. Qiuyinghong	Chongqing	Apparently healthy
12	<i>R. sativus</i> cv. Huaying	Changji, Xinjiang	Apparently healthy
13	<i>R. sativus</i> cv. Jinghong	Beijing	Apparently healthy
14	<i>R. sativus</i> cv. Duanye 13	Shantou, Guangdong Province	Leaf up-rolling

* Seeds were collected from different cities in 2008 but it does not mean they were produced there. Double stranded RNA segments were detected in all the varieties regardless of symptom appearance

By extracting dsRNAs from greenhouse grown seedlings of radish varieties, multiplex segments are always observed. Taking the Yidianhong variety as an example; Pattern one, two major dsRNA bands about 1,700 bp in size, with one brighter band and one much lighter; Pattern two, a single dsRNA band about 1,500 bp; Pattern three, two similar-sized dsRNA bands about 3,500 bp; Pattern four, two similar-sized dsRNA bands of about 1,500 bp. Actually, these four groups of dsRNAs correspond to the five proposed viruses after sequence analysis.

In order to find out the natural occurrence of potential dsRNAs in the radish, double stranded RNAs have been extracted from leaf tissues collected individually in the field, and the dsRNA patterns designate a more complex incidence of variations, showing that more dsRNA segments are expected (Fig. 6.2).

In the case of the Yidianhong variety, a single cell-line without dsRNA contamination is needed.

Virus-like particles, in a relatively high concentration, are detectable in preparations extracted from radish leaf tissues, and spherical virus-like particles are thus observed 28–38 nm in diameter. Analysis of the structure proteins of these particles, using SDS-PAGE, has shown that polypeptides with a molecular weight of 30–60 kD are detectable, and thus illustrated the existence of unidentified viruses (Fig. 6.3). All these above present the possibility of virus infection in the radish.

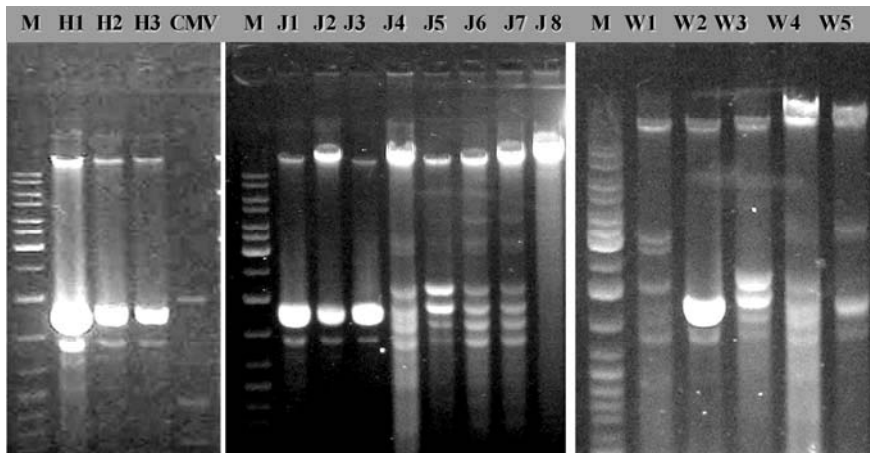


Fig. 6.2. Double stranded RNA patterns extracted from field radish grown in Zhejiang Province, China, Spring 2002. Arrow bar shows the segments of RaV1; The radish varieties are not the same; H1, H2 and H3: radish samples collected from Hangzhou; J1, J2, J3, J4, J5, J6 and J7: radish samples collected from Jiaxin, with J8 for healthy tobacco leaf as a negative control; W1, W2, W3, W4, W5: radish samples collected from Wenzhou. The dsRNA patterns show the diversity and common existence of dsRNAs in radish

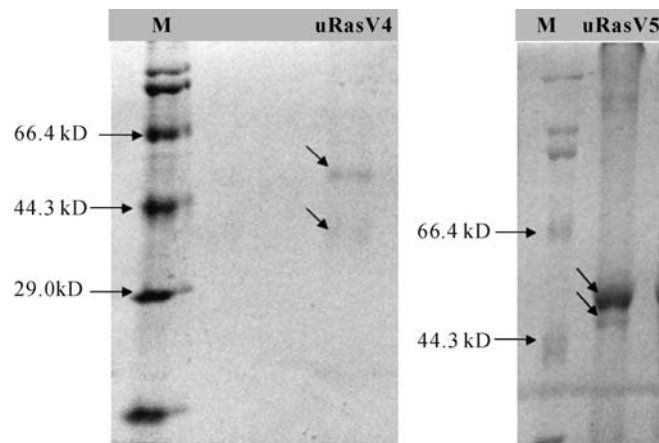


Fig. 6.3. SDS-PAGE analysis of structure proteins extracted from virus-like particles of some un-identified dsRNA viruses from the radish. M: protein molecular weight marker; uRasV4 and uRasV5: un-identified virus preparations from the radish (Yidianhong); the black arrows indicate the viral structure proteins

6.2.2 Genome Characterization of *Raphanus Sativus* Cryptic Virus 1

From a single plant of the radish Yidianhong, over four dsRNA bands were observed and extracted. By repeated cloning and sequencing, at least six segments have been found to make up two or more viruses. The diagram indicating the genomic structures is presented in Fig. 6.4.

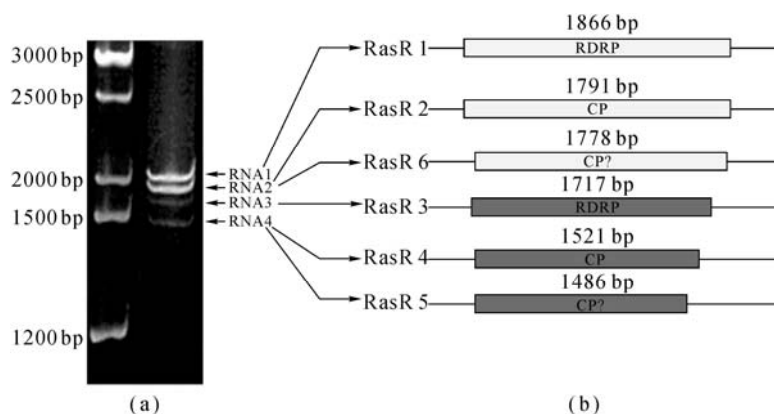


Fig. 6.4. Pattern of dsRNA extracted from a radish sample and the diagram of genomic structures for newly-suggested RaV3. 1% agarose gel electrophoresis was used. (a) Lane M: 1 kb DNA ladder; Lane 1: dsRNAs extracted from leaf tissues of *R. sativus* cv. Yidianhong; (b) The gene organization of RasR 1–6

Raphanus sativus cryptic virus 1 consists of RasR 1, RasR 2 and possibly RasR 6. They are 1,866, 1,791 bp and 1,778 bp respectively, all of which contained an adenosine-uracil (A/U) rich tail of 23, 44 and 46 nt in length at the 3' terminus. The base contents of RasR 1 (RasR 2 and RasR 6, in parenthesis) are 28.3% A (23.3%, 24.63%), 26.9% U (26.0%, 26.43%), 27.1% C (33.7%, 30.82%), and 17.7% G (17.0%, 18.11%), respectively. Each dsRNA segment contains a single ORF on its plus-strand and no significant ORFs could be found on the minus strands, by using the LaserGene program to search for putative ORFs. Multiple alignments of UTRs among RasR 1, RasR 2 and RasR 6 (70, 77 and 79 nt respectively) have found that they are highly conserved at the 5' UTR. Four identical stretches, including the terminal motif (5'-AGAAAAAUUU-3'), are commonly distributed among their 5' UTR (Fig. 6.5(a)). On the other hand, the 3' UTRs of RasR 2 (196 nt) and RasR 6 are much longer than that of RasR 1 (74 nt) and distant from it, but they have a conserved termini (Fig. 6.5(b)). Furthermore, secondary structure investigation of the 5' UTR shows that they have stretches of inverse complementary bases that are capable of forming similar stem-loop structures.

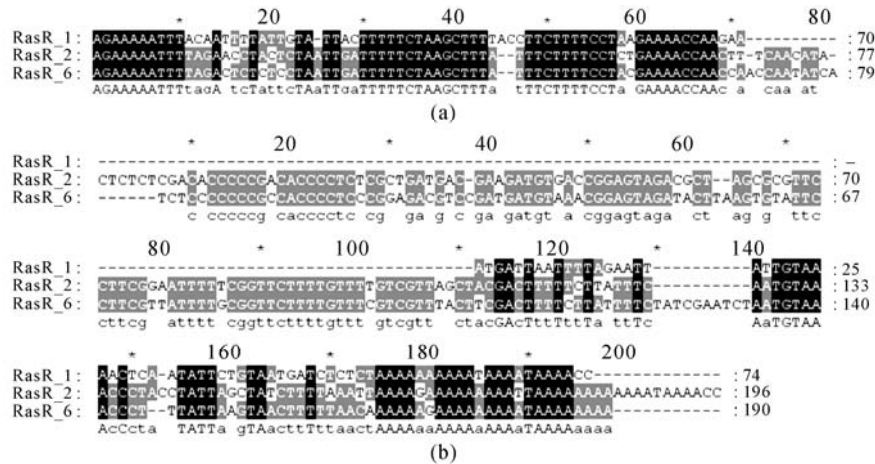


Fig. 6.5. Comparisons of 5' UTR (a) and 3' UTR (b) sequences among cDNAs for RasR 1, RasR 2 and RasR 6. The black shading regions in each column represent the identical parts of the aligned sequences. Different shading levels in each column, from black, gray, grayish, to unshaded, stand for different degrees of amino acid conservation. Black: 100%; gray: >80%; grayish: >60%; unshaded: <60%

Genome structure analysis has showed that RasR 1 contains one ORF from position 71 to 1,792, encoding a putative protein of 573 amino acid residues (aa) with an estimated molecular mass of 66.9 kD. A comparative database search of NCBI with the BLAST program revealed the presence of 26 proteins with similar sequences, all of which were putative viral RdRps. Of these 26 sequences, 22 were from members of the genus *Partitivirus*, including the tentative member oyster mushroom isometric virus II (AAP74192), and the remaining four were from the genus *Alphacryptovirus*. The RdRp encoded by *Helicobasidium mompa* V1-2 virus (HmV-V1-2, BAD32678) was found to be most closely related to that of RasR1 with an identity score of 54.5%, followed by *Helicobasidium mompa* dsRNA virus (HmV-dsRNA, BAC23065, 30.8%), *White clover cryptic virus 1* (WCCV 1, YP 086154, 30.5%), *Vicia cryptic virus* (VCV, YP 272124, 29.8%). According to multiple RdRps alignments, six out of eight conserved polypeptide motifs that were considered as markers of dsRNA viral RdRps were detected in RasR 1-encoded amino acid sequence (Fig. 6.6).

The ORF of RasR 2, initiated at position 78 nt, consisted of 1,518 bp and encoded a putative polypeptide of about 55.9 kD. Database searching revealed four amino acid sequences distantly related to RasR 2 with E -value $>2E-7$, all of which were putative coat proteins (CPs) from members of the family *Partitiviridae*. They were *Amasya cherry disease associated partitivirus* (ACD-PV, YP 138536) with 15.1% identity compared to RasR 2, *cherry chlorotic rusty spot associated partitivirus* (CCRS-PV, YP 138539, 16.3% identity), and two plant cryptic viruses, VCV (AAX39024, 19.5% identity) and WCCV 1 (YP 086755) (18.3% identity).

Virus	Motif										
	III	IV	V	VI	VII	VIII					
<i>Rhizoctonia solani</i> virus	KVRFVY	54	LDMSCEIQRLP	71	GVPSGILLTQFLDSFGNLYLII	19	DMGDDNS	43	ETLSY	8	RDVEKLI
<i>Helicobasidium mompa</i> dsRNA virus	KIRVVF	60	VDMSSEFLRSL	67	GIPSGLEITQFLDSFYMMIIL	16	VOGDDSL	45	NALGY	8	RDWRKLI
<i>Cherry chlorotic rusty spot associated virus</i>	KMRDII	59	LDMKRFKPKAY	71	GIPSGLEITQFLDSFYNYTHIA	16	VOGDPSI	45	EVLGY	8	RDELAML
<i>Pleurotus ostreatus</i> virus 1	KQRFVY	54	LDMSCEIQRLP	72	GVPSGILNFQFLDSFSLFLIF	19	DMGDDNS	43	ETLSY	8	RPLAKIV
<i>Discula destructiva</i> virus 2	KTRLEW	54	LDPSAFPSKVP	61	GVPSGWNFQFLDSVWN-NIIL	15	VLGDDSA	47	KLLGT	8	RSTDEWF
<i>Ceratocystis resinifera</i> virus	KVRDNI	54	LDMSSEFDTVP	93	GVPSGLLCTQFLDSVNLVLI	19	DMGDDNV	43	EILGY	8	RSLSKLI
<i>Discula destructiva</i> virus 1	KTRLEW	54	LDPSAFPSKVP	61	GVPSGWNFQFLDSVWN-NIIL	15	VLGDDSA	37	KLLGT	8	RSTDEWF
<i>Heterobasidion annosum</i> P-type virus	KVRFVY	54	FDVSRFDTLAP	102	GVPSGIEMFQFLDSVNLFLFV	19	DMGDDNL	43	EVLGY	8	RDVSKLI
<i>Fusarium solani</i> virus 1	KTRLEW	54	LDPSSEFTKVP	61	GVPSGWNFQFLDSVWN-NIIV	15	VLGDDSA	37	KLLGV	8	RETEWF
<i>Rosellinia necatrix</i> virus 1-W8	KQRFVY	58	LDMSSEFQRVP	72	GVPSGILNFQFLDSFONLFLII	19	DMGDDNS	43	ETLSY	8	RPLGLII
<i>Helicobasidium mompa</i> V1-1 virus	KQRFVY	54	LDMSCEIQRLP	72	GVPSGLENFQFLDSFGNLYLII	19	DMGDDNS	43	ETLSY	8	RPLGKIV
<i>Ceratocystis polonica</i> virus	KVRDNI	54	LDMSSEFDTVP	93	GVPSGLLCTQFLDSVNLVLI	19	DMGDDNV	43	EILGY	8	RSLSKLI
<i>Atkinsonella hypoxylon</i> virus	KVRFVY	54	LDMSSEFHLAP	93	GVPSGILNFQFLDSVNLTLIF	19	DMGDDNV	43	EVLGY	8	RISKLIV
<i>Penicillium stoloniferum</i> virus S	KTRLEW	54	LDPSSEFTKVP	61	GVPSGWNFQFLDSVWN-YIIV	15	VLGDDSA	37	KLLGT	8	RETNEWF
<i>Fusarium poae</i> virus 1	KQRFVY	54	LDMSCEIQRLP	72	GVPSGILNFQFLDSFGNLYLII	19	DMGDDNS	43	ETLSY	8	RPLGKIV
<i>Amasya cherry disease associated virus</i>	KMRDII	59	LDMKRFKPKAY	71	GIPSGLEITQFLDSFYNYTHIA	16	VOGDPSI	45	EVLGY	8	RDELAML
<i>Gremmeniella abietina</i> MS2 virus	KTRLEW	54	LDPSSEFTKVP	61	GVPSGWNFQFLDSVWN-YIIV	15	VLGDDSA	37	KLLGT	8	RDNEWF
<i>Gremmeniella abietina</i> MS1 virus	KTRLEW	54	LDPSSEFTKVP	61	GVPSGWNFQFLDSVWN-YIIV	15	VLGDDSA	37	KLLGT	8	RDNEWF
<i>Oyster mushroom isometric virus</i> II	KVRLVF	60	LDMSCEFRYAR	74	GIYSGYMQTQFLDSFYMMIIF	16	VOGDPSI	44	EVLGY	8	RDPIALL
<i>White clover cryptic virus</i> 1	KMRDII	59	LDMSRFKPKAY	70	GIPSGLEITQFLDSFYNYTHIA	16	VOGDPSI	45	EVLGY	8	RDEIAML
<i>Vicia cryptic virus</i>	KMRDII	59	LDMSRFKPKAY	70	GIPSGLEITQFLDSFYNYTHIA	16	VOGDPSI	45	EVLGY	8	RDEIAML
<i>Pyrus pyrifolia</i> RNA 1	KTRNVI	54	LDMKCFATVS	50	GIPSGSYFSTLIGSLII-RLRI	16	TOGDDSL	37	HELGR	8	REIKRCL
<i>Beet cryptic virus</i> 3	KVPCVW	55	LDMSSEFSSVT	50	GIPSGSYFSTLIGSLII-RLRI	16	TOGDDSL	37	TELGR	8	RSLDKCL
RasR 1	KIRTFE	59	LDMSCEHRVY	66	GVPSGLEICTQFLDSFYNYTHIA	17	VLGDDVI	45	QVLSY	8	RDSNQLL
<i>Helicobasidium mompa</i> V1-2 virus	KVRFVY	59	LDMSSEFMRVY	79	GVPSGLEICTQFLDSFYNYTHIA	17	DMGDDAL	45	TVLSY	8	RSAEDVL
<i>Penicillium stoloniferum</i> virus F	KTRAVW	56	LDMSCEFTSVS	65	GIPSGSEFTQFLDSVWN-YIIV	15	VLGDDSS	41	KPLGY	8	RSTEWL

Fig. 6.6. Conserved amino acid sequences of putative RdRps from members of the family *Partitiviridae*. Numbers of amino acid residues between flanking conserved motifs are listed. Different shading levels in each column, from black, gray, grayish, to unshaded, stand for different degrees of amino acid conservation. Black: 100 %; gray: >80%; grayish: >60%; unshaded: <60%. RasR 1 is indicated in bold

The ORF of RasR 6, initiated at position 80 nt, consisted of 1,506 bp and encoded a putative polypeptide of about 55.1 kDa. BLAST searching showed that four amino acid sequences were closely related with RasR 6-encoding peptide, the same for the related protein of RasR 2-encoding peptide, all of which were CPs from members of the family *Partitiviridae*. They were ACD-PV with 30% identity compared to RasR 2, CCRS-PV (25% identity), and VCV (23% identity) and WCCV 1 (21% identity). Multiple alignments of these proteins revealed the presence of several conserved regions. And phylogenetic analysis revealed that RasR 2 and RasR 6 are closely related to each other (Fig. 6.7).

Based on the above information, both RasR 2 and RasR 6 are tentatively encoding the CPs of RasV1. That is to say, RasR 2 and RasR 6 might co-use one replicase (RasR 1). Regarding the assembled virions, there are two possible scenarios: RasR 2-encoding peptide and RasR 6-encoding peptide each as a subunit composing the CP of RasV1 co-packaged the genome and replicase; the other is RasR 2 and RasR 6 co-using the same replicase (RasR 1) but each as a CP packaging their genomes separately. This is an unusual and interesting phenomenon, and it needs more direct evidence to support the above hypothesis. The function and origin of RasR 2 and RasR 6 (including other tri-segments partitiviruses) should be carefully considered. Since RasR 1, RasR 2 and RasR 6

are highly conserved at the 5' UTR and possess a conserved motif at the 3' terminus. Furthermore, the field radish sample harboring only ? ^WHAT?? is easily discovered, and by hybridization tests for more field samples, RasR 1, RasR 2 and RasR 6 are always occurring together. That is to say, all the three segments must be from one virus. The similarity of RasR 6 related sequences are compared in Fig. 6.8.

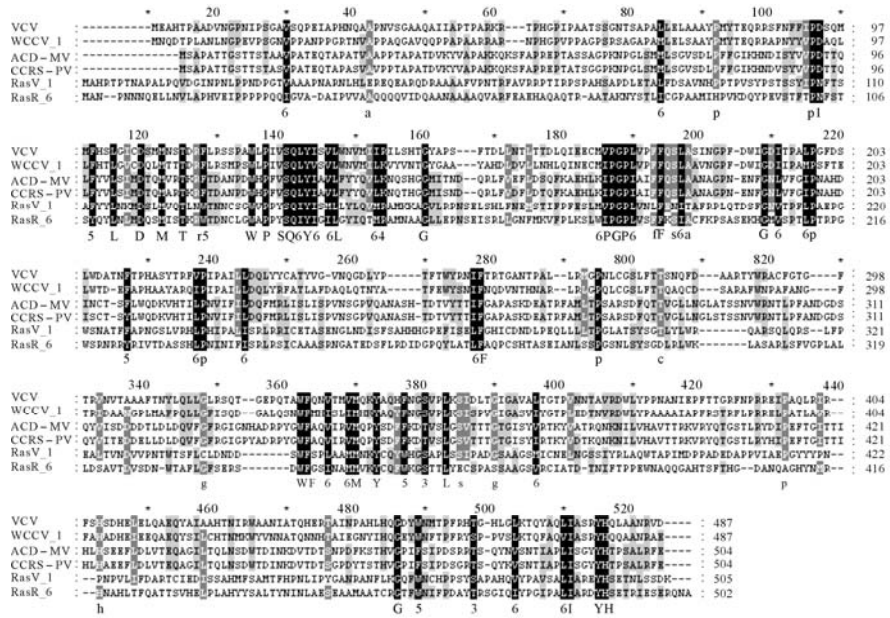


Fig. 6.7. Multiple alignments between the predicted amino acid sequences of RasR 2 and RasR 6 and CPs of members of the family *Partitiviridae*. The meaning of different levels of shading are the same as Fig. 6. 6

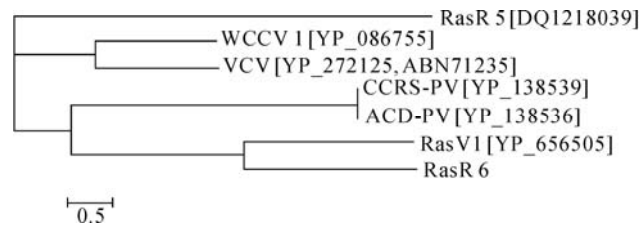


Fig. 6.8. Phylogenetic tree generated from multiple alignments of *Partitiviridae* viral CPs and RasR 6

These conformational signals, along with conserved terminal motifs, may play a role in viral replication, translation and assembly. Considering dsRNA virus evolution and increasing divergence, their evolutionary relationships should be hypothesized on the basis of homologies found in the conserved motifs of RdRps. A sequence of comparison of RasR 2 and RasR 6 is given in Fig. 6.9.

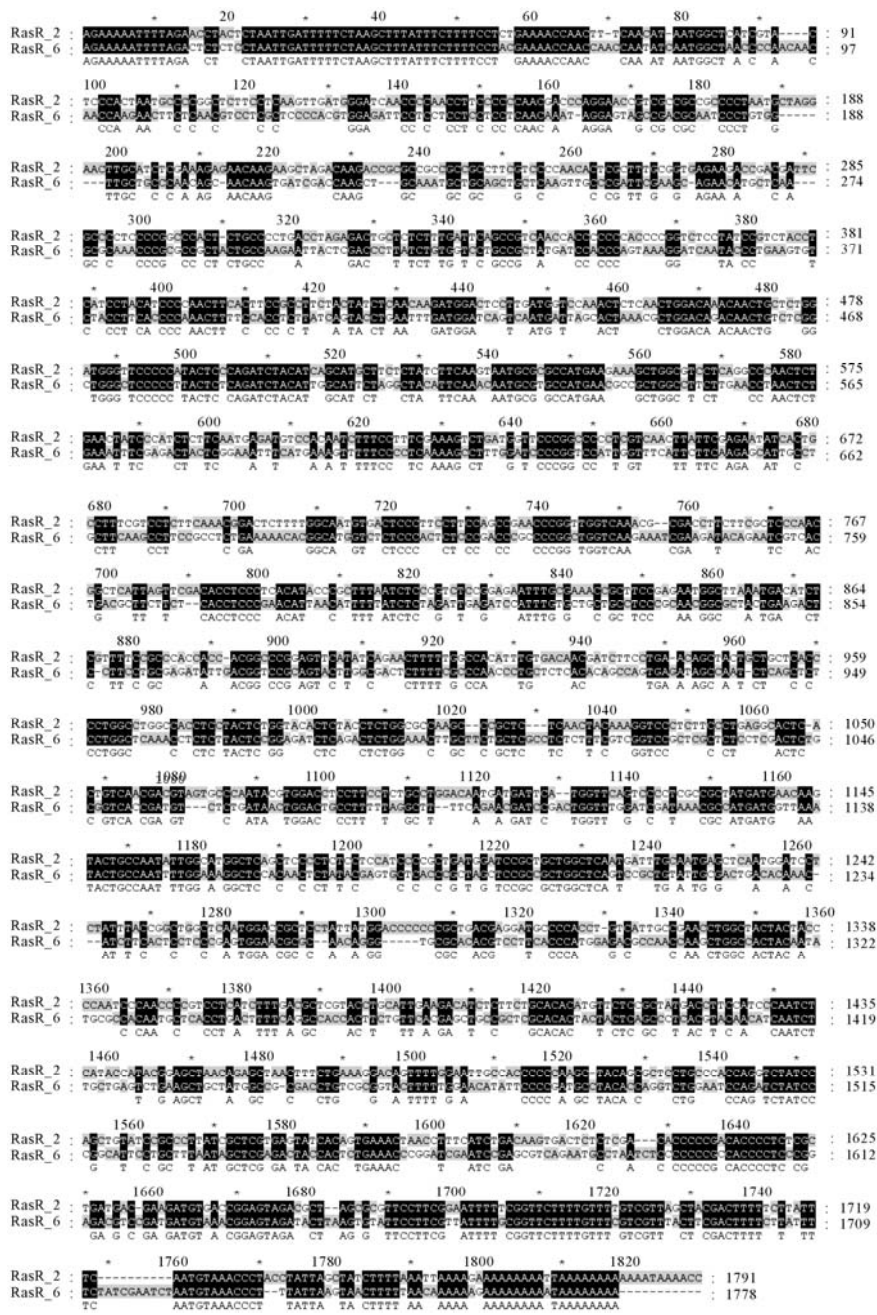


Fig. 6.9. Comparisons of full-length nucleic acid sequence between RasR 2 and RasR 6

The spherical virus particles of RasV1 observed under an electro-microscope are of about 33–35 nm in diameter, with no obvious morphological diversity detected yet.

6.2.3 *Genome Characterization of Raphanus Sativus Cryptic Virus 2*

Concomitant with the occurrence of RaV1, which are RasR1, RasR2 and RasR3, RasV2 appears in two minor bands. Repeated cloning and sequencing have revealed that there are three segments composing the genome of another dsRNA virus. It is found that, just like those of RasV1, the smallest band is composed of two individual dsRNA segments, namely RasR 4 and RasR 5. Among segments of RasV2, RasR 3, RasR 4 and RasR 5 are found to be 1,717, 1,521 and 1,485 bp, respectively. RasR 3 and RasR 4 co-migrated in gel, since the difference in size between them is only 36 bp. Their G+C% have been determined as 43.2%, 46.6% and 46.0% respectively, with an obvious imbalance of base composition since base G only occupied 20.4% in RasR 3, 18.9% in RasR 4 and 20.4% in RasR 5. All three segments had an identical 5' terminal motif (5'-GATAATG-3'), but the similarity between RasR 3 and RasR 4 at their 5' un-translated regions (UTRs) is poor (11.8%), while relatively higher between RasR 3 and RasR 5 (64.7%), or between RasR 4 and RasR 5 (54.1%) (Fig. 6. 10). On the other hand, the 3' UTRs of the three segments were much less similar to each other. In addition, there were no significant similarities estimated between UTRs of the minor segments and corresponding regions of the genome of RasV1.

Genome structure analysis has showed that RasR 3 encodes the RdRp, while RasR 4 and RasR 5 tentatively encode the CPs. RasR 3 has one single ORF from the position 179, which encoded a putative protein of 477 aa with a molecular mass of approximately 55.3 kDa. The GenBank database search by BLASTP program caught ten similar amino acid sequences with *E*-value < 2E–11, all of which were RNA dependent RNA polymerases (RdRps) encoded by members of the family *Partitiviridae*, including *Fragaria chiloensis* cryptic virus (uFccV, AAZ06131, 63.8% identity) (Tzanetakis et al., 2008), *Beet cryptic virus 3* (BCV3, AAB27624, 34.5% identity) (Xie, Antoniw, and White, 1993), *Pyrus pyrifolia dsRNA 1* (PyrR1, BAA34783, 34.4% identity) (Osaki, Kudo, and Ohtsu, 1998) and seven other *partitiviruses* with low identity beneath 20%. Six conserved motifs (motif III to motif VIII), typical of RdRps of the family *Partitiviridae*, were present in RasR 3-encoded polypeptide as well. A phylogenetic reconstruction derived from multiple alignments of RdRps, including that of RasR 1 and RasR 3, categorized the two segments into different groups, on account of their low identity of 12.3%.

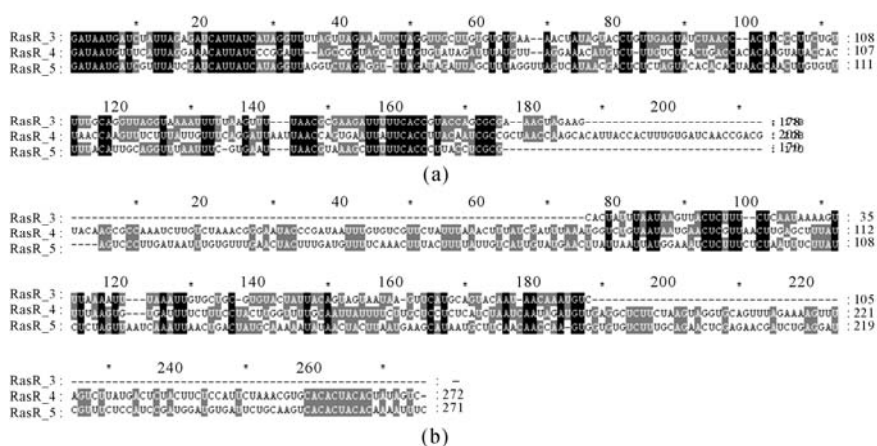


Fig. 6.10. Comparison of UTRs of both ends of RasR 3, RasR 4 and RasR 5. (a) 5' UTR alignment; (b) 3' UTR alignment. Different shading levels in each column stand for different degrees of nucleotide conservation. Black: 100%; gray: 66%; non-shaded: 0%

RasR 4 and RasR 5 each harbored a single ORF initiated at the positions 209 and 171, potentially encoding a protein of 346 (38.2 kDa) and 347 aa (38.8 kDa) respectively, almost identical in size and molecular mass. Furthermore, the amino acid residue compositions of the two putative polypeptides are similar to each other as well. Alignment analysis denoted that they share 17.1% identity, with several conserved residues in both sequences (Fig. 6.11). However, neither the nucleic acid sequence nor the sequence of translated products currently available from the GenBank database clustered with any of the two polypeptides.

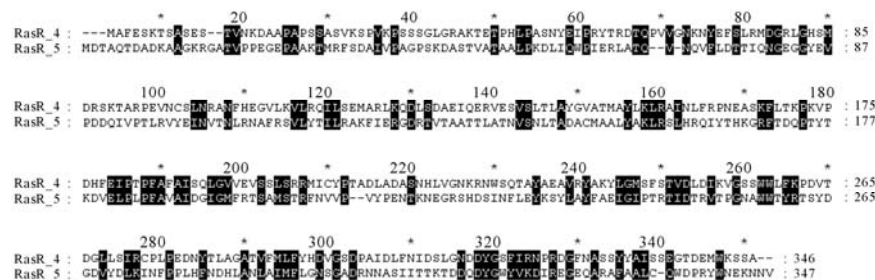


Fig. 6.11. Comparison of putative protein encoded by RasR 4 and RasR 5

Depending on to date acquaintance, RasR 3 encodes a polypeptide resembling the RdRps of the family *Partitiviridae*, whereas the function of RasR 4 and RasR 5 is as yet unknown, but on account of their presence in viral particles as well as the identical 5' terminal motif they share, the proposal that these three are of viral origin and consist of the genome of a partivirus (named RasV2) appears convincing. Moreover, in terms of these two pieces of circumstantial evidence, they might originate from the same species that is new in the family *Partitiviridae*. Since the three minor dsRNA segments are always detected together with the

segments of RaV1, it could be considered that RasV3, RasV4 and RasV5 are composed of a satellite virus or segments of a defective virus depending on RaV1.

And it is speculated that both RasR 1 and RasR 3 encode RdRps resembling that of the family *Partitiviridae* and on the basis of their distinction in size and sequence features of their UTRs at both ends and relative remoteness from each other in phylogeny, it is proposed that there is a co-infection by two unique viruses of the same family. One includes RasR 1 RasR 2 and RasR 6 (*Raphanus sativus* cryptic virus 1) and the other includes RasR 3, RasR4 and RasR 5 (*Raphanus sativus* cryptic virus 2).

RasV1, RasV2 and uFcCV are similar in genome structure. These three viruses are likely to exist as two different and independent virions which co-use the same virus replicase, viral RdRp. It is easy to predict that at least one of RasR 4 and RasR 5 is the structure gene of RasV2, based on its genome characterization and these two segments' coding capability.

6.2.4 Correlation of *Raphanus Sativus* Cryptic Virus 2 with *Raphanus Sativus* Cryptic Virus 1

Referring to the electrophoretical profile, in which the two major dsRNA bands are remarkably brighter than the remaining ones, the two supposed species might develop unevenly. *Raphanus sativus* cryptic virus 1 would dominate in the host, while *Raphanus sativus* cryptic virus 2 is just maintained at a very low level. Precedents for viral co-infection have been recounted recently. Osaki et al.(2004) reported an assorted infection of two species of the genus *Partitivirus* in *Helicobasidium mompa*. Kim et al. reported two partitiviruses co-infecting *Penicillium stoloniferum*. Likewise, members of different families, such as *Chrysoviridae* and *Partitiviridae*, or *Totiviridae* and *Partitiviridae*, would also co-exist in the same host (Coutts et al., 2004; Covelli et al., 2004). Accordingly, we could not leave out the possibility of different viruses mutually inhabiting the same radish plant.

Regardless of the variety, dsRNAs extracted from 23 field-grown radish plants underwent dot-blotting hybridization analysis. dsRNAs samples were extracted individually from plants and spotted onto the nylon membrane, and six specific probes were labeled with ³²P, corresponding to RasR 1–RasR 6, by using their specific primers and cDNA-containing plasmids. The hybridization results showed that 56.5% of the detected radish plants were infected by RasV1, or RasV1 and RasV2. The percentage of RasV1-and-RasV2 co-infecting the plant was 39.1%, and that of RasV1-solely infecting the plant was 17.4%, RasV2-solely infecting the plant was not found to occur. That is to say, RasV2 always co-infected the radish plant with RasV1. At the same time, RasR 1, RasR2 and RasR6 always occurred together in the same way as RasR3, RasR4 and RasR5, which shows that RaV1 and RaV2 are both composed of three necessary segments. The detection primers are illustrated in Table 6.2 and the results are shown in Fig. 6.12 and Table 6.3.

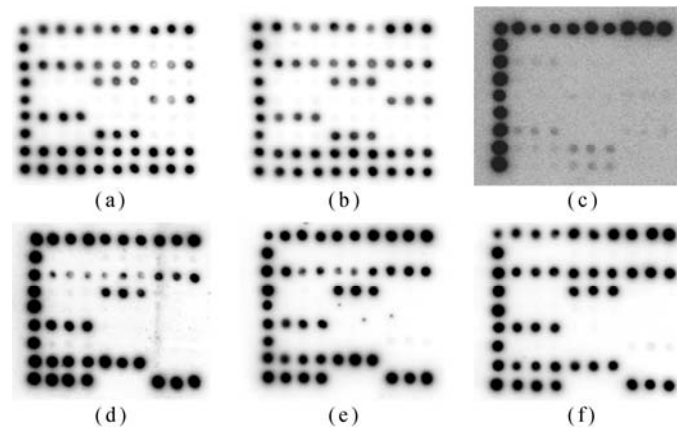


Fig. 6.12. Detection for dsRNA in field radish samples using dot blot hybridization. (a)–(f) Dot blot hybridization result respectively using RasR 1–RasR 6 as probe template. The PCR products of RasR 1–RasR 6 amplified from their cDNA plasmids with their corresponding primers were used as positive controls, and the dsRNA sample extracted from no dsRNA-harboring plant was used as negative control

Table 6.2 Specific primers in ORF of RasR 1–RasR 6 used for dot hybridization

dsRNAs	Primers	Length and position
RasR1	RasR 1-F: 5'-GTTTGCGAAATCACCTAACGA-3' RasR 1-R: 5'-GTGCTTGAGGATTCCGAAAAT-3'	1120 bp, nt 124–1243
RasR2	RasR 2-F: 5'-GATTCAGCCGTCAACCAC-3' RasR 2-R: 5'-GGGGTAGTAGTAGCCAGGTT-3'	1011 bp, nt 330–1340
RasR 3	RasR 3-F: 5'-CAGTTCCCTTCGTGTCCAA-3' RasR 3-R: 5'-CTCCACATAAACGGTTTCGCA-3'	1054 bp, nt 228–1281
RasR4	RasR 4-F: 5'-GTCCTCCGCAAGTGTCAAAT-3' RasR 4-R: 5'-CTAAGCGGACGATTTCCACAT-3'	976 bp, nt 274–1249
RasR 5	RasR 5-F: 5'-GCACAAACAGACGCTGACAAA-3' RasR 5-R: 5'-GATCATAGACATCGCCGTCGTA-3'	902 bp, nt 180–981
RasR 6	RasR 6-F: 5'-GCCCAACAGCAACAAGTGAT-3' RasR 6-R: 5'-GTGTAGGCATCGGGGAATAT-3'	1298 bp, nt 194–1491

Table 6.3 The result of dot blot hybridization for detecting field occurrence of RasR 1–RasR 6

Samples	RasV1			RasV2		
	RasR 1	RasR 2	RasR 6	RasR 3	RasR 4	RasR 5
L1						
L2						
L3	√	√	√	√	√	√
L4	√	√	√	√	√	√
L5	√	√	√	√	√	√
L6						
L7	√	√	√	√	√	√
L8						
L9						
L10						
L11	√	√	√			
L12	√	√	√	√	√	√
L13						
L14						
L15						
L16	√	√	√			
L17						
L18	√	√	√	√	√	√
L19	√	√	√	√	√	√
L20	√	√	√			
Y1	√	√	√	√	√	√
Y2	√	√	√			
Y3	√	√	√	√	√	√

The failed detection does not mean the non-detection of all dsRNA viruses. RaV1 and RaV2 could be detected from some of those negative individuals in their off-spring seedlings, and dsRNAs belonging to other viruses could also be detected from the same preparation

6.2.5 *Genome Characterization of Suggested Raphanus Sativus Cryptic Virus 3*

A dsRNA band smaller than that of RasR4 and RasR5 has been observed independently from RaV1 and RaV2. And the corresponding dsRNA represented virus was named RasV3. Actually, this band contains two dsRNA sequences. Characteristics of the two segments are also exhibited in Fig. 6.13. The larger, namely RasV3-dsR1, is 1,609 bp and the other, namely RasV3-dsR2, is 1,581 bp. Base component analysis showed that RasV3-dsR1 is composed of 31.70 % (25.93%) A, 20.88 % (17.58%) G, 26.10% (19.03%) U and 21.32% (27.45%) C, with the main ORF in one strand covering 1,446 nt starting with an AUG at nt 101

and ending with an UAA at nt 1,546. The main ORF of RasV3-dsR2 in one strand is 1,125 nt in length, starting with an AUG at nt 94 and ending with an UAG at nt 1,125. Comparisons of 5' UTR and 3' UTR between the two novel cDNAs has shown that they are highly conserved at 5' UTR and the identical region (5'-AGAAUUU-3') is discovered (Fig. 6.14). The first four nucleotide residues 5'-AGAA-3' are also found at the same position of the genome sequences of *Raphanus sativus* cryptic virus 1. The 3' UTR of RasV3-dsR2 was much longer than that of RasV3-dsR1, but they have an identical region (5'-AUUUUUUUU-3').

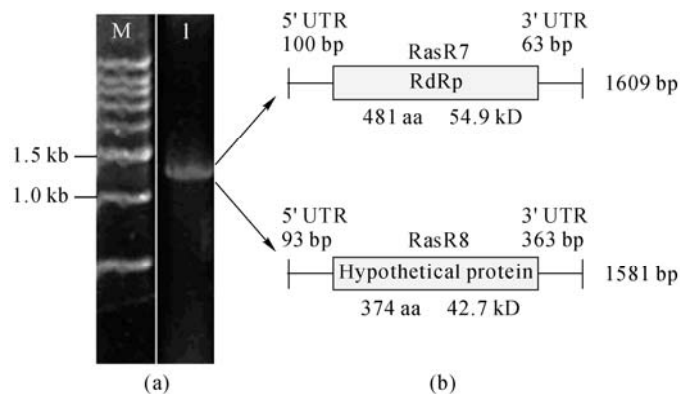


Fig. 6.13. dsRNA extracted from a radish sample and the diagram of genomic structures for newly suggested RasV3. 1% agarose gel electrophoresis was used. (a) Lane M: 1 kb DNA ladder; Lane 1: dsRNAs extracted from leaf tissues of *Raphanus sativus* cv. Yidianhong; (b) The gene organization of RasV3 dsR1 and RasV3 dsR2

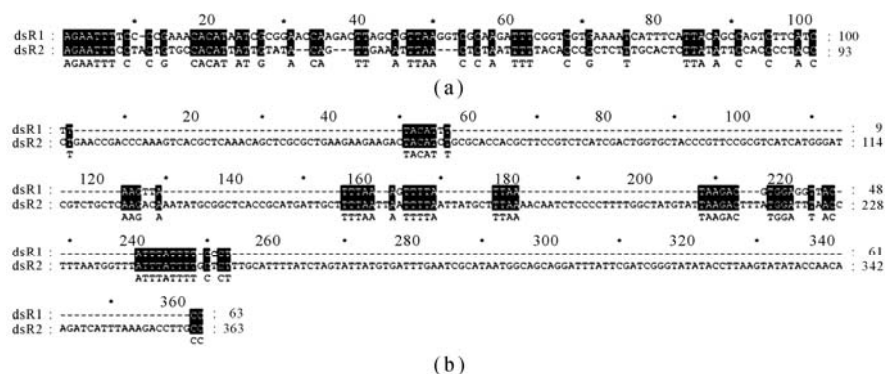


Fig. 6.14. Comparison of UTRs of both ends of RasV3 dsR1 and RasV3 dsR2. (a) 5' UTR alignment; (b) 3' UTR alignment

More analysis has proved that RasV3-dsR1 encoded a putative protein of 481 amino acid residues with the molecular weight of 54.9 kDa, and BLASTP search showed that 9 protein sequences were found similar to this putative protein sequence. All these 9 proteins were putative RdRps which were encoded by plant-infecting viruses belonging to the family *Partitiviridae*, including *Pyrus*

pyrifolia cryptic virus, *Beet cryptic virus 3*, *Black raspberry cryptic virus*, *Pepper cryptic virus 1*, *Raphanus sativus cryptic virus 2*, *Rosa multiflora cryptic virus*, *Rose cryptic virus 1* [ABZ10945], *Fragaria chiloensis cryptic virus* and *Pinus sylvestris partitivirus*. RdRp sequence of *Pepper cryptic virus 1* had the highest similarity with RasV3-dsR1 encoded putative protein but it was 67.2%. When multiple sequences alignment among these similar sequences and RasV3-dsR1 encoded putative protein sequence was performed, the result revealed that five out of eight conserved motifs including GDD which were conservative in RdRp of dsRNA viruses were detected (Fig. 6.15). RasV3-dsR2 encoded a putative protein of 374 amino acid residues with a molecular weight of 42.7 kDa, and BLASTP search showed no similar sequence, but according to their structure similarity at both ends, they should be regarded as belonging to the same virus.

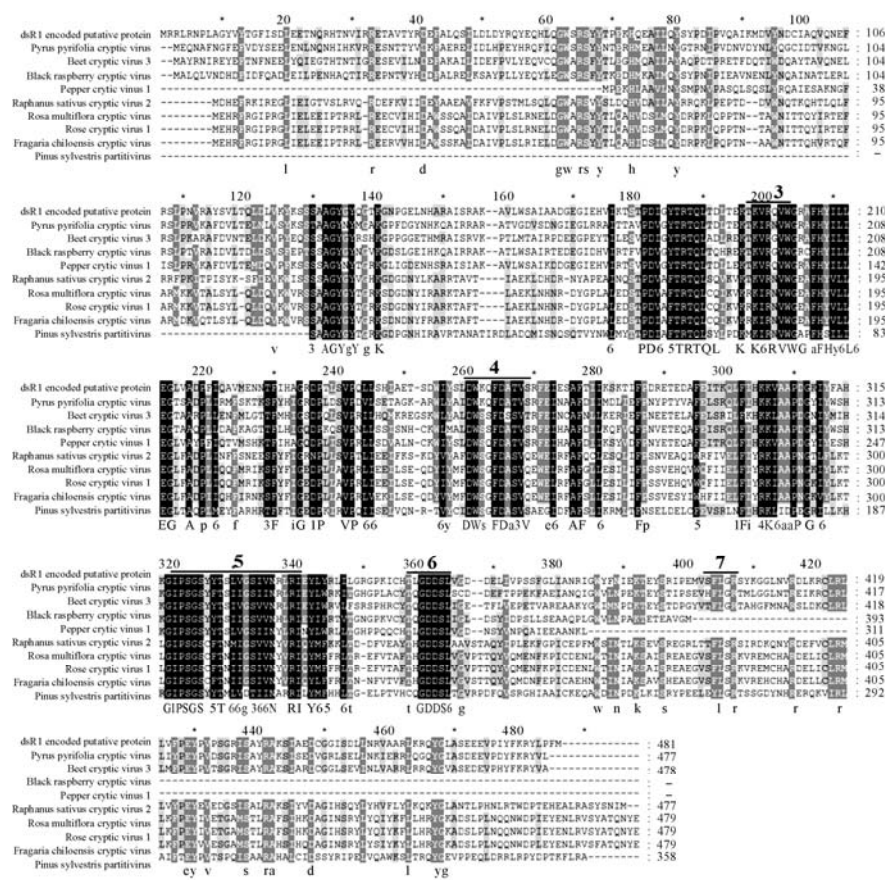


Fig. 6.15. Conserved amino acid sequences of putative RdRps from members of the family *Partitiviridae*. Numbers of amino acid residues between flanking conserved motifs are listed. Different shading levels in each column, from black, gray, grayish, to unshaded, stand for different degrees of amino acid conservation. Black: 100%; gray: >80%; grayish: >60%; unshaded: <60%

Virus-like spherical particles of about 30nm were extracted from naturally infected radish plants. Viral RNAs were extracted from VLPs and used as templates for RT-PCR. Sense strand cDNA and antisense strand cDNA were obtained through reverse transcription using forward or reverse primer. Each cDNA was used as a template for PCR with forward and reverse primers. The electrophoretic result of each PCR product showed that the corresponding fragments of RasV3-dsR1 and RasV3-dsR2 were obtained, indicating that both sense and antisense strand of RasV3-dsR1 and RasV3-dsR2 existed in the VLPs and viral dsRNAs were identical with the dsRNAs extracted from the leaf tissues.

Since RasV3-dsR1 and RasV3-dsR2 have no significant sequence homology with the genome sequences of RasV1 and RasV2, UTR analysis of RasV3-dsR1 and RasV3-dsR2 indicated that these two dsRNAs may constitute the genome of a new dsRNA virus (namely *Raphanus sativus cryptic virus 3*, RasV3). This suggestion was also supported by the presence of RasV3-dsR1 and RasV3-dsR2 in the VLP preparations.

6.2.6 The Possible Existence of More dsRNA Viruses in Radish

More segments belonging to independent potential dsRNA viruses have been observed from the radish Yidianhong and other varieties, e.g. those of about 1,800, 3,500, 5,000 bp and over segments only detectable occasionally. The above dsRNAs are more or less detectable from cruciferous plants, indicating the possible distribution of them across this family. But to date, the described RasV1 and RasV2 have only been detected in radish.

Again, according to the phylogenetic tree generated from multiple all assigned and tentative members of the family *Partitiviridae*, the relationship between RasV1 and RasV2 to "RYEV" described in Japan is still unclear, even though both are associated with leaf yellow edging of the radish and their dsRNA genomes are apparently of similar sizes. This may become clear by future studies involving comparative analysis.

TuMV and CMV are principal viruses infecting the radish and other cruciferous crops. In our survey, TuMV are well distributed in the radish in early and later spring in eastern China, and CMV occasionally occurs in autumn, which could also have been detected with dsRNA analysis. But in the author's experience, dsRNA viruses are more widely and deeply distributed in the radish, and a clear understanding of this group of viruses, mostly partitiviruses, will be an interesting base for plant virus study and also for radish characters.

6.3 Double Stranded Viruses in *Vicia Faba*

In comparison with the limited research attention paid to dsRNA viruses infecting

plants, mycoviruses, those viruses infecting fungi, have been noticed for quite a long time. Plants, especially field crops, are infected not only by different viruses but also by pathogenic fungi and co-existent fungi at large.

In contrast to many pathogenic viruses with single stranded RNA genomes, dsRNA viruses infecting plants are underestimated. It is always asked in academic congresses, and in journals, about the possible currency of plant dsRNA viruses origin or mycovirus contamination, etc., and the wide distribution of multiplex dsRNA segments in many “dsRNA-favourite” plant species provides another picture of virus-plant interaction. Taking the broad bean (*Vicia faba*) as an example, dsRNAs viruses and a fungal species from leaf tissue are introduced to show up the diversity and common existence of the dsRNA viruses associated with this crop.

6.3.1 Two dsRNA Viruses Infecting *V. faba*

Three predominant dsRNA segments, approximately 1.5–3.5 kbp, FaR1, FaR2 and FaR3, are detected in all the tested seedlings grown from commercial seeds of *V. faba*, as well as in three independent field *V. faba* cultivars grown in Hangzhou, eastern China (Fig. 6.16). In addition, two larger dsRNA segments were also observed in some field grown broad beans at relatively low concentration.

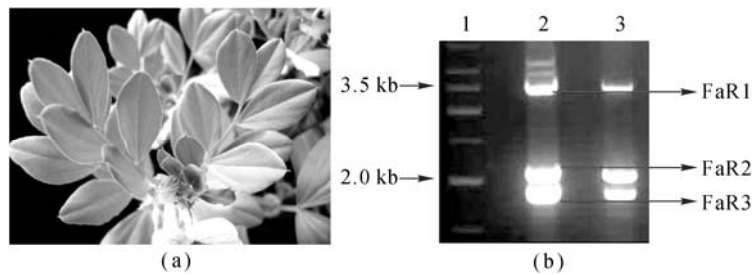


Fig. 6.16. Plant appearance and the dsRNA pattern of the broad bean collected in Hangzhou, China. (a) Plant appearance of field broad bean from which the dsRNA were extracted; (b) dsRNA patterns. 1: double stranded DNA marker; 2: dsRNA extracted from a field plant; 3: dsRNA extracted from a greenhouse-grown seedling with seeds

Using a modified SPAT protocol, FaR2 and FaR3 were fully sequenced, and found to be 2,013 bp and 1,759 bp in length. The largest ORF on their positive strands were predicted to encode two proteins, which were identical to the RdRp and the CP of *Vicia cryptic virus* (VCV) respectively. This accordingly indicates that FaR2 and FaR3 are genomic segments of VCV. The larger FaR2 was 2,012 bp in length and contained a major open reading frame (ORF) encoding a putative RdRp. The smaller FaR3 was 1,779 bp in length and comprised a single ORF on its plus-strand encoding CP (Blawid et al., 2007).

Based on the high concentration in dsRNA preparation and the common

distribution of FaR1 and FaR2, VCV is considered to be well spread among broad bean varieties and areas which are cultivated. But according to the survey, other viruses are not so commonly detected as FaR1, FaR2 and FaR3, which widely occurred with VCV in most cases tested.

The largest segment, FaR1 is found to be 3,434 bp in length. The result of searching a similar sequence with BLASTN has shown that the southern tomato virus (STV) isolates MS-7 [EU371896] and MT-1 [EU413670], which have almost identical genomic sequences, 66% similarity with FaR1. And the STV clone T-11-2 RNA-dependent RNA polymerase [DQ361007] has a higher similarity of 73% with FaR1. Multiple ORFs were discovered on its positive strand and the two largest ORFs (ORF1 and ORF2) are each predicted to encode a putative protein. ORF1, initiating at nt 143–145 and ending at nt 1,325–1,327, encodes a protein of 394 amino acids, of 43.4 kDa. ORF2, ranging from 1,041 to 3,317 encodes another protein of 758 amino acids, of 85.4 kDa. ORF2 partly overlapped with ORF1 (Fig. 6.17) and it is possibly encoded as a fusion protein with ORF1. Secondary structure prediction indicated that there are pseudo-knot structures (nt 1,325–1,388; not shown) which probably cause frame-shift. Searching for similar sequences with BALASTP, has found that the protein encoded by FaR1-ORF1 has a similarity of 24% to predicted protein [EE90173] of *Populus trichocarpa*, and of 23% to STV putative coat protein p42 [ABO36237] and its overlapping fusion protein p122 [ABO36238], as well as STV fusion protein [ABZ10949] (E -value $\leq 8E-9$). Multiple alignments and secondary structures comparison of FaR1-ORF1 and putative coat protein p42 [ABO36237] of STV showed that they were distinct from each other (Fig. 6.18). The discrepancy of FaR1 against FaR2 and FaR3 is displayed in Fig. 6.19. A positive hybridization signal was detected when total dsRNAs extracted from leaf tissue of *V. faba* were hybridized with the ^{32}P labeled cDNA probe of FaR1, but no cross hybridization was detected between FaR1 and FaR2 or FaR3. The comparison of differences between amino acid sequences of FaR1-ORF1 with that of P42 of the southern tomato virus is shown in Fig. 6.18. The results reveal the viral character of FaR1 and its relation with the described dsRNA virus.

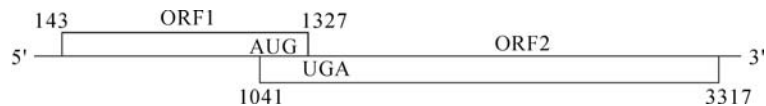


Fig. 6.17. Diagram of the novel mono-partite virus genome

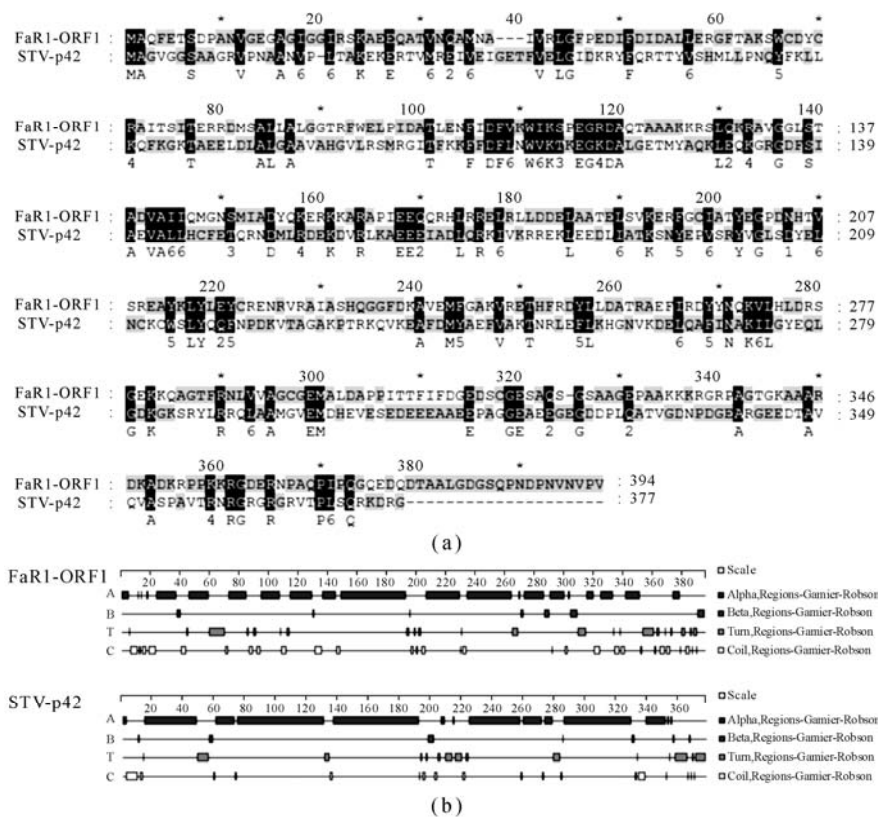


Fig. 6.18. Comparison between aa sequence of FaR1-ORF1 with P42 of *Southern tomato virus*. (a) Result of multiple alignments of amino acid sequences of putative CPs of FaR1-ORF1 and STV-p42 [ABO36237]. Multiple alignments of the sequences were performed with program CLUSTALX 1.8 and displayed with program GeneDoc 2.7. Different shading levels (black, gray) represent distinct degrees of nucleotides conservation. Black: 100%; gray: >80%; (b) Secondary structures predicted putative CPs of FaR1-ORF1 and STV-p42 [ABO36237]. The secondary structural units of Alpha-helix, Beta-sheet, Turn and Coil are represented by red, green, blue and yellow boxes and their relative distributions and contents are presented as A, B, T and C, respectively

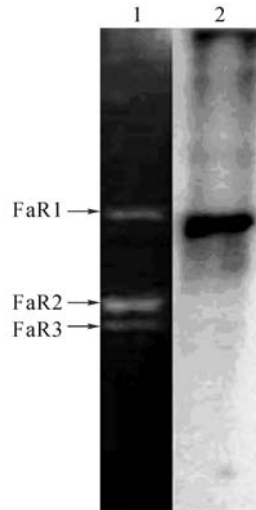


Fig. 6.19. Results of Northern blotting analysis using cDNA of FaR1 as probe. Lane 1: Total dsRNAs extracted from *Vicia faba* (FaR1, FaR2 and FaR3); Lane 2: The same total dsRNAs hybridized with [³²P]dCTP-labeled cDNA probe of FaR1

Seven proteins have been found to be similar to the putative protein encoded by FaR1-ORF2 (E -value $\leq 5E-8$). Two of them are STV RNA-dependent RNA polymerase-like (RdRpL) proteins [ABC96788] and [ABC96787], with 58% and 47% similarities, respectively. Two other proteins recorded from STV, namely p122 [ABO36238] and protein [ABZ10949], having been identified as fusion proteins showed 50% similarity to the deduced protein encoded by FaR1-ORF2. In addition, polymerase [ABO36236] of Blueberry fruit drop virus was displayed with 43% similarity to putative protein of FaR1-ORF2. And the predicted protein [EEE90713] of *Populus trichocarpa* had 38% similarity and the RdRp [NP_624325] of *Zygosaccharomyces bailii virus Z*, a totivirus was of limited similarity of 23% to the protein determined by FaR1-ORF2. The analysis of multiple alignments between putative protein of FaR1-ORF2 and STV fusion protein p122 [ABO36238] indicated that, like STV protein p122 [ABO36238], protein encoded by FaR1-ORF2 contained the typical motifs (4–6) of partitivirus RdRp as well (Fig. 6.20). Thus, protein encoded by FaR1-ORF2 is a putative viral RdRp. To clarify the possible classification of the virus determined by segment FaR1, multiple alignments and phylogenetic analysis are conducted with RdRps from representative members of *Partitviridae*, *Totitviridae* and *Chrysoviridae* families as well as the protein encoded by FaR1-ORF2. The phylogenetic analysis showed an evident grouping of ORF2 of FaR1 with proteins encoded by STV. That is, they possessed closer evolutionary relationships. As the result acquired by Sabanadzovic et al. shows, however, these two viruses were found to be scarcely related to members of *Partitviridae*, *Totitviridae* or *Chrysoviridae* (Fig. 6.21).

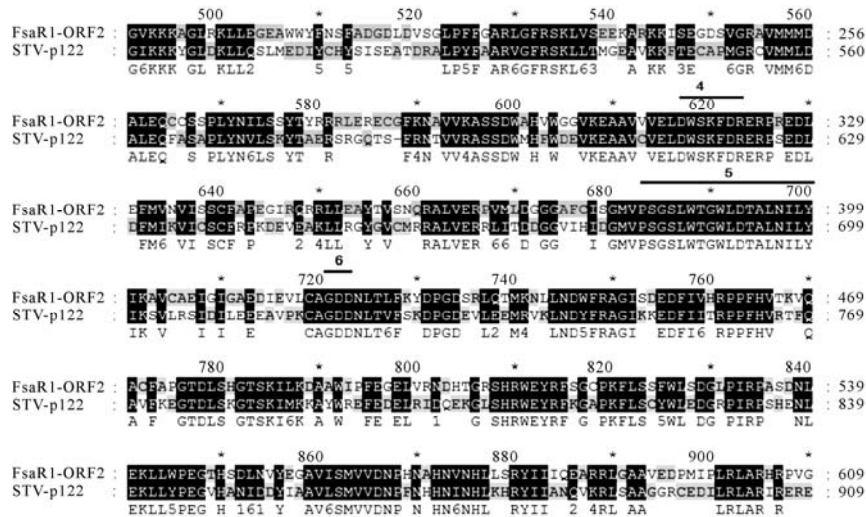


Fig. 6.20. Comparison between aa sequence of FaR1-ORF2 with RdRp of southern tomato virus. Result of multiple alignments of amino acid sequences of putative RdRps of FaR1-ORF2 and STV-p122 [ABO36238]. The conserved motifs (4–6) of partitiviruses were marked with bold lines above. The meanings of different shading levels are as Fig.3(a) described

Additionally, the 5' UTR of FaR1-ORF1 and the 3' UTR of FaR1-ORF2 are 142 bp and 117 bp, respectively, and their corresponding A+U contents are 61.97% and 70.09%. Secondary structure prediction showed that both UTRs could form hairpin-like structures which might assist RdRp recognition in the process of virus replication. Furthermore, there are some similarities between the secondary structures of FaR1-UTRs and STV-UTRs (Fig. 6.22).

According to all the above mentioned, segment FaR1 contains a probable genome of 3434 bp in size, and it is similar, but different from, the genomic segment of STVs, which have been suggested as novel plant viruses, but not fungal viruses. In this case, the virus containing FaR1 does not appear to be a fungal virus, either. Secondary structures predicted the protein determined by FaR1-ORF1 is distinct from those of p42 encoded by STV, so is the amino acid sequence, although FaR1-ORF2 and STV encoding putative RdRps share more identical amino acids after multiple alignments. According to the display of prediction, both protein determined by FaR1-ORF1 and p42 of STV are rich in alpha helix, but the size of their individual alpha helix is different. The ones in putative CP of FaR1-ORF1 are short and discrete, while those of STV-p42 are longer and centralized. Additionally, putative CP of FaR1-ORF1 is composed of more discontinuous coils than that of STV. However, both putative CP of FaR1-ORF1 and STV-p42 share the common characteristic that fewer beta sheets are contained in their predicted secondary structures, which is unlike CPs of current partitiviruses and totiviruses. And it is also likely that there is no specialized CP for these kinds of viruses, and their genomic segments are exposed to the cytoplasm of plant cells. Thus, they are usually affected by factors from the

intracellular surroundings. In spite of this, the functional RdRps directing viral replication are found reserved with the conserved motifs. Maybe this is the reason why they remain in nature safely. The secondary structure similarity between UTRs of FaR1 and STV may imply the conservation of their RdRps, which recognize the unique structure type while conducting replication of the viral genome. Found in its relatively small size and simple structure, lucubrate study of such totivirus might bring new possibilities to understand dsRNA replication, transmission and interaction with hosts.



Fig. 6.21. Phylogenetic analysis on members of *Partitiviridae*, *Totiviridae* and *Chrysoviridae* families with FaR1-ORF2 protein. Numbers at the nodes of branches represent bootstrap values (shown when $\geq 50\%$). Members of the family *Partitiviridae*: *Gremmeniella abietina* RNA virus MS2 (YP_138540), *G. abietina* RNA virus MS1 (NP_659027), *Aspergillus ochraceus* virus (ABC86749), *Beet cryptic virus 3* (AAB27624), *Amasya cherry disease-associated mycovirus* (YP_138537), *Vicia cryptic virus* (YP_272124), *White clover cryptic virus 1* (YP_086754). Members not classified: *Tomato dsRNA virus T-11* (ABC96788) and *T-21* (ABC96787) (STV RNA-dependent RNA polymerase-like proteins), *Tomato yellow stunt virus* (ABO36238) (STV fusion protein p122), *Helicobasidium mompa* dsRNA mycovirus (BAC23065). Members of the family *Totiviridae*: *Gremmeniella abietina* RNA virus L2 (YP_044807), *Helminthosporium victoriae* virus 190S (AAB94791), *Saccharomyces cerevisiae* virus L-A (AAA50508). Members of the family *Chrysoviridae*: *Cherry chlorotic rusty spot associated chrysovirus* (CAH03664), *Amasya cherry disease associated chrysovirus* (YP_001531163), *Helminthosporium victoriae* 145S virus (YP_052858), *Fusarium oxysporum* chrysovirus 1 (ABQ53134). FaR1-ORF2 (EU371896) is indicated in bold; Viruses of the same family or genus were grouped, such as those members of the family *Totiviridae*, *Chrysoviridae* and *Partitiviridae* ([1]: *Alphacryptovirus*; [2]: *Partitivirus*)

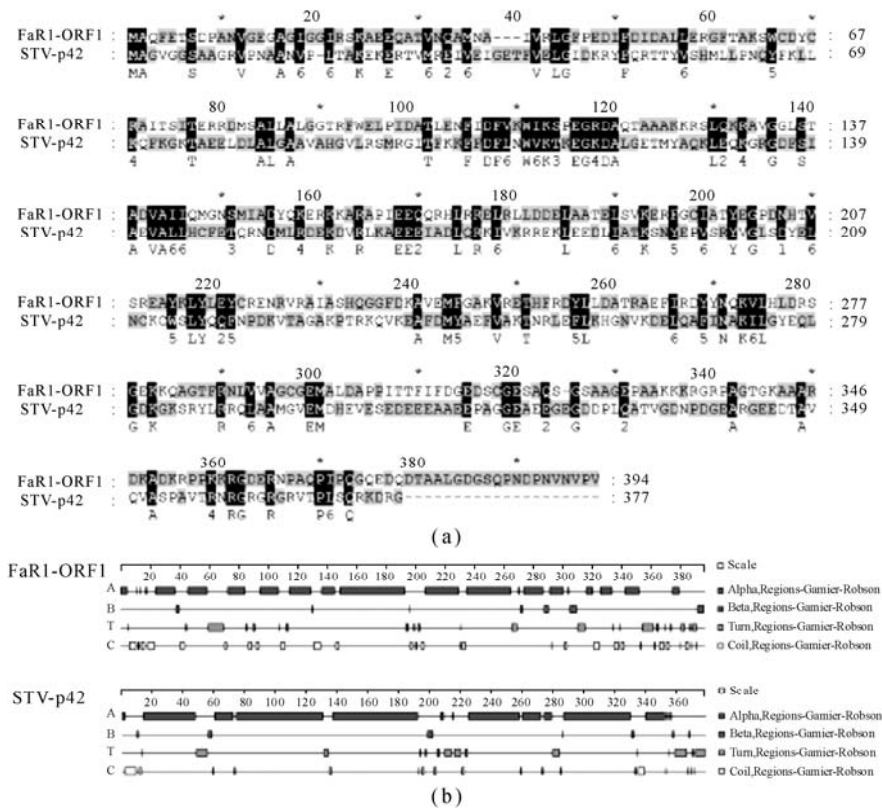


Fig. 6.22. (a) Result of multiple alignments of amino acid sequences of putative CPs of FaR1-ORF1 and STV-p42 [ABO36237]. Multiple alignments of the sequences were performed with program CLUSTALX 1.8 and displayed with program GeneDoc 2.7. Different shading levels (black, gray) represent distinct degrees of nucleotides conservation. Black: 100%; gray: >80%; (b) Secondary structures predicted putative CPs of FaR1-ORF1 and STV-p42 [ABO36237]. The secondary structural units of Alpha-helix, Beta-sheet, Turn and Coil are represented by red, green, blue and yellow boxes and their relative distributions and contents are presented as A, B, T and C, respectively

The virus determined is demonstrated to be grouped with STVs, and their RdRps possess conserved motifs as partitiviruses do. However, they do not belong to members of *Partitiviridae* with one-sequence genome, which is the typical genomic characteristic of members of *Totiviridae*. Neither do they belong to *Totiviridae* in light of the characteristics of assumed CPs, the smaller size and the fewer beta sheets. Therefore, just as Sabanadzovic et al. deduced, being present in nature, this new virus taxon possibly represented an intermediate transition from present *Totiviridae* to plant partitivirus.

In contrast to tomatoes, where STVs were originally isolated, *V. faba* in which the FaR1 segment was detected, did not show any symptom of viral infection. This phenomenon is quite similar to that caused by some cryptic plant viruses. It is therefore suggested that the virus containing FaR1 is a novel cryptic virus

infecting *V. faba*, with ORF1 coding for a putative CP and ORF2 coding for a putative RdRp. The new virus is suggested as *Vicia faba* cryptic virus M.

The family *Totiviridae* includes all the viruses of fungi and protozoa that have virions and a monopartite, linear, dsRNA of 4.6–7.0 kb as the genome. Its genome contains two large, usually overlapping, reading frames encoding the coat protein (gag) and an RNA-dependent RNA polymerase. Some members may have a smaller, 5'-proximal, ORF. *Totiviridae* is composed of four genera, *Giardiavirus* (36-nm diameter particles, infecting protozoan parasites), *Leishmanivirus* (33-nm diameter particles, infecting protozoan parasites), *Totivirus* (40-nm diameter particles, infecting yeasts and smut fungi), *Victorivirus* (40-nm diameter particles, infecting filamentous fungi and phylogenetically distinct from other genera). Recently, a totivirus-like plant dsRNA virus was also reported in plants. A dsRNA virus with a genome of 3.5 kb was isolated from field and greenhouse-grown tomato plants of different cultivars and geographic locations in North America. Cloning and sequencing of the viral genome showed the presence of two partially overlapping open reading frames (ORFs), and a genomic organization resembling members of the family *Totiviridae* that comprises fungal and protozoan viruses, but not plant viruses. The 5'-proximal ORF codes for a 377 amino acid-long protein of unknown function, whereas the product of ORF2 contains typical motifs of an RNA-dependant RNA-polymerase and is likely expressed by a +1 ribosomal frame shift. Despite the similarity in the genome organization within members of the family *Totiviridae*, this virus shared very limited sequence homology with known totiviruses or with other viruses. Repeated attempts to detect the presence of an endophytic fungus as the possible host of the virus failed, supporting its phytoviral nature. The virus was efficiently transmitted by seed but not mechanically and/or by grafting. Phylogenetic analyses revealed that this virus, for which the name southern tomato virus (STV) is proposed, belongs to a partitivirus-like lineage and represents a species of a new taxon of plant viruses.

The discovery of FaR1 supports the existence of STV. The virus described here and STV represent distinct members of a novel viral taxon different from the families *Totiviridae* and *partitiviridae*. With the discovery of more isolates of this new type of virus, the taxon of it will be quickly established (as shown in Fig. 6.21).

6.3.2 *A Partitivirus Infecting Aspergillus sp. Associated with Leaf Tissue of Vicia faba*

Fungal viruses (mycoviruses) have been found to be commonly hiding in many kinds of fungi, many of which are plant associated. Mycoviruses have no extra cellular phase; they are transmitted intracellularly through cell division, sporogenesis and cell fusion. Therefore, they are transmitted passively with their hosts and their natural host ranges are limited to individuals within the same or closely-related vegetative compatibility groups.

Since there are multiplex segments ready to be detected and isolated from broad bean plants, their possible origination and association have been investigated through isolating plant-pathogenic and exterior microbes. In the later grown stages, brown spots are commonly observed on the surface of the leaf, and the isolation of those dsRNA virus infected broad beans has yielded the principal fungus identified as *Aspergillus ochraceus* (Fig. 6.23).

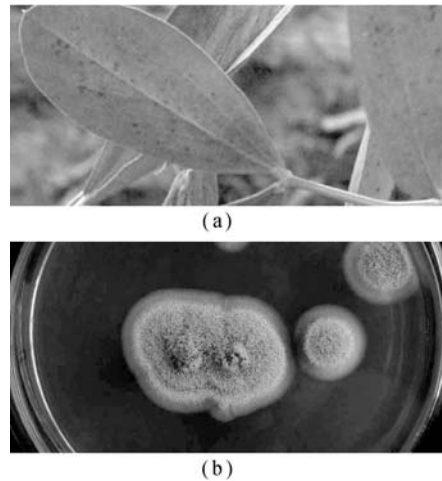


Fig. 6.23. Appearance of *V. faba* plants infected by *A. ochraceus* (a) and the culture characteristics of this fungus (b)

From all of the strain of *A. ochraceus* obtained from broad bean plants isolated in Hangzhou, eastern China during the year 2007–2008, multiplex dsRNA segments were detected widely. Taking *A. ochraceus* FA 0611 isolate for example, three dsRNA segments were detected. However, sequence analysis of dsRNAs showed that segment AoR1 was almost identical to the dsRNA 1 of *Aspergillus ochraceus* virus (AoV). The nucleic acid sequence of AoR2 was found encoding a putative CP, and segment AoR3 has no similar sequence found in the GenBank. AoR3 is considered as a satellite segment of this newly-sequenced partitivirus. Similarity and structure studies revealed that this new partitivirus, suggested as *A. ochraceus* virus 1 (AoV 1), has no relation with those dsRNA viruses infecting the broad bean.

The cDNA of AoR1 is found to be 1,754 bp in length. The search for similar sequences from the GenBank has revealed that it is 94% identical to AoV dsRNA 1, which was firstly sequenced from mycovirus complex in *A. ochraceus* (ATCC 28706) (Kim et al., 2006). A deduced RdRp, with 97% similarity to that encoded by AoV dsRNA 1, is found to correspond to the largest ORF of AoR1. Thus, AoR1 and AoV dsRNA 1 could be regarded as a dsRNA segment from the same mycovirus infecting *A. ochraceus* strains of different origins. AoR2 and AoR3 are 1,555 bp and 1,220 bp, respectively. The G/C contents for AoR2 and AoR3 were tested as 50.93% and 44.18%, respectively. The search for similar sequences reveals that AoR2 is 63% identical to segment S2 of PsV-S, a partitivirus infecting

similar to those of corresponding segments of partitiviruses, such as PsV-S, *Gremmeniella abietina* RNA virus MS1, *G. abietina* RNA virus MS2, *Discula destructiva* virus 1 and *D. destructiva* virus 2 (Table 6.4). The terminal motif sequences are accordingly suggestive as characteristics for members of the genus *Partitivirus*, including a novel member consisting of AoR1 and AoR2. AoR3 has a similar UTR with AoR2 in length, and multiple alignment of their UTRs shows that AoR3 contained the conserved sequence (5'-CGCAAAA-3') at the 5' terminus as well (Fig. 6.24(c)). However, it was less similar to AoR2 in the 3' UTR (Fig. 6.24(d)).

Table 6.4 Comparison of the 5' and 3' terminal sequences of AoR1 and AoR2 with those contained in *Partitiviruses*

Segments	5'	Terminal sequences	Terminal sequences	3'
AoR1[EU118277]	5'	CGCAAAA CU	UAAAUAA CUCC	3'
AoR2[EU118278]	5'	CGCAAAA CU	GUCAUAU CUCC	3'
PsV-S S1 [AM040148]	5'	CGCAAAA UC	AAUAAAUCUCU	3'
PsV-S S2 [AM040149]	5'	CGCAAAA UU	AGUAAAUCUCU	3'
GaRV-MS1 dsRNA1 [AY089993]	5'	CGCAAAA UA	AUUAACAAUCA	3'
GaRV-MS1 dsRNA2 [AY089994]	5'	CGCAAAA UU	AACCAACCUCU	3'
GaRV-MS2 dsRNA1 [AY615211]	5'	CGCAAAA UA	AUUAACAAUCA	3'
GaRV-MS2 dsRNA2 [AY615212]	5'	CGCAAAA UU	AACCAACCUCU	3'
DdV1 dsRNA1 [AF316992]	5'	GCGCAAAA AG	GUAAAAA CUCC	3'
DdV1 dsRNA2 [AF316993]	5'	CGCAAAA UU	CAUAAAC CUCC	3'
DdV2 dsRNA1 [AY033436]	5'	GCGCAAAA AC	AGUAAAACUCA	3'
DdV2 dsRNA2 [AY033437]	5'	GCGCAAAA AG	CAUAAAA CUCC	3'

Viruses used in preparation are *P. stoloniferum* virus S (PsV-S), *G. abietina* RNA virus MS1 (GaRV-MS1), *G. abietina* RNA virus MS2 (GaRV-MS2), *Discula destructiva* virus 1 (DdV1) and *D. destructiva* virus 2 (DdV2). Identical nucleotides with those of AoR1 and AoR2 are marked in bold and with grayish background color

The largest ORF on the positive strand of AoR2 is found to be coding for a protein of 433 amino acids (aa) with a molecular mass of approximately 47.0 kDa (P47.0). A database search for the proteins with similar sequences from the GenBank revealed that P47.0 has 50%–63% identity with the putative capsid proteins of seven documented partitiviruses (Table 6.5). Amongst those, it is found to be most closely related to PsV-S CP [YP_052857], with an identity of 63%. Results of the phylogenetic analysis with P47.0 and members of the family *Partitiviridae* revealed that P47.0 is grouped with CP of PsV-S and is more closely related to members of genus *Partitivirus* than those of genus *Alphacryptovirus* (Fig. 6.25).

Table 6.5 The identity among AoR2 CP and those of genus *Partitivirus*

Partitivirus	Identity
PsV-S [YP_052857]	63%
GaRV-MS1 [NP_659028]	56%
GaRV-MS2 [YP_138541]	56%
BfPV1 [CAM33267]	58%
DdV2 [NP_620302]	57%
DdV1 [NP_116742]	50%
OPV1 [CAJ31887]	50%

The nomenclature or preliminary identified viruses including PsV-S, GaRV-MS1, GaRV-MS2, *Botryotinia fuckeliana partitivirus 1* (BfPV1) (unpublished), DdV2, DdV1, *Ophiostoma partitivirus 1* (OPV1)

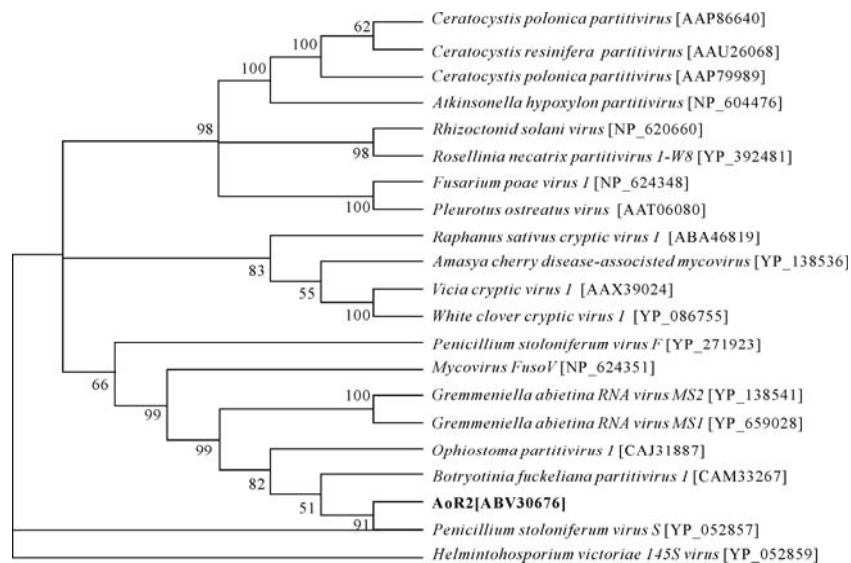


Fig. 6.25. Multiple alignments of the capsid proteins of the family *Partitiviridae* with AoR2 (indicated in bold). The phylogenetic analysis was performed with maximum parsimony tree and *Helminthosporium victoriae* 145S virus (HvV-145S) from the family *Chrysoviridae* was used as an outgroup [2]. The numbers at the nodes of the branches indicate the bootstrapping values (shown only when >50%)

A major ORF on the positive strand that putatively encoded a protein composed of 293 aa (33.6 kDa) was deduced for AoR3. However, the putative protein was found to have no similar sequences available from the GenBank, including those encoded by AoR1 and AoR2. Thus, the function of AoR3 remains unclear.

The newly-suggested AoV 1 is determined to be related to PsV-S infecting *P.*

stoloniferum, based on the sequence similarities. AoV 1 RdRp [AoR1: ABV30675] appears more similar to that of PsV-S [YP_052856] in the predicted secondary structures (Fig. 6.26), and they have higher identity (71%) in the aa sequences.

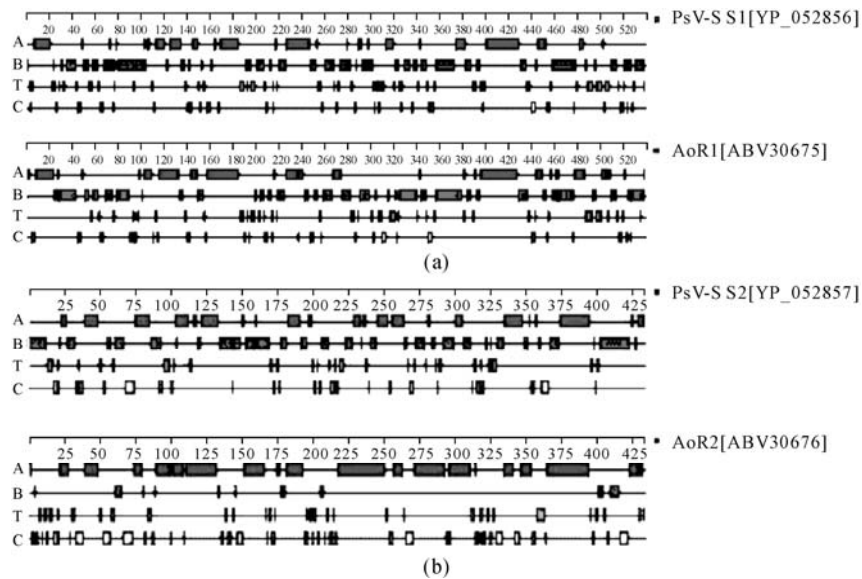


Fig. 6.26. Comparisons of the predicted secondary structures of RdRps and CPs encoded by PsV-S, AoR1 and AoR2. (a) Comparison between the predicted secondary structures of the putative RdRps encoded by PsV-S S1 and AoR1; (b) The comparison between the predicted secondary structures of the putative CPs encoded by PsV-S S2 and AoR2. The secondary structural units of Alpha-helix, Beta-sheet, Turn and Coil are represented by red, green, blue and yellow boxes and their relative distributions and contents are presented as A, B, T and C, respectively

In contrast, AoV 1 CP [AoR2: ABV30676] is less similar to PsV-S CP [YP_052857], with 63% identity. Compared with CP of PsV-S, more large Alpha helixes but fewer Beta sheets were predicted in CP deduced from AoR2. The appearance of AoR3 in FA 0611 is another characteristic difference from PsV-S, from which only two segments have been detected as the genomic molecules. Thus, the newly suggested partitivirus AoV 1, obtained from *A. ochraceous* in Hangzhou, China, is in some degree shown to be related to, but distinct from, PsV-S infecting *P. stoloniferum*.

Additionally, for some tripartite dsRNA cryptic viruses, the two smaller segments were both determined to encode coat proteins which are closely similar to each other. But these types of cryptic viruses have been found only in plant hosts, such as *Fragaria chiloensis* cryptic virus (FCCV) infecting the strawberry, RasR cryptic virus infecting the radish and a novel cryptic virus infecting the rose. Since these viruses have been shown to be more closely related to members of the fungi-infecting *Partitivirus* genus rather than members of plant-infecting *Alphacryptovirus*, it has been suggested that they evolve from fungal ancestors.

Although AoV 1 contains tripartite segments, sequence analyses revealed that AoR2 encoded a putative CP with homology similar to that of partitiviruses, whereas AoR3 putatively encoded a protein with no similarity to the protein encoded by AoR2. Therefore, these characteristics of AoR3 are more related to those of the additional segments which have been inferred as being satellite RNAs of partitiviruses infecting fungi.

Collectively, the newly-sequenced double stranded AoV 1 is regarded as a mycovirus infecting *A. ochraceous* which is plant pathogen or a broad bean related fungus, but not a plant virus. Its origination and distribution are waiting to be better understood by a general explanation through further investigation.

No direct relationship could be found between the viruses compared above using conventional methods.

6.4 A Novel dsRNA Virus Infecting *Primula Malacoides* Franch

Plants infected with double stranded viruses often exhibit yellow edge symptoms. Even though not all cases of dsRNA virus infection display the same symptoms at any one time, the emergence of yellow edges in general shows the existence of dsRNA segments belonging to one or more viruses. As follows, we will show a new partitivirus infecting a herb, *Primula malacoides* with yellow edge symptom.

Primula malacoides Franch, a perennial herb, is a winter and spring ornamental flower. There are relatively few study of viruses infecting *P. malacoides* Franch. Two tentative potyviruses, namely *Primula mosaic virus* and *Primula mottle virus*, were reported from *P. obconica* and *P. malacoides* respectively (ICTVdB, 2006a; 2006b). No genomic information about these two viruses has been documented. Yellowing-edge symptoms, which subsequently developed into withering symptoms, were commonly observed on primula (*P. malacoides*) plants during a survey in 2005–2008 (Fig. 6.27). With the commercial seeds imported from North America, both red flower or yellow flower seedlings reach a similar appearance. To confirm that these symptoms are indicative of infection by a plant virus, dsRNA diagnosis is made from leaf tissues of the primula plants collected from open fields. A dsRNA band of approximately 2.3–2.5 kbp has been accordingly observed in agarose gel electrophoresis and compared with those dsRNAs of *Cucumber mosaic virus* (Fig. 6.28(a)).

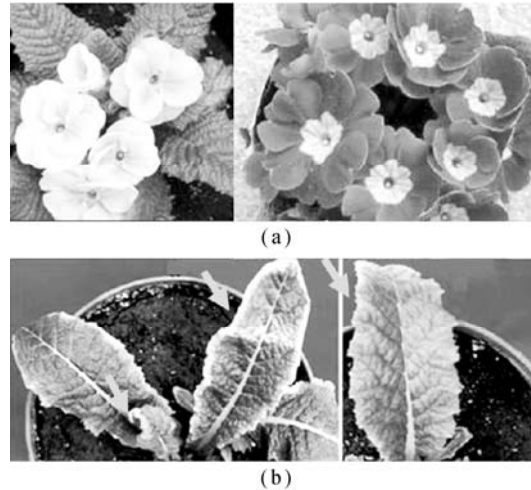


Fig. 6.27. Plants of *P. malacoides* grown from hybrid seeds imported from America and symptoms observed. (a) Flowering plants; (b) *Primula* seedlings with typical yellow edge symptoms

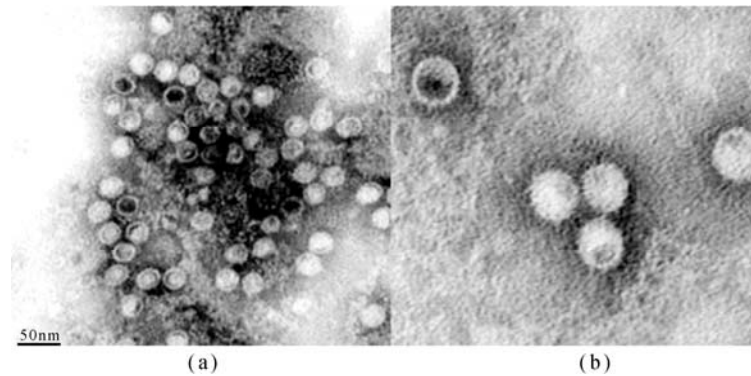


Fig. 6.28. Electron micrographs of viral-like particles extracted from natural-infected leaves of primula plants. The size bar is equal to 50 nm

To confirm the association of PmV1 with plant tissues, attempts have been made to obtain plant pathogenic fungi, endophytic fungi, plant-associated and surface-contamination fungi using potato dextrose agar (PDA) as the culture medium. No plant pathogenic or endophytic fungi are isolated, but several fungal species of genera *Aspergillus* and *Penicillium* were detected as plant associated and surface-contaminating fungi. Neither dsRNAs nor virus-like particles have been detected from the mycelium of the above microbes. Spherical virus-like particles, 30–35 nm in size, are obtained from partial purification preparation extracted from symptomized leaf primula tissues and observed under an electron microscope, using the method described in this chapter (Fig. 6.28). Agarose gel electrophoresis profiles of the total nucleic acids extracted from virions gave

dsRNA patterns quite similar to those extracted from plant tissues (Fig. 6.29(a)). Their double-stranded RNA properties are confirmed by the absence of digestion with DNase I and RNase A in low salt concentration, and SDS-PAGE analysis showed two major proteins from the virions. Their molecular weight values matched the calculated molecular masses (84.2 kDa and 74.8 kDa) of RdRp and CP putatively encoded by dsR1 and dsR2, respectively.

By repeated sequencing the RT-PCR products yielded from a modified single-primer amplification technique (see methodology in this chapter), two identical nucleotide sequences, namely dsR1 and dsR2, have been obtained from both leaf tissue and the purified virus-like particles.

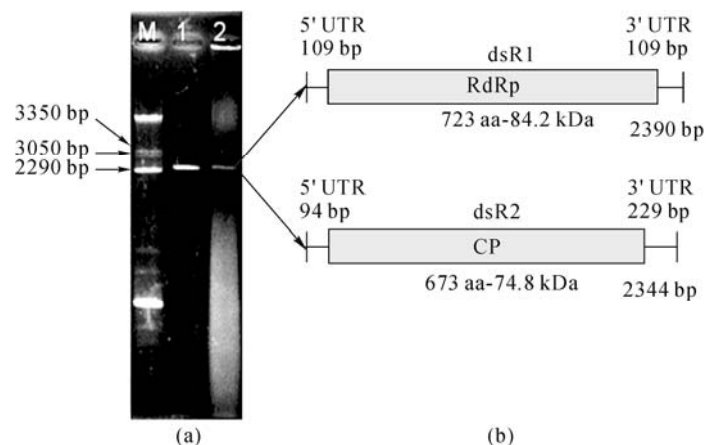


Fig. 6.29. Properties of dsRNAs extracted from primula and their genomic diagrams. (a) Agarose profile. M: dsRNAs from tobacco leaves infected by CMV with a 382 nt satellite; 1: viral RNAs extracted from virions which were isolated from primula leaves; 2: dsRNAs from primula leaves; (b) Genomic organization of dsR1 and dsR2. The open bars represent open reading frames defined by genome analysis encoding the putative RNA-dependent RNA polymerase (RdRp) and capsid protein (CP). The untranslated regions are indicated as a single line, with their corresponding sizes indicated above

The newly-sequenced dsR1 and dsR2 are found to be of 2,390 bp and 2,344 bp, respectively. The base contents of dsR1 (dsR2) are 30.75% A (25.64%), 24.98% C (27.47%), 29.62% T (31.91%) and 14.64% G (14.97%), respectively. One major open reading frame (ORF) is found to exist in one strand of each segment (designated the positive strand), but no functional coding element could be predicted from their complementary strands. The 5' UTRs of the positive strands of dsR1 and dsR2, 109 bp and 93 bp, respectively, showed high sequence identity with each other (Fig. 6.30(a)). The secondary structure analysis of the positive strands showed that their 5' UTR sequences formed similar RNA stem-loop structures. Such structures have also been reported in other partitiviruses, including *Rhizoctonia solani virus 717* (Rhs V-717) and *Pleurotus ostreatus virus* (PoV), which were presumed to be involved in virus assembly and dsRNA replication (Lim et al., 2005; Strauss et al., 2000). The 3' UTRs of dsR1 and dsR2 were 109

bp and 229 bp, respectively, and both contained a 3' proximal interrupted poly (A) tail, terminating with the sequence CCCC (Fig. 6.30(b)).

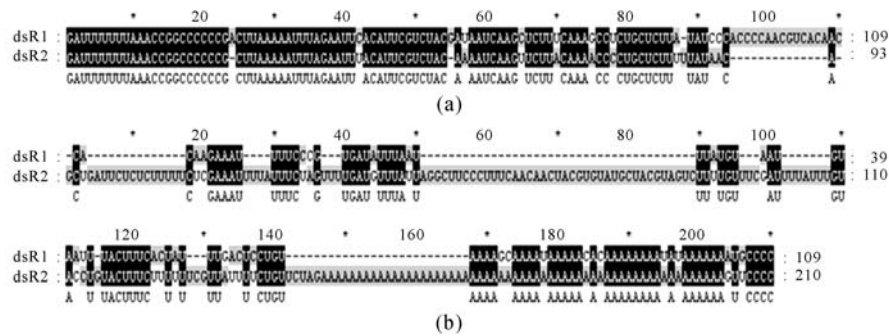


Fig. 6.30. Comparison of 5' UTR (a) and 3' UTR (b) between dsR1 and dsR2. The alignment was performed using the R-coffee method

Analyses of amino acid sequences putatively coded by the major ORFs yielded a 723 aa protein from dsR1, corresponding to nucleotides 110–2,281 bp, and a 673 aa protein from dsR2, corresponding to nucleotides 94–2,115 bp, with molecular weights of 84.2 kDa and 74.8 kDa, respectively (Fig. 6.30(b)). BLASTP search showed that the predicted protein of dsR1 was related clearly to sequences of RdRps of members of the family *Partitiviridae*. The most closely-related viruses are those infecting fungi, such as PoV infecting *Pleurotus ostreatus*, which is one of the major cultured edible mushrooms. Other related viruses include *Rosellinia necatrix partitivirus 1* (uRnPV-1; the “u” added on the abbreviation denotes unclassified partitivirus in this paper) infecting *Rosellinia necatrix*, which is a plant pathogenic ascomycete; *Helicobasidium mompa partitivirus V1-1* (HmPV V1-1) infecting *Helicobasidium mompa*, which is a violet root rot fungus; *Fusarium poae virus 1* (FpV1) infecting *Fusarium poae* (Peck) Wollenw, which is a cereal grain fungus *Rhizoctonia solani*, which is a cosmopolitan, soil-borne plant pathogenic fungus; *Atkinsonella hypoxylon virus* (AhV) infecting *Atkinsonella hypoxylon* (Peck), which is a filamentous ascomycete causing choke disease in several grasses; *Ceratocystis resinifera partitivirus* (CrPV) infecting *Ceratocystis resinifera*, which is a weak pathogen of *Picea* and *Pinus* tree species; *Ceratocystis polonica partitivirus isolate 1* (CpPV_1) and *Ceratocystis polonica partitivirus isolate 2* (CpPV_2) infecting the blue-stain fungus *Ceratocystis polonica*, which is pathogenic to European spruce (*Picea abies*) in Europe; and *Heterobasidion annosum virus* (HaV) infecting root rot fungus *Heterobasidion annosum*, which is a pathogen that causes root and butt rot in conifers. Sequence alignments among the above ten sequences with the predicted protein sequence of dsR1 showed the motifs (F, 3-8) characterizing viral RdRps, which are conserved within positive, negative ssRNA and dsRNA viral RdRps (Fig. 6.31).



Fig. 6.31. Sequence alignment of putative proteins of dsR1 and RdRps of reported partitiviruses. Viruses and Genbank accession numbers are: PoV (AAT07072), FpV1 (AAC98734), uRnPV-1 (AB113347), HmPV_V1-1 (AB110979), RhsV-717 (AF133290), AhV (I39125), CrPV (AY603052), CpPV_1 (AY247204), CpPV_2 (AY260756), and HaV (AF473549). The alignment was done using the Clustal W method. The conserved motifs of RdRp are indicated according to Bruenn as indicated

The CPs of four partitiviruses (RhsV-717, uRnPV-1, PoV and FpV1), whose replicases are also found to be closely-related to the predicted protein encoded by dsR1 as shown above, are found to be highly similar to the predicted protein encoded by dsR2.

It is suggested that dsR1 and dsR2 are the genomic components of a new partitivirus species isolated from primula, which is named as *Primula malacoides* virus 1 (PmV1). Furthermore, phylogenetic analysis of RdRp sequences of dsRNA viruses from the family *Partitiviridae*, using a chrysovirus *Helminthosporium victoriae* 145S virus (Hv145SV) as outgroup, indicated that dsR1-encoded putative RdRp clustered together with RdRp sequences of the members of the *Partitiviridae* (Fig. 6.32). Among the *Partitiviridae*, the dsR1-encoded putative RdRp is found to be much closer to members of the genus *Partitivirus*, including uRnPV1, HmPV V1-1, FpV1, RhsV-717, PoV, AhV, CrPV, CpPV_1, CpPV_2 and HaV as mycoviruses, than to members of the genus *Alphacryptovirus*, including VCV, WCCV-1 (*White clover cryptic virus 1*) and BCV3 as cryptoviruses, the latter infecting *Vicia faba*, white clover and beet, respectively. An explanation for this similarity to members of the genus *Partitivirus* is considered below.

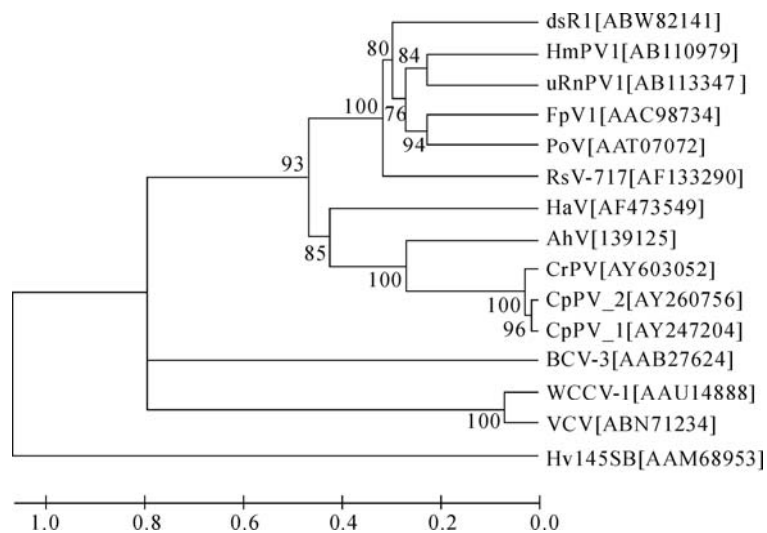


Fig. 6.32. Phylogenetic tree based on alignment of dsR1-encoded putative protein and RdRp sequences of some dsRNA viruses. The phylogenetic tree was linearized assuming equal evolutionary rates in all lineages. *Helminthosporium victoriae* 145S virus (Hv145SV, AAM68953) was used as outgroup. The neighbor joining method with a 1000-replicate bootstrap search was utilized, and bootstrap values were indicated at the branch points. The dsR1-encoded putative RdRp is indicated by the sign

6.5 Derivation and Evolutionary Relationship of dsRNA Viruses Infecting plants

Besides the viruses described above, many other plant dsRNAs viruses have also been reported. Partitiviruses representing all members of the family *Partitiviridae*, were found to be widely distributed in plants (Boccardo et al., 1987) and fungi (Ghabrial, 1998), and classified into three genera, *Alphacryptovirus* and *Betacryptovirus* infecting plants, and *Partivirus* infecting fungal species (Ghabrial et al., 2005). In addition, a virus infecting protozoa was also found to be related to partitiviruses (Khrantsov and Upton, 2000). The genome of most partitiviruses identified to date is composed of two dsRNAs, ranging from 1.4 to 3.0 kbp, which are encapsidated by isometric particles about 30–40 nm in diameter. The larger dsRNA encodes RNA dependent RNA polymerase (RdRp), and the smaller dsRNA encodes capsid protein (CP) (Ghabrial et al., 2005). However, a third dsRNA segment, suggested to be a satellite or an additive dsRNA with unknown function, has been detected in some partivirus species (Oh and Hillman, 1995; Salem et al., 2008; Tuomivirta and Hantula, 2005; Tzanetakis et al., 2008). Partitiviruses infecting plants are usually designated as cryptoviruses. Cryptoviruses are transmitted through seed and pollen but not by mechanical inoculation. In most cases, plant-infecting cryptoviruses cause no obvious symptoms (Boccardo et al., 1985; Kassanis et al., 1977). Some cryptoviruses were found well adapted to their hosts and they could persist for years under tissue culturing conditions and even survive thermotherapy (Szegô et al., 2005).

As early as 1977, *Beet cryptic virus* (BCV), a member of the family *Partitiviridae*, was observed to have isometric particles about 30 nm in diameter (Kassanis et al., 1977). Although this virus was found to be widespread in different cultivars of *Beta vulgaris*, it induced no apparent symptoms. Subsequent research revealed that there were three kinds of BCVs, designated BCV1, BCV2 and BCV3, infecting various beet cultivars (Antoniw et al., 1986; Xie et al., 1993). Kentex et al. detected virus-like particles (VLPs) isolated from several cultivars of *Vicia faba*, and regarded them as particles of *Vicia cryptic virus* (VCV) (Kentex et al., 1978). Abo-Elnasr et al. found that VLPs of VCV contained three dsRNAs of about 2,014, 1,852 and 1,779 bp, respectively (Abo-Elnasr et al., 1985). Recently, the genome of VCV was sequenced and it was found to contain two segments, including one 2,012 bp dsRNA putatively encoding viral RdRp and another 1,779 bp dsRNA putatively encoding viral CP. In addition to these two dsRNAs, a third dsRNA of about 1.9 kbp, encoding a putative partivirus-related RdRp, was reported and suggested to have no apparent characteristics associated with VCV (Blawid et al., 2007). In the 1980s, Boccardo et al. isolated three dsRNA viruses *White clover cryptic viruses* (WCCV) 1, 2, and 3, which were latterly classified in the family *Partitiviridae*, based on their biology and physical chemistry characteristics (Boccardo et al., 1985). And furthermore, RNA-dependent RNA polymerase activities were detected in purified particles of WCCV 1 and 2, which had different requirements for optimum activity (Boccardo and Accotto, 1988). However only the genome of WCCV1 has been determined and characterized

recently. The results showed that it is of typical partitivirus genomic structures, and composed of one dsRNA (1955 bp) putatively encoding viral RdRp and another dsRNA (1708 bp) putatively encoding viral CP. Similar viruses have also been detected in alfalfa, beet, radish, Italian ryegrass, carnation, meadow fescue, hop trefoil, red clover, spinach, carrot etc. (Dodds, Morris, and Jordan, 1984). Although no genome information of *Alfalfa cryptic virus 1* (ACV1) can be obtained now, ACV1 is the first plant cryptic virus the function of whose genome segments was studied and confirmed *in vitro*. The genome of ACV 1 consists of two dsRNAs, one with an estimated Mr of 1.27×10^6 Da (about 1920 bp, RNA 1) encoding RdRp whose activity was tested, and the other of Mr 1.17×10^6 Da (about 1772 bp, RNA 2) expressing the capsid protein of ACV 1 (Accotto et al., 1990).

In recent years, especially since 2000, with fast development of gene manipulating techniques, more of these cryptic plant dsRNA viruses have been found and genomically characterized. Tzanetakis and Martin found a new partitivirus named *Fragaria chiloensis cryptic virus* infecting a Chilean *Fragaria chiloensis* plant while cloning the genome of *Fragaria chiloensis latent virus* (Tzanetakis and Martin, 2005). Like RasV1 and 2, *Fragaria chiloensis cryptic virus* is composed of three dsRNA segments: the largest one putatively encodes viral polymerase, and the other two encode two closely-related proteins predicted to be the coat proteins of the virus (Tzanetakis et al., 2008). Latterly, another tripartite partitivirus (rose) was reported in *Rosa multiflora* plants showing rose spring dwarf symptoms, which was named *Rosa multiflora cryptic virus* (Salem et al., 2008). There were also other partitiviruses infecting tree plants reported, such as the pear tree (*Pyrus pyrifolia*) and even the ancient Gymnosperm, pine (*Pinus sylvestris*).

The family *Chrysoviridae* currently consists of the single genus *Chrysovirus*. It contains dsRNA viruses that infect fungi and which have four genome components. Its virions are isometric (icosahedral), not enveloped, 35–40 nm in diameter and have a genome with four linear dsRNAs ranging from about 2.9–3.6 kb in size. Some chrysovirus sequences have now also been isolated from plants; it is not clear yet whether these are genuine plant pathogens, or whether they have been isolated from a parasitic fungus within the plant. A series of dsRNAs were isolated from cherry leaves showing Cherry chlorotic rusty spot (CCRS) and Amasya cherry disease (ACD). Sequence determination of four of these dsRNAs revealed that they were essentially identical for CCRS and ACD. And two chrysovirus, named *CCRS associated Chrysovirus* and *ACD associated Chrysovirus*, were characterized. Their genome consisted of four dsRNA segments. The largest (3399 bp), which putatively encoded a protein of 1087 aa with the eight motifs conserved in RNA-dependent RNA polymerases, had the highest similarity to those coded by dsRNA 1 of chrysovirus. The three other closely migrating dsRNAs had the properties of the other components of a chrysovirus and in CCRS and ACD versions, respectively, these were chrys-dsRNA 2 (3125 and 3128 bp), chrys-dsRNA 3 (2833 bp) and chrys-dsRNA 4 (2499 and 2498 bp), potentially encoding the viral capsid protein (993 and 994 aa) and two proteins (884 and 677 aa, respectively) of unknown function (Covelli et al., 2004). As supposed by Covelli et al., species of the genus *Chrysovirus* have only been

described in fungi. This suggests a fungal aetiology for CCRS and ACD, that is to say that both CCRS associated Chrysovirus and ACD associated Chrysovirus infect the fungus that possibly causes the cherry disease. However, it is more likely to be two chrysoviruses infecting the cherry plant.

Linear large dsRNAs have commonly been found in various healthy plants ranging from algae to higher plants and fungi, such as barley (*Hordeum vulgare*), kidney bean (*Phaseolus vulgaris*), melon (*Cucumis melo*), bottle gourd (*Lagenaria siceraria*), Malabar spinach (*Basella alba*), seagrass (*Zostera marina*), and the fungus *Helicobasidium mompa* (Brown and Finnegan, 1989; Fukuhara et al., 2006; Ishihara et al., 1992). Phylogenetic analyses indicate that they share a common ancestor with the alpha-like supergroup of single-stranded RNA (ssRNA) viruses (Gibbs et al., 2000). And it is suggested they be classified into a new genus *Endornavirus*.

dsRNAs viruses are widely distributed in *planta* and fungi. And in the same family, cryptoviruses always have a closer relationship with mycoviruses. Even some evidence supports the possibility of horizontal transmission between them.

As follows, the evolution relationship and taxonomy of the family *Partitiviridae* are comprehensively analyzed and discussed. Currently, the family *Partitiviridae* is classified into three genera, *Partitivirus*, *Alphacryptovirus* and *Betacryptovirus* and this classification is based predominantly on virion morphology, host range, size of dsRNA segments and serological relationships. Viruses of genus *Alphacryptovirus* have relatively small genomes compared with those of *Betacryptovirus*. However, in present taxonomy, few genome characteristic and evolution criteria at the molecular level are considered in the classification of the family *Partitiviridae*.

Table 6.6 Information of documented partitiviruses used for alignment and phylogenetic analyses

Virus	RdRp accession no. (nucleic acid, protein)	Taxonomy status ^b
<i>Amasya cherry disease associated partitivirus</i> (ACD-PV) ^a	<u>AJ781168</u> , <u>CAG77604</u>	<i>Partitiviridae</i> , <i>partitivirus</i>
<i>Atkinsonella hypoxylon virus</i> (AhV)	<u>L39125</u> , <u>AAA61829</u>	<i>Partitiviridae</i> , <i>partitivirus</i>
<i>Cherry chlorotic rusty spot associated partitivirus</i> (CCRS-PV)	<u>AJ781401</u> , <u>CAH03668</u>	<i>Partitiviridae</i> , <i>partitivirus</i>
<i>Discula destructiva virus 1</i> (DdV-1)	<u>AF316992</u> , <u>AAG59816</u>	<i>Partitiviridae</i> , <i>partitivirus</i>
<i>Discula destructiva virus 2</i> (DdV-2)	<u>AY033436</u> , <u>AAK59379</u>	<i>Partitiviridae</i> , <i>partitivirus</i>
<i>Fusarium poae virus 1</i> (FpV1)	<u>AF047013</u> , <u>AAC98734</u>	<i>Partitiviridae</i> , <i>partitivirus</i>
<i>Fusarium solani virus 1</i> (FsV1)	<u>D55668</u> , <u>BAA09520</u>	<i>Partitiviridae</i> , <i>partitivirus</i>
<i>Gremmeniella abietina RNA virus MS1</i> (GarV-MS1)	<u>AY089993</u> , <u>AAM12240</u>	<i>Partitiviridae</i> , <i>partitivirus</i>

(To be continued)

(Table 6.6)

Virus	RdRp accession no. (nucleic acid, protein)	Taxonomy status ^b
<i>Gremmeniella abietina</i> RNA virus MS2 (GarV-MS2)	AY615211 , AAT48886	Partitiviridae, partitivirus
<i>Penicillium stoloniferum</i> virus F (PsV-F)	AY738336 , AAU95758	Partitiviridae, partitivirus
<i>Penicillium stoloniferum</i> virus S (PsV-S)	AM040148 , CAJ01909	Partitiviridae, partitivirus
<i>Pleurotus ostreatus</i> virus (PoV)	AY533038 , AAT06080	Partitiviridae, partitivirus
<i>Rhizoctonia solani</i> virus 717 (RhsV-717)	AF133290 , AAF22160	Partitiviridae, partitivirus
Rosellinia necatrix partitivirus 1 (uRnPV-1)	AB113347 , BAD98237	Partitiviridae, unclassified
<i>Vicia faba</i> cryptic virus (VCV)	AY751737 , AAX39023	Partitiviridae, alphacryptovirus
White clover cryptic virus 1 (WCCV-1)	AY705784 , AAU14888	Partitiviridae, alphacryptovirus
<i>Aspergillus ochraceus</i> virus (AoV)	DQ270031 , ABC86749	Partitiviridae, partitivirus
<i>Botryotinia fuckeliana</i> partitivirus 1 (BfPV1)	AM491609 , CAM33266	Partitiviridae, partitivirus
<i>Ceratocystis polonica</i> partitivirus isolate 2 (CpPV_2)	AY260756 , AAP86639	Partitiviridae, partitivirus
<i>Ceratocystis polonica</i> partitivirus isolate 1 (CpPV_1)	AY247204 , AAP79988	Partitiviridae, partitivirus
<i>Ceratocystis resinifera</i> partitivirus (CrPV)	AY603052 , AAU26069	Partitiviridae, partitivirus
<i>Helicobasidium mompa</i> partitivirus V1-1 (HmPV V1-1)	AB110979 , BAD32677	Partitiviridae, partitivirus
<i>Helicobasidium mompa</i> partitivirus V1-2 (HmPV V1-2)	AB110980 , BAD32678	Partitiviridae, partitivirus
<i>Helicobasidium mompa</i> virus (HmV)	AB025903 , BAC23065	Partitiviridae, partitivirus
<i>Heterobasidion annosum</i> virus (HaV)	AF473549 , AAL79540	Partitiviridae, partitivirus
<i>Ophiostoma</i> partitivirus 1 (OPV-1)	AM087202 , CAJ31886	Partitiviridae, partitivirus
<i>Vicia faba</i> partitivirus 1 (uVfPV-1)	DQ910762 , ABJ99996	Partitiviridae, unclassified
Beet cryptic virus 3 (BCV-3)	S63913 , AAB27624	Partitiviridae, alphacryptovirus
<i>Pyrus pyrifolia</i> cryptic virus (PpCV)	AB012616 , BAA34783	Partitiviridae, partitivirus
<i>Cryptosporidium</i> partitivirus (uCPV)	U95995 , AAC47805	Partitiviridae, unclassified
<i>Fragaria chiloensis</i> cryptic virus (uFcCV)	DQ093961 , AAZ06131	Partitiviridae, partitivirus
<i>Raphanus sativus</i> cryptic virus 1 (uRsCV-1)	AY949985 , AAX51289	Partitiviridae, unclassified
<i>Raphanus sativus</i> cryptic virus 2 (uRsCV-2)	DQ218036 , ABB04855	Partitiviridae, unclassified
<i>Pinus sylvestris</i> partitivirus (uPsPV)	AY973825 , AAY51483	Partitiviridae, unclassified

All the *Partitiviridae* members (including tentative members) reported to date are included. The characters in the brackets represent the abbreviated name of the virus used in this chapter. The “u” added to the abbreviation denotes unclassified partitivirus. ^b The classification status of the virus is given

The phylogeny of the family *Partitiviridae* based on RdRp ORF sequences of all sequenced partitiviruses showed that all sequenced partitiviruses clustered into two major groups, namely Group A and Group B. Each group contains two subgroups (Fig. 6.33(a)). The members of Subgroup I to IV are listed in Table 6.6 and Table 6.7.

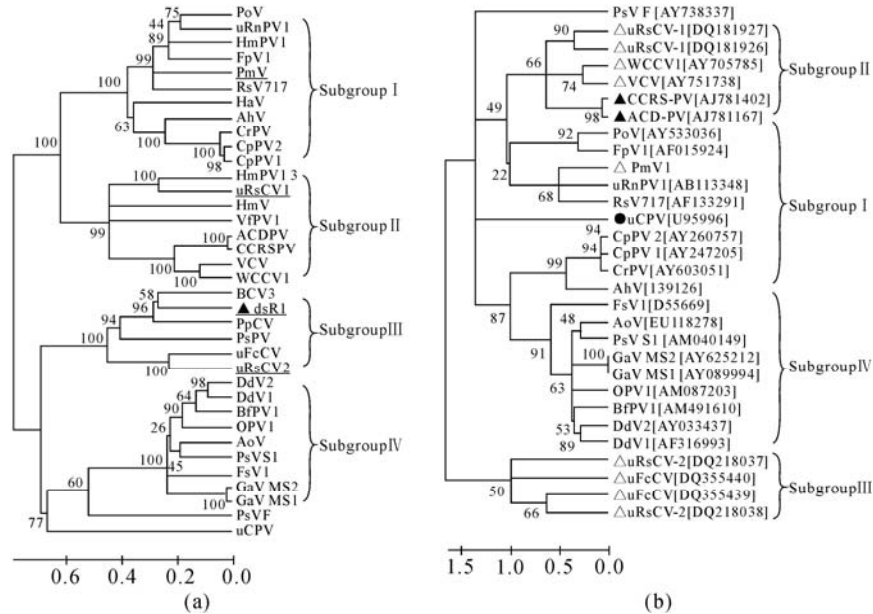


Fig. 6.33. Inferred phylogenetic tree of partitivirus. (a) Phylogenetic tree based on alignment of all available partitivirus RdRp ORF sequences. The RdRp ORF sequence of PsPV is incomplete; (b) Phylogenetic tree based on alignment of all available partitivirus CP ORFs sequences. Accession numbers of CP sequences are shown in the tree along with the viruses. The evolutionary distances were computed using the Maximum Composite Likelihood method. Bootstrap values are indicated at the branch points. The putative-RdRp-corresponding partitivirus infecting the plants is indicated with Δ , the partitivirus infecting the protozoas is indicated with \bullet . ACD-PV and CCRS-PV indicated with \blacktriangle , whose genomes were isolated from cherry leaves but might be of fungus origin. The unmarked viruses were reported in fungi

Interestingly, both Group A and Group B contain a fungal subgroup and a plant subgroup. All members of Subgroup I infect fungal species except the newly-described virus PmV1 from primula. All viruses of Subgroup II infect plant species, while HmV and HmPV V1-2 were described as having a fungal origin. All viruses of Subgroup III infect plant species. And all viruses in Subgroup IV are mycoviruses infecting fungi. Subgroup I was found to be clustered together with Subgroup II to form Group A, and Subgroup III was found to be clustered together with subgroup IV to form another independent group Group B. PsV-F (*Penicillium stoloniferum virus F*) infecting *Penicillium stoloniferum*, and uCPV (*Cryptosporidium partitivirus*) infecting a protozoa species of *Cryptosporidium*, are clustered as outgroup individuals. Apparently, the evolutionary history of the

partitivirus is directional and of high host specificity. This suggests that partitiviruses evolved into four different groups.

The inferred phylogenetic tree of partitiviruses based on alignment of ORF nucleotide sequences of CPs also has a similar topology as above (Fig. 6.33(b)), indicating parallel evolution of CP with RdRp, but with faster adaptation and mutation.

Table 6.7 Composition information and coding fragment of partitiviruses used for alignment and phylogenetic analyses

Subgroup	Virus ^a	Base composition (%) ^b					Length of the RdRp ORF (bp)	Length of the RdRp-encoding dsRNA (bp)
		U	A	C	G	G+C		
I	PmV1	29.6	30.1	25.1	15.2	40.3	2172	2290
	RsV 717	29	29.5	26.1	15.4	41.5	2193	2363
	FpV1	28.4	27.8	28.5	15.2	43.7	2022	2203
	PoV	25.9	24.8	32.9	16.5	49.4	2121	2223
	uRnPV1	25.8	28.3	30.5	15.4	45.9	2130	2299
	HaV	28.8	25.5	30.4	15.3	45.7	2205	2325
	HmPV1 1	28.9	24.7	31.5	14.9	46.4	2121	2247
	CpPV 2	29.9	29.6	24.1	16.4	40.5	1992	2156
	CpPV 1	30.7	29.7	23.2	16.3	39.5	1992	2315
	CrPV	30.1	28.7	24.6	16.6	41.2	1992	2207
AhV	31.3	30.5	22.2	16	38.2	1998	2180	
II	HmV	27.1	24.7	30.1	18.1	48.2	1797	1928
	HmPV1 2	26.1	24.5	30.7	18.7	49.4	1617	1776
	VFPV1	27	29.6	25.7	17.8	43.5	1729	1915
	ACD-PV	23.7	28.8	29.8	17.6	47.4	1866	2002
	CCRS-PV	23.6	28.8	30	17.5	47.5	1866	2012
	VCV	25.3	27.3	29.8	17.6	47.4	1851	2012
	WCCV1	28	27.3	26.6	18	44.6	1851	1955
	uRsCV-1	26	27.1	28.2	18.6	46.8	1721	1866
III	BCV3	24.8	30.9	21.4	22.8	44.2	1437	1607
	PpCV	25	32.4	19.9	22.7	42.6	1434	1592
	PsPV	24.3	30.5	24.3	20.8	45.1	974	1078
	uFcCV	26.5	27.9	25.2	20.3	45.5	(incomplete)	(incomplete)
	uRsCV-2	27	27.5	24.3	21.1	45.4	1434	1717
	DdV1	25.1	27.1	20.4	27.4	47.8	1620	1787
IV	DdV2	25	28	20.2	26.8	47	1620	1781
	BfPV1	25.4	27.5	21.7	25.3	47	1623	1793
	OPV1	24.4	24.9	24.6	26	50.6	1620	1744
	GaV MS1	24.4	24.5	23.3	27.7	51	1620	1787
	GaV MS2	25.1	24.2	23	27.8	50.8	1620	1781
	PsV S	27.4	23.3	23.2	26.1	49.3	1620	1753
	AoV	27.4	25.4	22.1	25.1	47.2	1620	1754
	FsV1	25.7	24.1	22.8	27.4	50.2	1560	1645
	PsV F	31	27.4	20.3	21.3	41.6	1617	1677
	uCPV	30.4	33.1	16.4	20	36.4	1575	1786

^a Full virus names are listed in Table 6.6; ^b Values are calculated by MEGA 4

To support the above results and viewpoints, more aspects are considered based on nucleic acid sequence characteristics. The inferred phylogeny is well supported by base composition analysis and length characteristics of the aligned RdRp ORFs, and UTR alignments of genomic segments. The disparity of G+C base content of aligned RdRp ORFs amongst four subgroups is not obvious, but the G base content varies in subgroups. The G base content ranges from 15.2% to 16.6% in Subgroup I, from 17.6% to 18.7% in Subgroup II, from 20.3% to 22.8% in Subgroup III and from 25.1% to 27.8% in Subgroup IV (Table 6.7). Thus, the G base content of Group B (Subgroup III and Subgroup IV) is much higher than Group A (Subgroup I and Subgroup II).

The length range of the aligned RdRp ORFs (corresponding to the polypeptides length) among the four subgroups was found to be clearly different, with few exceptions. The ORF size varies from 1,992 to 2,205 bp in Subgroup I, from 1,721 to 1,866 bp in Subgroup II (except that HmPV V1-2 is 1,617 bp), from 1,434 to 1,440 bp in Subgroup III, and from 1,620 to 1,623 bp (except that FsV1 was 1,560 bp) in Subgroup IV (Table 6.7). Taken together, the RdRp-encoding ORF sequences of the species in Group A are longer than those in Group B. Interestingly, most members of Subgroup IV were highly conserved at their 5' UTR regions through extensive UTR alignment analysis. In the CP-encoding sequences of Subgroup IV, all 5'UTRs contained strictly conserved segments, including CGCAAAA (r1), UUUU (r2), CUGUGUAUACGG (r3) and GCCUCCUUCA (r4), even though occasional base changes occurred in these conserved regions. In the viral RdRp-encoding dsRNA sequences of Subgroup IV, all the 5'UTRs also present three highly conserved regions, including CGCAAAA, UUUU and GCCUCCUUCA, corresponding to r1, r2 and r4 in the CP-encoding dsRNA sequences, respectively (Fig. 6.34). Interestingly, the amino acid sequences of RdRps of Subgroup IV are highly conserved (not shown). The conserved regions in Subgroup IV provide further evidence supporting the inferred phylogeny of the partitivirus. The RdRp ORF of PmV1 is 2,172 bp and its G base content is 15.2%. These characteristics are clear in the spectrum of Subgroup I, and consistent with the above phylogenetic result.

Based on the inferred phylogeny of all partitiviruses with the available genome information, a suggestion about reconsidering the taxonomy of the family *Partitiviridae* was given. And it is more feasible to classify the partitivirus into four genera: *Alphacryptovirus* and *Betacryptovirus*, corresponding to Subgroup II and Subgroup III, whose members mainly infect plant hosts, and *Alphapartitivirus* and *Betapartitivirus*, corresponding to Subgroup I and Subgroup IV, whose members mainly infect fungal hosts. The proposal that viruses in Subgroup II and Subgroup III should be classified into the suggested genera *Alphacryptovirus* and *Betacryptovirus* is compatible with the current classification, such as WCCV1, the typical member of genus *Alphacryptovirus*, included in Subgroup II. This classification is also well supported by the host specificity of the partitivirus during transmission and evolution (Ghabrial., 1998) and the genome characteristics of the partitivirus, such as base composition, length of ORFs and conservation of the 5' UTR (Table 6.6 and 6.7; Fig. 6.34). As shown in several reports, partitiviruses are transmitted vertically through cell division, seeds or pollen

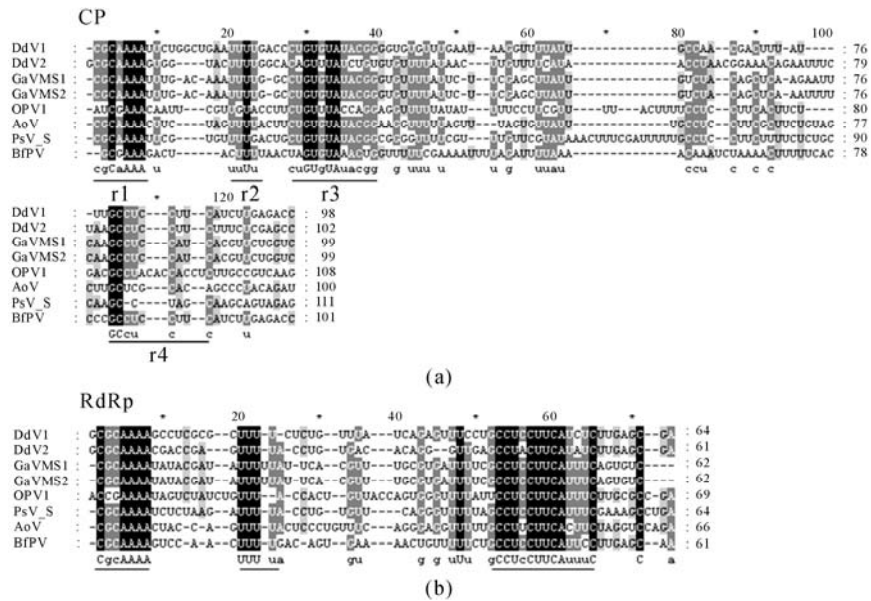


Fig. 6.34. Conserved regions in 5'UTR of genome sequences of Subgroup IV. (a) Alignment of 5' UTR of CP-encoding dsRNAs, performed by R-coffee (Wilm et al., 2008), showing four conserved regions (r1, r2, r3, r4); (b) Alignment of 5' UTR of RdRp-encoding dsRNAs, also by R-coffee, showing three strictly conserved regions

(Boccardo et al., 1985; Kassanis et al., 1977). However, Deng and Boland found evidence of horizontal transmission, provided that two strains (with high similarity) of the same partitivirus infected two different fungi, *Ceratocystis polonica* and *Ceratocystis resinifera* (Deng and Boland, 2007). The possible transmission between the fungal and plant hosts has been inferred (Crawford et al., 2006). Thus, it is possible that the ancestor of PmV1 was transmitted to primula from a fungus, and HmV and HmPV V1-2 were transmitted from a plant ancestor by accident. Viruses in the genus *Betacryptovirus* have a relatively larger genome (each genomic dsRNA larger than 2.0 kbp), compared with those in the genus *Alphacryptovirus*. However, no genome sequence information of the genus *Betacryptovirus* is available now (Ghabrial et al., 2005). Therefore, it is hard to establish their evolutionary relationship with other partitiviruses. In Subgroup I and Subgroup II, we suspect that there are more divergent evolutionary structures among partitiviruses infecting plants and fungi. The discovery of the intermediate viral species, such as PmV1, HmV and HmPV V1-2, will help to clarify the origin and evolution of viruses of the family *Partitiviridae*. Some partitiviruses were found to be tripartite, with the suggestion that the third dsRNA was a satellite or an additive dsRNA with unknown function (Oh and Hillman, 1995; Salem et al., 2008; Tuomivirta and Hantula, 2005; Tzanetakis et al., 2008).

Based on the inferred phylogenetic analysis, newly-detected or uncertain classified viral species could be easily distinguished. Coutts et al. (2004) deduced that ACD-PV (CCRS-PV), isolated from cherry leaf tissues, infected the plant

pathogenic fungus. They suggested that ACD-PV (CCRS-PV) should be classified in the genus *Partitivirus* (Coutts et al., 2004). However, it is more reasonable to classify them into the suggested genus *Alphacryptovirus* according to its evolutionary relationship with other partitiviruses. ACD-PV (CCRS-PV) is more likely to be a cryptovirus that infects the cherry, rather than a myco-partitivirus.

6.6 Conclusion

One cryptovirus always exists universally in different cultivars of the same species (Szegö et al., 2005; Tzanetakís et al., 2008; Veliceasa et al., 2006). And interestingly, if one cryptic dsRNA virus was found in one plant species, various cryptic dsRNA viruses would be detected in different individuals. With regard to these phenomena, it is expected that many more cryptic viruses than we can imagine can be found in the future. Thus it is time to pay more attention to these once “discriminated viruses”.

Actually, as we all know, more symptomless dsRNA viruses were found in fungi than *in planta*. However, in the author’s point of view, it is more reasonable and scientific to take the plant-dsRNA virus system as the investigation model system than to use the fungi-dsRNA virus model. At the macroscopic level, in comparison with most fungi, planta possesses a much larger body organism, and is easy to technically isolate and distinguish from each other. And planta grows much more slowly, thus it is easier to control and observe. With these biological advantages, the transmission of dsRNA viruses and planta-virus interaction can be effectively investigated. Furthermore, dsRNA virus species can be kept, and their activities in host cells can be disclosed, based on the highly-developed tissue culture-regeneration and cell culture technology. Certainly, the plant-dsRNA virus system also has many disadvantages such as, the biggest one, the time taken to study the phenotype changes induced by the viruses. And in order to make clear the relationship between mycoviruses, especially myco-cryptic dsRNA viruses and plant cryptic dsRNA viruses, it is necessary, and agricultural science is needed, to study the mycovirus-fungi-planta-cryptovirus comprehensively.

We present some future issues as follows:

(1) What about the cellular phytopathology property of these plant dsRNA viruses? Do they evoke severe destruction in the host plant in certain circumstances, such as high temperature and drought? To answer these questions, reverse genetics systems (i.e. infectious systems) are the first and fundamental step. So far as we know, in planta these dsRNA viruses only transmit through cell division like their hosts’ genome. Thus, reasonably, establishing an infectious system by using transgenic techniques through agrobacteria is a worthwhile and valid way to proceed, further confirming the transmission paths of these viruses. If, as in previous reports, more and more plants will be infected for the reason that these viruses can quickly spread through seed and pollen and, once infected, there is no valid way to cure these plant species, thus, it is more urgent to diagnose and

distinguish the healthy plant individuals (no infecting dsRNA viruses) from those with infected dsRNA viruses. We can use the healthy ones for plant breeding and spread them in agricultural production. Because of the non-infection among different individual plants (much less to say different species) and vertical transmission of these dsRNA viruses, it is much easier and fundamental to realize the origin and the relationship of these dsRNA viruses in *planta* and fungi through deep investigation of certain dsRNA virus's distribution in related plants of the natural host and divergence among these plants. For example, using RasV1 as a model virus, we can study the distribution of RasV1 in the family *Cruciferae* plants, and determine the genomes of the isolates from different host plants. Then we can analyze these results through comparative genomic methods. In combination with these hosts' evolutionary relationship, we could obtain a much clearer picture of the transmission and evolution of RasV1.

(2) The relationship between dsRNAs in *planta* and in fungus: Do the fungi transmit mycoviruses to plants or vice versa? Do these events still occur in the ' biosphere nowadays ? And through what ways?

6.7 Methodology

In the section, we introduce plant material and dsRNA extraction, purification of virus particles, amplification of unknown dsRNA sequence by modified single-primer amplification technique (SPAT), sequence analysis, dot blot hybridization.

6.7.1 *Plant Material and dsRNA Extraction*

Both field plants and the ones generated from seeds were grown at 15–25°C and at 50%–75% relative humidity in a greenhouse. *Aspergillus ochraceus* isolate FA 0611 was originally obtained from foliage of *Vicia faba*, a local cultivar grown in a suburb of Hangzhou city. And this isolate was identified according to morphological and molecular characteristics, and was cultivated on potato dextrose agar (PDA) at 28°C before use. It is suggested the mycelia be grown in a PDA liquid medium with inter-phase shaking for 6–9 d before harvesting. The harvested mycelia are vacuum dried over a piece of filter paper.

Fresh leaf tissues, with the main vein removed in advance, are recommended as the best material for dsRNA extraction. Prepared leaf tissue frozen below –80°C is optional material. Other plant organs, such as roots and seeds, can also be used for dsRNA extraction. Firstly, ground the plant tissues into powder using liquid nitrogen. Then, add 10 ml 2× STE (pH 8.0), 300 µl β-mercaptoethanol, 6 ml phenol (saturated with tris base, pH 8.0), 4 ml chloroform, 1.4 ml 10% SDS, and homogenize fully for 20 min in the shaker. Then, centrifuge for 15 min. The aqueous supernatant was collected and blended with ethanol to make its final concentration 17%. dsRNA in the mixture was bound to a CF11 cellulose column,

washed with a solution of 17% ethanol-STE buffer, and then eluted with 1× STE. The suspension was precipitated by adding an equal volume of isopropyl alcohol and washed with 75% ethanol. Finally, the precipitate was resuspended in deionized water. dsRNAs were fractionated by electrophoresis in a 5% polyacrylamide gel. Details of the protocol diagram are given in Fig. 6.35. The purified dsRNA was used for sequencing analysis and dot blot hybridization.

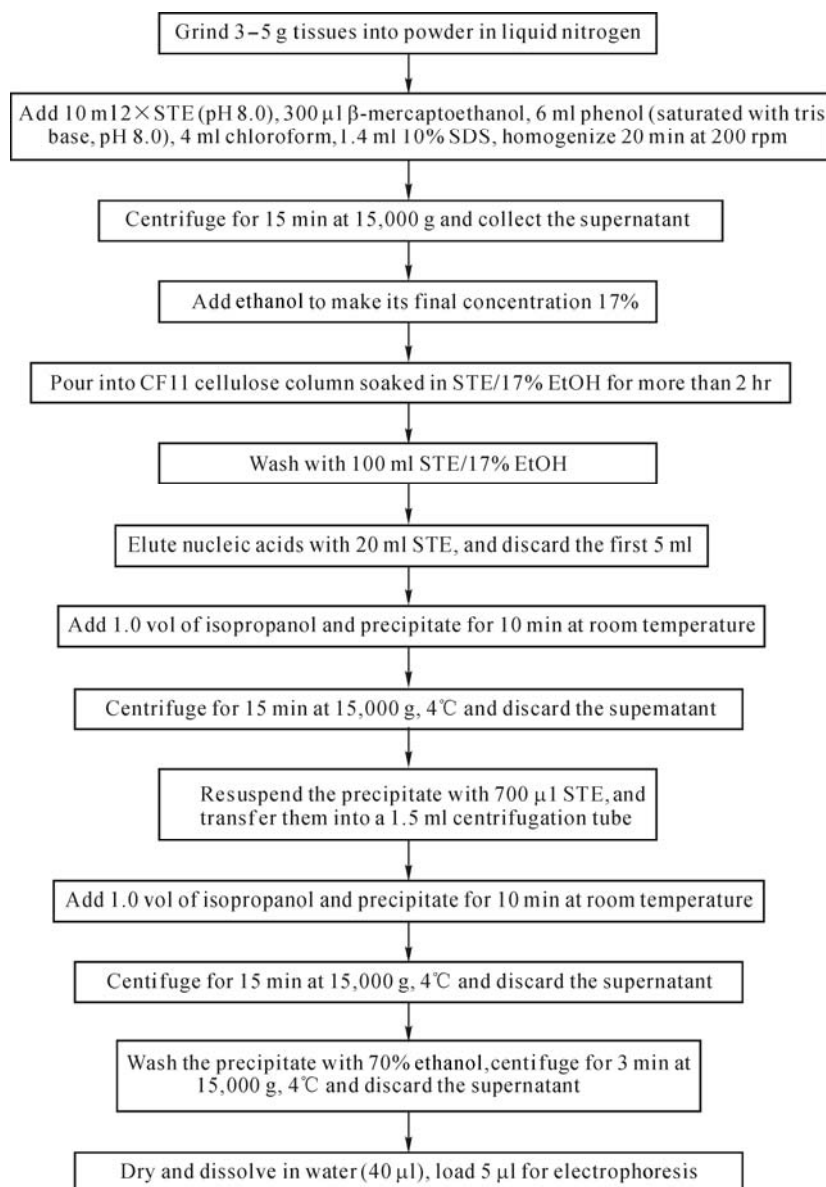


Fig. 6.35. Protocol diagram for dsRNA purification from plant leaf tissue

6.7.2 Purification of Virus Particles

Purification of VLPs from plant tissues and fungi materials was performed as described by Chen et al. (2006). Fresh leaf tissues or mycelia (vacuum dried) were homogenized in 0.5 mol/L phosphate buffer together with chloroform and *n*-butanol (pH 7.4) by using an electric blender. Cell debris was removed by centrifugation at 6,000×g for 30 min. The aqueous supernatant was mixed with 6% (W/V) polyethylene glycol (PEG 6000) and 0.1 mol/L NaCl (final concentration) and stirred overnight. The precipitate after centrifugation at 10,000×g for 30 min was resuspended with 0.01 mol/L phosphate buffer (pH 7.4) and re-centrifuged at 10,000×g for 30 min. The aqueous supernatant was collected for an ultracentrifugation at 78,000×g for 90 min. The pellet was resuspended with 0.01 mol/L phosphate buffer to keep the purified virus particles. To extract viral genomes from VLPs, treatment with Trizol reagent (Bio Basic INC., Canada) and chloroform was used, removing other viral components. Then we precipitate with an equal volume of isopropyl alcohol and wash with 75% ethanol. The precipitate was resuspended with DEPC-treated-H₂O.

Morphological characterization of virions was observed under an electron microscope after the virions were prepared by fixing with 1% formaldehyde and dialysis using demonized water. SDS-polyacrylamide gel electrophoresis (PAGE) analysis of virus particles was conducted to determine the molecular mass of the coat protein of the virus particle.

6.7.3 Amplification of Unknown dsRNA Sequence by Modified Single-primer Amplification Technique (SPAT)

A simplified single-primer amplification technique (SPAT) was used to obtain full-length cDNA clones of dsRNAs (Fig. 6.35) (Chen et al., 2006). A 3' amino-blocked ligase adaptor (primer A: 5'-PO₄-TCTTCGGGTGTCCTTCCTCG-NH₂-3', synthesized by Sangon, China) was ligated to the 3' end of the individual dsRNA segments using T4 RNA ligase (TaKaRa, Dalian, China) and DNA ligase (Promega, USA). The mixture was incubated at 15°C for 16 hours as described by the manufacturer. In particular, primer A was designed to be identical to a stretch of the genome of potato spindle tuber viroid with a 3'-NH₂ blocking group to avoid either significant resemblance to any other sequences from plants, or inter-concatenation of primers. The partial duplex was repaired with TaqTM DNA polymerase (TaKaRa, Dalian, China) at 68°C for 3 hours and purified using a PCR clean-up kit (V-gene, China). The tailed dsRNA was denatured at 99°C for 3 min with 15% dimethyl sulfoxide (vol/vol, final concentration), transferred into liquid nitrogen immediately for 1 min, and then onto ice for a further 5 min incubation. cDNA was synthesized using the complementary primer B (5'-CGAGGAAGGACACCCGAAGA-3') and SuperScriptTM II RNase H- Reverse Transcriptase (Invitrogen, USA) according to manufacture's recommendations. The PCR

reaction was done with Prime B and TaKaRa LA Taq™. The resulting products were gel-purified and ligated into the pMD18-T vector (TaKaRa, Dalian, China). The recombinants were transformed into competent *E. coli* DH5α cells and screened for inactivity of β-galactosidase. The inserted sequences were determined using M13 reverse and forward primers (Bioasia, China).

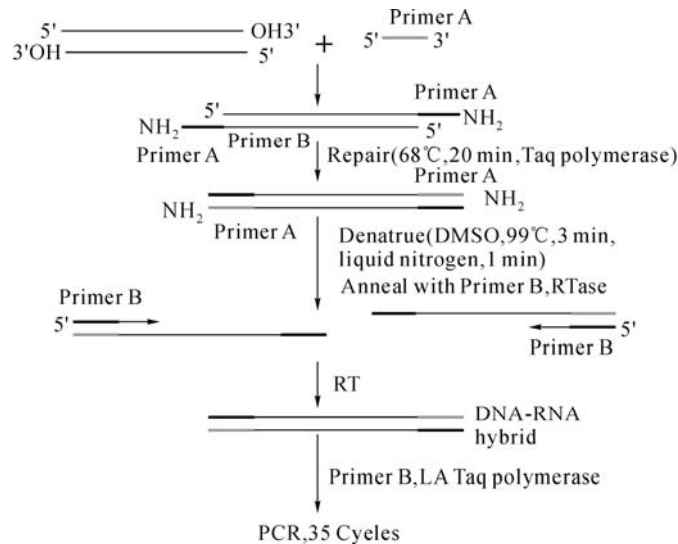


Fig. 6.36. Diagram of modified single primer amplification technique (M-SPAT)

6.7.4 Sequence Analysis

The LaserGene program (DNASTAR, Madison, USA) was used for dsRNA sequence annotations, including nucleotide statistics and open reading frame (ORF) searching. Similar sequences corresponding to the cDNAs and their corresponding putative proteins were retrieved from the Genbank (<http://www.ncbi.nlm.nih.gov/>) by using the BLAST program (Altschul et al., 1990). Sequence alignment was done by the Clustal W method (Thompson et al., 1994) or R-coffee (Wilm et al., 2008), and viewed with the Genedoc program (Nicholas et al., 1997). The phylogenetic analysis was conducted using MEGA version 3 (Kumar et al., 2004). RNA secondary structure predictions were performed using RNAstructure (Mathews et al., 2004).

6.7.5 Dot Blot Hybridization

Dot blot hybridization was performed to identify the unity between the cDNAs (plasmids) and their corresponding dsRNAs, and to detect related viruses. Purified and recovered dsRNA segments were dissolved in sterile DEPC-treated-H₂O and added to 3 volumes of denaturing solution containing 69.0% (vol/vol) formamide, 8.9% (vol/vol) formaldehyde, and 1.4× SSC. After being denatured at 99°C for 3 min, the mixture was transferred onto ice for 5 min, blended with an equal volume of 20× SSC, spotted onto the nylon membrane (Pall, USA) with 5 ul of each spot, and immobilized at 80°C for 2 h. Pre-hybridization and hybridization were performed as described by Sambrook and Russell (Sambrook and Russell, 2001). Probes specific for the clones of certain nucleic acid sequences were produced by PCR with primer B. ³²P labeling of probes was conducted with the random primer DNA labeling Kit (TaKaRa, Dalian, China). Membranes were incubated in the hybridization solution with specific probes (final concentration, 5× SSC, 5× Denhart's, 50% formamide (vol/vol), 1% SDS) overnight and washed at 42°C in 2× SSC with 0.1% SDS twice, 1× SSC with 0.1% SDS once, and 0.1× SSC with 0.1% SDS once, each time for 15 min. Finally, hybridization signals were detected and recorded using a Bio-imaging Analyzer System 1800 (Fujifilm, Japan).

References

- Abo-elnasr MA, Jones AT, Mayo MA (1985) Detection of dsRNA in particles of *Vicia cryptic virus* and in *Vicia faba* tissues and protoplasts. *J Gen Virol* 66: 2453-2460.
- Accotto GP, Marzachi C, Luisoni E, et al. (1990) Molecular characterization of alfalfa cryptic virus 1. *J Gen Virol* 71(2): 433-437.
- Altschul SF, Gish W, Miller W, et al. (1990) Basic local alignment search tool. *Journal of Molecular Biology* 215(3): 403-410.
- Antoniw JF, Linthorst HJM, White RF, et al. (1986) Molecular cloning of the double-stranded RNA of *Beet cryptic viruses*. *J Gen Virol* 67(9): 2047-2051.
- Bartel DP (2004) MicroRNAs: genomics, biogenesis, mechanism and function. *Cell* 116(2): 281-297.
- Bernstein E, Caudy AA, Hammond SM, et al. (2001) Role for a bidentate ribonuclease in the initiation step of RNA interference. *Nature* 409(6818): 363-366.
- Blawid R, Stephan D and Maiss E (2007) Molecular characterization and detection of *Vicia cryptic virus* in different *Vicia faba* cultivars. *Arch Virol* 152: 1477-1488.
- Boccardo G and Accotto GP (1988) RNA-dependent RNA polymerase activity in two morphologically different *White clover cryptic viruses*. *Virology* 163(2): 413-419.
- Boccardo G, Lisa V, Luisoni E, et al. (1987) Cryptic plant viruses. *Adv Virus Res* 32: 171-214.
- Boccardo G, Milne RG, Luisoni E, et al. (1985) Three seedborne cryptic viruses containing double-stranded RNA isolated from white clover. *Virology* 147(1): 29-40.
- Brown GG and Finnegan PM (1989) RNA plasmids. *Int Rev Cytol* 117: 1-56.

- Carter WA and De Clercq E (1974) Viral infection and host defense. *Science* 186(4170): 1172-1178.
- Chen L, Chen JS, Liu L, et al. (2006) Complete nucleotide sequences and genome characterization of double-stranded RNA 1 and RNA 2 in the *Raphanus sativus* cv. Yidianhong [corrected]. *Arch Virol* 151(5): 849-859.
- Child SJ, Hanson LK, Brown CE, et al. (2006) Double-stranded RNA binding by a heterodimeric complex of murine cytomegalovirus m142 and m143 proteins. *J Virol* 80(20): 10173-10180.
- Coutts RH, Covelli L, Di SF, et al. (2004) Cherry chlorotic rusty spot and *Amasya* cherry diseases are associated with a complex pattern of mycoviral-like double-stranded RNAs. II. Characterization of a new species in the genus *Partitivirus*. *J Gen Virol* 85(Pt 11): 3399-3403.
- Covelli L, Coutts R, Covelli L, et al. (2004) Cherry chlorotic rusty spot and *amasya* cherry disease are associated with a complex pattern of mycoviral-like double-stranded RNAs. I. Characterization of a new species in the genus *Chrysovirus*. *J Gen Virol* 85: 3389-3397.
- Crawford L, Osman T, Booy F, et al. (2006) Molecular characterization of a *Partitivirus* from *Ophiostoma Himal-ulmi*. *Virus Genes* 33(1): 33-39.
- Deng F and Boland GJ (2007) Natural occurrence of a partitivirus in the sapstaining fungus *Ceratocystis resinifera*. *Canadian Journal of Plant Pathology* 29(2): 182-189.
- Dodds JA, Morris TJ and Jordan RL (1984) Plant viral double-stranded RNA. *Ann. Rev. Phytopathol.* 22: 151-168.
- Doherty EA and Doudna JA (2001) Ribozyme structures and mechanisms. *Annu Rev Biophys Biomol Struct* 30: 457-475.
- Fenner BJ, Goh W and Kwang J (2007) Dissection of double-stranded RNA binding protein B2 from betanodavirus. *J Virol* 81(11): 5449-5459.
- Fire A, Xu S, Montgomery MK, et al. (1998) Potent and specific genetic interference by double-stranded RNA in *Caenorhabditis elegans*. *Nature* 391(6669): 806-811.
- Fukuhara T, Koga R, Aoki N, et al. (2006) The wide distribution of endornaviruses, large double-stranded RNA replicons with plasmid-like properties. *Arch Virol* 151(5): 995-1002.
- Ghabrial SA (1998) Origin, adaptation and evolutionary pathways of fungal viruses. *Virus Genes* 16(1): 119-131.
- Ghabrial SA, Buck K, Hillman B, et al. (2005) Partitiviridae. In: Eighth Report of the International Committee on Taxonomy of viruses (Fauquet CM, Mayo MA, Maniloff J, et al. (Eds.)), Elsevier/Academic Press London, pp. 581-590.
- Ghabrial SA and Suzuki N (2009) Viruses of plant pathogenic fungi. *Annu Rev Phytopathol* 47: 353-384.
- Gibbs MJ, Koga R, Moriyama H, et al. (2000) Phylogenetic analysis of some large double-stranded RNA replicons from plants suggests they evolved from a defective single-stranded RNA virus. *J Gen Virol* 81(1): 227-233.
- Hollings M (1978) Mycoviruses: viruses that infect fungi. *Adv Virus Res* 22: 1-53.
- ICTVdB M (2006a) Primula mosaic virus. In: ICTVdB - The Universal Virus Database, version 4 (Büchen-Osmond, C (Ed)). Columbia University, New York, USA.
- ICTVdB M (2006b) Primula mottle virus. In: ICTVdB - The Universal Virus Database, version 4 (Büchen-Osmond, C (Ed)). Columbia University, New York, USA.

- Ishihara J, Pak JY, Fukuhara T, et al. (1992) Association of particles that contain double-stranded RNAs with algal chloroplasts and mitochondria. *Planta* 187(4): 475-482.
- Jacobs BL and Langland JO (1996) When two strands are better than one: The mediators and modulators of the cellular responses to double-stranded RNA. *Virology* 219(2): 339-349.
- Kassanis B, White RF and Woods RD (1977) *Beet cryptic virus*. *Phytopathologische Zeitschrift* 90: 350-360.
- Kentex RH, Cockbain HJ and Woods RD (1978) *Vicia cryptic virus*. Report of Rothamsted Experimental Station for 1977, p. 222.
- Khrantsov NV and Upton SJ (2000) Association of RNA polymerase complexes of the parasitic protozoan *Cryptosporidium parvum* with virus-like particles: heterogeneous system. *J. Virol.* 74(13): 5788-5795.
- Kumar M and Carmichael GG (1998) Antisense RNA: function and fate of duplex RNA in cells of higher eukaryotes. *Microbiol Mol Biol Rev* 62(4): 1415-1434.
- Kumar S, Tamura K and Nei M (2004) MEGA3: Integrated software for molecular evolutionary genetics analysis and sequence alignment. *Brief Bioinform* 5(2): 150-163.
- Lemke PA and Nash CH (1974) Fungal viruses. *Microbiol. Mol. Biol. Rev.* 38(1): 29-56.
- Libonati M, Carsana A and Furia A (1980) Double-stranded RNA. *Mol Cell Biochem* 31: 147-164.
- Lim WS, Jeong JH, Jeong RD, et al. (2005) Complete nucleotide sequence and genome organization of a dsRNA partitivirus infecting *Pleurotus ostreatus*. *Virus Res* 108(1-2): 111-119.
- Lincoln TA and Joyce GF (2009) Self-sustained replication of an RNA enzyme. *Science* 323(5918): 1229-1232.
- Mathews DH, Disney MD, Childs JL, et al. (2004) Incorporating chemical modification constraints into a dynamic programming algorithm for prediction of RNA secondary structure. *Proceedings of the National Academy of Sciences of the United States of America* 101(19): 7287-7292.
- McCabe PM, Pfeiffer P and Van Alfen NK (1999) The influence of dsRNA viruses on the biology of plant pathogenic fungi. *Trends Microbiol* 7(9): 377-381.
- Morris TJ and Dodds JA (1979) Isolation and analysis of double-stranded RNA from virus-infected plant and fungal tissue. *Phytopathology* 69: 854-858.
- Natsuaki T, Yamashita S and Doi Y (1983) Radish yellow edge virus, a seed-borne virus with double-stranded RNA, of a possible new group. *Ann. Phytopath. Soc. Japan* 49: 593-599.
- Natsuaki T, Yamashita S, Doi Y, et al. (1979) Radish yellow edge virus, a seed-borne small spherical virus newly recognized in Japanese radish (*Raphanus sativus* L.). *Ann. Phytopath. Soc. Japan* 45: 313-320.
- Nicholas KB, Nicholas HB, Deerfield II D W (1997) GeneDoc: analysis and visualization of genetic variation. *EMBnet news* 4(2): 1-4.
- Oh CS and Hillman BI (1995) Genome organization of a partitivirus from the filamentous ascomycete *Atkinsonella hypoxylon*. *J Gen Virol* 76(6): 1461-1470.
- Osaki H, Kudo A and Ohtsu Y (1998) Nucleotide sequence of seed- and pollen-transmitted double-stranded RNA, which encodes a putative RNA-dependent RNA polymerase, detected from Japanese pear. *Biosci Biotechnol*

- Biochem* 62(11): 2101-2106.
- Osaki H, Nomura K, Matsumoto N, et al. (2004) Characterization of double-stranded RNA elements in the violet root rot fungus *Helicobasidium mompa*. *Mycol Res* 108(Pt 6): 635-640.
- Salem NM, Golino DA, Falk BW, et al. (2008) Complete nucleotide sequences and genome characterization of a novel double-stranded RNA virus infecting *Rosa multiflora*. *Arch Virol* 153(3): 455-462.
- Sambrook J and Russell DW (2001) *Molecular cloning: A Laboratory Manual*, 3rd ed. Science Publishing House, Beijing, pp. 517-589.
- Strauss EE, Lakshman DK and Tavantzis SM (2000) Molecular characterization of the genome of a partitivirus from the basidiomycete *Rhizoctonia solani*. *J Gen Virol* 81(2): 549-555.
- Szegő A, Tóth EK, Potyondi L, et al. (2005) Detection of high molecular weight dsRNA persisting in *Dianthus* species. *Acta Biologica Szegediensis* 49(1-2): 17-19.
- Thompson JD, Higgins DG and Gibson TJ (1994) CLUSTAL W: improving the sensitivity of progressive multiple sequence alignment through sequence weighting, position-specific gap penalties and weight matrix choice. *Nucl Acids Res* 22(22): 4673-4680.
- Tian B, Bevilacqua PC, Diegelman-Parente A, et al. (2004) The double-stranded-RNA-binding motif: interference and much more. *Nat Rev Mol Cell Biol* 5(12): 1013-1023.
- Tuomivirta TT and Hantula J (2005) Three unrelated viruses occur in a single isolate of *Gremmeniella abietina* var. *abietina* type A. *Virus Research* 110(1-2): 31-39.
- Tzanetakis IE and Martin RR (2005) *Fragaria chiloensis* cryptic virus: A new strawberry virus found in *Fragaria chiloensis* plants from Chile. *Plant Disease* 89(11): 1241.
- Tzanetakis IE, Price R and Martin RR (2008) Nucleotide sequence of the tripartite *Fragaria chiloensis* cryptic virus and presence of the virus in the Americas. *Virus Genes* 36(1): 267-272.
- Veliceasa D, Enunlu N, Kos PB, et al. (2006) Searching for a new putative cryptic virus in *Pinus sylvestris* L. *Virus Genes* 32(2): 177-186.
- Wang Y, Xu Z, Qu F, et al. (1988) Studies in the active principle inducing interferon in the extract of raphanus sativus. *Chinese J Virol* 4: 204-207.
- Weber F, Wagner V, Rasmussen SB, et al. (2006) Double-stranded RNA is produced by positive-strand RNA viruses and DNA viruses but not in detectable amounts by negative-strand RNA viruses. *J Virol* 80(10): 5059-5064.
- Wilm A, Higgins DG and Notredame C (2008) R-Coffee: a method for multiple alignment of non-coding RNA. *Nucl. Acids Res.* 36(9): e52.
- Xie WS, Antoniw JF and White RF (1993) Nucleotide sequence of beet cryptic virus 3 dsRNA2 which encodes a putative RNA-dependent RNA polymerase. *J Gen Virol* 74(7): 1467-1470.
- Xie WS, Antoniw JF, White RF, et al. (1993) A third cryptic virus in beet (*Beta vulgaris*). *Plant Pathology* 42(3): 465-470.
- Xu Z and Li L (2001) Studies on anti-epidemic type B encephalitis virus and anti-reticular cell sarcoma effects of extract of raphanus sativus-root in mice. *Chinese J Virol*(17): 338-340.
- Xu Z, Li L, Wang Y, et al. (1987) Protective effect of extract of raphanus sativus root on virus infection in vivo. *Chinese J Virol*(3): 99-101.

Index

18S Rna, 32, 34, 52
1a protein, 4, 6, 31
2a protein, 4, 6, 127
³²P-labeled DNA probe, 70, 73, 90
3a protein, 4, 6, 45
Δ2b, 102-104, 118

A

AGO1, 126, 136, 138
Alfalmovirus, 125
Alphacryptovirus, 218, 235, 240
*Amasya cherry disease associated
partitivirus*, ACD-PV, 218, 251
Amelioration, 31, 126
aminosilane slide, 67-69
aminosilane-coated glass slide, 49, 66
amplicon, 52, 54, 55
antiviral defense, 137, 163
apical necrosis, 99
arginine-rich nuclear localization signal,
136
artificial attenuated strain, 117
attenuated CMV, 117
attenuation, 107-108, 110

B

Beet cryptic virus 3, BCV3, 222, 228,
235
Betacryptovirus, 249, 251, 255
broad bean, *Vicia faba*, 230
Bromoviridae, 50, 97, 162
bubble-formed mosaic, 108

C

calibration factor, CF, 81, 84-85
cDNA, 6, 11, 40
character substitution, 21, 23, 28
chemical modification, 68, 168, 264
*cherry chlorotic rusty spot associated
partitivirus*, CCRS-PV, 218, 251
chimeric DNA fragment, 156
chimerical recombination, 97
chlorosis, 31, 98, 100
Chrysoviridae, 224, 233, 250
cis-acting elements, 35
Clade, 7, 11, 14
Cluster, 11, 14-16
CMV-Fny, 7-9
CMV-Fny derived mutant
CMV-Q strain
CMV-Sd, 7-8
CMV-Tsh, 6-8
codon degeneracy, 23
coefficient variation, CV, 77
co-infection, 2, 98, 104
complementary mutagenic primer, 154
complex infection, 30, 80, 102
Conformation of tomato miRNA
conserved terminal motif, 220
Copy number, 4, 75-76
CoreNucleotide BACs, 165
correlation coefficient, 76, 84
Cross-protection, 97, 100, 117
Cruciferae, 212, 258
crude sap, 72, 74, 130

Cryptovirus, 248-249, 251
 C_t standard deviation values, 76
 C_t value, 76-78
Cucumber mosaic virus, CMV, 1-5
 cucumovirus, 1, 6, 45
 CY3 label, 49
 CY5 label, 49, 66, 167
 CY5-labeled DNA probe, 66, 69-70
 cycle 0, F_0 , 81

D

dark green chlorosis, 213
Dasheen mosaic virus, DsMV, 17, 20
 days post inoculation, dpi, 32
 deleterious-compensatory model, 30
 detection limit, 56, 61, 69-70
 detection signal threshold, 174, 187
 diagnosis of plant virus, 47
 Disease index, 106-107, 112-113
 Divergence, 10-12
 dot blot hybridization, 49, 225, 258
 double-antibody sandwich enzyme-linked immunosorbent assay, DAS-ELISA, 18, 47, 55
 Double-stranded RNA, dsRNA, 47, 51, 110
 dsRNA pattern, 4, 213, 215
 dystrophin gene, 49

E

edge chlorosis, 213
 epidemiological investigation, 58
 Exacerbation, 31, 126

F

Fragaria chiloensis cryptic virus, uFccV, 223
 fruit distortion, 57, 98

G

G+C base content, 255
 GDD, 228
 gene centering, 169
 gene normalization
 Gene replacement, 125, 159

Giardavirus, 237
 glass slides, 49, 66-70
Glycine max, Soybean, 164
 GSS, 165, 175-176

H

Helicobasidium mompa V1-2 virus, 218
 helper virus, 31, 33, 36
 high ionic strength, 48, 66
 horizontal distance, 23, 26, 28
 hypersensitive response, HR, 165

I

Identity, 6-8
 immunocapture RT-PCR, IC-RT-PCR, 58
 In situ synthesis microfluidic chip, 167
In vitro transcription, 119, 130
 Infectious clone, 43, 48, 97
 infectious viruse, 48, 97
 internal control, 50, 52-56
 interspecific reassortant, 6
 intraspecies hybrid viruse, 82, 128, 131
 intraspecific reassortant, 6
 ITSP sequencing data, 165

K

K-H tests, 21-22

L

lab-on-a-chip, 51, 75-76
Leishmaniovirus, 237
Lettuce mosaic virus, 17
 LinRegPCR method, 85
 long-distance systemic movement, 39

M

maximum parsimony, 22-23, 26
 mechanical inoculation, 16, 100, 249
 metamorphic, 38-39
 microarray, 47-49
 microRNA, miRNA, 136, 159, 163

mild mosaic, 20, 99-100
 miRNA expression profile, 190, 193, 194
 miRNA microarray, 167-169
 miRNA pathway, 136, 138, 164
 miRNA sequence database, miRBase, 180, 185
 miRNA target, 166, 170, 173
 move protein
 Muller's ratchet predict, 30
 Multiple alignment, 217, 219-220
 Multiplex RT-PCR, 49, 51, 54

N

N_0 value, 84, 86-88
nad2 mRNA, 52-53, 55
 NADH *dehydrogenase* mRNA, 50, 56
 necrosis, 1, 6, 31
 necrosis determinant, 140
 necrotic streak, 99
 non-redundant mature miRNA sequence, 166, 173
 northern blotting, 36, 44, 81
 nucleic acid hybridization, 47-48, 51

O

opening read frame, ORF
 overlap-extension PCR, 154, 156

P

Pairwise, 12, 14-15
 parental viruses, 10, 126, 128
Partitiviridae, 218-220
Partitivirus, 218, 224, 228
 pathogenesis, 31, 38, 126
 Pathogenicity, 44, 51, 105
 PCR efficiency, 147, 172-173
 phenotype divergence, 130
 phylogenetic analysis, 7, 10, 18
 phylogenetic tree, 22-28
Pinellia ternate, 10
Pinus sylvestris partitivirus, 228, 252
 Plant hormone, 174, 179
 plant stunt, 57, 98
 plant-dsRNA virus system, 257

Pleurotus ostreatus virus, PoV, 245, 252
 polyacrylamide gel electrophoresis, PAGE, 74
 post-transcriptional gene silencing, PTGS, 104, 136, 163
Potato leaf roll virus, PLRV, 51, 55
Potato spindle tube viroid, PSTVd, 66
Potato virus A, PVA, 51, 55, 66
Potato virus S, PVS, 51, 55
Potyvirus, 2-3, 5
 pre-miRNA, 166, 175, 182
Primula malacoides, 243, 248
Primula mosaic virus, 243
Primula mottle virus, 243
 pseudorecombinant
 PTGS suppressor, 163,
Pyrus pyrifolia dsRNA 1, PyrR1, 222

R

Radish yellow edge virus, RYEV, 213
Raphanus sativus, 147, 212
Raphanus sativus cryptic virus 1, 217, 224, 227
Raphanus sativus cryptic virus 2, 222, 224, 228
Raphanus sativus cryptic virus 3, 226, 229
 Rapid amplification of cDNA ends, RACE, 169
 Real-time RT-PCR, 34-35, 50
 reassortment
 recombination, 9, 17, 30
 Relative quantitation, 119-120
 reproductive growth, 178, 190, 194
 restriction enzyme analysis, 7, 10, 62
 restriction pattern, 10, 63-65
 reverse transcript-polymerase chain reaction, RT-PCR
Rhizoctonia solani virus 717, RhsV-717, 245, 252
 RNA dependent RNA polymerase, RdRp, 222, 249
 RNA transcript, 32-33, 36-37
 RNA-induced silencing complex, RISC,

163
RNA-silencing suppressor, 180

S

Sanger miRNA Registry Database, 164
satRNA, 5-6, 10
secondary structure, 5, 29, 31
Sensitivity of multiplex RT-PCR, 61
simplified single-primer amplification technique, SPAT, 41, 260
site missing, 24
site-directed mutagenesis, 44, 140, 157
Small interfering RNA, siRNA, 163
Solaniose, 11
Southern tomato virus, STV, 231, 237
Soybean mosaic virus, SMV, 5, 17, 40
spatial constraint, 197
ssRNA, 4-5, 10
stem looped RT-PCR, 164
stem-loop, 38, 166, 170
subgenomic promoter region, SgPr, 4
subgroup I (CMV), CMV I
subgroup II (CMV), CMV II
subgroups IA and IB, 6, 9
SYBR Green I, 51, 75-76
SYBR Green-based stem-loop assay, 198
symptom expression, 15, 109, 122
symptom-induction domain, 140
synergic interaction, 112, 117
synergy, 6, 98, 111
systemic leaves, 32-37
systemic necrosis, 98, 138, 140

T

taxonomy of virus, 263
termination codon, 126, 129, 143
the ratios of nonsynonymous to synonymous mutations, Ka/Ks, 30
thermal optima, 9

thermal profile, 76
threshold cycle value, Ct
Titration, 50
 T_m value, 76-77
Tobamovirus, 40, 57-58
Tomato aspermy virus, TAV, 31, 126
Tomato EST, 165, 174
tomato miRNA, 164-165, 174
Tomato mosaic virus, ToMV, 1
top necrosis, 57, 98, 100
Totiviridae, 224, 233, 236
transcription factor, 178-180
transition, 24, 28, 236
transversion, 24, 28
tri-segments patitivirus, 219
true-leaf stage, 99, 118, 120
TuMV, 2-3, 30

U

Untranslated region, UTR, 42, 245

V

vegetative growth, 102, 174, 178
Vicia cryptic virus, VCV, 218, 230, 249
viral progeny RNA, 120, 132-136
Virion, 29, 39-42
viroid, 47-50
virulence, 28, 126-128
virulence determinant, 134, 138
virus inoculation, 40, 168-169

W

Watermelon mosaic virus, WMV, 5, 17
White clover cryptic virus 1, WCCV 1, 218, 248, 252
yellowing edge, 213, 215

Y

Zucchini yellow mosaic virus, ZYMV, 10, 98, 111